SURFACTANTS

AND

ENHANCED OIL RECOVERY

Thesis submitted for the degree of

Doctor of Philosophy at Brunel University

JENNIFER PILC

APRIL 1988

DEPARTMENT OF CHEMISTRY
BRUNEL UNIVERSITY
UXBRIDGE
MIDDLESEX

ACKNOWLEDGEMENTS

My Phd has been funded by Mobil North Sea Ltd., to whom I am very grateful, but further, I want to thank William Hurd for his particular support and technical advice.

I am greatly indebted to my supervisor, Paul Sermon, who has patiently guided and encouraged me throughout. Also, I wish to express my gratitude to my colleague and friend, Stephen Lawrence, for his help and ideas.

I would like to thank various Companies and Institutions who have also in the practical aspects of the work - Hoechst AG. (Frankfurt, West Germany), Anachem (Luton, UK), I.C.I. (Cleveland, UK), Rohm and Haas (Croydon, UK), Queen Mary College and University College (London, UK).

I am especially grateful to Jenny Taylor for reading my hand writing and typing the thesis.

Finally, I owe many thanks to my friends and colleagues at Brunel University who helped to make my time there so enjoyable.

ABSTRACT

A large number of commercial and some novel Brunel synthesised surfactants have been studied with a view to their potential usefulness for enhanced oil recovery (EOR) application. Ethoxylated phenols and their sulphonated derivatives were given especially high priority. The surfactants were well-characterised in order to understand their EOR potential. High pressure liquid chromatography, mass spectrometry, Raman spectrometry, nuclear magnetic resonance spectrometry and other quantitative techniques were used.

Aspects of their behaviour (as single components and as blends with co-surfactants and co-solvents) which have been considered in terms of:

(i) phase behaviour with brine and hydrocarbons

(ii) adsorption onto various oxide surfaces

(iii) interfacial properties such as surface tension, wetting, contact angles and viscosity

(iv) stability

Three different blends using sulphonated surfactants which:

(i) produce a microemulsion which is stable to high salinity brines over a large temperature range

(ii) exhibit low adsorption onto reservoir rock

(iii) interfacial tension as low as 10^{-2} mNm^{-1}

have been subsequently optimised. Core flooding tests carried out under reservoir conditions produced an additional 20% of the original-oil-in-place.

CONTENTS

Chapter 4 Physical Properties of Surfactants.

Chapter 5 Solubilisation.

CHAPTER 1

1.1. Crude Oil.

1.1.1. The Origin of Petroleum and its' Reservoirs.

As soon as any biological organism dies, its' remains are at once attacked by aerobic bacteria. However, as muds rapidly deposit on the sea bed, the flow of water and therefore oxygen is diminished and the environment becomes net reducing rather than oxidising. Depending on the temperature, pressure and time, various oils are formed from the insoluble organic matter. It is believed that most crude oils are formed between 333K and 423K; after which the heavier hydrocarbons are cracked to form methane gas. Most of the world's oil occurs between the depths of about 0.6 to 1.5 km.

Throughout the world, the composition of crude oil varies. Table 1.1 illustrates examples of this range and some of the important characteristics.

A typical oil reservoir consists of crude oil being trapped within a porous rock by natural forces resulting from viscosity, interfacial tension and capillarity (see Fig. 1.1). The oil is generally viewed as having migrated from the region of formation under the action of gravity (1). The rocks have a highly variable composition and comprise of sandstones, limestones, dolomites and clay minerals. A reservoir may contain brine, oil and gas and may be at a steady-state but not necessarily at equilibrium since reservoir fluids are

ORIGIN	NORTH AFRICA	NORTH SEA	MIDDLE EAST	NORTH AMERICA	SOUTH AMERICA
Light gasoline (0-343K)	8.8	5.8	4.7	2.4	0.1
Naphtha (343-413K)	16.0	11.0	7.9	6.5	1.1
Kerosine (413-523K)	26.3	18.6	16.4	15.6	4.4
Diesel Fuel (523-623K)	18.2	19.1	15.3	19.6	9.6
Residue (>623K)	27.5	43.5	54.4	55.5	84.8
Density (288K) $Kgdm^{-3}$	0.801	0.842	0.869	0.890	1.000
Viscosity (311K)	1.4	4.5	9.6	13.4	19,400
Sulphur (%wt)	0.1	0.3	2.5	1.0	5.5
Metals					
Vanadium ppm	<2	8	50	25	1415
Nickel ppm	<2	4	13	13	17

TABLE 1.1 Composition Variation of Crude Oil throughout the World. (% weight)

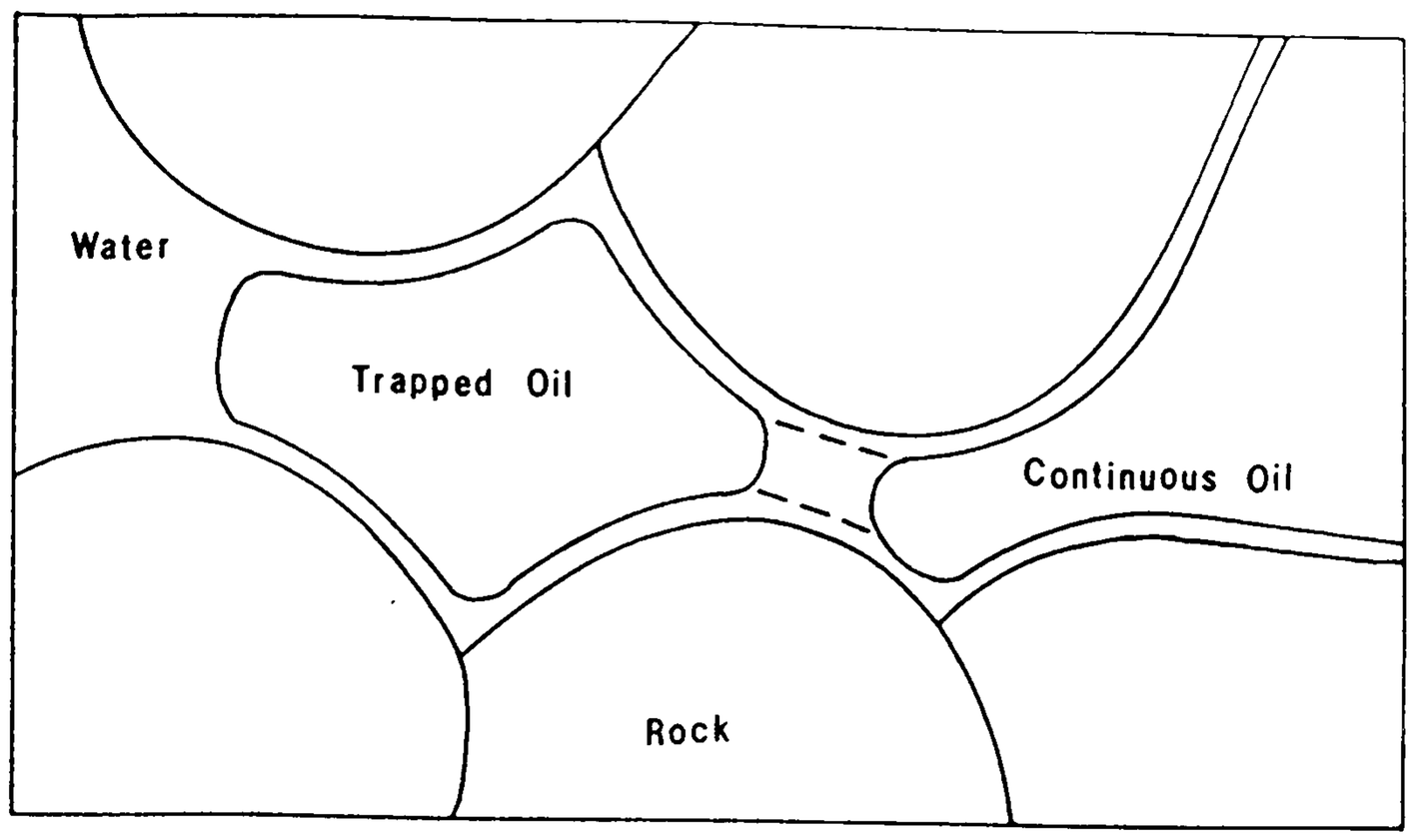

Fig.1.1 Crude oil trapped in a porous matrix by natural forces.

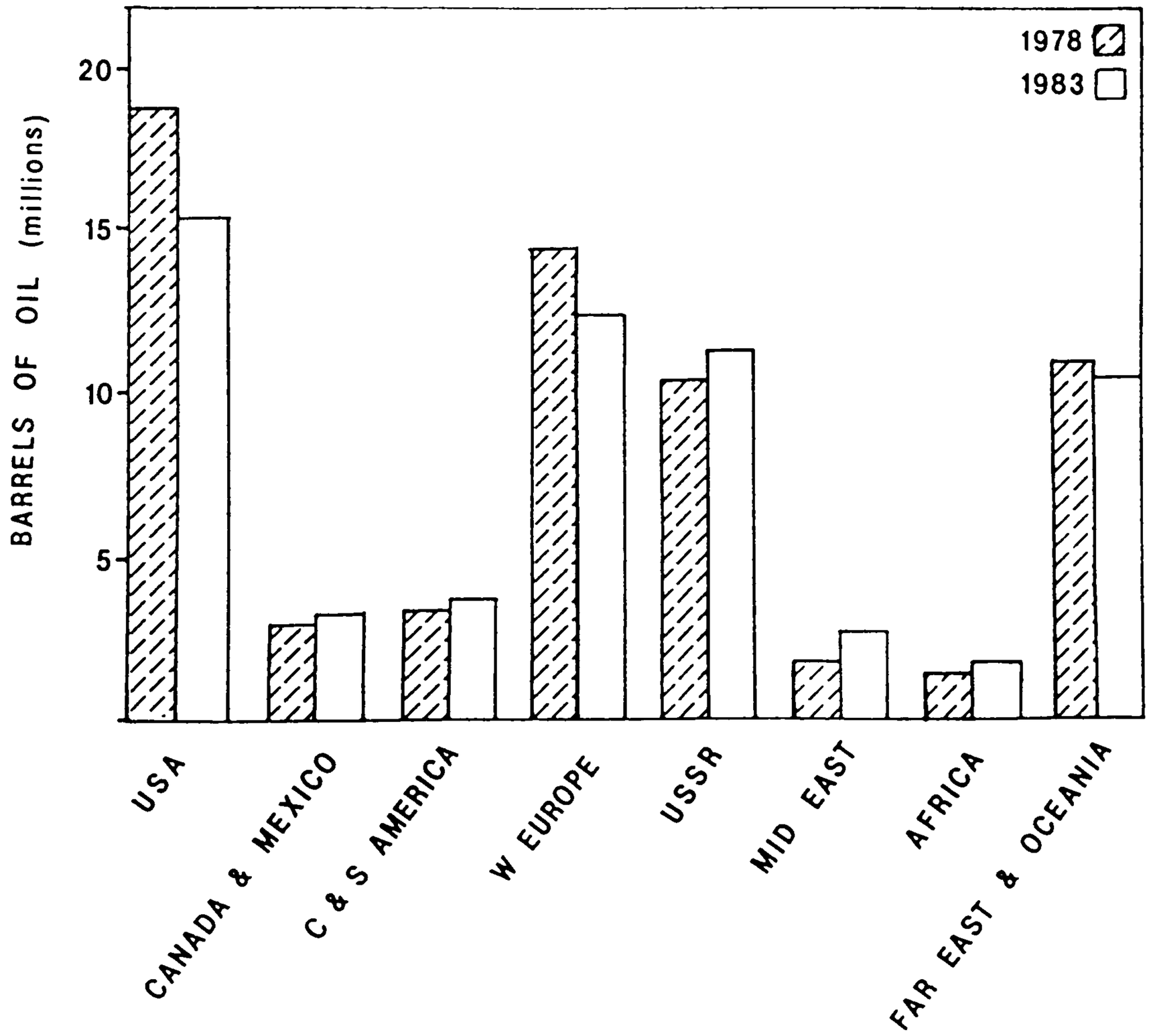

Fig.1.2 World consumption of crude oil.

frequently not well mixed or uniform.

1.1.2 Oil Reserves, Production and Consumption

The consumption of crude oil throughout the world in 1978 and 1983 is shown in Fig. 1.2. There has been a 5% decline over the 5 years with the greatest difference in the U.S.A. and Western Europe. There are many reasons for this, e.g. an increase in the use of gas and a greater efficiency in automobile engines.

The source of this crude oil is shown in Fig. 1.3. The 1978 figures show little change except for the Middle East, where production decreased by about 34%. The distribution of the oil reserves is illustrated in Fig. 1.4. One striking feature is the ratio of the reserves to production, particularly for the Middle East where the reserves are far greater. The reverse is true for the United States which must import a large fraction of oil to meet its demand.

1.1.3 Causes of Residual Oil

(i) Microscopic

Capillary forces which allow displacement of oil by water also result in the trapping of oil across the water-oil interface. Fig. 1.5. shows two pore spaces which have a common inlet and outlet. The capillary force at the water-oil interface "draws" the water and causes it to move into the upper and lower pore spaces, displacing oil as it moves. This action assumes that the pore walls are water-wet (which is the case

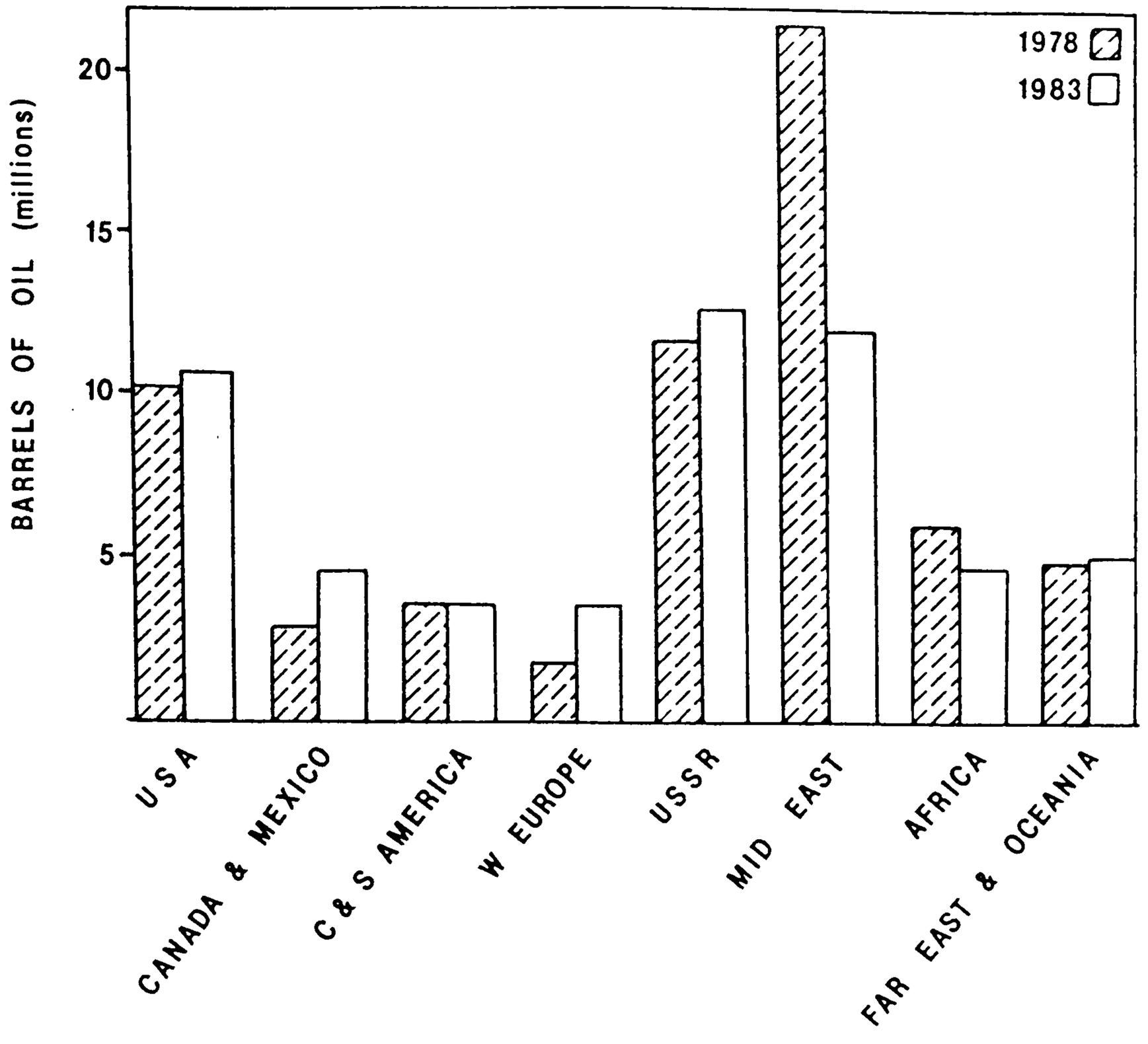

Fig.1.3 World production of crude oil.

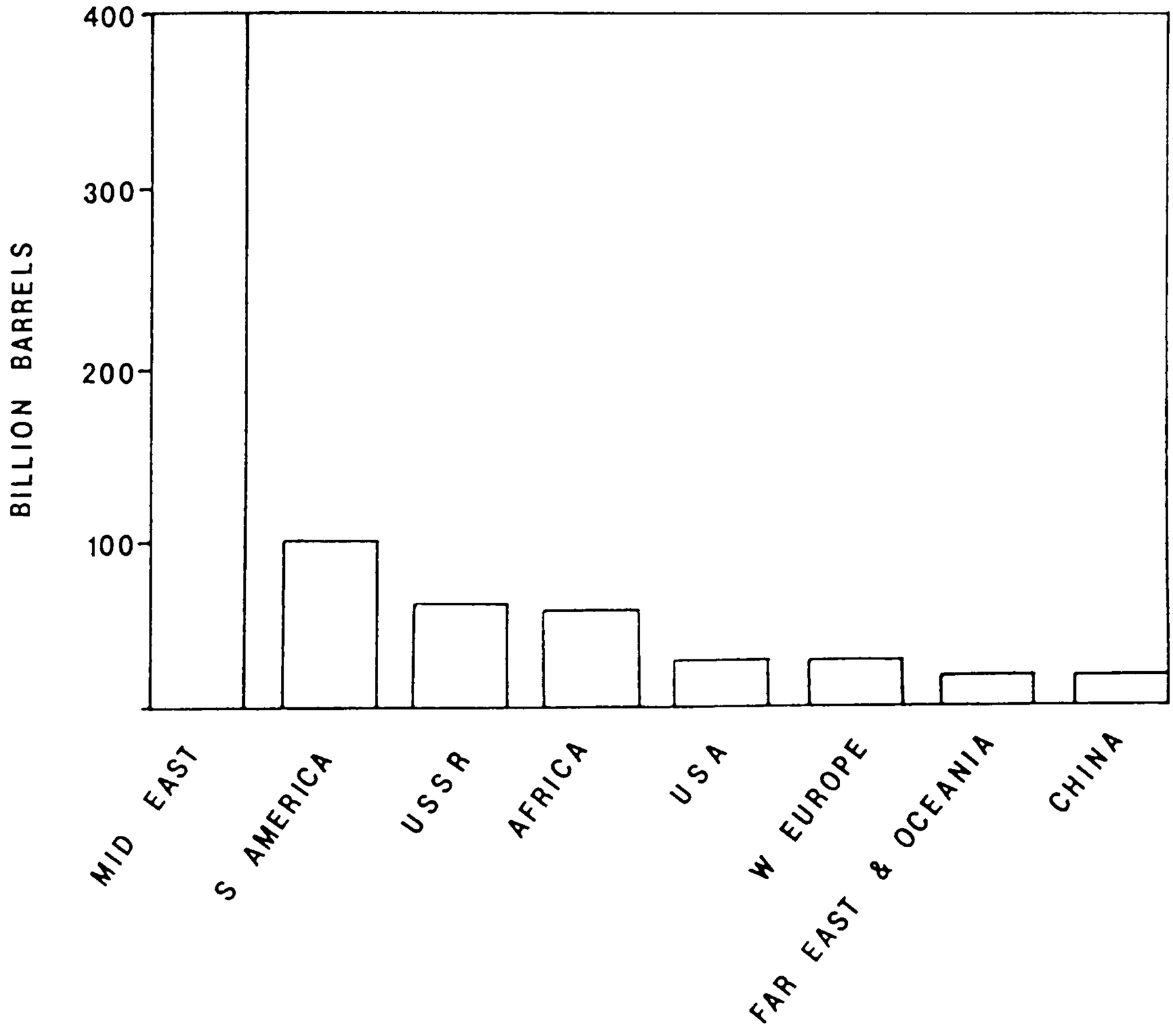

Fig.1.4 World reserves of crude oil (1984).

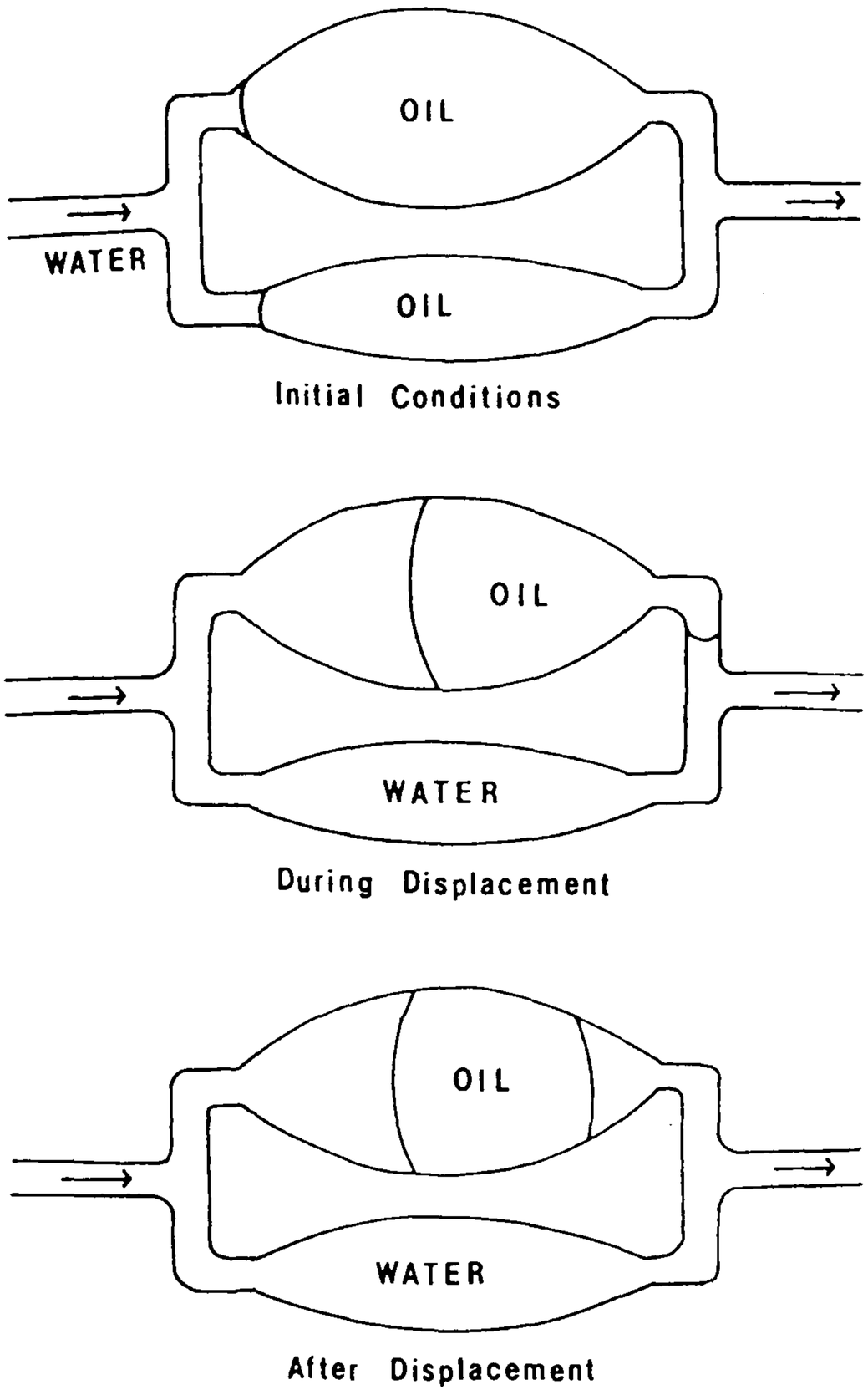

Fig.1.5 Idealised pore model showing capillary forces simultaneously displacing and trapping residual oil.

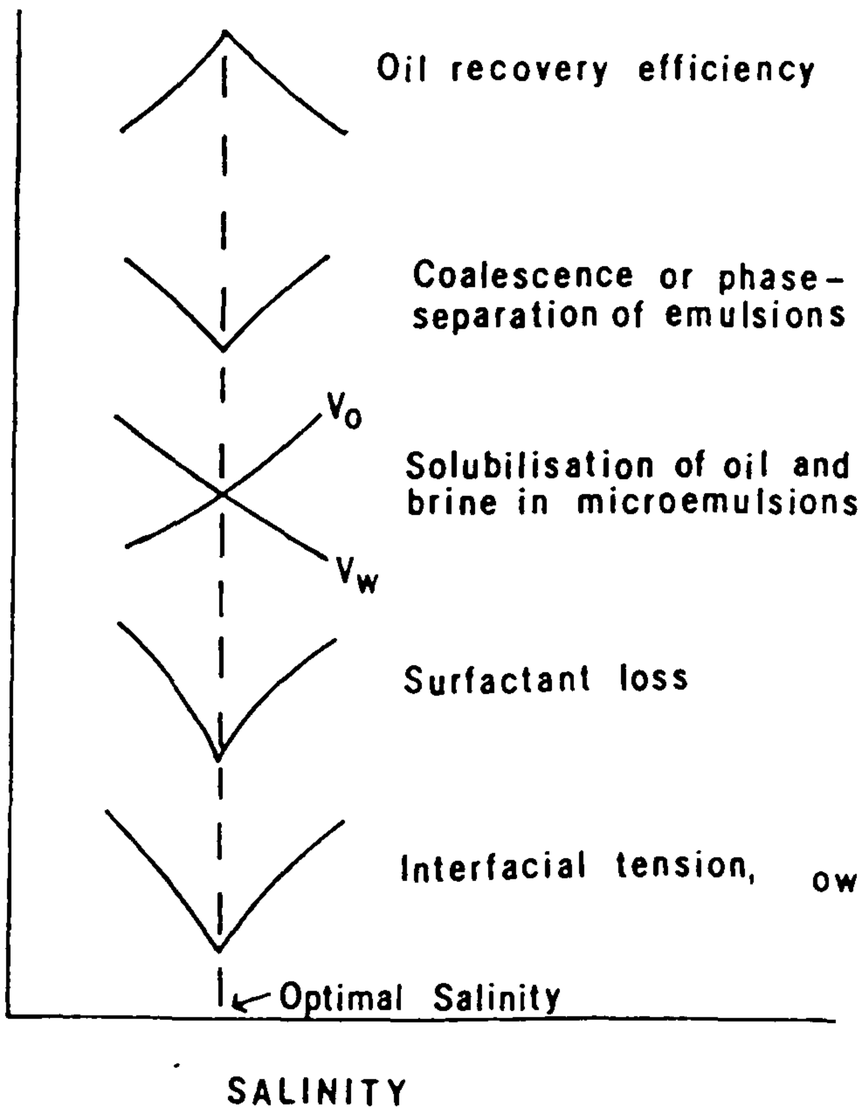

Fig.1.6 Various phenomena occurring at the optimal salinity

generally for reservoir rock). The centre diagram shows water has displaced all the oil from the smaller pore but only part of the oil from the larger one. This is because:

a) the smaller diameter pore has increased capillary pull and,
b) the oil volume displaced by water is far less.

A capillary force is exerted on the downstream end of the large pore and further displacement ceases, trapping it between the two interfaces. The lower diagram depicts the trapped oil after all the capillary forces have reached equilibrium. The path of water flow has been established through the smaller pore space, and continued water injection cannot dislodge the residual (trapped) oil droplet.

(ii) Macroscopic

Residual oil also arises from permeability variations in the rock matrix. The oil lies in the unswept pockets or is by-passed by the waterflood. A high viscosity of the oil relative to the displacing fluid (usually water) causes a break-through of the displacing phase.

1.1.4 Mechanisms of Oil Mobilisation

(i) Low Interfacial Tension Flood

In order to mobilise oil ganglia trapped in a water-wet pore by interfacial forces, the oil/water interfacial tension (IFT) must be reduced to very low levels (~10^{-1}

mNm^{-1}). Fig. 1.1 illustrates the role of ultralow IFT for the movement of a trapped oil ganglion. The subsequent coalescence of these ganglia is necessary to form an oil bank. The capillary pressure resistance to flow is proportional to the oil/water interfacial tension divided by the diameter of the pore constriction (~10μm for North Sea sand formations).

(ii) Spontaneous Emulsification

This arises from the diffusion of surfactants across the oil/water interface. Consider a drop of surfactant containing solubilised oil suspended in water. The surfactant will diffuse into the aqueous phase and simultaneously solubilise fine drops of oil into the water.

An oil/brine/surfactant/alcohol system often forms a middle phase microemulsion (see chapter 5) in an appropriate salinity range. When this system is pumped through a porous media, a minimum pressure drop (or apparent viscosity) is observed at the optimal salinity. Fig.1.6 summarises these and other factors contributing towards maximum oil recovery at optimimum salinity.

(iii) Interfacial Rheology.

Movement of oil/water interfaces through pores of varying geometry will involve compression and expansion of the oil/water interface. If this interface is highly elastic or viscous it could present a resistance to oil

mobilisation. Highly compressible interfacial films can exist under reservoir conditions at the crude oil/water interface. Such films stabilise oil drops released from pore surfaces resisting the formation of an oil bank necessary for efficient oil displacement.

(iv) Surface Wetting

Consider the pore doublet (Fig. 1.5) consisting of 2 pores of unequal diameter from which oil must be displaced. If the system is water wet, water will imbibe into the narrow pore leaving oil trapped in the wider pore. This system has low permeability. In the oil-wet case, oil will be trapped in the narrower pore. This system has high permeability. An actual surface may have regions of mixed wettability owing to surface heterogeneities. This can lead to oil trapping, for example when an oil/water interface advances through a water-wet capillary and meets an oil-wet section. In this case, an oil blob would be retained on the oil wet surface. As shown in Fig. 1.7, the contact angle of oil on the rock surface depends on the wettability of the rock. This is discussed further in Chapter 4.

1.2 Oil Recovery Techniques

In the early years of oil production, pioneers gave relatively little thought to production techniques. The drilling sites were selected purely on a speculative basis and consequently the odds of finding a producing well were generally poor. Early production techniques were crude. One method involved dropping an explosive

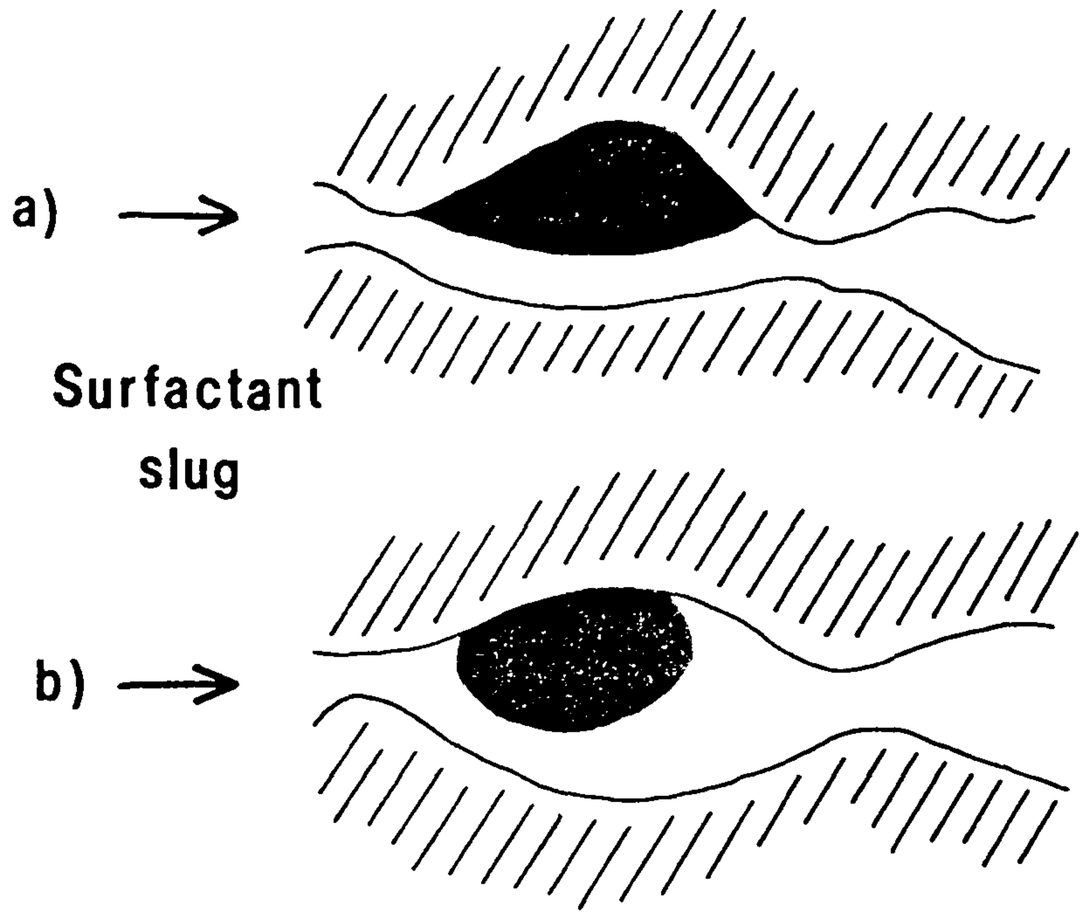

Fig.1.7 The effect of rock wettability on the contact angle an oil drop: a) represents an oil-wet rock surface whereas b) represents a water-wet surface

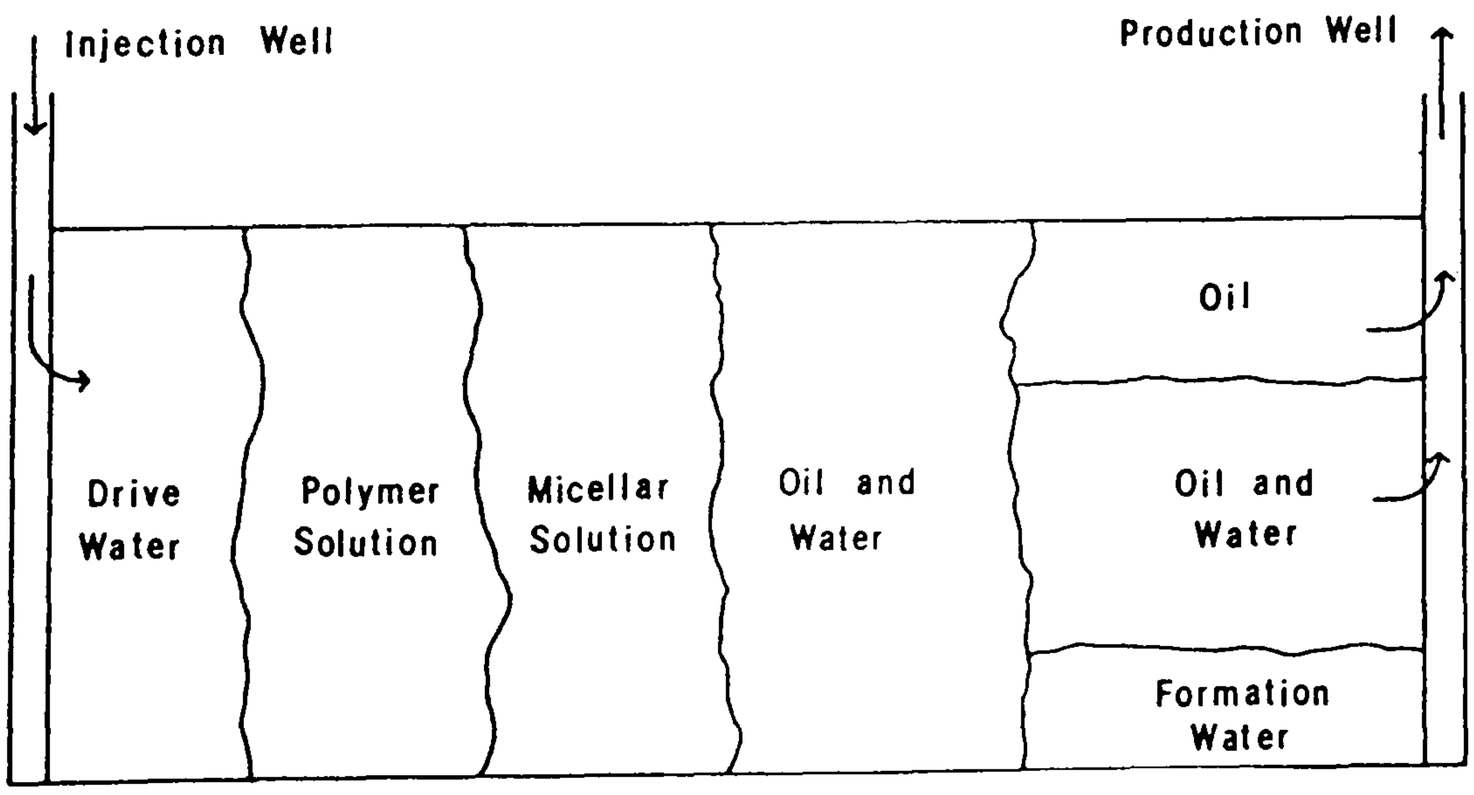

Fig.1.8 Example of a micellar-polymer EOR process.

assembly into the well bore which shattered the rock formation thus reducing the resistance to flow of the oil. Another was the stimulation of wells with acid and is reported in the literature as far back as 1895.

These techniques began to wane with the advent of hydraulic fracturing, whereby pressurised liquid is injected to fracture the formation. A porous zone was created through which the oil could flow with relative ease. The application of a vacuum to the well head was also used for some time before giving way to more efficient methods such as gas or air drives which "lifts" the oil from the depths of the well; these were reported as early as 1864 in Pennsylvania.

These early techniques may be classed as secondary recovery methods employed after the natural decline of a producing reservoir. The first successful attempt to force oil from underground rocks by the injection of another fluid occured apparently by accident. Early oil production began in Pennsylvania around 1865, wells were often abandoned improperly and surface water was allowed to enter the productive zone. Early operators feared that the water would "drown" the oil and many states had laws which prohibited the injection of water. However, the increased production from this water flooding was observed consistently and by 1940, it was considered to be "unquestionably the most efficient method ever devised for increasing oil recovery" (2).

Early engineers realised that water-flooding still bypassed some oil and in 1917 a patent was granted for the addition of alkali to the flooding water. In chemical flooding, surface active agents were assumed to be effective for releasing oil from the rock.

It was even reasoned that since water displaces oil largely by capillary action, better displacement would occur if the interfacial tension, γ, could be <u>increased</u> to improve the capillary driving force. Some of the early experimenters also reported that very little improvement in oil recovery could be expected with many of the surface active materials. One detailed study indicated that oil recovery actually decreased slightly when the oil-water interfacial tension, γ_{ow} was decreased (3). Enhanced or tertiary oil recovery is generally considered as the third or (last phase) of useful oil production. Defining EOR requires some knowledge of traditional processes, namely primary and secondary oil recovery.

1.2.1. Primary Recovery

When the first well is drilled into a new oil field, the oil and gas are usually found at high pressure. In many cases, the pressure of the confined fluids will be of the order of MPa. In the early stages of production, most of this pressure is released as the fluids are allowed to expand and they flow to the well bore, through to the well head. Much of the expansion comes from gas, either in a gas cap or by gas desorbing from solution. Although the initial reservoir pressure is often enough to force

the oil to the surface, the pressure falls steadily until it is necessary to install pumps or apply other means to force the oil from the bottom of the well.

1.2.2. Secondary Recovery

The principal method is water-flooding which seeks to maintain the pressure in a reservoir by adding supplementary energy. The injection of fluids (often sea water) replaces the volume lost by the oil and gas. As the water to oil production approaches an economic limit of operation, the tertiary phase of oil production begins. Water is relatively inexpensive to obtain, inject and is incompressible. However, the older the well, the higher the water to oil ratio required for recovery and it may then become uneconomic and time consuming. It was first used over 100 years ago, and gained popularity in the 1950's when field applications increased rapidly.

The fraction of oil that will be recovered from water flooding is a function of the following factors:

(i) areal sweep efficiency
(ii) a contact factor
(iii) displacement efficiency.

This simplified approach estimates the extent of recovery assuming one homogeneous strata with average reservoir properties. Another method assumes the reservoir is composed of many strata of different properties. Each layer is treated independently.

1.2.3. Tertiary Recovery

Fields in which waterfloods were initiated and reached the stages of depletion are plugged and abandoned. The third crop of oil which can be recovered involves a more complex secondary production with chemical modification of injection fluids. However, a tertiary method may be more efficient if applied prior to the application of secondary recovery. For example, polymer injection is more effective when utilised as an enhanced secondary technique than when it is applied only near the completion of a regular waterflood.

1.2.4. Enhanced Oil recovery

The term enhanced oil recovery refers to injection of fluids or special forms of energy into a reservoir for purposes other than regular pressure maintainance. It always involves the addition of chemical or thermal energy to stimulate production. The oil recovered is that which is obtained by means other than through the natural energy of the reservoir. The combined total oil production by primary, secondary and tertiary methods is generally less than 40% of the original-oil-in-place (OOIP).

The main reasons for the remaining or residual-oil-in-place (ROIP) are:

(i) some oil is too viscous to flow at economic rates;

(ii) oil is trapped as isolated microscopic

drops in pore spaces of the water-swept regions (20- 30% ROIP);

(iii) only part of the reservoir can be contacted by a waterflood, so 80-70% of the ROIP is located in unswept regions.

Even though 100% recovery is not conceivable, the potential target of EOR (the ROIP) is greater than the reserves produced by conventional methods.

While the broad umbrella of EOR covers many methods, the techniques can be grouped under four general headings:

a)	Thermal Methods -	Steam Drive Hot Water Flooding In-situ Combustion
b)	Gas Flooding -	Carbon Dioxide Flooding Inert Gas Flooding Nitrogen Flooding
c)	Chemical Methods -	Surfactant Flooding Polymer Flooding Alkaline Flooding
d)	Novel Technologies	Microbial EOR Electrical Methods Oil Mining Foam Drive.

It is most likely that future recovery methods will use a combination of these techniques, each designed for a specific reservoir. The application of each type is dependent upon reservoir characteristics including the type of oil.

Surfactants and EOR

For a surfactant to have EOR potential it must meet several requirements:

(i) good solubility/dispersibility in saline

water

(ii) partial solubility in oil

(iii) lowering of the interfacial tension in oil/water systems (<1mNm^{-1})

(iv) ability to form micellar structures

(v) stabilisation of oil/water emulsions

(vi) low retention by adsorption on the rock surface or through trapping of the microemulsion.

These must met be throughout the flood as the fluid flows through a complex heterogeneous reservoir and the fluid banks begin mixing with each other.

Holstein (4) concluded that for optimum performance, surfactants must be tailored to the temperature, salinity and crude oil conditions encountered in the reservoir. The number of surfactants suited for EOR measures decreases rapidly when highly saline reservoir brines are involved at high temperatures.

1.3. Enhanced Oil Recovery Techniques

1.3.1. Thermal Techniques

The purpose of thermal recovery is to heat the reservoir (and its oil) by generating heat at the surface and transporting it into the reservoir by the injecting fluid. Usually water is used, resulting in either a steam injection or hot waterflood project. Heat reduces the crude viscosity, which improves sweep efficiency. The rate of viscosity improvement is greater in the more viscous low-gravity crudes and at smaller temperature

increases. Little benefit is gained after reaching a certain temperature.

a) Steam Drive.

The injection of steam for oil recovery started in the late 1950's and now accounts for more oil recovered than by all other EOR techniques (5). Steam is continuosly injected into a well which carries mechanical as well as thermal energy. A high oil displacement rate requires a minimum of heat loss through surface lines, injection well bores and to over- and under-lying formations. Heat loss due to the injection temperature and equipment can be controlled but that due to reservoir characteristics cannot. To overcome high formation pressures in deep zones, steam at a higher pressure and temperature is necessary, resulting in a greater heat loss. Also the longer the bore (the deeper the well) the greater the loss of thermal energy. Application at lower pressure is therefore energetically a more efficient process.

b) Hot Water-Flooding

This is the most basic type of thermal recovery and needs the fewest and least expensive equipment changes to extend water-flooding. It is less attractive than steam injection which naturally has a much higher heat content. Hot water flooding can be used in some reservoirs where steam cannot. These include formations sensitive to fresh water and those at high pressure where steam temperature would be excessive.

Application. Both processes are limited to those reservoirs containing viscous oils that are the most susceptible to viscosity reduction by heat. A reservoir depth of less than 1000m and a sand thickness between 10-15m are necessary to limit formation heat losses. A permeability of 50md (millidarcy) or more assists the flow of viscous oils and is important since response depends on injection rate. Examples of hot water and steam drive are given by Martin (6) and Bursell (7).

Advantages

(i) it is the best technique to boost meager primary or secondary recovery.

(ii) displacement efficiency is increased since injection rates are higher causing more oil to flow.

Disadvantages

(i) losses of costly surface generated heat are high and so cannot be utilised in reservoirs which are deep, thin or have low permeability.

(ii) operation at high temperature entails added safety risks to personnel.

(iii) gravity override by steam may result in only the upper part of the formation being contacted.

(iv) the initial investment is high since the water used must be of a high quality, usually softened to prevent scale problems in the steam generators. Also, the high viscosity crudes usually considered for thermal projects are lower priced.

(c) In-situ Combustion

The concept of in-situ combustion dates back to 1880 when its' application was first suggested for the production of combustible gases from coal seams. This method was first used for the recovery of crude oil in 1934. Commonly referred to as 'fire flooding' this thermal

technique ignites the oil in the reservoir and the fire sustained by air injection. In some reservoirs ignition is spontaneous. The speed of the oxidation process between oxygen in the injected air and reservoir oil is sufficient to develop temperatures to ignite the oil. In others ignition is aided by using downhole heaters or preheating the injection air. The vapourised light components and steam formed ahead of the flame are carried forward and condense in the cooler portion of the reservoir. The heavy residual carbon deposit remains as fuel to be burned. In the condensing zone, the condensed light hydrocarbons displace oil miscibly, the condensed steam causes a hot water-flood and the combustion gases provide a gas drive.

Application. The gravity of the crude should not be too high or else too much fuel will be deposited for burning. The gravity should also not be too low or the deposit will not be able to support combustion. The oil content of the reservoir should be greater than normal for the process to be economic since large amounts may be burned during application. The reservoir thickness should be at least 10m to prevent excessive heat loss and at a depth range of 100-120m. Shallow depths limit injection pressure and air compression costs are high for deep reservoirs.

Examples of successful and unsuccessful projects are given in references (8) and (9) respectively.

Advantages.

- the process is not limited to heavy crudes,
- high displacement efficiency can be achieved although some oil is burned and not produced,
- the injection fluid, air, is readily available.

Disadvantages.

- producing equipment can be severly damaged by heat and corrosion as the flame nears the producer,
- heat distribution is inefficient. A relatively large hot zone is formed behind the flame where little benefit is gained. This can be overcome by alternately injecting with water,
- air compression costs can be high depending on the required pressure.

1.3.2. Gas Flooding

This process shares the basic aim with micellar methods to eliminate the effects of interfacial tension. The chief criterion is to achieve a minimum miscibility pressure at which 100% displacement efficiency can be achieved. Among the methods which have been ued for oil recovery are the liquified petroleum gas (LPG), miscible slug process (10), the enriched gas miscible process (11), and the high pressure lean gas miscible process (12). The main problem is choice of a suitable driving agent. Natural gas, propane and other liquified petroleum gases are in great demand and are increasing in price. The economics are strengthened if gas plant facilites are on site or near, to save on transportation cost. Apart from their increasing petrochemical value, hydrocarbon gases are poorer performers than carbon

dioxide.

Carbon Dioxide Miscible Process.

Carbon dioxide is effective in displacing oil from a reservoir by vapourisation and swelling. It is not miscible with oil upon first contact but under favourable conditions of temperature, pressure and oil composition, a miscible front is generated in the reservoir. Multiple contacts between the leading edge of the CO_2 and oil cause a tansfer of components from the oil to the CO_2. Holm and Josendol (13) found that CO_2 can disperse crude oil more efficiently than other gas processes. This feature of the CO_2 process makes it applicable to a large number of reservoirs.

Field studies of CO_2 flooding to date have led to encouraging residual oil saturations. Injection of alternate CO_2/water slugs, the "carbonate" water-flood, has been successfully employed in Hungary (14). Less encouraging results (15) were due to miscibility being hindered by the waterflood.

Application. The CO_2 process is applicable to a high percentage of reservoirs. The pressure required with a given oil ranges from 10-40MPa. Prospective reservoirs must be of a sufficient depth to withstand the pressure without fracturing the overlying rock.

Advantages.

- the sweep and displacement efficiency is high: CO_2 is 2-4 times as viscous as methane over the usual range of pressures.

- under some reservoir conditions, the density of CO_2 is close to that of crude oil and

approaches that of water. This greatly minimises the effects of gravity override.

- the miscible front, if lost, regenerates itself.

Disadvantages.

- to obtain a favourable mobility ratio, the injection of CO_2 alternately with water is requied.

- CO_2 forms carbonic acid with water which is highly corrosive. Special metal alloys and coatings for facillities are needed. Dual injection systems are required - one for CO_2, two for water.

- CO_2 is generally not readily available and transportation costs are large. Substantial sources of naturally occuring CO_2 have not been identified in the U.K. A few North Sea oil reservoirs (in the Norwegian Sector), do contain some useful amounts in the associated gas but this is not sufficient for general application.

1.3.3 Chemical Methods

(i) Surfactant Flooding.

Micellar or surfactant solution flooding is one of the most promising methods. Only a brief outline of the principle will be reviewed here; a detailed understanding follows in Chapter 5.

The basic concepts involved in surfactant flooding are old, a patent having been issued for such a process as early as 1927. Water soluble compounds have been described (16,17) and Holbrook (18) suggested, among others, fatty acid soaps, organic perfluoro compounds and polyglycolether. Laboratory results showed that these solutions reduced the interfacial tension and improved the oil recovery.

The first mention in the literature of using microemulsions and swollen micelles was a patent filed in 1942 (19). In 1962 Gogarty and Olson (20) described the use of microemulsions in a new miscible-type recovery process which lead to the addition of cosurfactants and electrolytes. Since then publications have stressed coupling different salts with surfactants to reduce the interfacial tension to a minimum and to prevent the adsorption of surfactants within the reservoir. A surfactant process must meet several requirements to be successful in recovering residual oil:

(a) low IFT between crude oil and microemulsion to mobilise the oil.

(b) low IFT between the microemulsion and drive bank to prevent trapping of the emulsion in small droplets (c.f. the residual oil).

(c) microemulsion mobility must be less than the oil bank mobility

(d) drive bank mobility must be less than the microemulsion mobility

(e) low surfactant retention and adsorption

(f) maintainance of favourable conditions throughout the flood.

(c) and (d) are necessary to prevent the microemulsion channelling or fingering through the oil-water bank and the surfactant drive water through the microemulsion bank.

The general procedure for chemical EOR is illustrated in Fig. 1.8.

Preflush. Often the composition of the brine in a reservoir has an adverse effect on the micellar solution. To correct for this, a low salinity or controlled-tapered salinity water is injected to place a compatible aqueous buffer between the highly saline reservoir brine and the chemicals where the oil bank will be formed. The preflush also removes most of the divalent cations that are in the connate brine. Ca^{2+} and Mg^{2+} react with many sulphonates causing them to precipitate or become inactive. A brine-tolerant system has been designed (21) and Holm and Josendal (22) describe a preflush which reduces adsorption of surfactants and polymers.

Oilbank. This is the residual crude oil bypassed during the preflush stage. If the micellar slug is successful, this oil will be swept and concentrated into a uniform displacement bank.

Surfactant Slug. This is usually a complex solution of surfactant, brine and cosurfactant. The cosurfactant is usually a short-chain polar compound, soluble in oil and water and designed to accelerate the process of emulsification. The surfactant helps to stabilise the emulsion once it has formed. It displaces all the water ahead of it towards the producing well.

Polymer/Water Bank. Surfactant solutions must be displaced themselves by an equally viscous liquid for which the usual choice is an aqueous polymer solution. It serves as a mobility buffer between the surfactant slug and the drive water. The high molecular weight water soluble polymers offer increased resistance to flow

and improves the volumetric sweep efficiency.

Drive Water. Finally as well as to propel the fluids to the production well, the salinity of the injected water following the injected chemicals is gradually increased to the normal concentration of the oilfields.

The term surfactant refers to a class of chemicals able to solvate water and oil equally well. They achieve this by the dual nature of their molecular structure. One end of a typical surfactant molecule consists of a long hydrocarbon chain (hydrophobic), the other end is either ionic or highly polar (hydrophilic). Surfactants are classed as either anionic (negatively charged hydrophile), cationic (positively charged) or nonionic (neutral but polar hydrophile). Amphoteric surfactants containing both positive and negative parts also exist.

The clays that make up part of the oil reservoir consist primarily of calcium, magnesium, iron and aluminiun silicates. The negative charge of these silicates tends to predominate at the surface (see Fig.1.9) resulting in adsorption of positive ions from the surrounding fluid. Thus cationic surfactants are heavily adsorbed with consequent wastage of expensive chemical in solution. Even nonionics incorporate a fractional positive charge. The remaining class the anionics, include the alkali metal salts of carboxylic or sulphonic acids. Of these, sulphonates are favoured for their resistance to precipitation by divalent metallic ions.

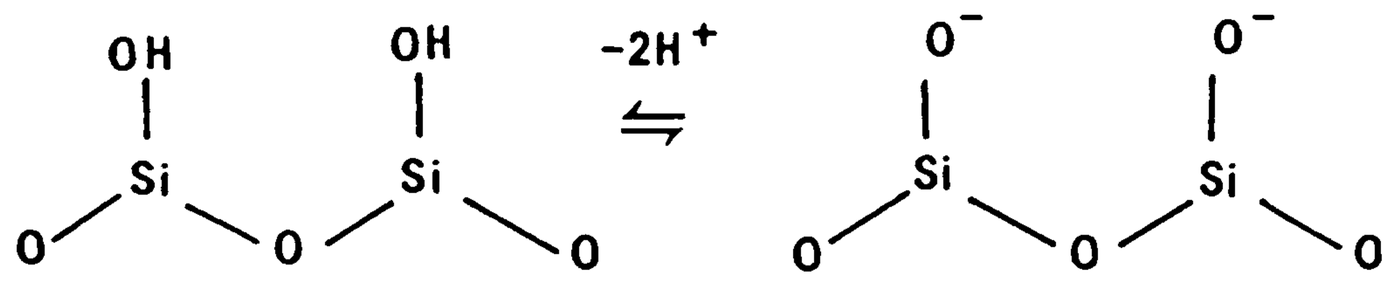

Fig.1.9 The polarity of a silica surface.

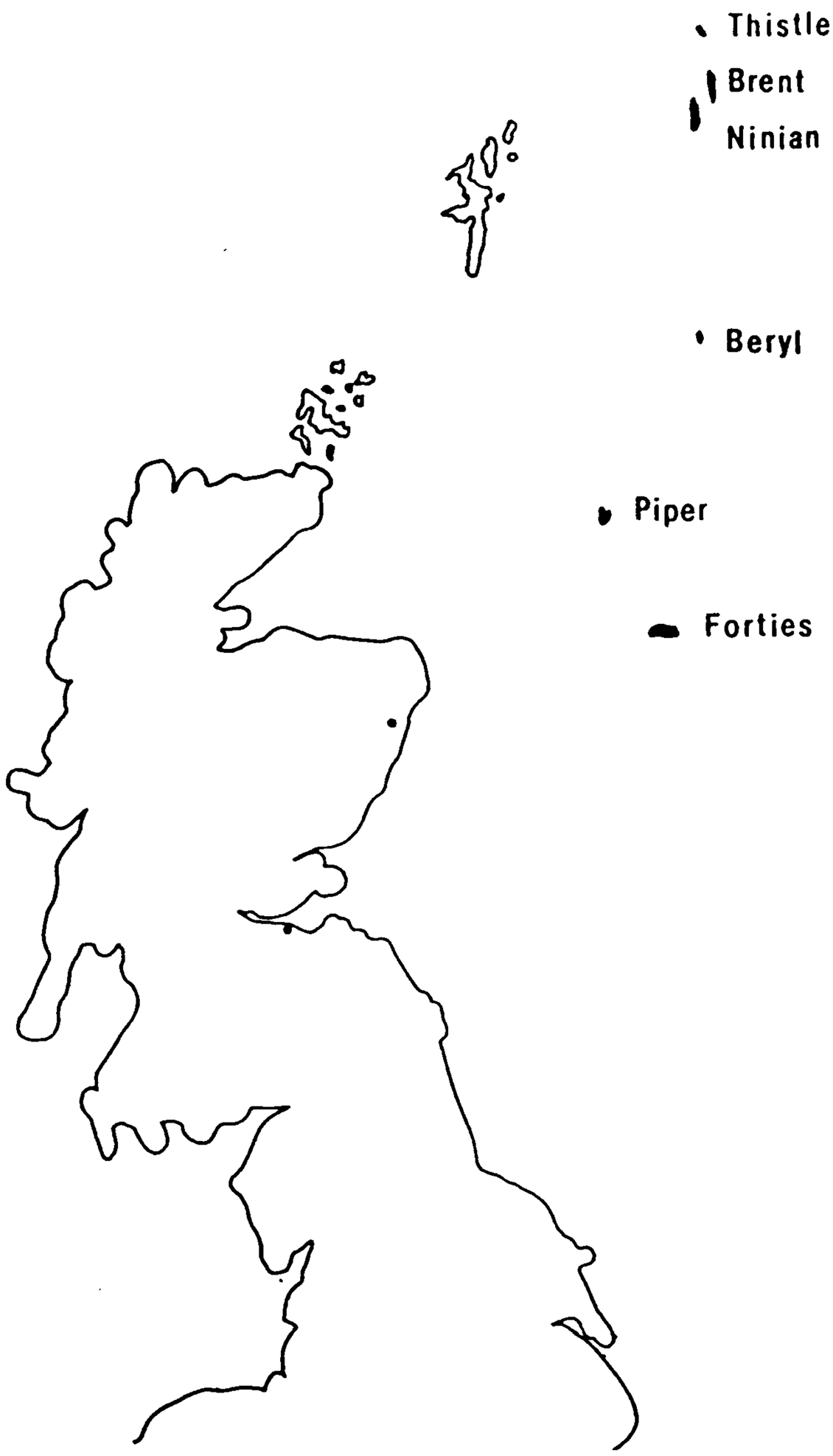

Fig.1.10 Location of six of the major North Sea oil fields.

The objective of a surfactant system is to generate an ultra low interfacial tension at the oil/water interface. To achieve this there must be a certain salt concentration. An oil-in-water emulsion consists of oil globules suspended in water. Such an emulsion is readily formed in water at low salinity in which each globule carries a high surface charge density. In a highly saline brine, a water-in-oil emulsion is formed with the surfactant molecules pointing 'inwards' towards a highly ionic centre within each droplet. At some intermediate (optimal salt concentration) a phase inversion for which oil-in-water and water-in-oil emulsions are equally formed and the IFT has reached a minimum.

Another important feature of micellar flooding is the ability to adjust their viscosities. Economically this is done by altering its' composition (of cosurfactant, cosolvent, electrolyte etc.,) and therefore its' mobility until it is equal to or less than the total mobility of the oil-water bank, which results in increased sweep efficiency. It also reduces water fingering through the chemical slug, diluting and displacing it.

The size of the micellar solution slug is usually designed to be from 5% to 10% of the reservoir pore volume. The lower limit is set to achieve effective recovery and the upper limit is the maximum the economics will allow.

Essentially two different concepts have developed for using surfactants (23).

1) Low Tension Flooding. A solution containing a low concentration of surfactant is injected. Large pore volumes of the solution are injected to reduce the IFT between oil and water. Residual oil will approach zero only after the passage of large volumes of surfactant solution. It tends also to suffer from lack of mobility control. Addition of a polymer improves this even though studies indicate that oil recovery is sustained at a lower level for a longer period but a higher recovery is obtained with a high concentration, microemulsion flooding and a low pore volume system.

2) Microemulsion Flooding. A relatively small pore volume of a higher concentration surfactant solution is injected. The amount of dispersed phase in the microemulsion is high and becomes a surfactant-stabilised dispersion of either water in hydrocarbon or hydrocarbon in water. As the slug moves through the reservoir, it is diluted by the formation of fluids and adsorption to the rock and the process can revert to a low concentration flood.

Micellar flooding is applicable to many reservoirs which have been water-flooded successfully, particularly sandstone formations. It is limited in use in carbonate reservoirs where the brine contains excessive divalent ions which causes high adsorption of the surfactant. The process is best applied to medium gravity crude, the higher viscosity crude would require highly viscous micellar and polymer slugs for a favourable, mobility ratio which would not be economical.

Advantages.

- micellar solution followed by a polymer buffer is an ideal displacing fluid providing a high sweep and displacement efficiency.

- the field operation is only slightly different from a water-flood needing the addition of only mixing and filtering equipment.

- very deep reservoirs pose no problems provided the rock has sufficient permeability.

Disadvantages.

- a large investment in high cost chemicals must be made very early. The income is based on two undefinable parameters: the residual oil saturation in the reservoir and the amount of oil that will be recovered.

- in early surfactant flooding, the adsorption of the surfactant on the rock will reduce the process to a water-flood. This can be overcome by using a specific blend of surfactant, cosurfactant and electrolyte, or a cheap sacrificial chemical which will be preferentially adsorbed.

- when micellar flooding follows a depleted water-flood only water is produced for a period of 6 months-2 years.

b) Polymer Flooding. A polymer operation is similar to a surfactant-polymer flood. Since the polymer phase is used, it is also called a thickened or polymer waterflood. A preflush is often needed since many polymers react with divalent cations. The presence of free oxygen in the mix water is also detrimental as it causes degradation. The molecular weight is reduced and therefore requires an oxygen scavanger.

c) Alkaline Flooding (In-situ). It is possible to 'manufacture' surfactants in-situ by flooding a reservoir with an alkali. The slug interacts chemically with naturally-ocurring surface active acids in the crude oil to produce surfactants at the oil-water interface.

$$RCO_2\text{-}R' + NaOH \Rightarrow R'\text{-}OH + RCO_2Na$$

carboxylic acid — alcohol — soap

This lowers the IFT and an emulsion is formed. The flow properties of this type of emulsion generates a highly non-uniform pressure gradient which is capable of overriding the capillary forces and effectively displaces oil from the pores. Unfortunately, this attractive inexpensive process suffers from the following reactions which can deplete the slug components:

a) divalent cations in the reservoir water causes precipitation of hydroxides and pore plugging. This can be overcome by a good brine preflush and an alkaline slug at high monovalent salinity.

b) Sodium hydroxide combines chemically with silica particularly at high temperature and high pH. Flooding with sodium carbonate can remedy this but in general caustic reacts too slowly with silica in sandstone to cause problems.

Laboratory tests (26) show that caustic flooding does not significantly reduce residual oil saturation in the swept region, but the oil recovery improvement is due to better displacement of the mobile oil. This technique is therefore suited to reservoirs containing high viscosity crudes with naturally occuring surface active organic acids (e.g. naphthenic). Kuuskraa (25) gives a comprehensive review of the significant field tests in the U.S.A. covering

the major enhanced oil recovery techniques.

1.4. Problems of Oil Recovery Techniques.

(i) Environmental.

The use of chemical additives in the oilfields provoked environmental concern. Gas EOR requires the processing of large quantities of chemicals which in many cases are near farming areas. Policies and regulations on standards of air, water and land contamination are more stringent than those used in the case of primary and secondary recovery techniques. Air pollution caused by the concentrated use of thermal methods resulted in restrictions on the allowable amounts of hydrocarbon and oxide of sulphur and nitrogen that could be released. This has had a severe impact on the economics of tertiary/enhanced recovery since treatment or recovery of pollutants is necessary in all cases.

Even the injected chemicals must be considered as potential sources of pollution of fresh-water aquifiers through faults or abandoned wells.

(ii) Economics.

The commercial application of any chemical flooding process depends on an adequate return on investment. Chemical supply and cost are the most critical factors in an economic analysis but also included is the amount of the oil recovered and the time required. It is possible to make reasonable estimates of the volumes and costs of the fluids to be injected. Polymer and steam processes

are the least costly while miscible and surfactant flooding are the most expensive. The resource availability of the injectants, trained manpower, equipment and capital is also critical particularly when considering the inflationary pressures on the price of these goods and services.

Any increase in oil production is not likely to be obtained for several years after implementation of the EOR scheme in conventional reservoirs because of their size.

(iii) Political

Due to the present political climate, price seems to be the most important key to EOR. The crude supply, and therefore the price, can be affected by political developments in the oil exporting nations. Higher recoveries offset, to some extent, the need for higher crude oil prices. Reduced tax concessions also aid the cost of injectants and the risk associated with the (amount of) increase in oil production that will be obtained from the oil process.

The chemical industry can make important contributions to overcoming these concerns. Since the potential chemical market can be large, most of the risk will be borne by the petroleum industry with EOR providing future hydrocarbon feedstock.

Overall, domestic energy policy will set the pace to which EOR must comply in order to compete with other

energy sources.

(iv) Technological

Some outstanding technical problems are:

(i) Operating under conditions of high temperature (up to 423K); high pressure (up to 50MPa); and salinity variation (up to 20% total dissolved solids).

(ii) Reducing loss of materials through adsorption and retention, ageing and shear degradation over the timescale required.

(iii) Understanding the complexities of crude oil displacing fluids, rock geometry and their interactions.

Good candidates for surfactant floding are in largely depleted fields. A large time-lag may lapse to keep the field open to allow for potential development, which still requires research and innovation. Including the time until production actually begins, this could take 15-20 years.

(v) Geological

The risk appears high because of the uncertainties in reservoir characteristics, eg. in defining the geology, estimating the amount of removable oil and uncertainty in predicting reservoir behaviour in terms of production. Adsorption onto rock is a main cause of the failure in usuing surfactants. In addition, surfactant loss can occur also by retention and/or precipitation of the surfactant into the oil phase. Inks and Lahring (26) found that nonionic surfactants tend to adsorb to a lesser extent than the anionic or cationic surfactants.

(vi) Crude Oil

The chemical composition of crude oils is very complex so that a multitude of components has to be considered rather than individual chemical species. The complexity increases when interfacial properties are considered as components present in very low concentration (eg. crude oil surfactants) can dominate these properties. In addition, the composition of oil varies according to its origin (see Table 1.1), hence each reservoir must be considered individually.

(vii) Scale Formation

Scale deposits are inorganic mineral deposits that form due to any changes in thermodynamic equilibrium caused by pressure drops, temperature fluctuations, pH or ionic stength changes. This results in the lowering of the solubility of particular inorganic ions in water. In general, analysis of the reservoir brine will provide a good indication as to what inorganic precipitates to expect in such a scale deposit.

These problems outlined above require an EOR method to be specific - one reservoirs characteristic may vary considerably from that of another, even if in the same field.

Conventional oil recovery is chemically quite complex. A water injection process often necessitates an oxygen scavenger, scale inhibitors, corrosion inhibitors, biocides and filtration equipment. Any EOR technique associated with a waterflood must be compatible within

	Range of Reserves in Tonnes x 10^6
Production to end 1984	825
Remaining reserves in present discoveries	750-1880
Reserves in potential future discoveries	
North Sea	250-875
West of Shetand	25-75
West of Scotland	0-550
Remainder of UK continental shelf	20-485
Total recoverable reserves (UK continental shelf)	1870-4940

TABLE 1.2 Range of Oil Reserves (discovered and undiscovered). (figures from the UK Department of Energy).

	Forties	Brent	Ninian	Piper	Thistle	Beryl
Initial Pressure (MPa)	22	41	45	24	41	34
Mean Porosity (%)	27	23	20	25	25	15
Temperature (K)	363	366	375	353	375	370
Oil Density ($kg.dm^{-3}$)	750	570	790	750	760	690
Oil Viscosity (mPa.s)	0.82	0.28	1.35	0.73	1.05	0.69
Formation salinity (ppm)	102000	26700	21400	75000	25000	89000

TABLE 1.3 Characteristics of Major North Sea Reservoirs.

this range of additives.

1.5 The North Sea

Some 30 oil reservoirs in the North Sea are being developed. The U.K. Department of Energy estimates that the possible reserves for these fields may be as high as 5,000 million tonnes (see Table 1.2). North Sea reservoirs have a number of characteristics that distinguish them from most American land reservoirs. Apart from the obvious difference associated with the operation of deep water platforms in stormy seas, the temperature of the fields are high and contain very saline water (Table 1.3). Fig.1.10 illustates the locations and approximate size of six of the major North Sea fields. These reservoirs are listed in Table 1.3, together with some of their most important characteristics. The production rates of these reservoirs has currently reached a plateau though still increasing slightly. This is due to a flood of oil on the market and coupled with a low oil price; huge exploration projects are uneconomic. Since conventional oil recovery methods leave a considerable amount of crude in the ground, extracting only about a third (primary 10% and secondary a further 20%) there is a huge incentive for further recovery. The various enhanced oil recovery techniques are targeted towards this remaining oil and are relatively new and developing technologies. The widespread success of these remains largely unproven due to uncertainties in determining the oil content of reservoirs and the oil quality. Coupled with the (wide) range of variation in the composition of the crude oil

and the rock formations, EOR presents a major problem to petroleum engineers and scientists more generally. The programme of work described in this thesis was undertaken to ascertain the contribution that surface chemists could make in the area of surfactant application to EOR.

1.6 Aims of the Research Presented

The majority of surfactant floods carried out to date, principally in the U.S.A., have used surfactant microemulsion systems containing petroleum sulphonates and solubilising short chain alcohols. However, such systems were considered not to be so applicable to the North Sea. The petroleum sulphonates are not very soluble in high salinity sea water which is used as the injectant. A micellar slug of such a sulphonate could have potential in the North Sea if coupled with a suitable cosurfactant and cosolvent that aids solubilisation of the oil and stabilises the microemulsion.

Mobil Research and Development Corporation (Dallas, Texas) suggested that the following groups of surfactants offer the greatest promise for EOR under Beryl reservoir conditions.

1. alkyl or alkylaryl polyethoxyalkane sulphonates or alkyl or alkylaryl propoxy-polyethoxyalkane sulphonates as a primary surfactant,

2. a branched chain alkane sulphonate or internal olefin sulphonate stabilised in brine by an alkyl or alkylaryl ether sulphonate,

3. an alkyl xylene or alkyl toluene

sulphonate stabilised in brine by a synthetic alkylaryl ether sulphonate.

This guideline, coupled with the conditions and properties of the Beryl field in the North Sea were the basis for the research to develop a micellar slug capable of enhanced oil recovery.

Chapter 2

2.1. Surfactants.

2.1.1. Introduction

Surfactants are among the most versatile of the products of the chemical industry. They have the property of adsorbing onto the surfaces or interfaces of a system and substantially altering the free energies of the surface or interface. They contain a hydrophobic group, usually a long-chain hydrocarbon and hydrophilic group; depending on the charge of these groups such materials can be classified as anionic, nonionic, cationic and amphoteric.

Anionic surfactants are the most important and most widely used class of surface active agents. The majority of the published literature deals with this category. Anionics are negatively charged organic compounds with bulky hydrophobic groups. The negative charge is carried by, for example, the sulphonic, or carboxylic groups. The most popular anionic surfactants are the alkylbenzenesulphonates, with either linear or branched hydrophobic alkyl chains.

Nonionic surfactants are the second most important class of surfactants. Their molecules do not possess either negative or positive charges. The most important types are reaction products between ethene oxide and various organic compounds, namely fatty alcohols, alkylphenols, fatty acids etc..

The cationic and amphoteric classes of surfactants are not in general as widely used as the anionics and nonionics. Cationic surfactants are organic compounds, having one or more functional groups, that are positively charged in aqueous solutions. This class includes quaternary ammonium salts, alkyl pyridinium salts that possess a positive charge over a wide pH range. Also, amino and amido compounds that can be protonated and behave as cations in solutions with a pH < 7.

Amphoteric surfactants contain acidic and basic functional groups and, depending on pH, may act either as anionic or as cationic surfactants in aqueous solution. Such compounds are alkylbetaines, sulphobetaines and some alkyl aminocarboxylic acids. These last two classes will not be discussed since they were not used for the present enhanced oil recovery study.

The surfactants used in this enhanced oil recovery work were all supplied by Hoechst Chemicals (Frankfurt, West Germany). They are not pure single-component compounds, but contain various amounts of precursors, by-products, catalyst and solvents. Tables 2.1 and 2.2 list these surfactants together with their average ethene oxide chain length and activity. Their structure is assumed to be as shown in Figs 2.1 and 2.2.

Another series of surfactants, the Tritons, (Rohm and Haas, Croydon, England) were also obtained, mainly with a view to studying the properties of surfactants that had been purified (to 99.9% purity); these are listed in

Tri-butylphenol ether Surfactant	Average number of EO. units
Sapogenat	
T040	4
T060	6
T080	8
T100	10
T110	11
T130	13
T150	15
T180	18
T300	30
T500	50
Nonylphenolethoxylate	
Arkopal	
N040	4
N050	5
N060	6
N090	9
N100	10
N110	11
N150	15
N230	23
N300	30

Table 2.1 Nonionic Surfactants.

Tributylphenolether Sulphonate	average number EO units	* % active component
T040S	4	26.0
T060S	6	29.7
T080S	8	30.1
T100S	10	35.0
T150S	15	21.4

TABLE 2.2. Anionic Surfactants.
* Sulphonate activity.

	Triton		Average Number of EO Units
a)	Octylphenol Series	X-114	7- 8
		X-100	9-10
		X-102	12-13
b)	Nonylphenol Series	N-101	9-10
		N-111	11
		N-150	15

TABLE 2.3 Pure Non-ionic Surfactants.

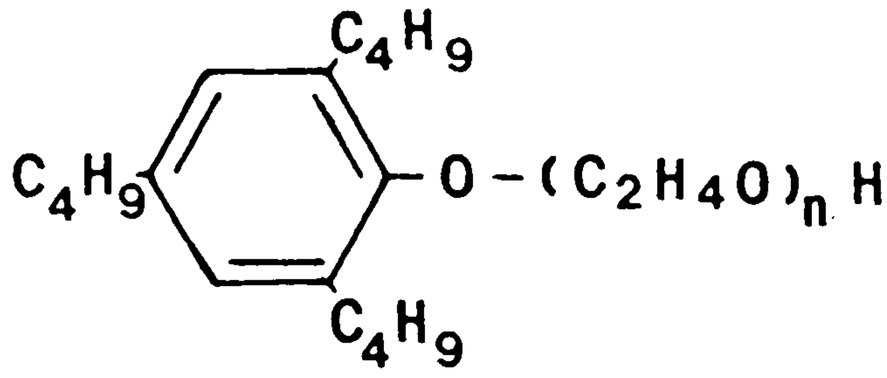

Fig.2.1 Structure of the Sapogenat surfactants.

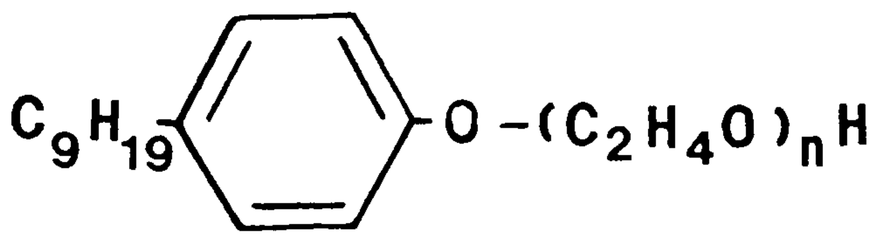

Fig.2.2 Structure of the Arkopal surfactants.

a)

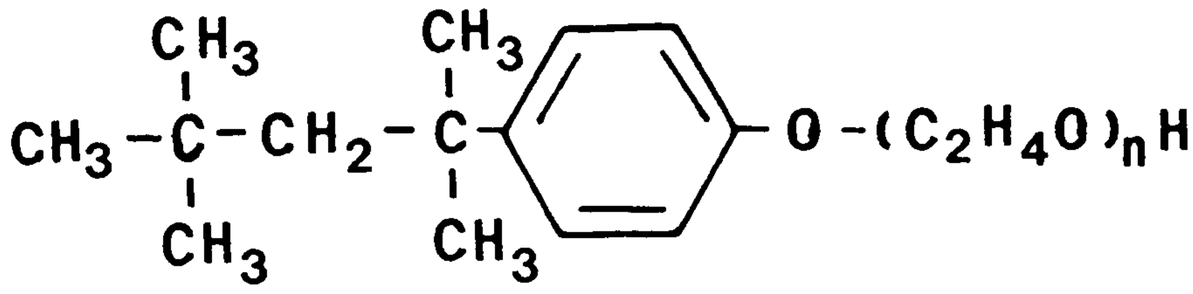

b)

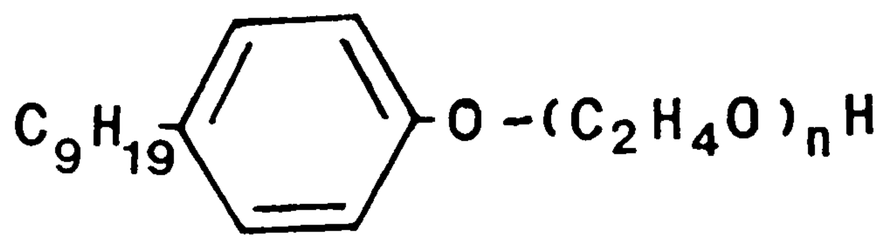

Fig.2.3 Structure of the Triton surfactants: a) octylphenol, b) nonylphenol.

been purified (to 99.9% purity); these are listed in Table 2.3, and have the structures shown in Fig. 2.3.

Most surfactant-based enhanced oil recovery processes involve the use of "natural petroleum" sulphonates as the primary component; these are defined as those produced by sulphonation of crude oil or crude distillates and are thus quite different from their synthetic counterparts. In general, they are more complex than the synthetics since the natural materials contain condensed rings that allow multiple-sulphonation to occur.

The precursors of the Hoechst surfactants were also obtained and were used to determine the extent of the impurities (e.g. iso-nonyl phenol, di-iso-nonyl phenol and tributyl phenol).

Two other surfactants from Hoechst, not belonging to the above classes, were also studied. They are B712 and SAS 60. Their composition in terms of chain lengths is given in Table 2.4.

2.1.2. Properties of Surfactants

(i) Micellisation

Micelle formation, or micellisation, is an important phenomenon since a vast array of properties depends on the existence of micelles in solution; these include detergency, solubilisation, interfacial and surface tension reduction.

Surfactant	C_{13}	C_{14}	C_{15}	C_{16}	C_{17}	C_{18}
SAS60	3	25	30	25	15	2
B712				~30	~45	~23

TABLE 2.4 % Chain Length Variation for the Secondary Alkanes Sulphonates.

At low concentration, surfactant molecules exist as monomers in aqueous solution. If the concentration is increased, a value called the critical micelle concentration (cmc), is reached where any further increase in surfactant concentration causes no increase in monomer concentration. At this point then, micelles are formed in equilibrium with monomer (see Fig. 2.4). For simplicity, the micelles are considered to be roughly spherical in the absence of any additives that are solubilised by the micelle. Fig. 2.5a illustrates the micelles of a nonionic surfactant. The interior region contains the hydrophobic groups surrounded by an outer region containing the hydrated hydrophilic groups and bound water. The radius of the micelle is approximately equal to the length of the fully extended hydrophobic group (29). For these nonionics, the outer region contains coils of hydrated ethene oxide chains.

In ionic micelles (Fig. 2.5b) the interior is surrounded by a region that contains the ionic head groups. This charge is balanced by counterions in the aqueous phase.

In a hydrocarbon medium, the structure of the micelle is similar but <u>reversed</u> with the inner region containing hydrophilic heads surrounded by an outer region comprising of hydrophobic and hydrocarbon groups. The hydrophilic heads in the core are held together by dipole-dipole interactions.

For a long time, it was understood that the polar heads dissolved in water, whereas the hydrocarbon tails

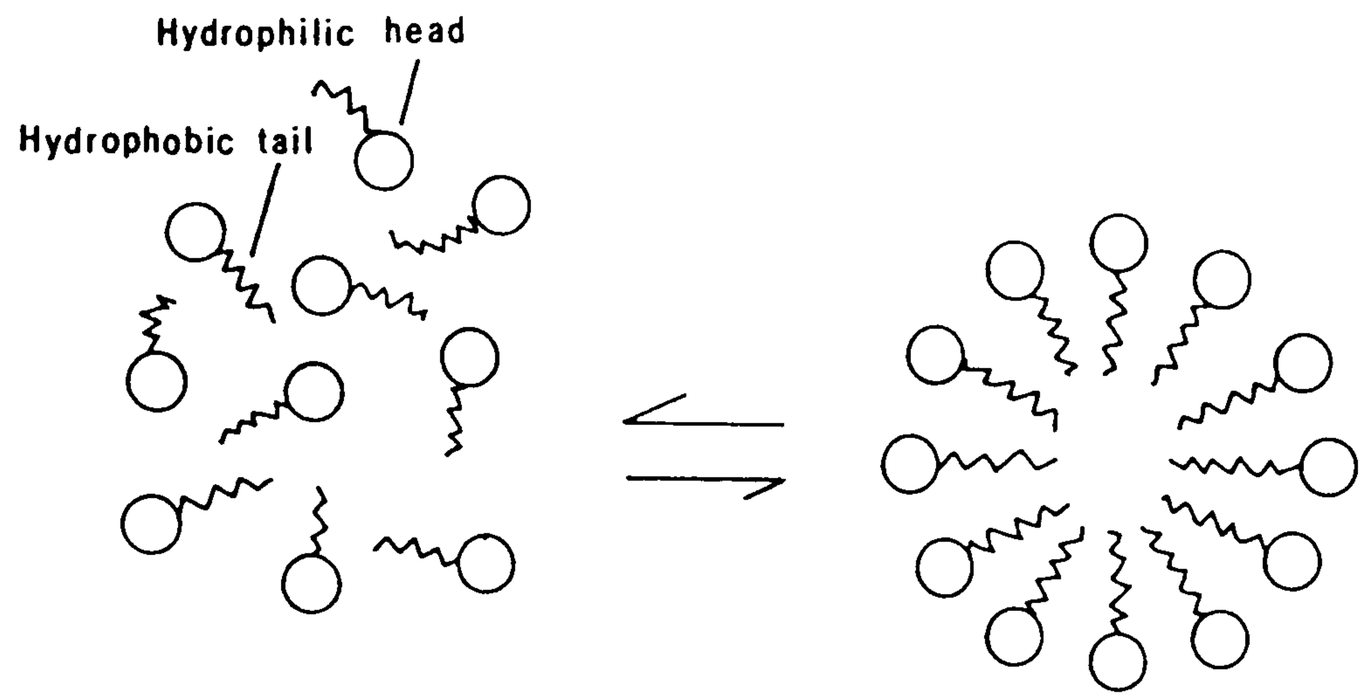

Fig.2.4 Micelles in equilibrium with monomer.

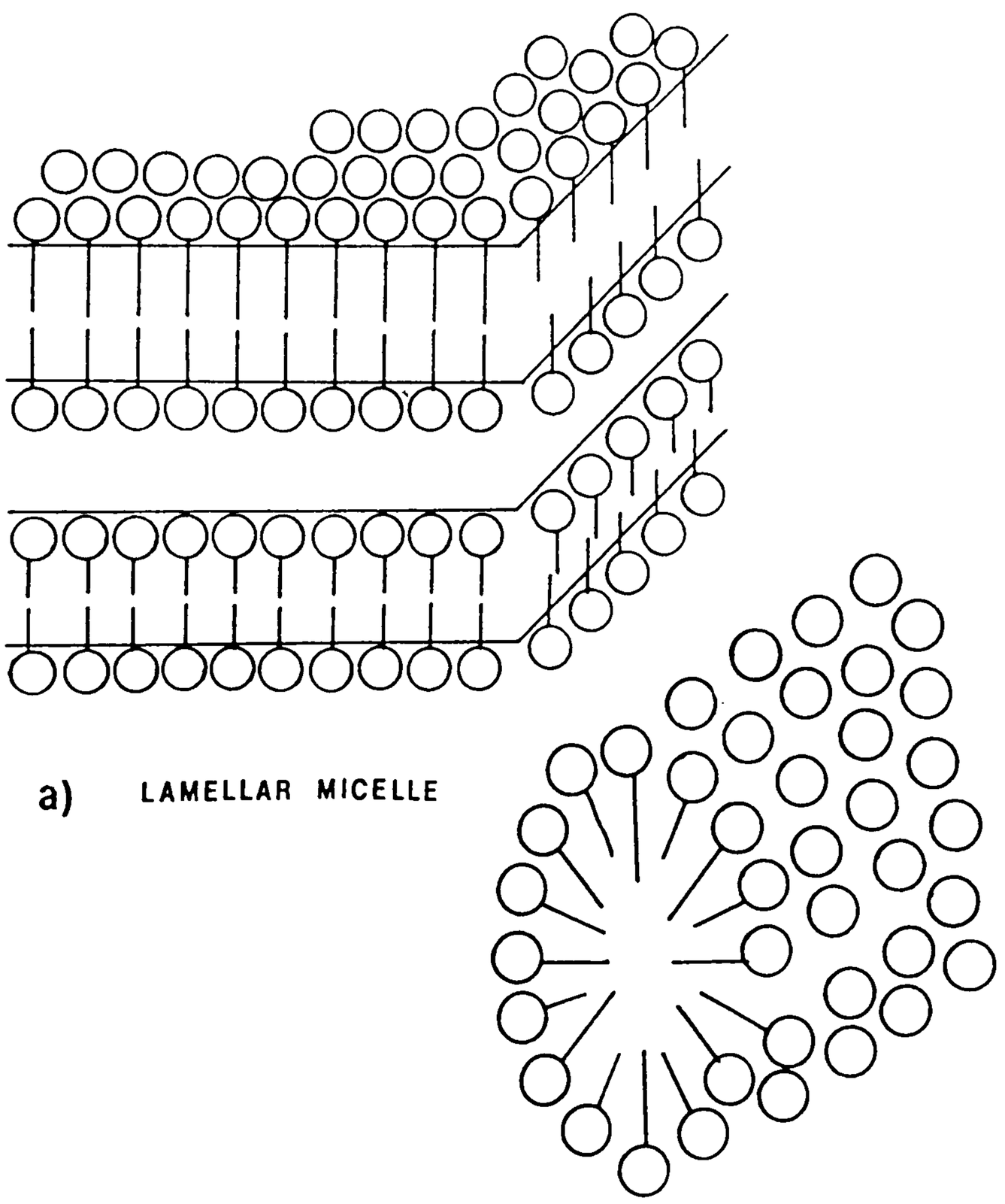

Fig.2.5 Shapes of micelles.

according to Langmuir's principle of differential solubility (30). This view has recently been challenged. Spectroscopic data (31, 32) and neutron scattering experiments (33) now indicate significant penetration of water into the cores of micelles.

Changes in temperature, concentration of surfactant, and the presence of ions in the liquid phase may all cause a change in the size, shape and aggregation number of the micelle.

In concentrated solutions (e.g. ten times the cmc), the micelles are generally non-spherical; in some cases the surfactants are believed to form lamellar micelles, Fig. 2.5a, or cylindrical micelles, Fig. 2.5b. These ordered arrangements of extended micellar structures are called liquid crystalline phases (34) and they may become very pronounced in the presence of certain additives.

At the cmc., changes occur in almost every measurable physical property that depends on the size or number of particles in solution. The determination of the cmc. for any type of surfactant (nonionic, anionic, cationic, amphoteric) can be made by studying the properties such as surface or interfacial tension and conductivity (35) as a function of surfactant concentration (See Fig. 2.6).

(ii) Micellar Aggregation Numbers

These are generally determined by light scattering (36), although they can also be obtained from sedimentation rates in an ultracentrifuge (37). Generally, the greater

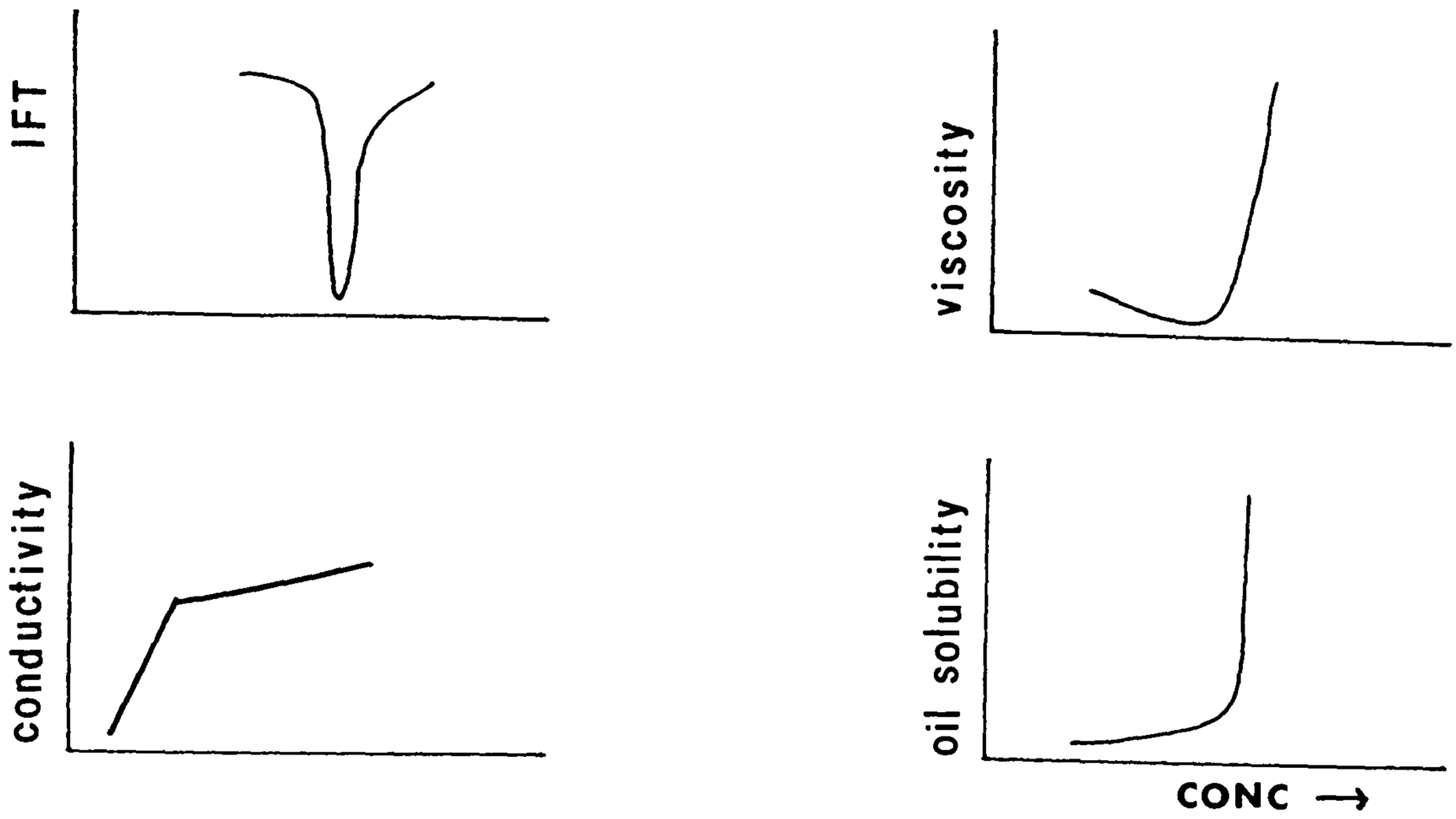

Fig.2.6 Physical property changes at the cmc.

the dissimilarity between surfactant and solvent, the greater the aggregation number. Thus, in aqueous solution, the aggregation number increases with an increase in hydrophobicity of the surfactant (i.e. an increase in the alkyl chain length), and therefore a decrease in the length of the ethene oxide chain.

(iii) Factors Affecting the CMC.

(a) The Hydrophobic Group

In aqueous medium, the cmc decreases as the length of the hydrophobic group increases. For nonionics, the decrease is greater than for anionics. Branching on the hydrophobic group also decreases the cmc (but if C=C's are present, the cmc is generally higher). The decrease becomes less marked as the chain lengthens and there is a limiting value (about 18 carbons) above which the cmc remains unchanged due to the oiling of the chains.

(b) Hydrophilic Group

In aqueous medium, ionic surfactants have a much higher cmc, than nonionics containing equivalent hydrophobic group. Surfactants containing more than one hydrophilic group in the molecule show larger cmc's than those with one and an equivalent hydrophobic group.

For the ethene oxide-based nonionics, the cmc decreases with a decrease in the chain length since this imparts hydrophobicity to the surfactant.

Most commercial ethene oxide nonionics are mixtures

containing hydrophilic chains of different lengths, and their cmc's are slightly lower than those of the single species. It has been suggested that this is due to the components with low EO content (in the mixture) which reduces the cmc more than it is raised by those with high EO content.

The cmc in aqueous solution also reflects the extent of binding of the counterion. The strength of the bond increases with increasing polarisability of the molecule.

(c) Electrolytes

In aqueous solution, the presence of an electrolyte decreases the cmc, the effect being more pronounced for anionics than nonionics. In the former, the depression is due to a reduction in the repulsion between the ionic head groups in the micelle. For nonionics, the effect has been attributed to the electrolyte salting out the hydrophilic groups.

The effects of the anion and cation in the electrolyte are additive and appear to depend on the radius of the ion. The smaller the hydrated radius, the greater the effect.

d) Organic Additives

Small amounts of organic materials may alter the cmc Most of these materials are probably present as impurities or by-products from manufacture. Polar organic compounds reduce the cmc; particularly shorter chain molecules which are incorporated into the micelle.

The larger chains are probably adsorbed mainly in the outer portion of the core, between the surfactant molecules. The work required for micellisation is decreased and, in the case of ionics, the repulsion between the charged heads is reduced. The depression of the cmc is greater for straight chain compounds than for branched and increases with chain length.

e) Temperature

The effect of temperature on the cmc is complex. The value appears first to decrease to a minimum and then increase as the temperature is raised. A temperature increase causes decreased hydration of the hydrophilic group which favours micellisation. However, it can also cause disruption of the water surrounding the hydrophobic group, an effect that disfavours micellisation. The resultant effect of these opposing forces determines whether the cmc decreases or increases over a particular temperature range. Paradies (38) studied a nonionic surfactant, Triton X100, using X-ray scattering. Much data on the shape and size of the micelle was obtained with various temperatures.

2.1.3 Synthesis of the Surfactants

An early paper discussing the preparation of the polyethene oxide derivatives is given by Miller et al. (39); this also reviews the literature prior to 1950. They are usually prepared by addition of ethene oxide to compounds containing active hydrogen atoms such as alkyl/alkyl phenols

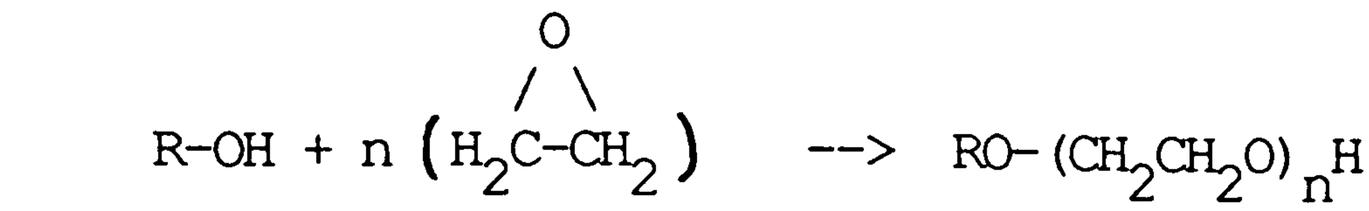

The product is a mixture of a variety of components. In most cases, the product specifications are related to the acid value, pH, hydroxyl number etc. - properties which are indicative of the average composition but not the individual components.

(i) Nonionic Surfactants

a) Sapogenat

Hoechst prepare the tri-butylphenol ethoxylates via the Friedal-Craft reaction. Using aluminium chloride as the catalyst, the phenol is alkylated in the ortho and para positions. This intermediate is then ethoxylated using potassium tertiary butoxide.

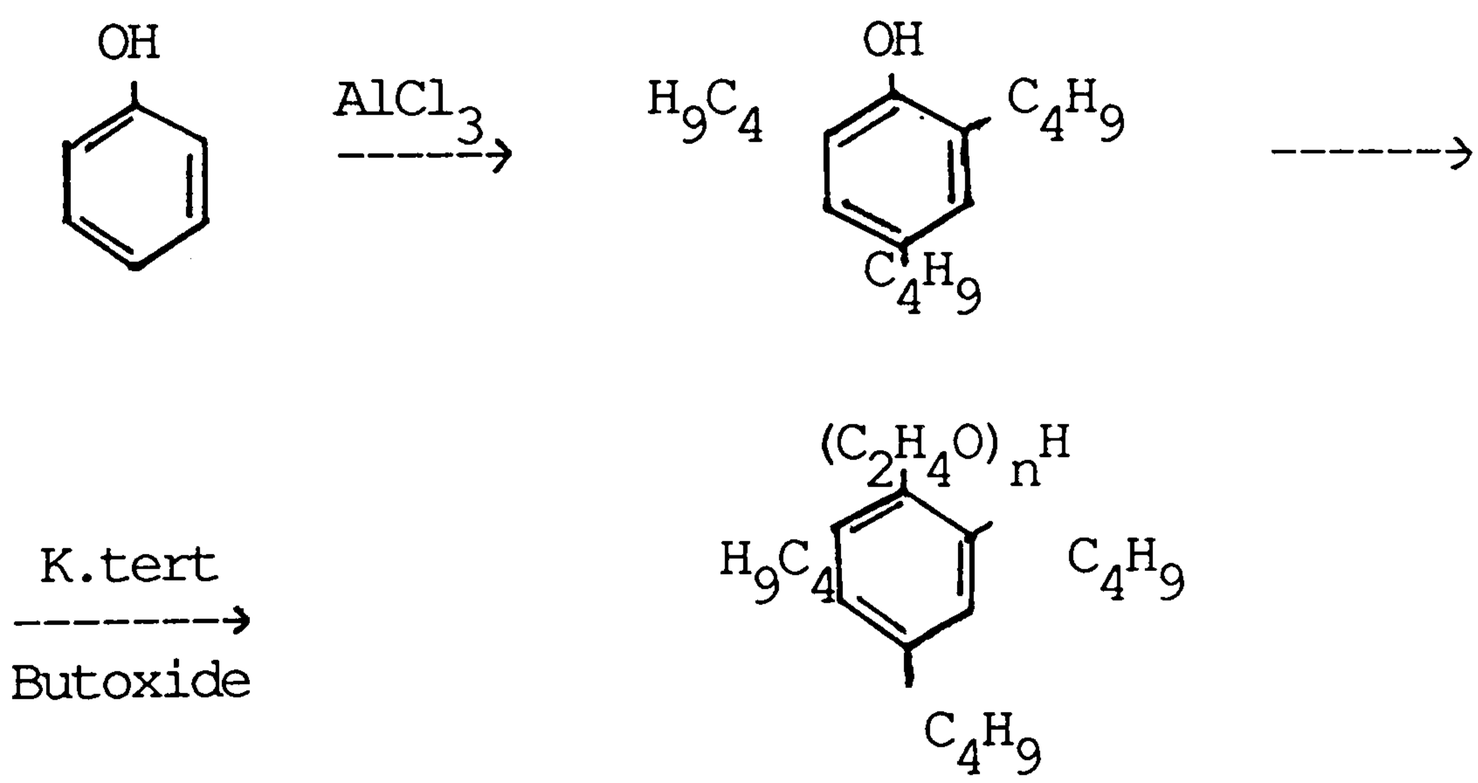

The number of ethene oxide units is controlled by the relative weights of the reactants and also by the duration of the reaction. The purity of the final product depends largely upon the purity of the precursors. It is assumed that the substituents on the ring are tri-tertiary butyl groups.

b) Arkopal.

The Hoechst preparation begins with the alkylation of phenol using Friedal-Crafts reaction as with the Sapogenats. The alkyl group is a C_8 fraction from a hydrocarbon cracking procedure. It is assumed to be mainly linear but may possess branching and double bonds.

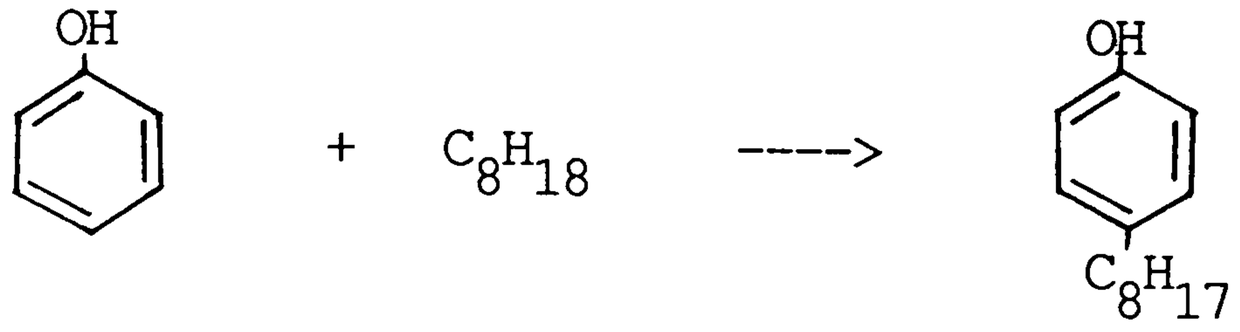

The product is 90% para substituted, which is then ethoxylated in an identical manner to the Sapogenats.

(ii) Anionic Surfactants.

a) Commercial Methods.

Reagents used for the preparation of sulphonates vary according to the components to be treated, Hoechst generally use the following reactions which avoid using oleum since it is difficult to handle although it produces the sulphonates.

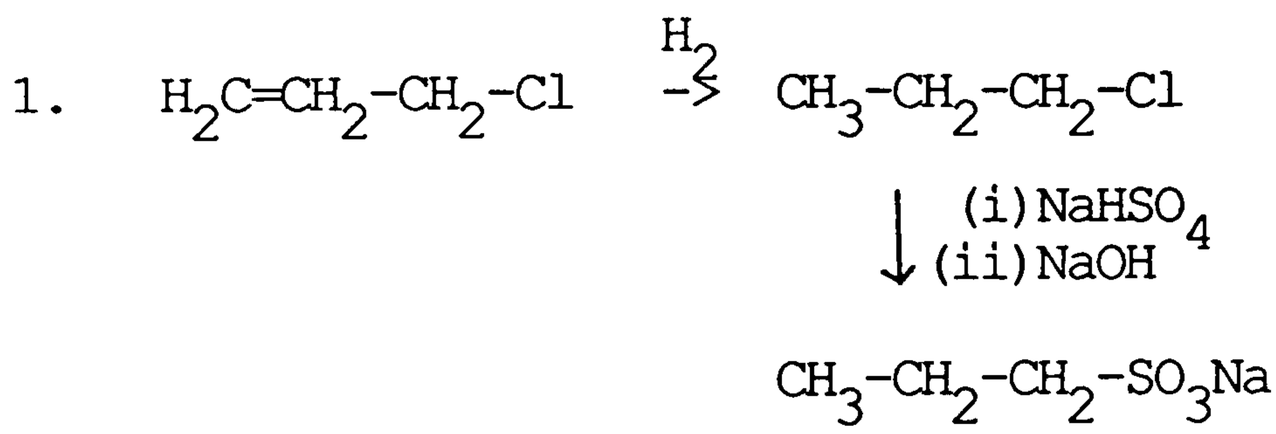

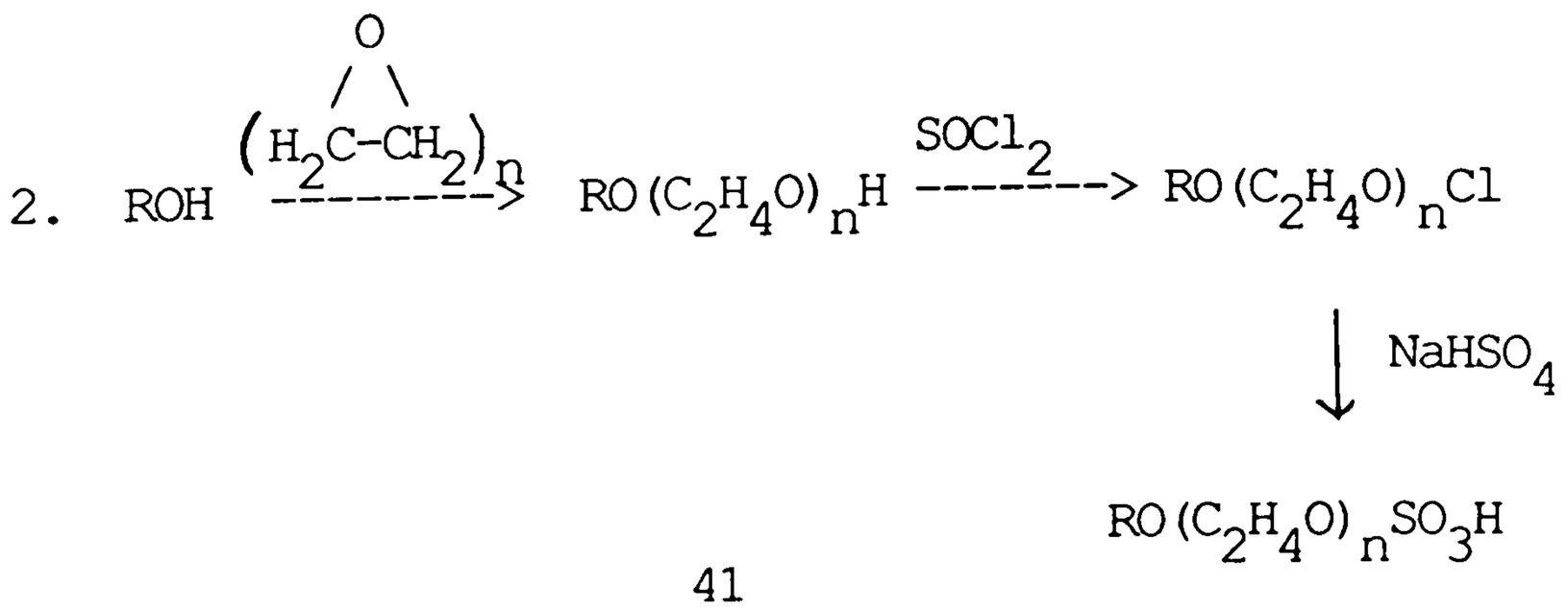

There are numerous other methods of which a few should now be discussed. Alkyl groups are theoretically most efficiently sulphonated by reacting with SO_3 in a dry atmosphere (40):

$$R\text{-}H + SO_3 \longrightarrow R\text{-}SO_3H$$

Sulphuric acid and oleum dissolved in 100% H_2SO_4 have been widely used for direct sulphonation (41):

$$R\text{-}H + H_2SO_4 \longleftrightarrow R\text{-}SO_2OH + H_2O$$

The Strecker reaction has also been used industrially in the preparation of surfactants in Triton series (42).

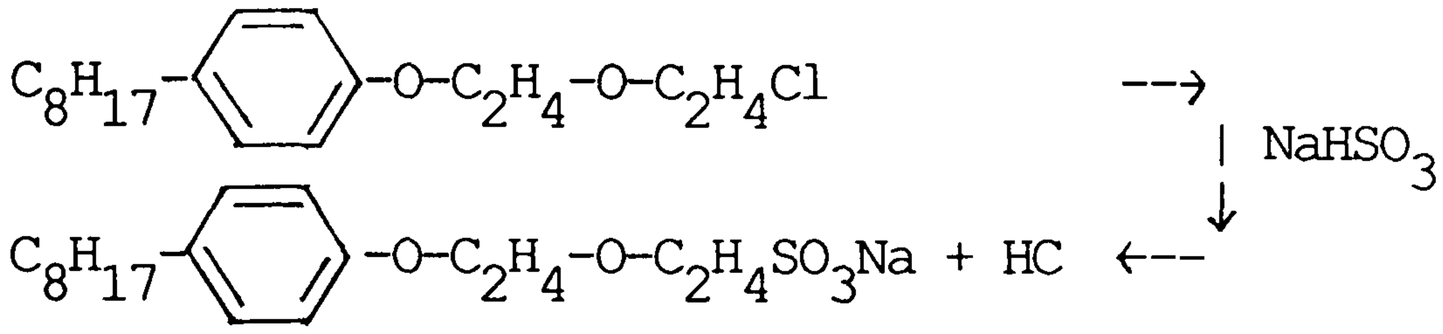

(b) Brunel Method

Two of the Sapogenat series (T180 and T300) were sulphonated at Brunel University. A material was produced that on separation and purification appeared to be of good clarity and reasonably pure. The yields however were low (26% and 32% wt) and also does not mean that the products were pure sulphonates.

The T180 and T300 nonionic surfactant was treated with concentrated H_2SO_4 and after 1h neutralised with a 20% NaOH solution until neutral (i.e. pH 7). The product was filtered, evaporated, washed with methanol and a light-

brown syrupy liquid (referred to in later chapters as T180s) or a cream waxy-solid (referred to as T300) remained.

Aromatic sulphonation is promoted by ortho and para directing substituents, here the tributyl groups. Increasing the size of these groups reduces the reaction rate due to steric hinderance(43). It is possible that some sulphate was formed simultaneously, though, this can be restricted by bulky ring substituents. Although the alkane sulphates are similar in structure to the alkane sulphonates, they are considerably more resistant to hydrolysis than the sulphonates. This is because the latter possess a rather unstable C-O-S bond.

Whichever of the above methods of synthesis and purification are adopted, it is virtually impossible to produce a pure sulphonated compound. The products are therefore mixtures with respect to the length of the polyetheneoxide chain and to sulphonate/sulphate components. The EO chain length follows a Poisson distribution (44). Methods have been reported for the determination of the general shape of these distribution curves by foaming properties (45) circular-thin-layer chromatography (46). Analysis of these surfactants including the non-ionics will be dealt with in detail in Chapter 3.

2.2. Absorbent Solids.

2.2.1. Sandstone.

Two different types of sandstone were supplied by Mobil North Sea Ltd. The Mobil Sandstone was obtained from the Beryl B Reservoir and the Berea sandstone, which is very similar to Beryl core rock, was drilled from an outcrop in Scotland. The composition of the rock is as follows:-

Mineral.	Formula.	Weight (%).
Quartz	SiO_2	87.2
Kaolinite	$Al_4Si_4O_{10}(OH)_8$	7.0
Illite	$K_{1-1.5}Al_4Si_{6.5-7}Al_{1-1.5}O_{20}(OH)_4$	2.4
Feldspar	WZ_4O_8 (W=Na,K,Ca,Ba: Z=Si,Al)	1.8
Dolomite	$CaMg(CO_3)_2$	1.6

The physical properties are:-

Density	Mobil sandstone	$2.21 g.cm^{-3}$
	Berea	$2.40 g.cm^{-3}$
Surface Area	Mobil	$0.285 m^2.g^{-1}$
	Berea	$0.513 m^2.g^{-1}$
Pore Volume	Mobil	$263 mm^3.g^{-1}$
	Berea	$119 mm^3.g^{-1}$

The rock was cleaned by refluxing with xylene and then ethanol prior to analysis and experimentation.

The most common method of measuring pore size distribution is through mercury porosimetry. The pressure necessary to insert mercury into a given pore to which mercury has access to is controlled by the size of the pore throat.

Both the above surface area and porosity results were obtained by this method using a Carlo-Erba 2000 Porosimeter. Although the two sandstones were assumed to be similar, the Mobil rock is approximately twice as porous as the Berea.

In practice, for the adsorption tests in particular, the Mobil sandstone was used in a powdered form. The rock was crushed and sieved through a 300um mesh.

The crushed form and the original Mobil rock were analysed by the BET (47) method (in a Sorptomatic 1800 instrument) for surface area:-

Solid chip Rock	~1$m^2.g^{-1}$
Crushed Rock	~2$m^2.g^{-1}$

The surface area deduced for the solid rock is quite different from the mercury porosimetry value. The surface area that is accessible to the gas used in the BET determination is not equivalent but higher than that available for mercury. So the former will give a higher value. Similarly, in a porous solid, the area available to a large surfactant molecule is likely to be much less than that available to a small gas molecule. Therefore, the surface areas should only be used as a rough guide as to the quantity a surfactant may adsorb.

Elemental Analysis

The Mobil and berea sandstones were studied using Scanning Electron Microscopy (SEM). The instrument used was a Cambridge Stereoscan 250 Mk 2 with a primary

electron voltage of 20kV and a beam tilt of 35°. Since the samples are non-conducting, they were coated with gold to produce a conducting surface. A beam of high energy electrons striking a non-conducting surface would otherwise only charge the sample and no image would be seen.

Electron micrographs of the sandstones are shown in Figs.2.7.(a-g).

The micrographs a) to e) are of the Mobil sandstone as a solid chip. From a), the structure appears to be not compact but fairly granular and quite homogenous. Many pores are clearly visible but it is difficult to give a range of pore diameter sizes.

At a higher magnification (micrograph b)) the structure takes on a layered appearance which is likely to provide more access to pore entrances. Overall, the rock still appears fairly homogeneous with some clearly defined straight edges.

Increasing the magnification further (c), it can be seen that the solid structure has fractured, probably when the chip was cleaved from the sandstone block. There is less homogeneity but the pore openings are clear to see. Using the scales of all the micrographs the pore diameters are in the range ~3-6μm.

Fig.2.7d) is a sample of the crushed and sieved Mobil sandstone. The structure is very homogeneous and is very

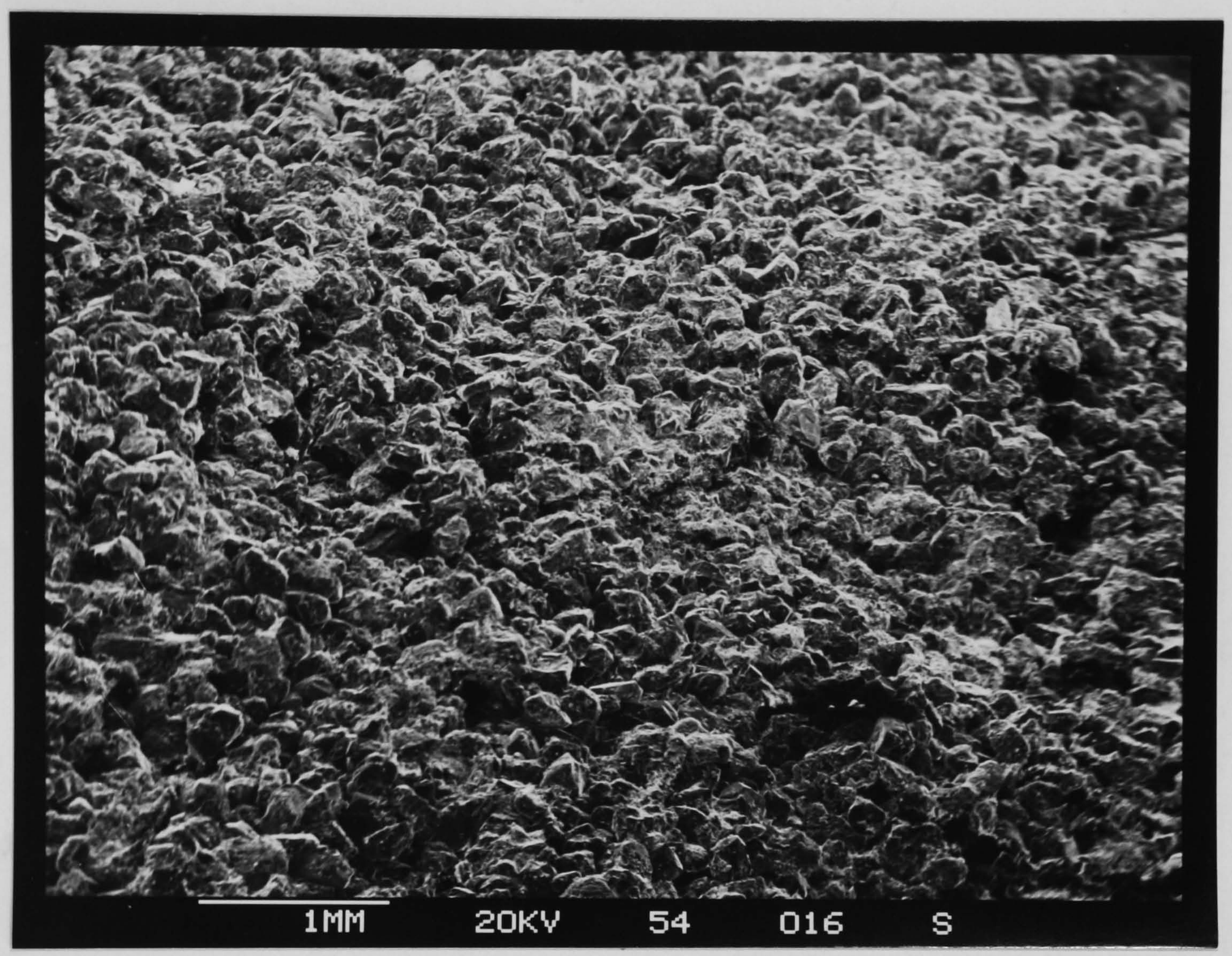

Fig.2.7a General view of Mobil sandstone.

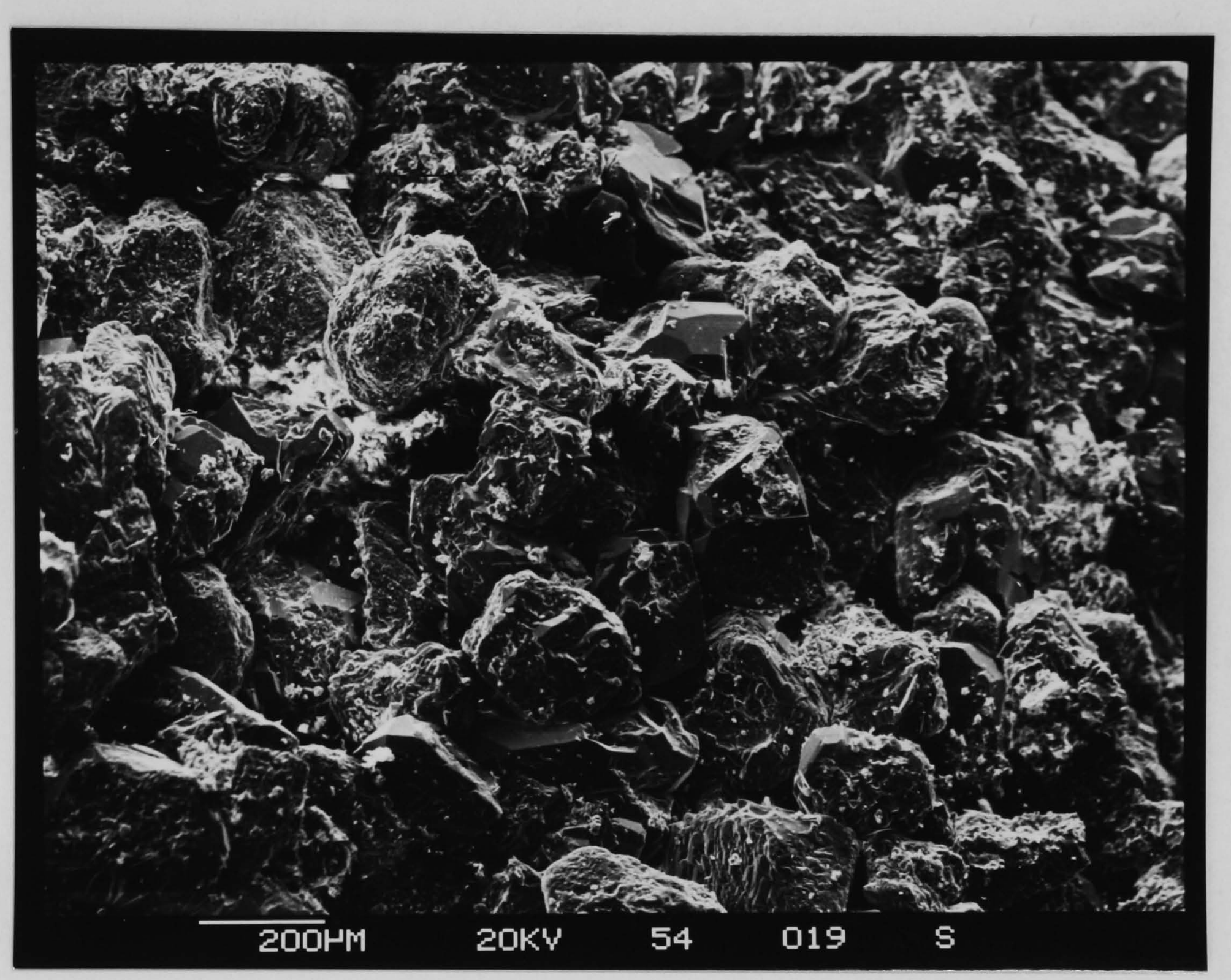

Fig.2.7b Enlargement of Fig.2.7a.

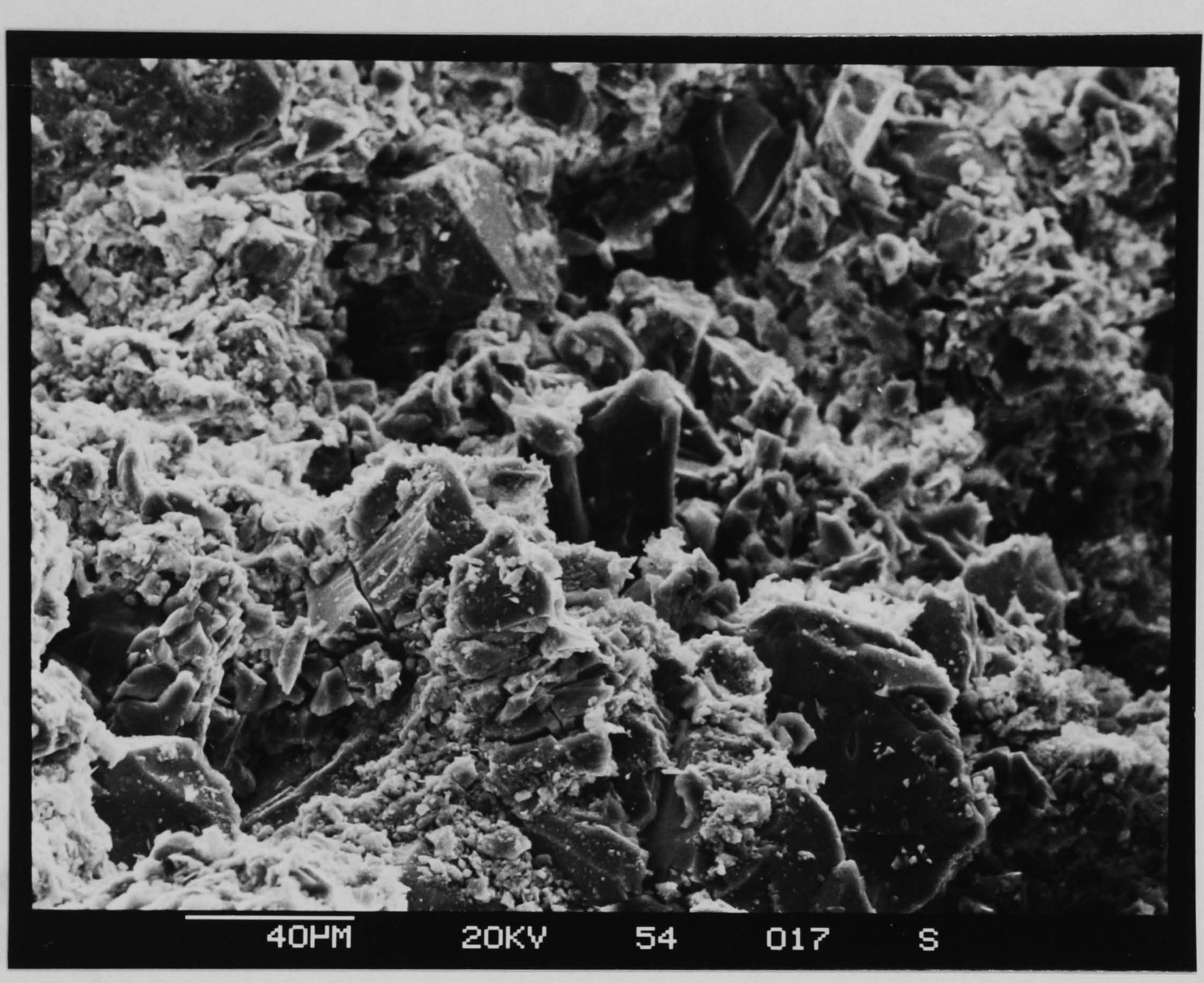

Fig.2.7c Enlargement of Fig.2.7b showing fracturing.

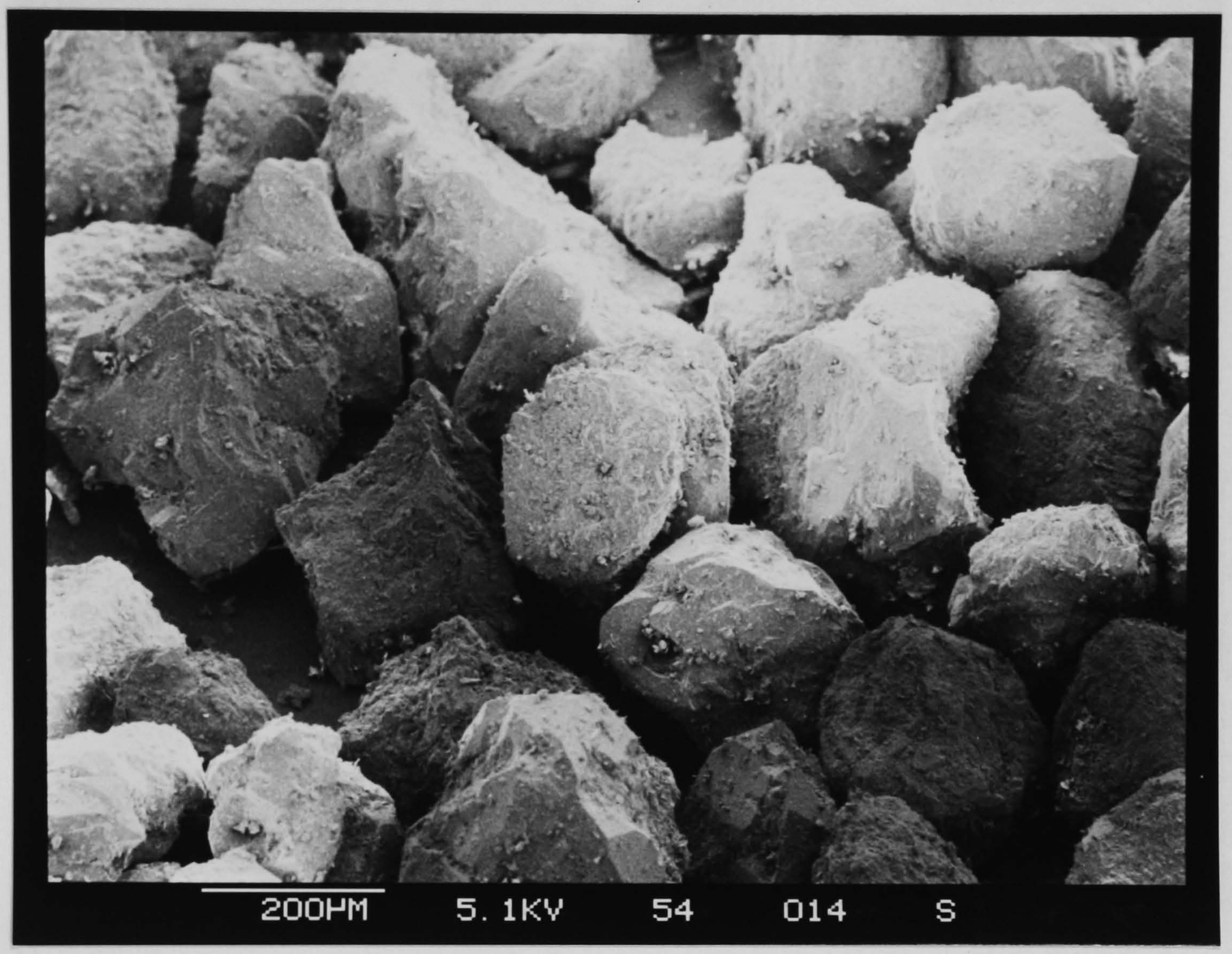

Fig.2.7d Powdered Mobil sandstone.

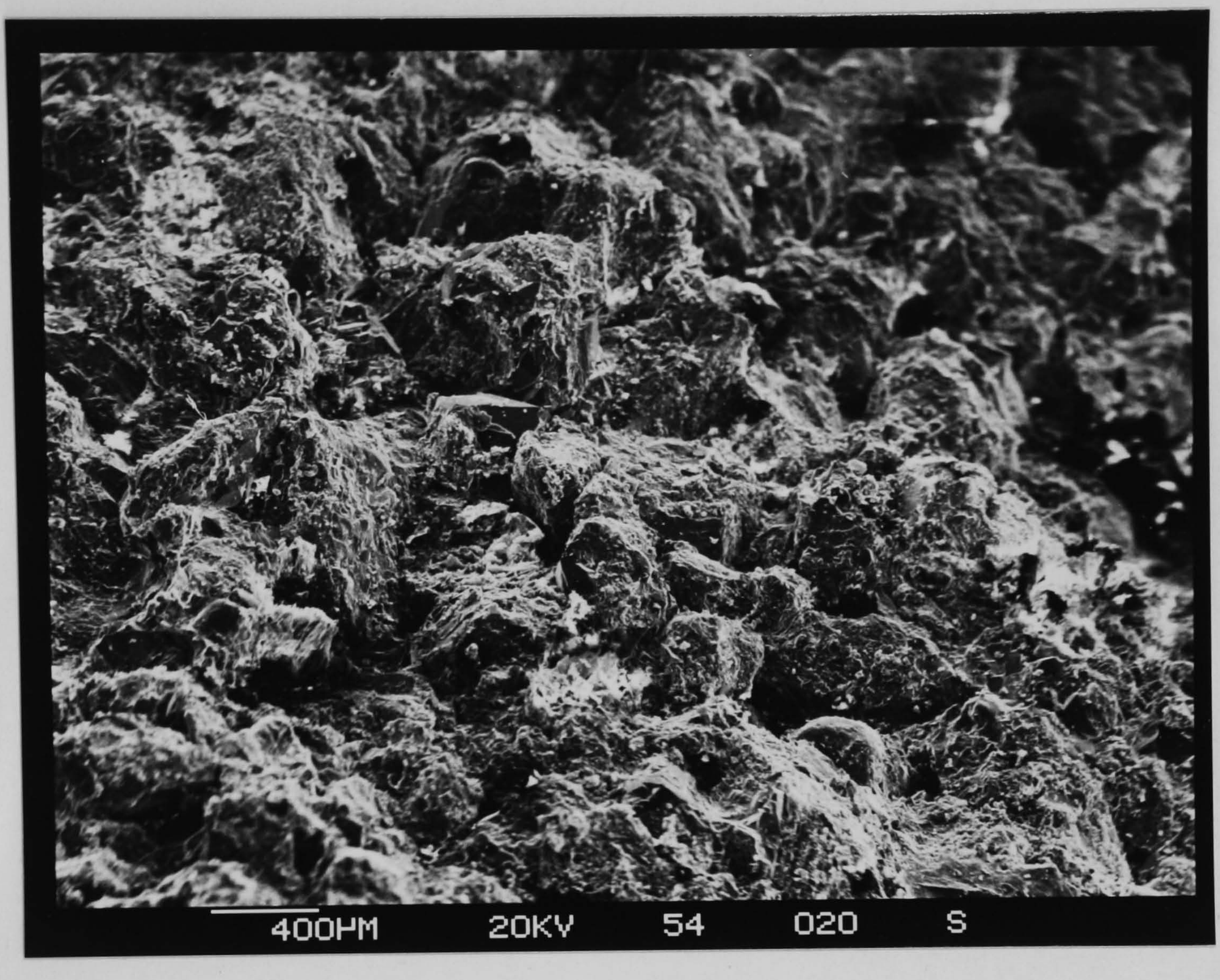

Fig.2.7e General view of Berea sandstone.

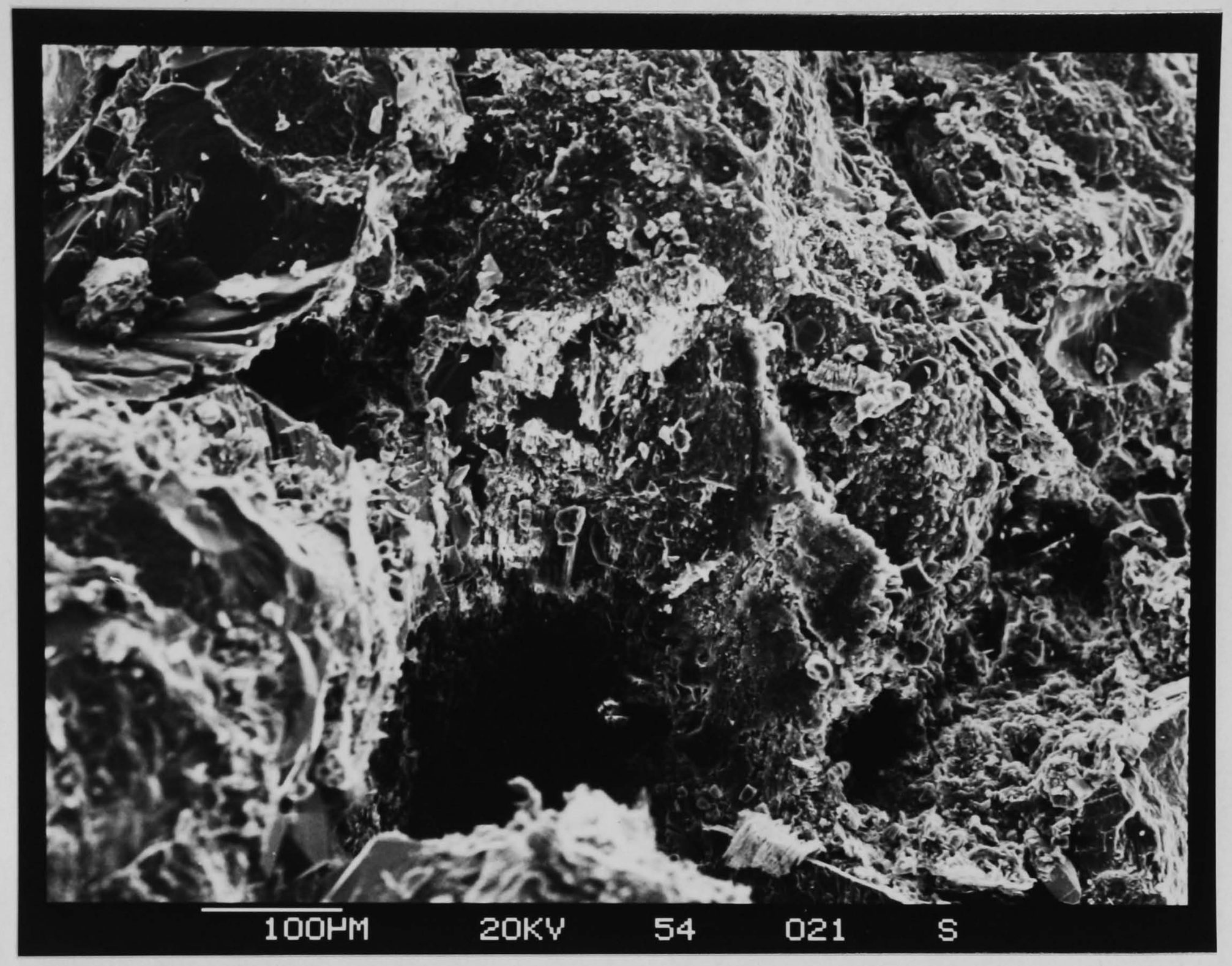

Fig.2.7f Enlargement of Fig.2.7e

different to the same magnification of solid rock as seen in Fig. 2.7c). The diameter of the particles ranges from 200-320um.

Figs. 2.7e) and f) are of the Berea outcrop taken from the Scottish coast approximately 160-240km from the Beryl oil field. Micrograph f) shows a general view of the surface which is strikingly different to the Mobil sandstone. The pores are clearly visible and are of a similar size, but the rock appears sintered and not granular. This could be due to the rock having been subjected to extreme heat and temperature at some time.

Microprobe analysis (Fig. 2.8) shows the following elements to be present with their percentage composition in brackets.

Mobil Sandstone: Mg(4.2); Al(7.7); Si(56.5); K(14.0); Ca(6.1); Ti(5.4); Fe(5.8).

Berea Sandstone: Mg(2.3); Al(8.2); Si(47); S(6.1); K(10.6); Ca(17.0); Fe(8.8).

By far the most abundant element is silicon, but this analysis shows less than previously thought. The elements common to both sandstones are present in similar proportions, although Berea contains three times more calcium than Mobil rock.

b) Idealised Oxides

In addition to the two reservoir sandstones, silica spheres and powdered alumina were used to provide ideal

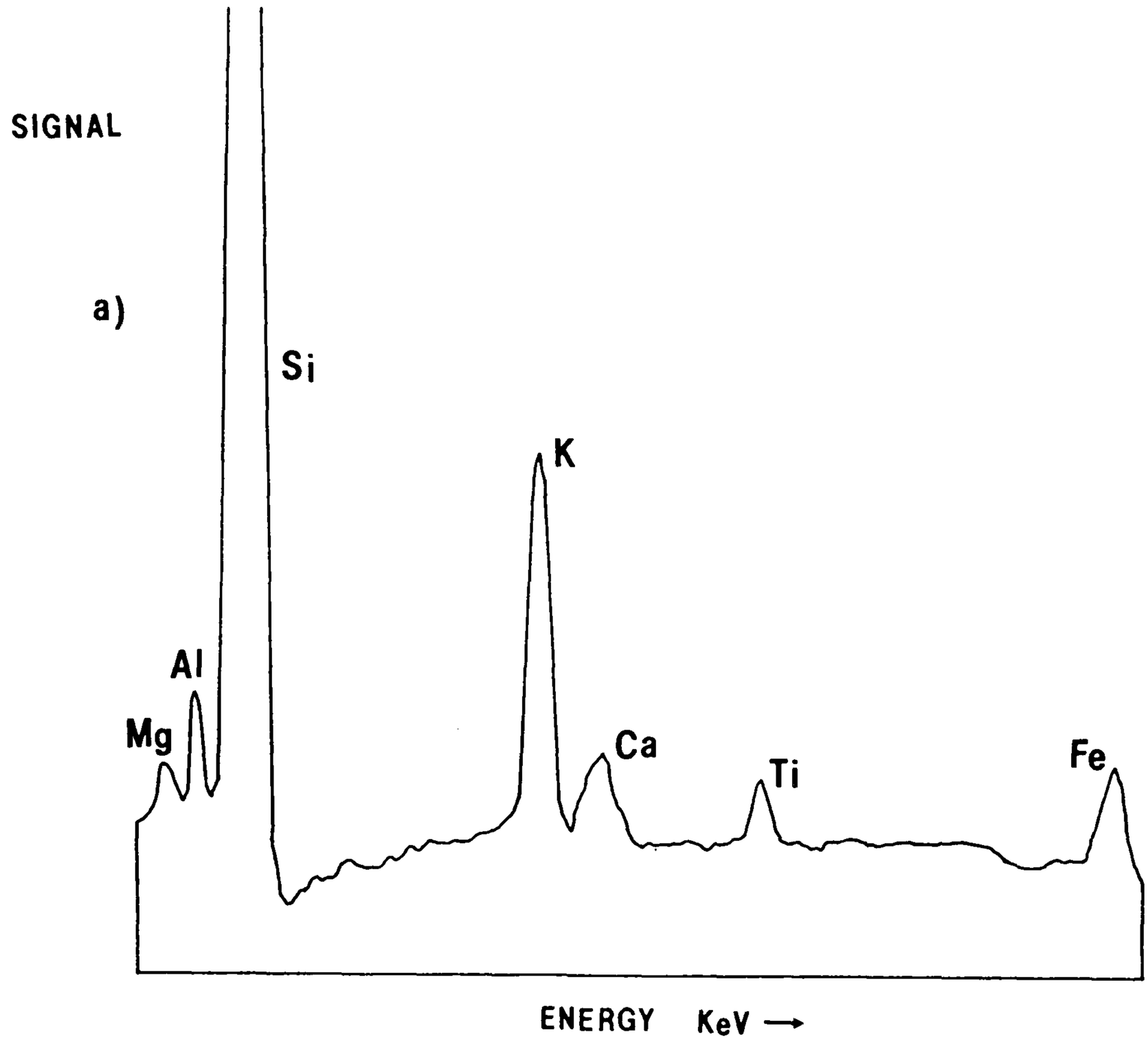

Fig.2.8 a) Elemental analysis of Mobil sandstone.

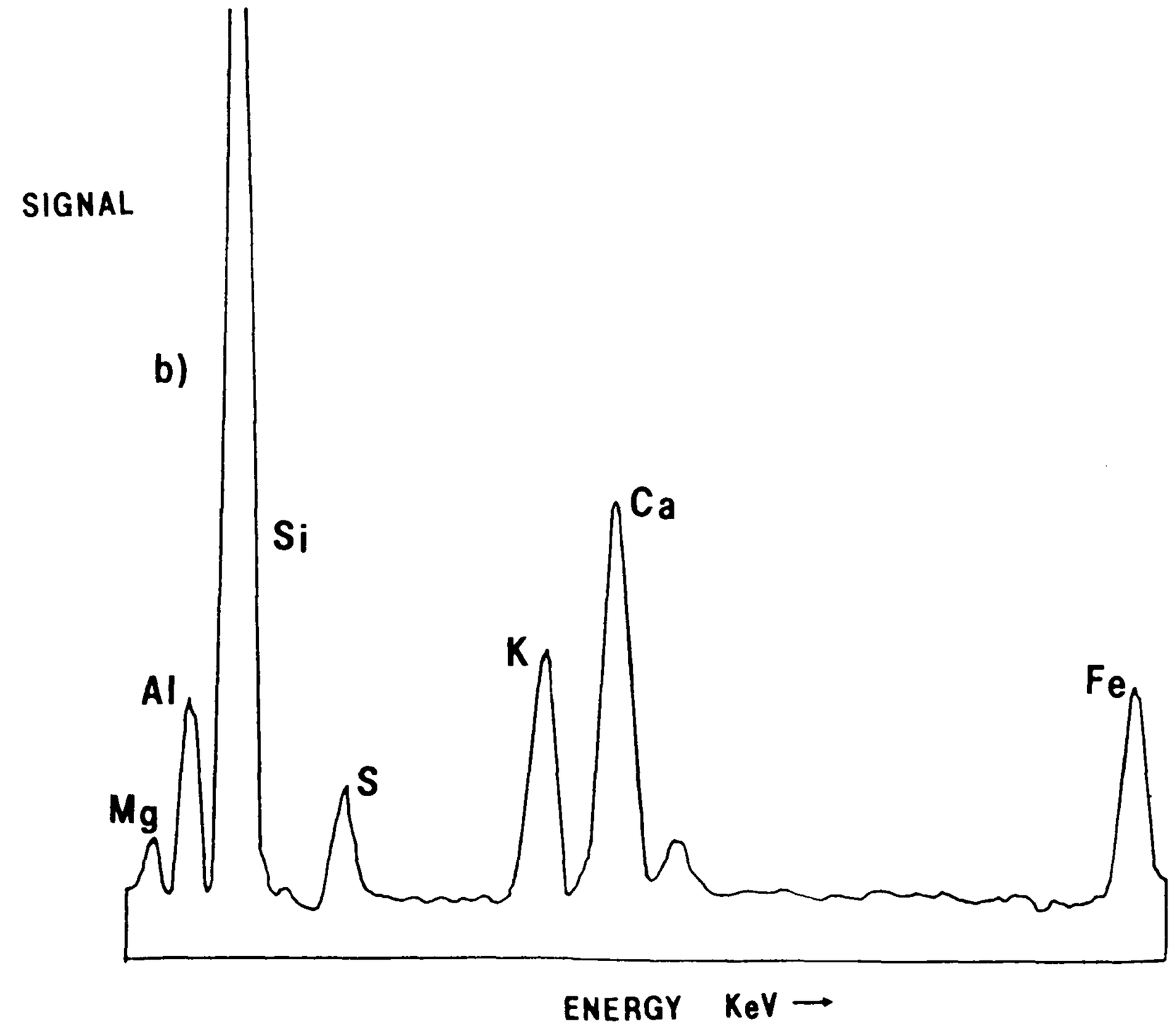

Fig.2.8 b) Elemental analysis of Berea sandstone.

surfaces to study surfactant adsorption. Silica was chiefly used since this is the most abundant element in the rock. Two types of silica spheres (Shell International Chemical Co. Ltd.) were used: 2.5-3mm diameter, S-980 A-2.5/3 and 1.5 mm diameter, S-980 A-1.5. The alumina was obtained from Laporte, Widnes, U.K.. They were chosen because of their high purity, uniformity of surface area and pore volume. The physical characteristics are given below:

Material	Range of Pore Radius nm	Surface Area $m^2 g$	Pore Volume $cm^3 g$
Alumina	15	14	0.315
Silica (2.5/3)	6-10	255	1.16
Silica (1.5)	30-60	58	0.95

The characteristics of these three materials vary quite considerably from the reservoir sandstones. They were used mainly for adsorption work only, and so the results cannot be quantitatively related to the reservoir rock system.

2.3 Brines

Initially a standard brine from BDH was used, but since this contains only one third of the concentration of total dissolved solids that the Mobil sea water has, its use was limited. An alternative, a synthetic brine, was prepared from the analysis as sent by Mobil North Sea Ltd.. This contains the same total dissolved solids (TDS) as Beryl B reservoir water. The salt contents of these two brines are listed in Tables 2.5 and 2.6.

Salt	Content (gdm^{-3})
Sodium Chloride	24.99
Calcium Sulphate Anhydrous	1.50
Magnesium Chloride Hexahydrate	2.99
Magnesium Sulphate Heptahydrate	2.00

TABLE 2.5 BDH Brine Composition

Salt	Content (gdm^{-3})
Sodium Chloride	75.60
Calcium Chloride	7.40
Potassium Chloride	1.65
Magnesium Chloride	1.05
Strontium Chloride	0.69
Calcium Bicarbonate	0.67
Ferric Chloride	0.32
Magnesium Sulphate	0.03

TABLE 2.6 Synthetic Beryl B Brine Composition.

2.4 Hydrocarbon and Synthetic Oils

It was often difficult to work with the actual reservoir oil since it is very dark and dirty. Also, some of the lighter hydrocarbons may evaporate in use, increasing the viscosity and generally altering its behaviour when considering adsorption, phase behaviour etc.

Therefore, two pure hydrocarbon mixtures were used to simulate the response of Beryl live crude oil and Beryl stock tank oil in laboratory flood experiments. Table 2.7 illustrates the characteristics for the pure-component synthetic oils at 370K and 1 atmosphere pressure. Tables 2.8 and 2.9 list the proportions of the pure components for the stock tank crude (STC) and synthetic live crude (SLC) respectively.

Important characteristics of the two pure hydrocarbon mixtures and of the two Beryl crude oils are compared in Table 2.10.

The components were selected to match, as closely as possible, with only three component mixtures, the viscosities, densities and molar volumes of the Beryl reservoir fluids as suggested by Puerto and Reed (48). The solvency characteristics of the fluids were matched also by using similar amounts of saturated hydrocarbons (paraffins and naphthenes), alkyl benzenes and polycyclic aromatic compounds. Some compromises were necessary in order to retain simple mixtures and priority was given to hydrocarbon types, density, and molar volumes. The stock tank crude was used diluted with iso-octane to

Component	Mole wt	Density (gdm^{-3})	Viscocity (Pa.s)	Molar Vol.(MV) $cm^3(g.mole)^{-1}$
n-octane	114.2	0.636	2.63	179.5
n-hexadecane	226.2	0.732	9.87	309.3
n-butylbenzene	134.2	0.796	4.40	168.6
1-methyl naphthlene	142.2	0.911	9.63	156.1

TABLE 2.7 Component Properties for Synthetic Oil.

Component	wt%	Mole %
n-hexadecane	40	28.95
n-butylbenzene	28	34.18
1-methyl naphthlene	32	36.87

TABLE 2.8 Beryl Stock Tank Crude.

Component	wt%	Mole %
n-octane	50	44.68
n-butyl benzene	23	26.61
1-methyl naphthlene	27	28.71

TABLE 2.9 Beryl Synthetic Live Crude.

Mixture (@ 370K)	Density (gcm^3)	Viscosity Pa.s	Molar vol. $cm^3(g.mole)^{-1}$
Beryl Stock Crude @ 1atm.	0.809	17.50	226
Synthetic Beryl STC @ atm.	0.810	7.95	221
Beryl Live Crude @ 2000psi	0.697	6.95	171
Synthetic Beryl Live Crude @ 1 atm.	0.749	4.27	168

TABLE 2.10 Characteristics of Live and Synthetic Oils.

simulate the viscosity of live crude at reservoir conditions in order to predict the response of live crude to surfactant flooding.

2.5. Characteristics of the Reservoir.

A particular reservoirs' characteristics may vary widely with another in the same field as stated earlier. Within the reservoir, conditions may differ as the rock composition changes with precise location. The formation water is often not well mixed and hence the crude oil components are also variable, even after migration. The reservoir conditions for Beryl B as supplied by Mobil North Sea Ltd., are as follows:-

Rock.

Temperature	370K
Pressure	34MPa(initial) to 14MPa(final)
Permeability	10 to 100 md (millidarcy)
Porosity	15%

Brine.

pH reservoir water	6.5 to 7.1
pH sea water	8.03

Total Dissolved Solids (TDS).

	$mg.dm^{-3}$
Reservoir	87520 to 88750
Seawater	36300

Oil.

Viscosity at bubble point	5.9Pa.s
Viscosity at 1 atmosphere(370K)	17.5Pa.s
Density @ 2000psi	0.69 $g.dm^{-3}$

CHAPTER 3

3.1 Introduction

Surfactants, particularly the nonionic and anionic classes, have been widely used for many years but there are relatively few analytical techniques that can accurately characterise these compounds. In most cases, these surfactants are industrial products of a series of reactions, with relatively little separation-purification. As a result, they are complex mixtures of unreacted chemicals and surfactant molecules of varying ethene oxide chain length.

Since the information necessary to understand the properties of these surfactants includes:

(i) distribution of ethene oxide oligomers;

(ii) percentage of each oligomer;

(iii) substituents on the aromatic ring;

(iv) conformation;

and (v) amounts of nonionic, anionic and impurities, several complimentary techniques are required to completely analyse them; these are described in the following chapter.

3.2. High Pressure Liquid Chromatography (HPLC)

3.2.1. Introduction

The aspect studied here by HPLC is the Poisson distribution of ethene oxide (EO) units as a result of the manufacturing process. One of the earliest papers (44) discusses the reaction of ethene oxide and includes a mathematical treatment of the Poisson curve.

Analytical chromatography separates molecules according

to their size and polarity and hence their retention on an adsorbent. In liquid adsorption chromatography, the solutes are selectively distributed between active sites on the surface of a solid in a liquid phase; this can be divided into normal and reverse-phase, depending on the polarity of the solid stationary-phase and the mobile liquid phase. In normal phase adsorption used here, the active sites on the surface of the solid are polar and the liquid phase less polar. The polarity is reversed for the reverse-phase system but in both cases, adsorption is a competitive process between the solvent and solute molecules.

Many chromatographic methods have been used to separate surfactant mixtures with varying degrees of success. In the early 1950s, two polyethene oxide alkylphenols were molecularly distilled and separated by conventional silica gel liquid chromatography. This method was time consuming but agreed well with the predicted Poisson theory. Thin-layer chromatography (TLC) has also been used to investigate the general spread of oligomers in polymeric molecules. In relation to surfactants, TLC suffers from poor reproducibility and analysis of the results is troublesome. Gas chromatography (GC) is successful, but can elute only a limited number of oligomers even if the volatility of the sample is increased by derivitisation (47). GC is restricted by the temperature that can be used and has the main disadvantage of the sample usually being destroyed. Circular thin-layer chromatography (CTLC) provides similar information concerning the spread of oligomers

(49) but little else.

There are a number of chromatographic parameters that may be varied. The pressure, flow rate and temperature are all equipment variables, as are the polarity of the mobile and stationary phases, pH, salt or buffer concentration; these can all be optimised to produce the best resolution. Nevertheless, many mixtures cannot be separated isocratically with <u>one</u> solvent composition for the mobile phase. The successive components of an oligomeric mixture generally shows only a slight difference in chromatographic behaviour and the number of oligomers in one sample is often considerable. Gradient elution is the most effective technique available for overcoming this problem. It uses a combination of solvents (e.g.up to three or four is common) and the proportion of each solvent present may be altered during the analysis.

Gradient-elution high-pressure liquid chromatography (GE-HPLC) has been used successfully for characterising surfactants. Much of the published literature describes the resolution of 9 or 10 EO units using reverse-phase chromatography; the resolution becomes poorer at higher EO numbers (47). Other papers describe the use of additives such as salts (51), buffers and pH variation (52). Derivitisation has also been described to enhance chromatographic separation (53) and additives used (e.g. anthracene) to achieve a good baseline (54).

Two comprehesive reviews on the HPLC of all classes of surfactants have been given by Jandera (55) and Garti(56).

The following section describes the separation of a wide variety of surfactants (nonionic and anionic) without the need for any additives or chemical pretreatment.

3.2.2. Experimental.

Apparatus: The GE-HPLC analysis was performed here using a Gilson gradient system (Anachem Ltd.). The samples to be analysed were injected through a 20µl ($20mm^3$) loop via an autosampler (model 231) and a diluter (model 401). Two pumps were used (model 302) capable of operating up to 60 MPa. The detector used was a Holochrome ultra-violet detector set at 254nm. It was assumed that all the oligomers have the same absortivity at this wavelength. A fraction collector (model 201) was used to collect the individual peaks for further analysis (see the next section on Mass spectrometry). All the apparatus was controlled by an Apple IIe computer. A differential refractometer (LDC) was used as a second detector in line with the UV to investigate the possibility that non-ultra-violet absorbing components might be present in the samples. A Pye Unicam oven (PU4031) was used to maintain the desired temperature of the columns.

Columns: A Du Pont technical report (57) recommended the use of a normal-phase cyano (CN) column which gives good resolution up to 10 EO units. After this, the baseline drifts due to the gradient and resolution is lost. The stationary phase consists of a monolayer of cyano groups bonded onto a silica support. Another paper (58) used a propyl amino (NH_2) column for the separation of one of the Triton series of surfactants. The suggestions from these two papers were followed with the conditions altered to

obtain better resolution. Both the columns used in this study (CN and NH_2) were of Zorbax make, and purchased from Du Pont. They measured 250 x 4.6mm and had a particle size of 10μm. A precolumn was placed immediately before the analytical columns (both the CN and NH_2 column) to protect them against severe contamination. They were stainless steel tubes (50 x 4.6mm) packed with Permaphase ETH (Du Pont).

Solvents: The solvents for the CN column were n-hexane, 2-methoxyethanol and 2-propanol. All were HPLC grade and purchased from Rathburn (Scotland). Solvent A for this analysis was 100% hexane. Solvent B was 2-methoxy ethanol/2-propanol in a ratio of 75/25. The solvents for the NH_2 column were also HPLC grade (Rathburn) and were tetrahydrofuran, n-hexane, water, and 2-propanol. Solvent A for this system consisted of 20% tetrahydrofuran and 80% hexane. Solvent B was 10% water and 90% 2-propanol. Initially, all the solvents were degassed but subsequently it was found that this was not necessary.

Samples: The surfactants were all prepared as 1% (wt/vol) solutions in solvent B for both sets of analyses. Ideally, the samples should be dissolved in the composition which initiates the gradient to produce better resolution, but here the solubility was poor. The sulphonated surfactants contained a precipitate when dissolved in the solvent (probably due to the method of synthesis). These samples were centrifuged, and the supernatant liquid used. The gradient profiles for the

For Sapogenats, Arkopals and Precursors	
Column	CN
Solvent A	Hexane (100%)
Solvent B	2-methoxy ethanol/2-propanol (75:25)
Flow rate	1.5cm^3 min^{-1}
Temperature	323K
Gradient profile	time(min): 0 %B: 2
	" : 50 ": 50

For Tritons	
Column	NH_2
Solvent A	Hexane/THF (80:20)
Solvent B	2-propanol/water (90:10)
Flow rate	1cm^3 min^{-1}
Temperature	323K
Gradient profile	time(min): 0 %B: 2
	" : 60 ": 100

TABLE 3.1 HPLC Analytical Conditions.

surfactants are listed in Table 3.1. Some of the samples did not require such a severe gradient but standard conditions were required for all the surfactants to allow comparison. After each sample was analysed, the column was regenerated until the original baseline was obtained. This was achieved by running a reverse gradient over 10 min and then flushing under the initial conditions for a further 10 min in order to equilibrate the column.

3.2.3 Results

Figures 3.1(a-j) show the HPLC traces for the nonionic surfactants and their corresponding sulphonates. Figures 3.2 and 3.3 show T130 and T500 which have no sulphonate analogues. T180 and its sulphonate, T180S, (which was prepared at Brunel) are shown in Fig. 3.4(a and b). Six other sulphonates were prepared at Brunel, one of which, N110S is depicted in Fig 3.5.

The chromatograms of the precursors phenol and tributyl-phenol are shown in Fig. 3.6.

The remaining chromatogram (Fig.3.7) illustrates an example of the Triton series.

3.2.4. Discussion

In normal phase chromatography (polar column and initially non-polar solvent), the nonionics are eluted first since they have less attraction for, and therefore lower retention on, the polar column. In Fig 3.1, (b,d,f,h,j) the final peaks of the nonionic distort the initial peaks of the sulphonate. Ideally, the nonionic

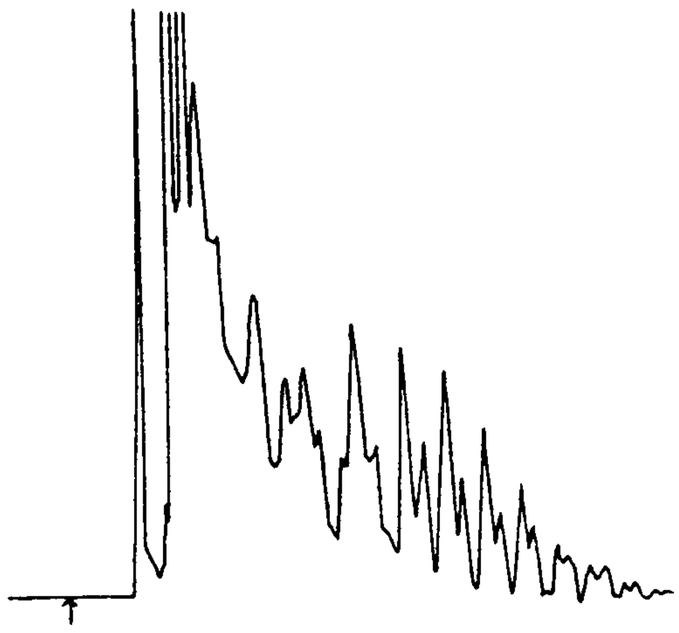

a) T040

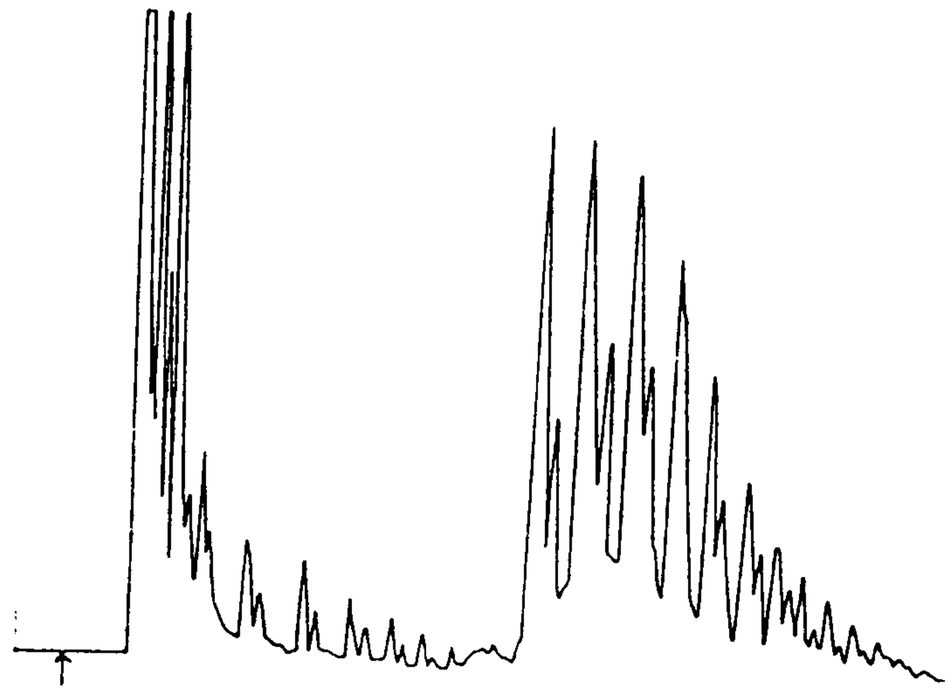

b) T040S

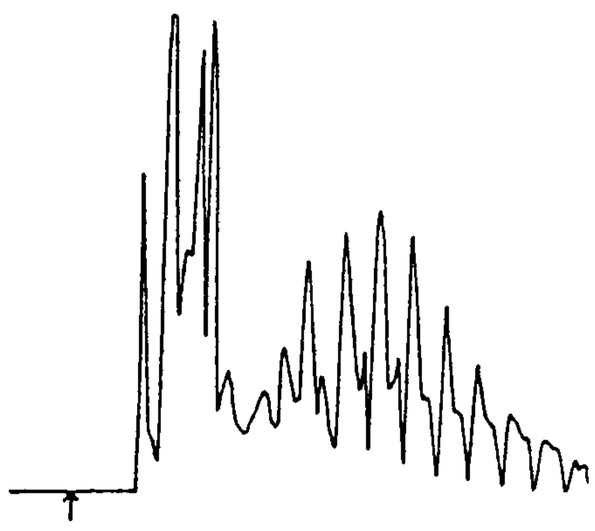

c) T060

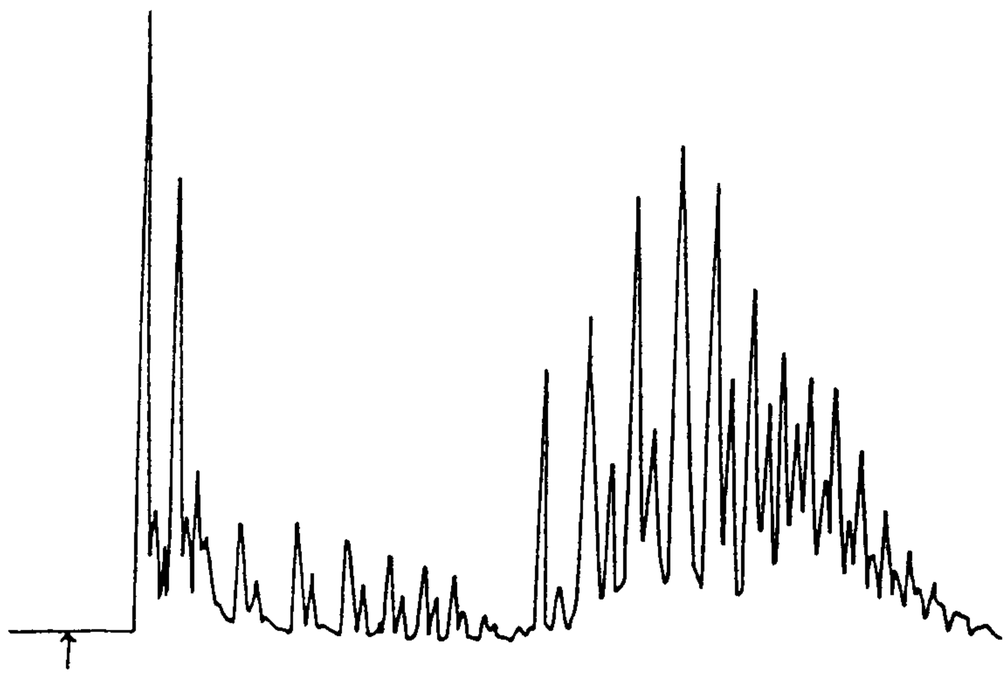

d) T060S

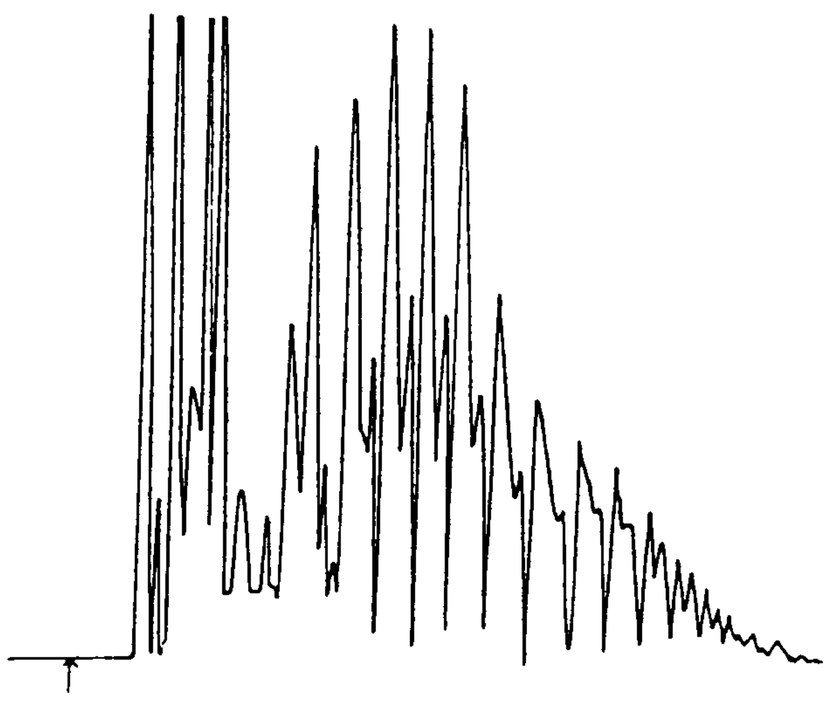

e) T080

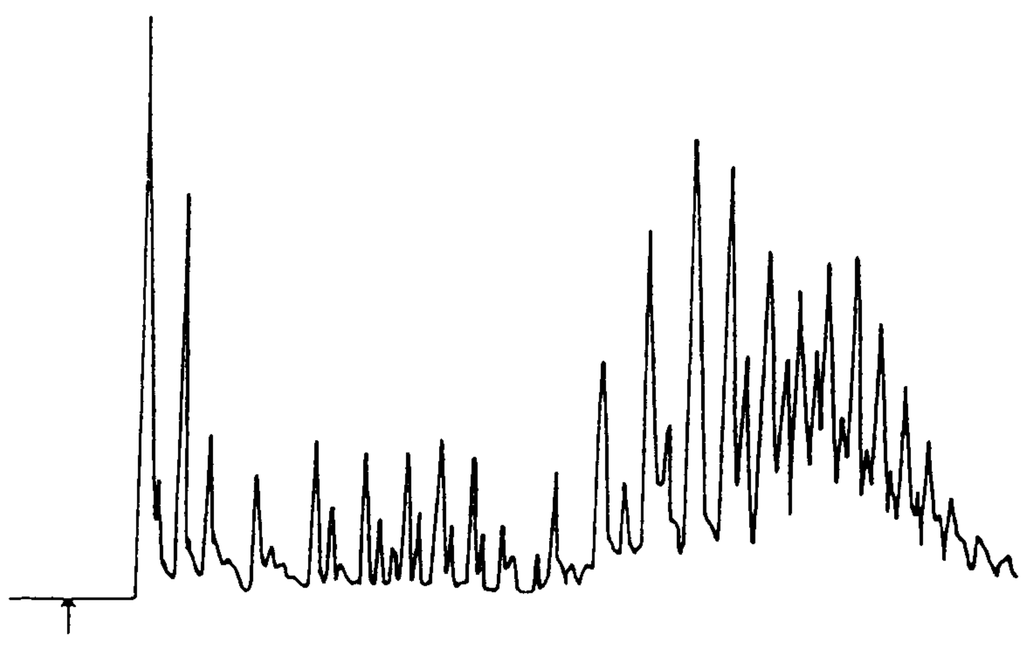

f) T080S

Fig.3.1 HPLC analysis of surfactants.

Fig.3.1 continued

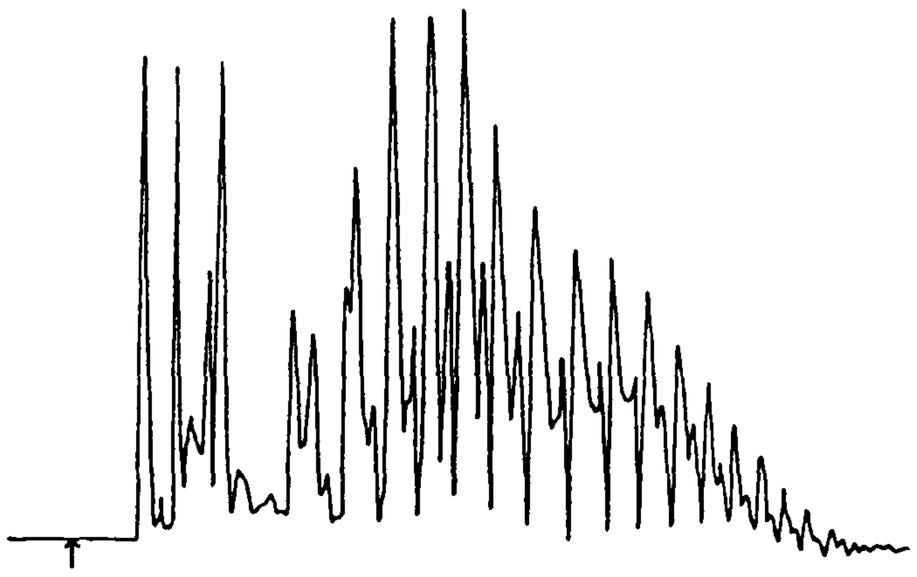

g) T100

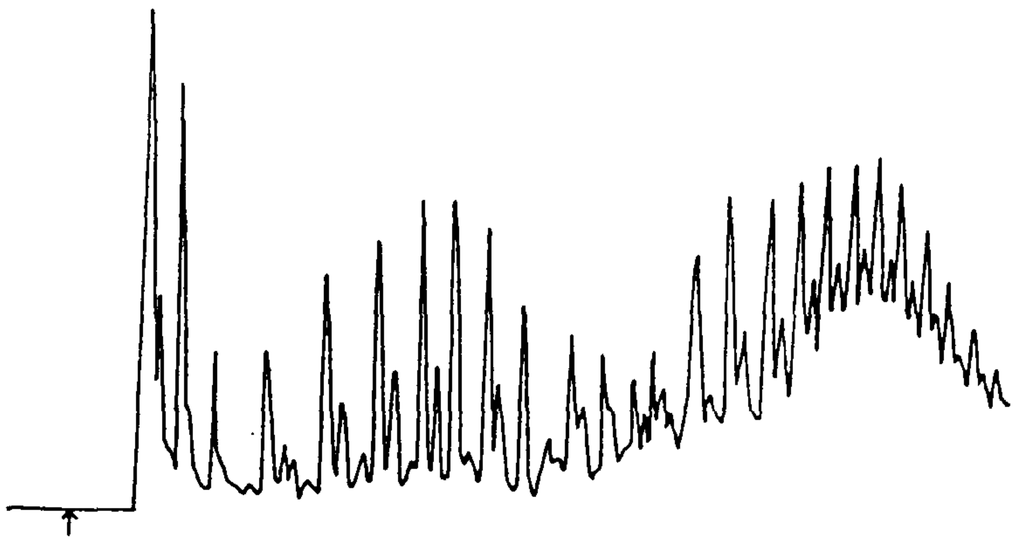

h) T100S

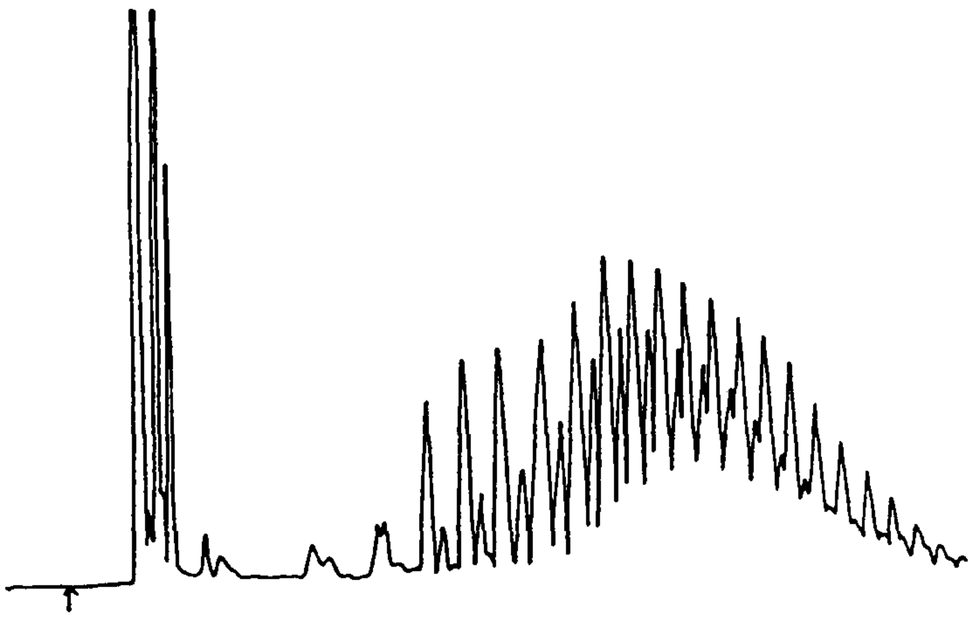

i) T150

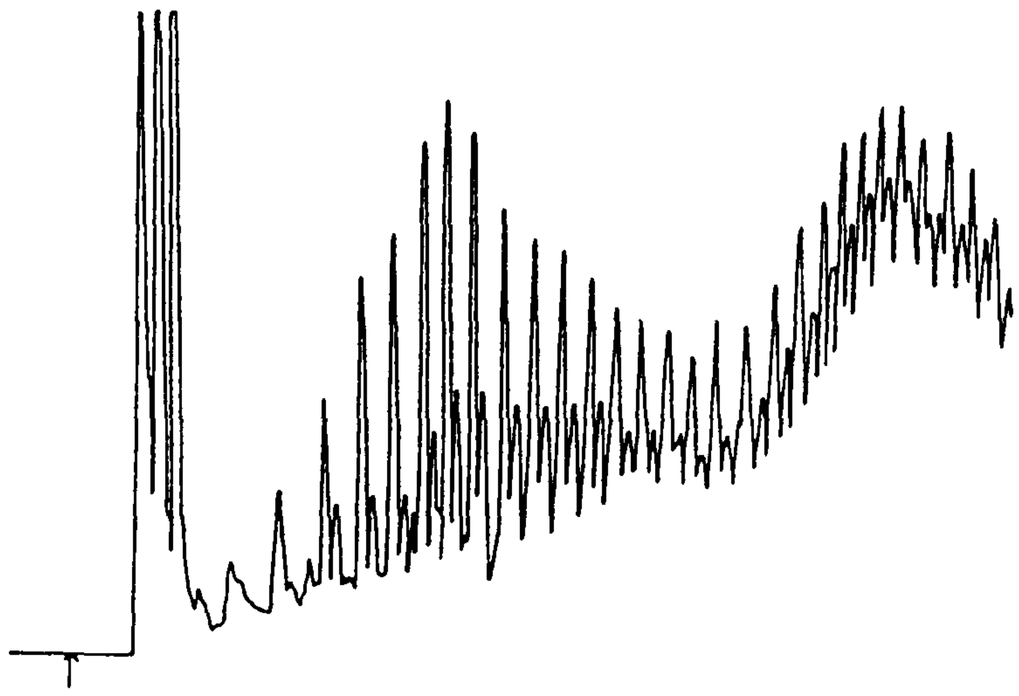

j) T150S

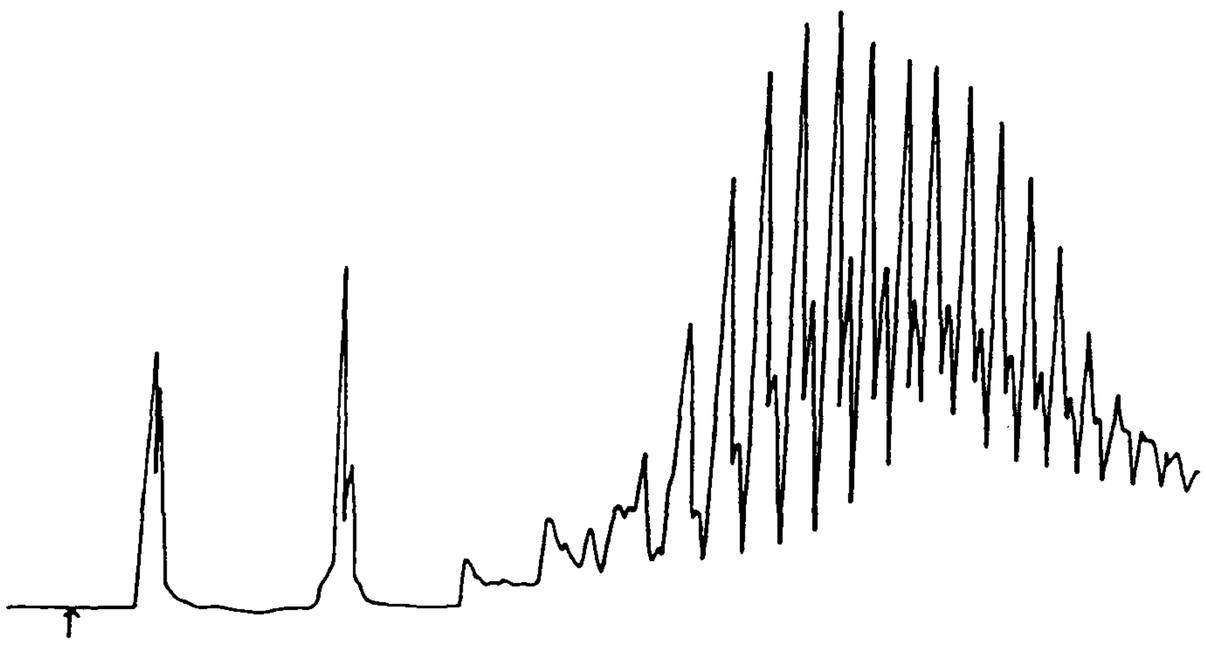

Fig.3.2 HPLC analysis of T130

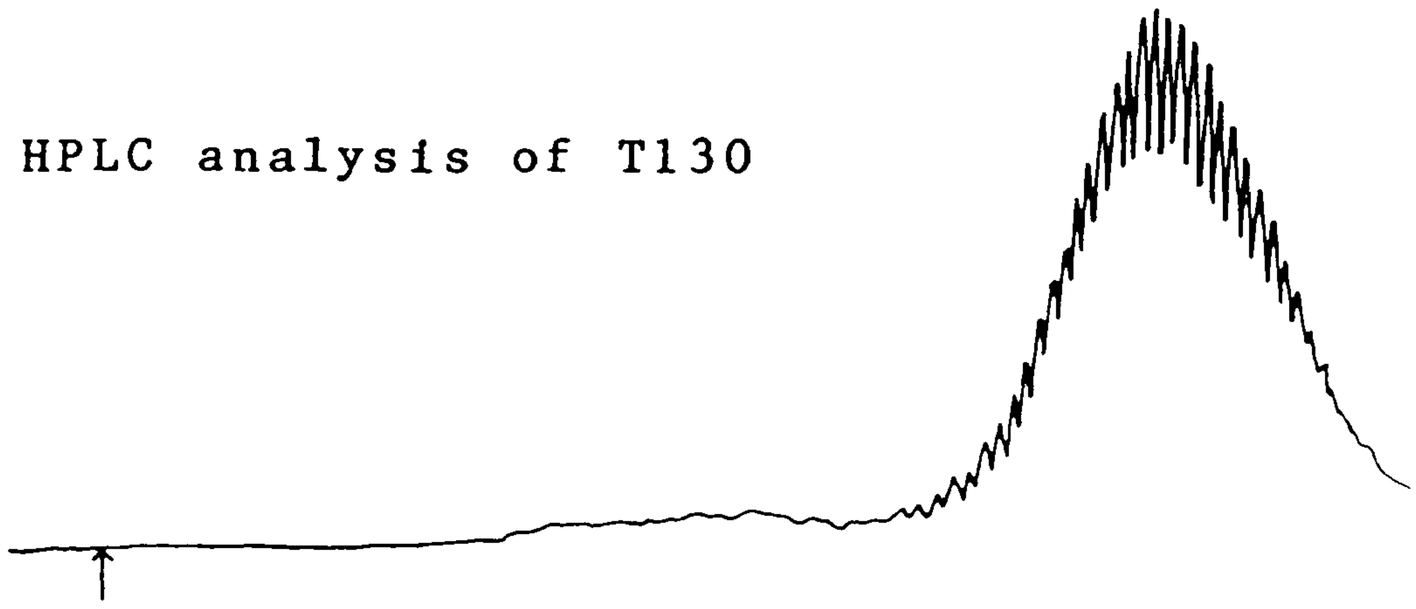

Fig.3.3 HPLC analysis of T500.

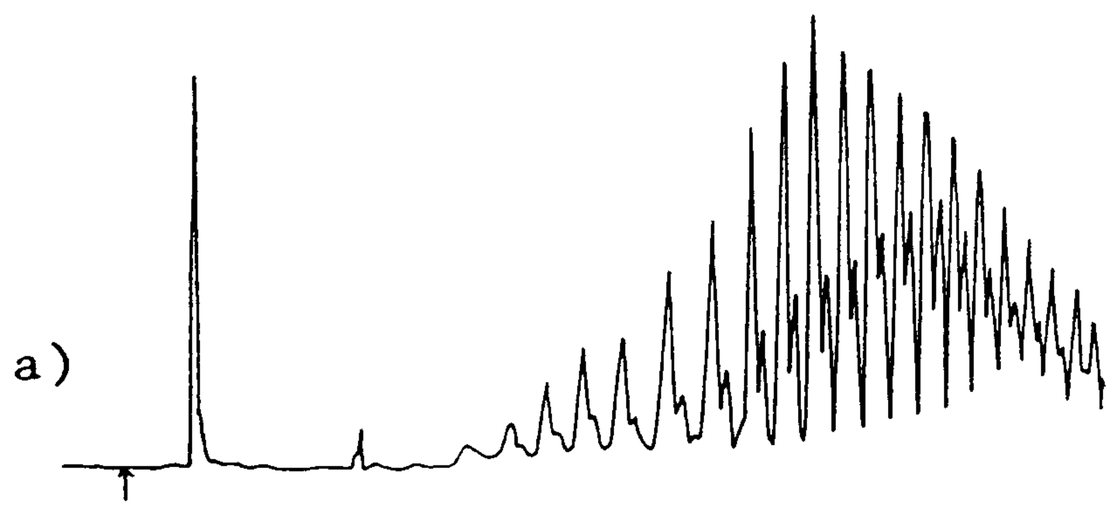

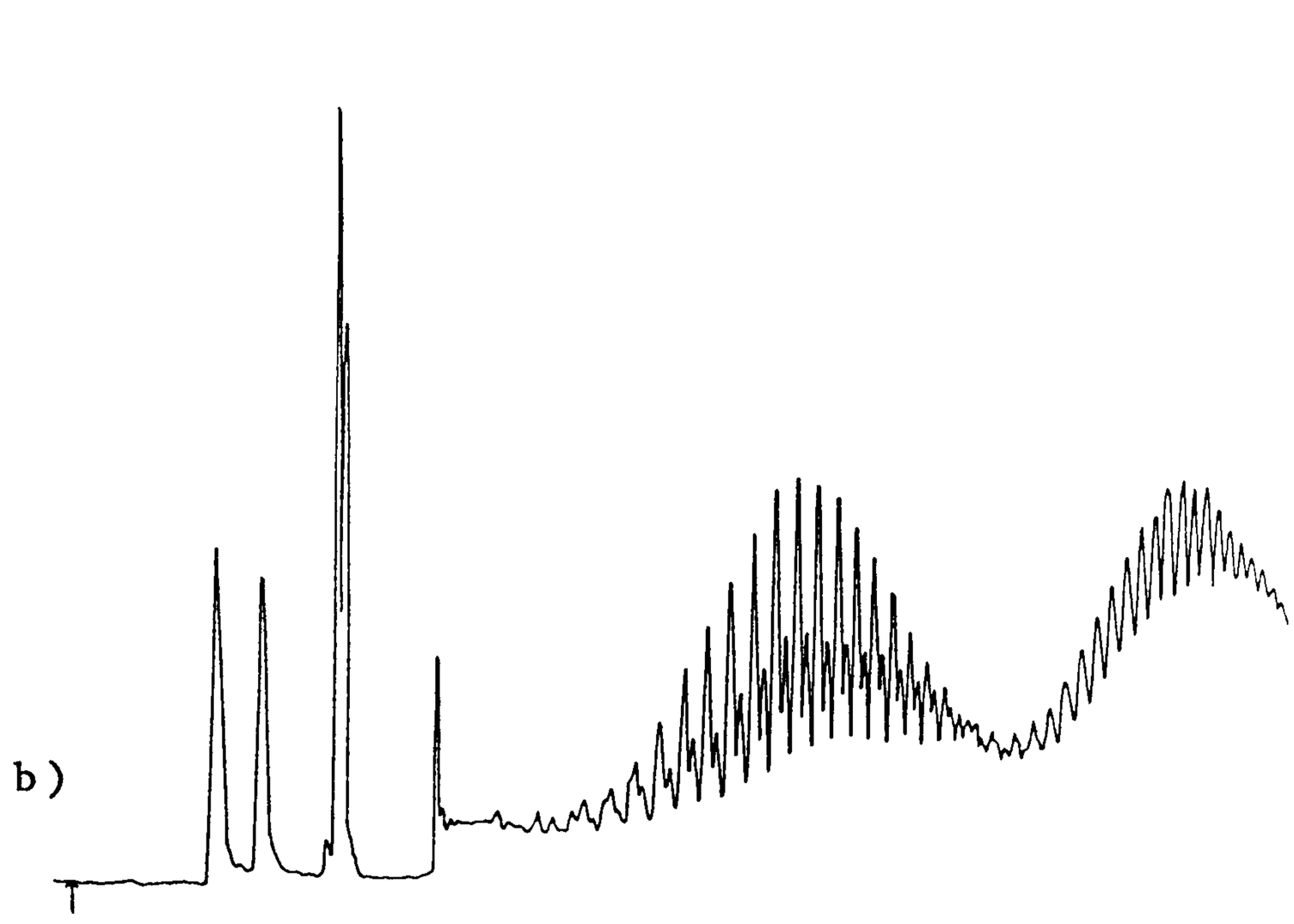

Fig.3.4 HPLC analysis of a) T180, b) T180S

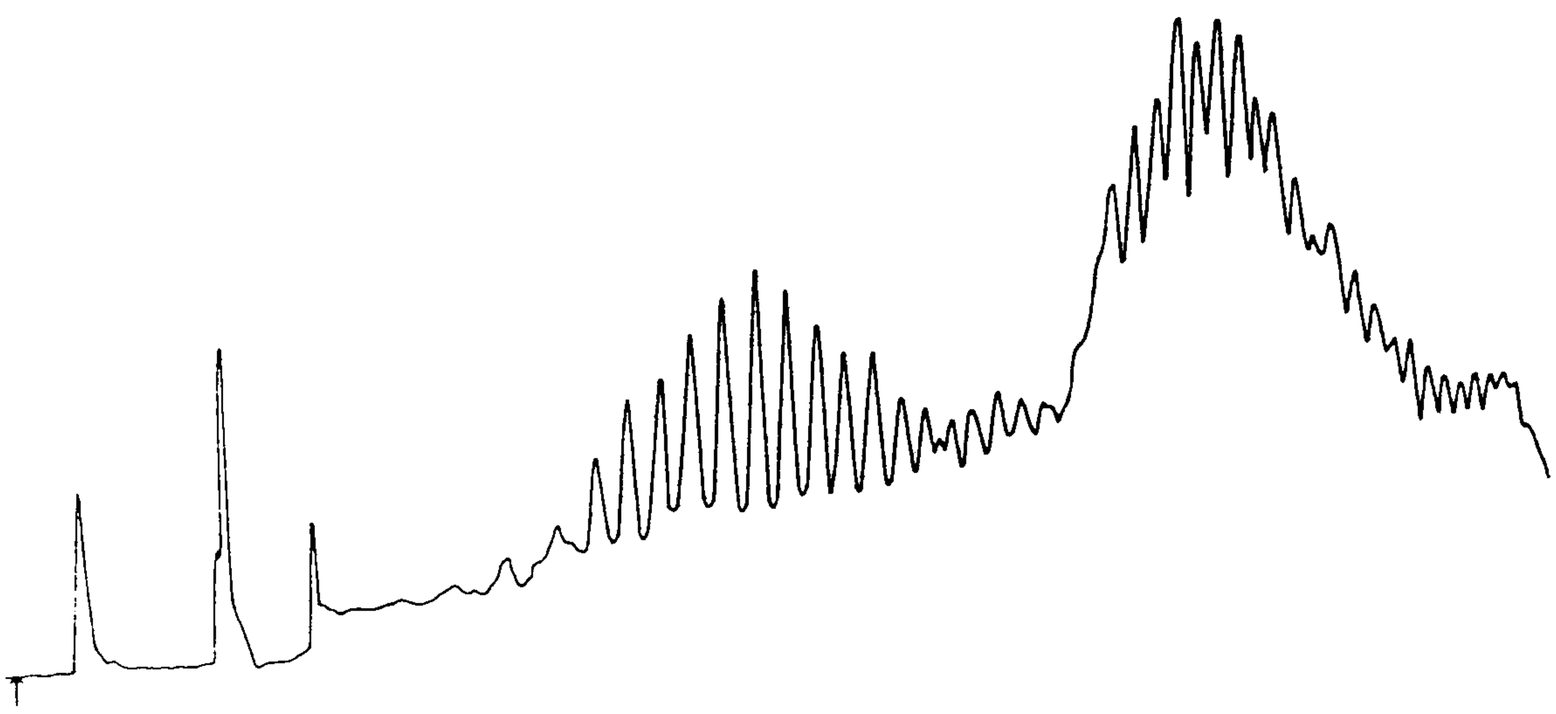

Fig.3.5 HPLC analysis of N110S

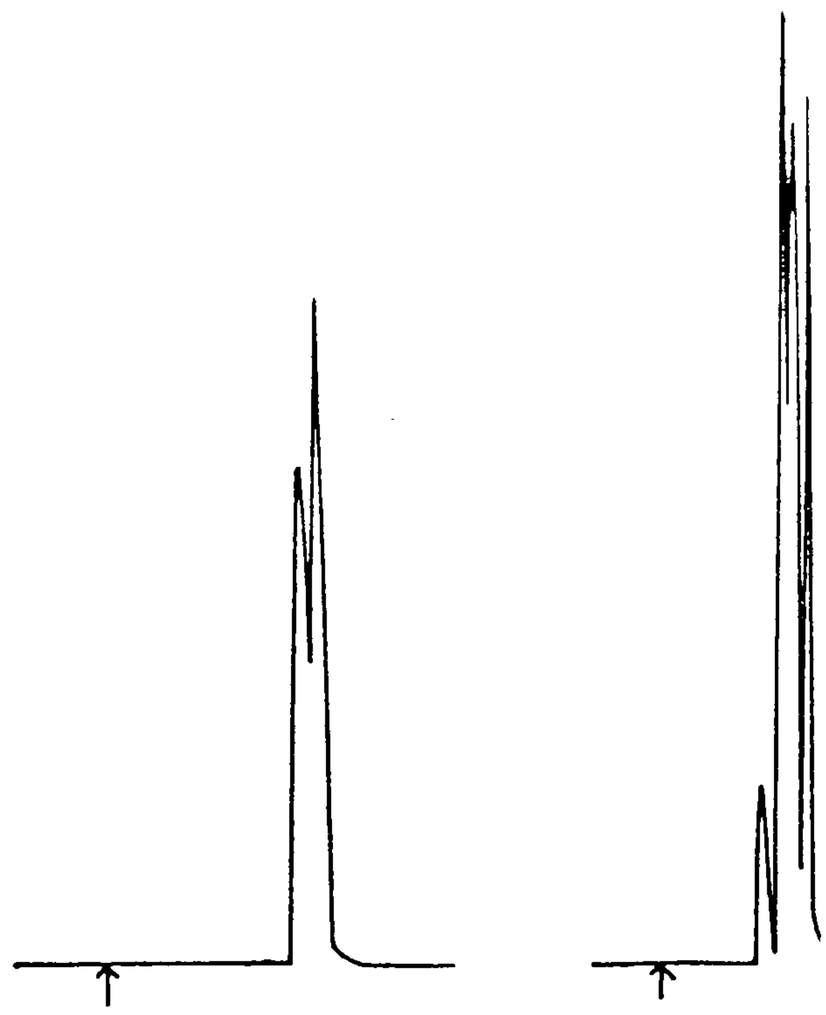

Fig.3.6 HPLC analysis of a) phenol b) tributylphenol

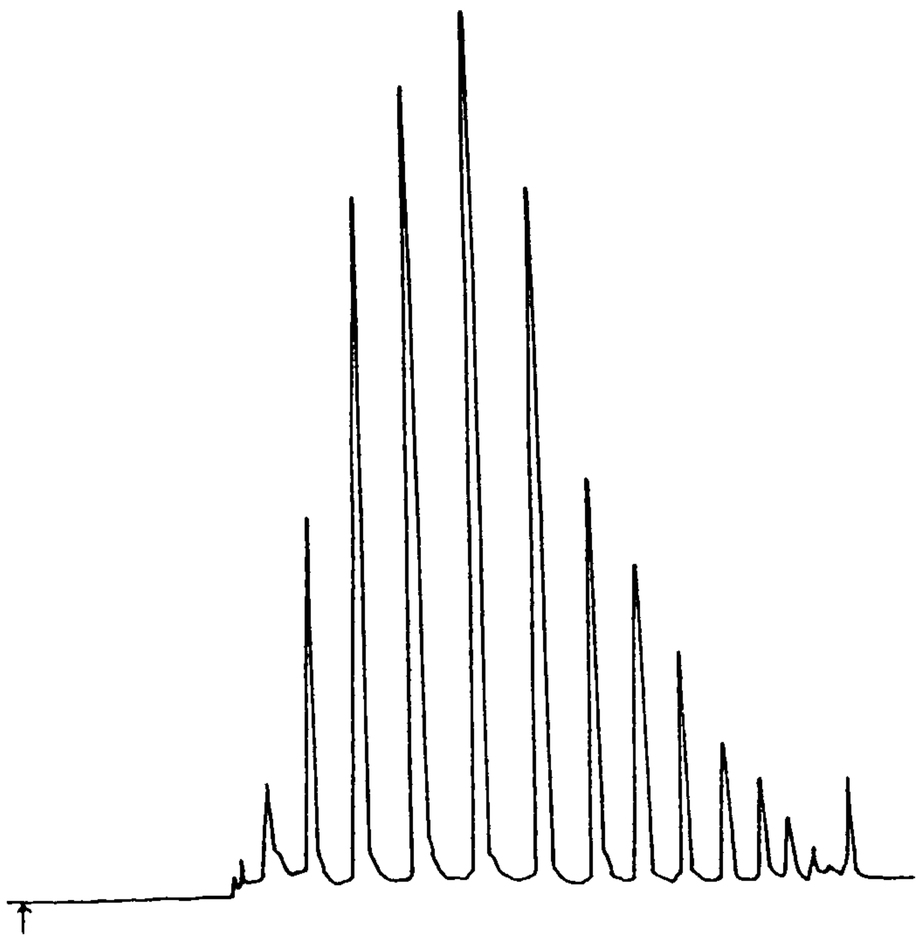

Fig.3.7 HPLC analysis of Triton X100.

part should be completely eluted and then the anionic flushed off the column. This could be achieved by using a slightly more polar column.

As the chain length increases, the proportion of nonionic material also increases. It is reasonable, therefore, to conclude that it becomes more difficult to sulphonate the surfactant as the precursor reactants are further ethoxylated.

The lower nonionic chain lengths are well resolved, but the separation of the larger molecules is more difficult and requires a different gradient. This is probably due to the "size exclusion effect" which is clearly seen in Fig. 3.3, the chromatogram for T500. The resolution between successive oligomers has decreased considerably. This could result from a reduction in the relative differences between the oligomers as the extent of ethoxylation increases. Also, as the molecular weight increases (and therefore the size) there is a decrease in the accessibility to the pores of the column packing, leading to similar retention times.

The chromatograms of the Sapogenat series are distorted at the beginning and the initial peaks are not well distinguished. This is particularly noticeable for the shorter chain surfactants (see Figs 3.1 a,c,e),whereas the longer chain lengths have a sufficiently long retention time to be separated from the first few peaks. Analysis of the retention times of the two precursors, phenol and tributyl phenol (Fig. 3.6), suggests that the

initial peaks are due to these materials. The tributyl phenol chromatogram is shown to be composed of several components which are attributed to ~~Di~~ various ring positions of the butyl groups. Further analysis of this compound using NMR allowed assignment of these peaks (see Section 3.4).

The Triton surfactant (X100) in Fig 3.7 shows very little distortion since these materials have been purified (99.9%) and hence have a much cleaner chromatogram. These surfactants show near perfect resolution, having level baselines and symmetrical peaks. They do show, however, the usual "bunching" of peaks at high molecular weight. This is an example of the octyl phenol series: the nonyl phenol Tritons produce a similar chromatogram.

Samples should ideally be dissolved in the same solvent composition that initiates the gradient to eliminate the "sample-solvent effect". The gradient is then smoothly changing the polarity of the eluting solvent. If a sudden change were introduced, it would cause negative peaks and distortion at the beginning of the chromatogram and impairment of the overall resolution along the column. The samples had poor solubility in solvent A and so solvent B was used. To overcome this sample-solvent effect, the gradient was started with a small percentage of B present to "couple" the sample and solvent.

Another possible reason for poor resolution is that the total composition of the sample may not be soluble in all of the solvents all of the time. The shorter (or longer)

chain lengths may be more soluble than other lengths. This can lead to precipitation of the sample during analysis and perhaps a gradual re-dissolution as the solvent flushes through the column.

A baseline drift can occur with gradient elution as the refractive index of the solvent changes. It can also be due to sample loading being too low and so the detector must be operated at a high sensitivity. Too high a concentration of sample will reduce the resolution as the sensitivity must be decreased. This change in the base-line is prominent in the trace from the refractive index detector. A rise in the baseline is observed but no peaks were positively detected. Polyetheneoxide could be formed in the manufacturing process but either the polymer was present at concentrations too low to be detected or it had very long retention times.

Gradient elution - HPLC has been shown to be an accurate and reliable analytical technique. It provides a great deal of information concerning the extent of ethoxylation and purity of the surfactant. This work on the separation of the nonionic surfactants and their sulphonated homologues has been published (59).

All of the chromatograms display the Poisson distribution. It is not necessarily valid to assume that, for example in T130, the largest peak is due to a surfactant molecule having 13 EO units. This is highly probable but the possibility that it could be due to 11 or 14 EO units cannot be ruled out. In order to

determine the composition of each peak, further analysis is necessary (e.g. mass spectrometry as described in the following section).

3.3. Mass Specrometry

3.3.1. Introduction

Numerous articles have assigned the various peaks in a liquid chromatographic spectrum of surfactants. Many assume that the peak having the largest area corresponds to the component which has the average number of ethene oxide units for that mixture. However, a more reliable assignment of peaks is required for an accurate analysis of the surfactant mixtures. Rothman (60) described the method of spiking, where a specific standard is used to identify the oligomer peaks by comparison of retention times. Nadeau and co-workers (61) employed a tedious method of separation by chromatography and molecular distillation and then assay by UV spectroscopy, to determine the number of EO units in that sample. This fraction was again run on the chromatograph and its retention time used to determine the chain length of one of the components. These methods only determine the structure of one component and assume that all the major peaks differ from the next by precisely one EO unit (62).

Most attempts to analyse these adducts stop at chromatographic separation, and qualitative analysis carried out shows that the molar distribution of EO adducts was directly proportional to the reaction time. The chromatograms obtained were always complex and so no peak identification was given.

Mass spectrometry (MS) is the most useful analytical technique for the study of separated oligomers. Reverse-phase chromatography has been used to separate nonionic surfactants and the fractions collected; they were then analysed successfully by field desorption mass spectrometry (FDMS) to obtain information on the oligomer distribution. For accuracy and speed, the chromatographic technique should be on-line with the MS (63). One of the Hoechst Arkopals (N060) and also Triton X100 was analysed by reverse phase chromatography followed by direct injection into the MS. Electron impact (EI) and chemical ionisation (CI) was used to produce well-defined total ion current traces.

In the present study, fractionation was used to identify the peaks in the LC chromatograms of T130 and T180. The mass spectrometry was carried out at University College, London (U.K.).

The Theory of Mass Spectrometry

A small amount of sample is deposited onto a probe which is inserted into the sample chamber. This is maintained at a high vacuum and the sample is vapourised either at room temperature or with heating. The vapour is passed into the ionisation chamber; this process most commonly consists of bombardment with high energy electrons (EI):

$$M + e^- \text{ (fast)} \longrightarrow M^+ + 2e^- \text{ (slow)}$$

Ionisation can also be accomplished by, for example, UV light (photo-ionisation), release of ions near a surface by applying a strong electrical field (field ionisation), or by charge exchange with previously ionised gaseous

molecules which then collide with the sample (CI).

The ions are then accelerated and focussed using a combination of magnetic and electrical fields and then scanned by varying either of the applied fields. A collector recognises the ions as a ratio of mass to charge (m/e). Every molecule will fragment characteristically to produce peaks of various m/e values which relate to its structure.

Two recent comprehensive reviews of coupling LC to MS (64,65) discuss the different interfaces, ionisation methods and other analytical coupling techniques.

3.3.2. Experimental

The chromatographic analysis for T130 and T180 was performed here on the Gilson gradient system, as described in the previous section. Each component eluted from the column was trapped using a fraction collector. The analysis was repeated 5 or 6 times in order to concentrate the component in each fraction and evaporated to near dryness. The first four peaks of each surfactant were prepared in this way. It is desirable to have no additives present (e.g. buffers, salts) in the column effluent as it can complicate the MS analysis.

Electron impact was carried out on a VG 7070H mass spectrometer, operating at 0.13mPa with ionising energy of 70eV, and the trap current 200 microamps. The samples were dissolved in dichloromethane and vapourised at 473K.

3.3.3. Results

T130 and T180 were separated using the CN column and the chromatograms are shown in Figs 3.8 and 3.9 respectively, together with their structures.

The mass spectra shown in Figs 3.10-3.13 are those for the peaks A,B,C, and D of T130.

The mass spectra for peaks E,F and G for T180 are illustrated in Figs 3.15-3.17.

Fig. 3.14 is an example of a library search for peak D or T130.

3.3.4. Discussion

In Fig. 3.8, peak A of T130 was originally thought to contain about 10 ethene oxide units (m.wt. 702), assuming that the largest peak was due to a chain length of 13 EO units. The mass spectrum in Fig.3.10 shows a peak at 570 which corresponds to a molecular ion having 7 EO units. The peaks relating to successive losses of EO units (1 unit = 44 m.wt,) can be seen at 526, (482 absent), 438, 394, 350 (306 absent) and 262. This last peak represents just the ring with the butyl groups. There are a number of smaller peaks in between and below 300 which are difficult to assign and if the complexity of the surfactant molecule is considered, many fragmentation processes can occur. This abundance of peaks could be due to, for example, loss of a butyl group (570-513), or loss of C_2H_5 (262-233), CH_3 (262-247, 288-273). There is unlikely to be a loss of CH_2 so the series of peaks which

differ by 14 should be considered as C_2H_4 loss and there are a number of series in which the peaks differ by 28 for example, 149-177, 189-217, 233-261, 247-275, 261-289.

Fig.3.11 shows the mass spectrum of peak B for T130. This peak could reasonably be expected to differ from peak A by 44 mass units and have a chain length of 8 EO units. This would produce a molecular ion at 614. The loss of EO units is seen at 570 (absent at 526 and 482), 438 and 394, 350, 306 and 262. The last peak is again due to the ring and butyl groups. Again there are numerous smaller peaks, due to losses as explained above.

Fig.3.12 shows the mass spectrum of the smaller peak C immediately following peak A. It was thought that this component contained the same number of ethene oxide units as the peak adjoining it (peak A) but was an isomer of the groups on the aromatic ring. Analysis of the spectrum shows a regular decrease in the peaks of 14 mass units. This cannot be due to loss of CH_2, rather C_2H_4 and the spectra should be considered as two series of mass units decreasing by 14. The numbers are all odd, hence the fragments must be protonated. The molecular ion at 463 reveals that, when divided by 14 (CH_2 unit), this peak is due to a straight chain hydrocarbon composed of 33 CH_2 units, similarly, peak D could then be expected to be a larger straight chain hydrocarbon. The mass spectrum Fig.3.13 does not show the same regularity that Fig.3.12. does. A library search (Fig.3.14.) suggests that some amine or bromine is present. This could not have come directly from the surfactant or solvents.

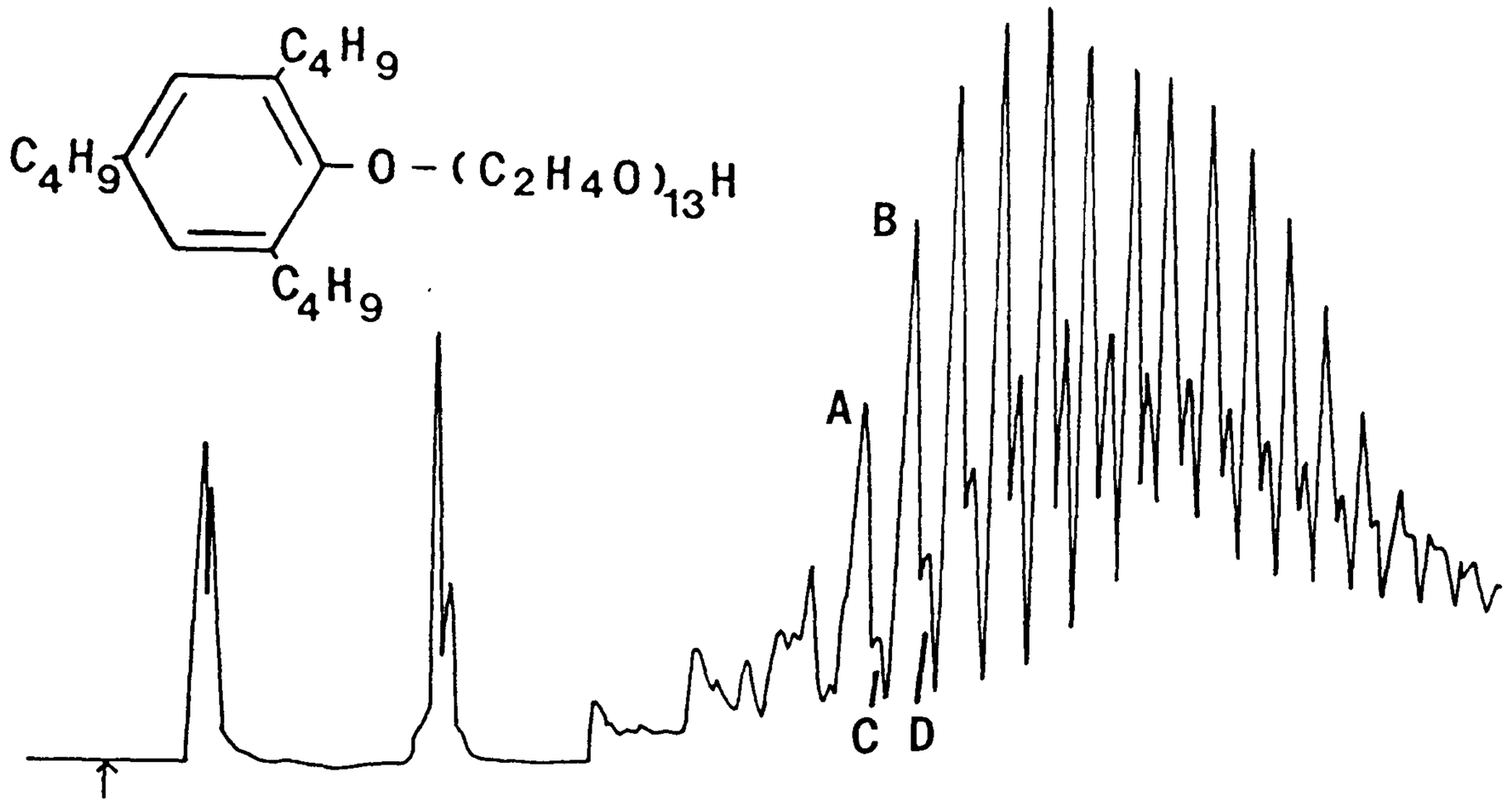

Fig.3.8 Structure and HPLC chromatogram of T130.

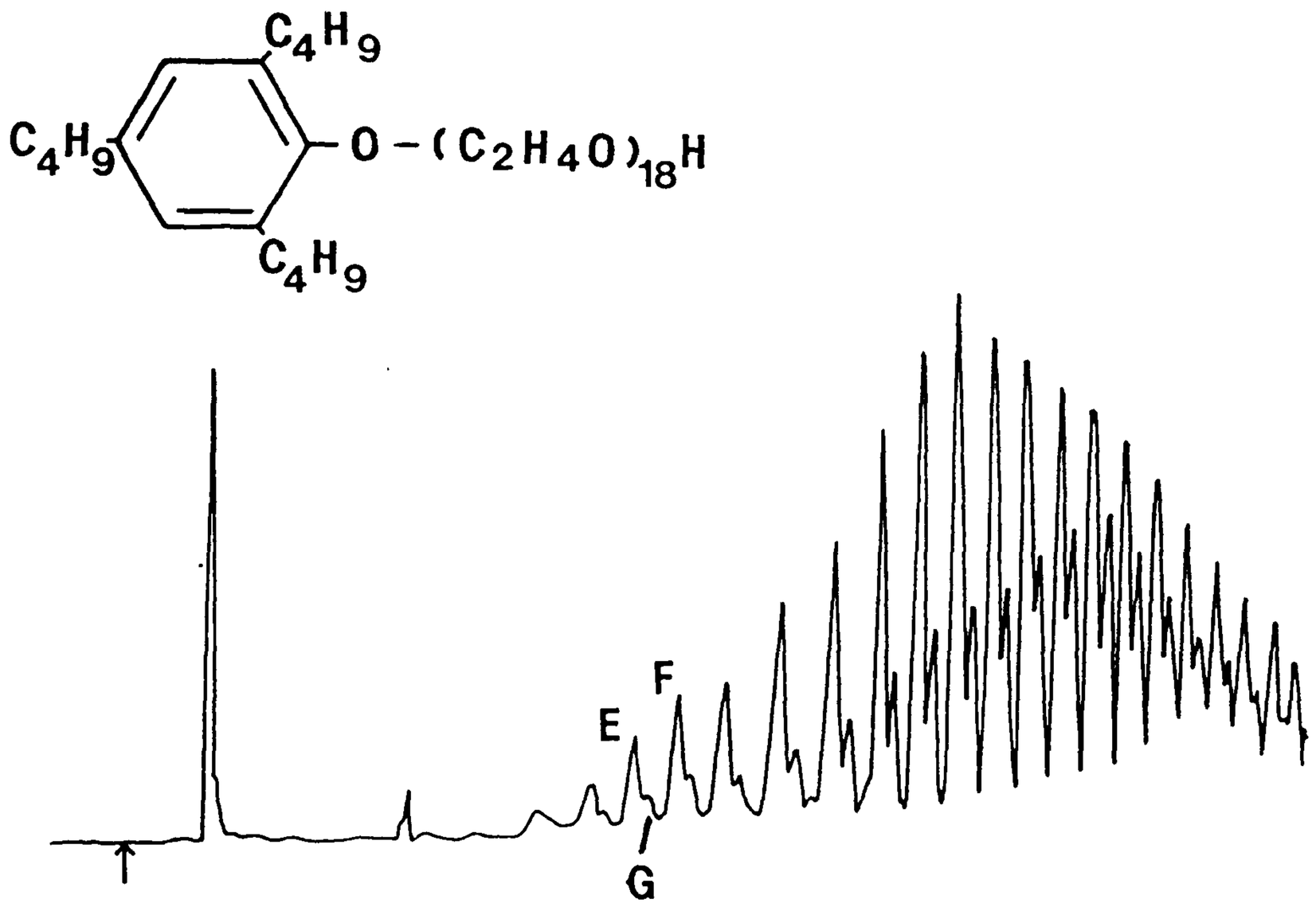

Fig.3.9 Structure and HPLC chromatogram of T180.

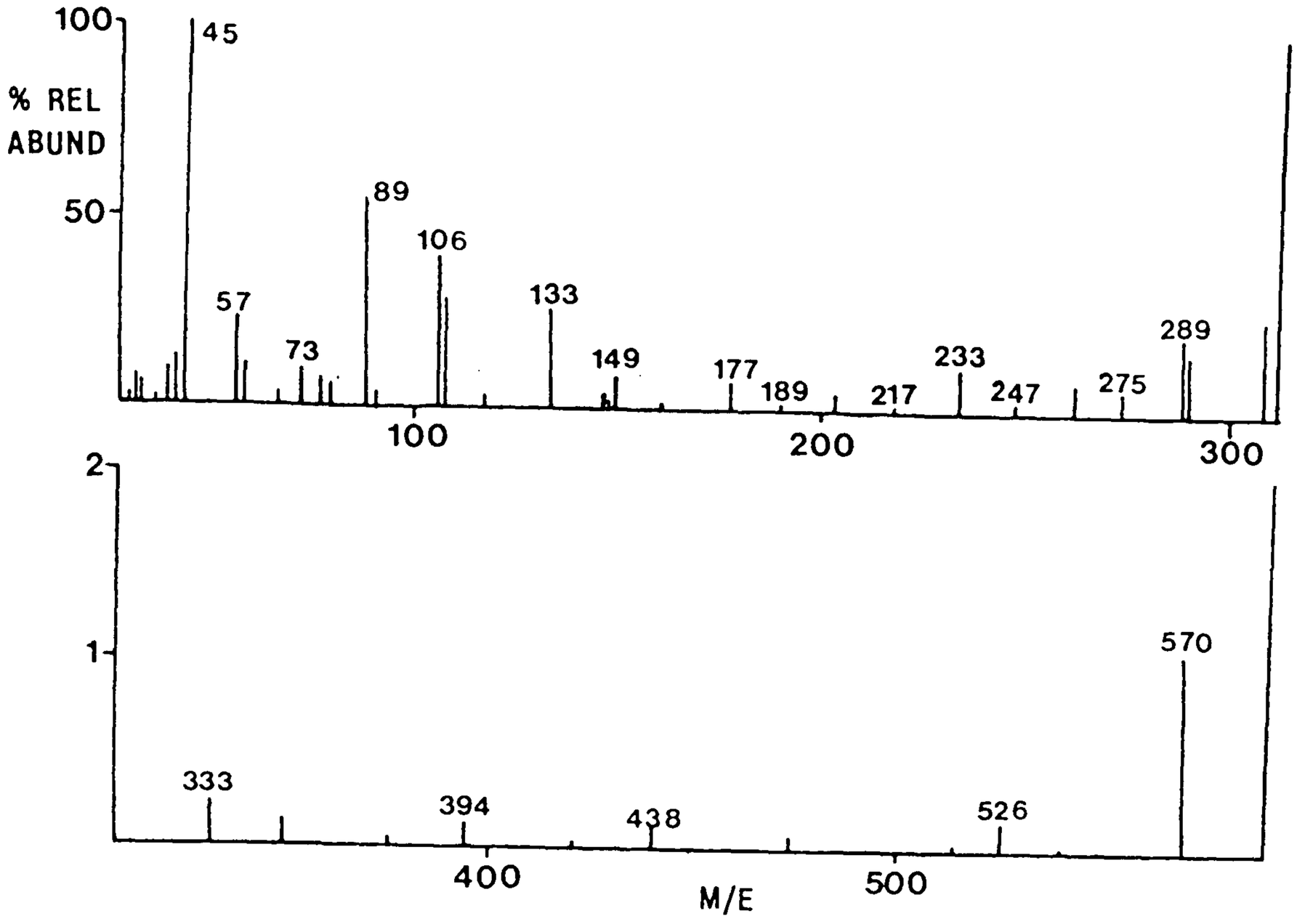

Fig.3.10 Mass spectrum of T130 peak A.

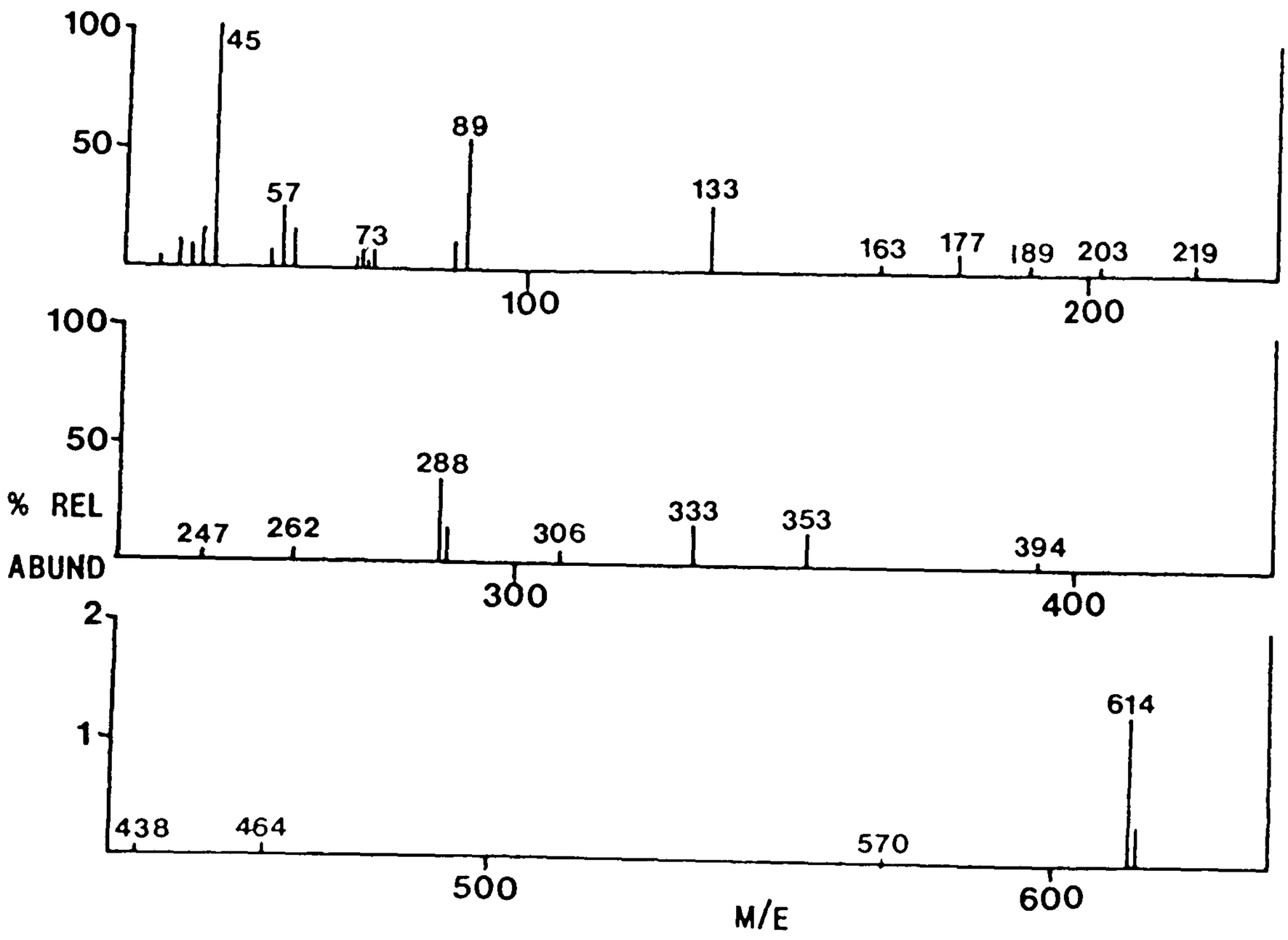

Fig.3.11 Mass spectrum of T130 peak B.

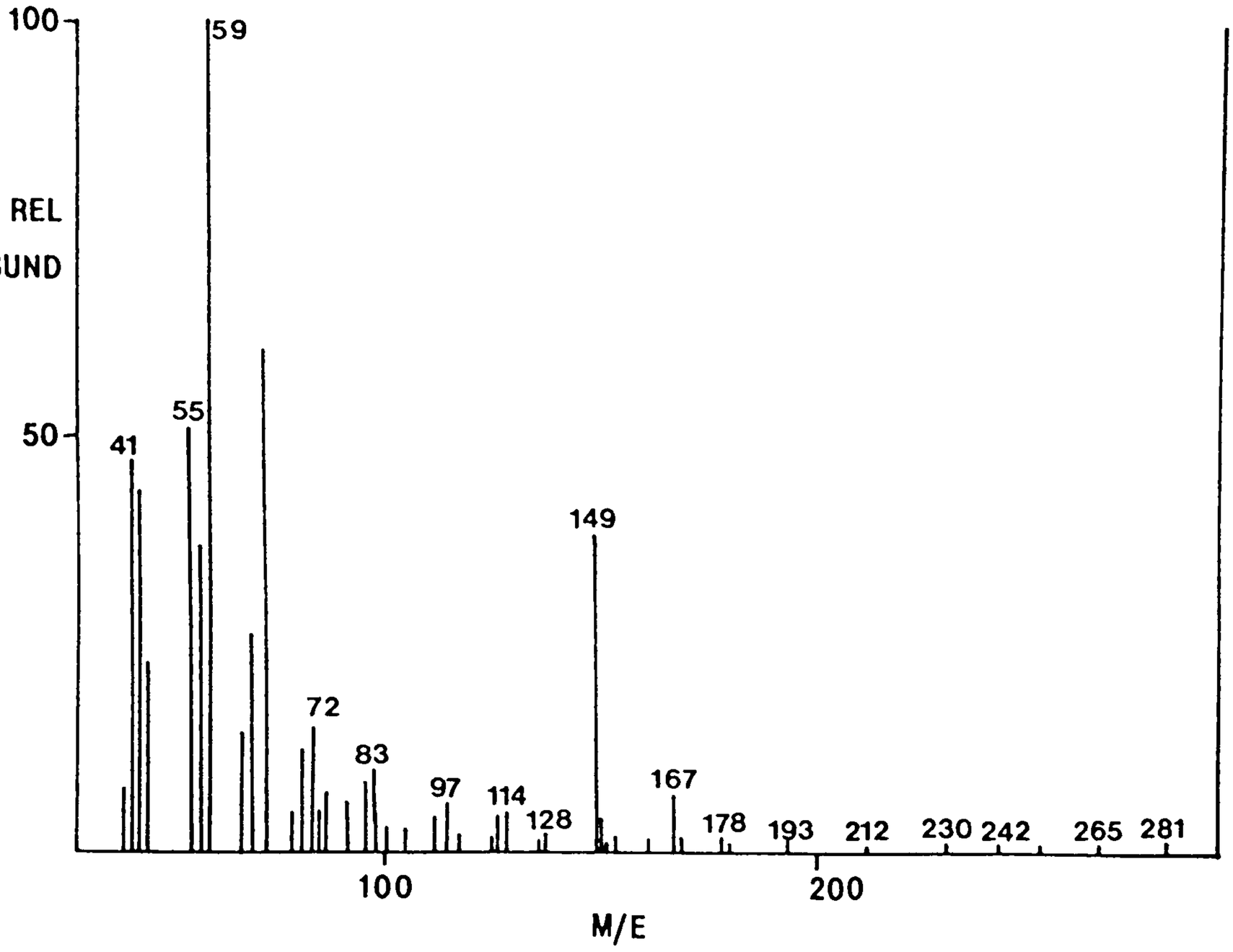

Fig.3.12 Mass Spectrum of T130 peak D

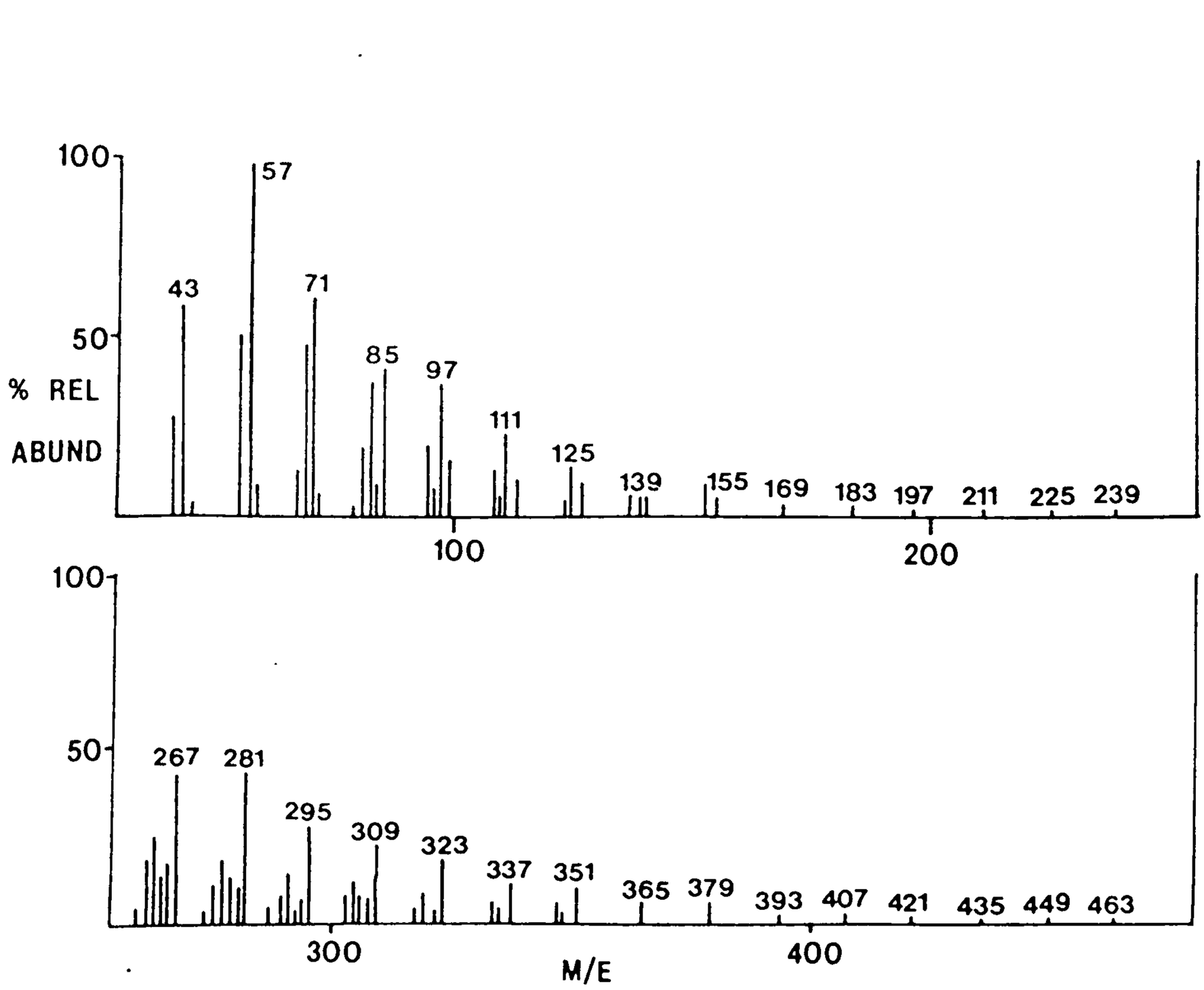

Fig.3.13 Mass spectrum of T130 peak D

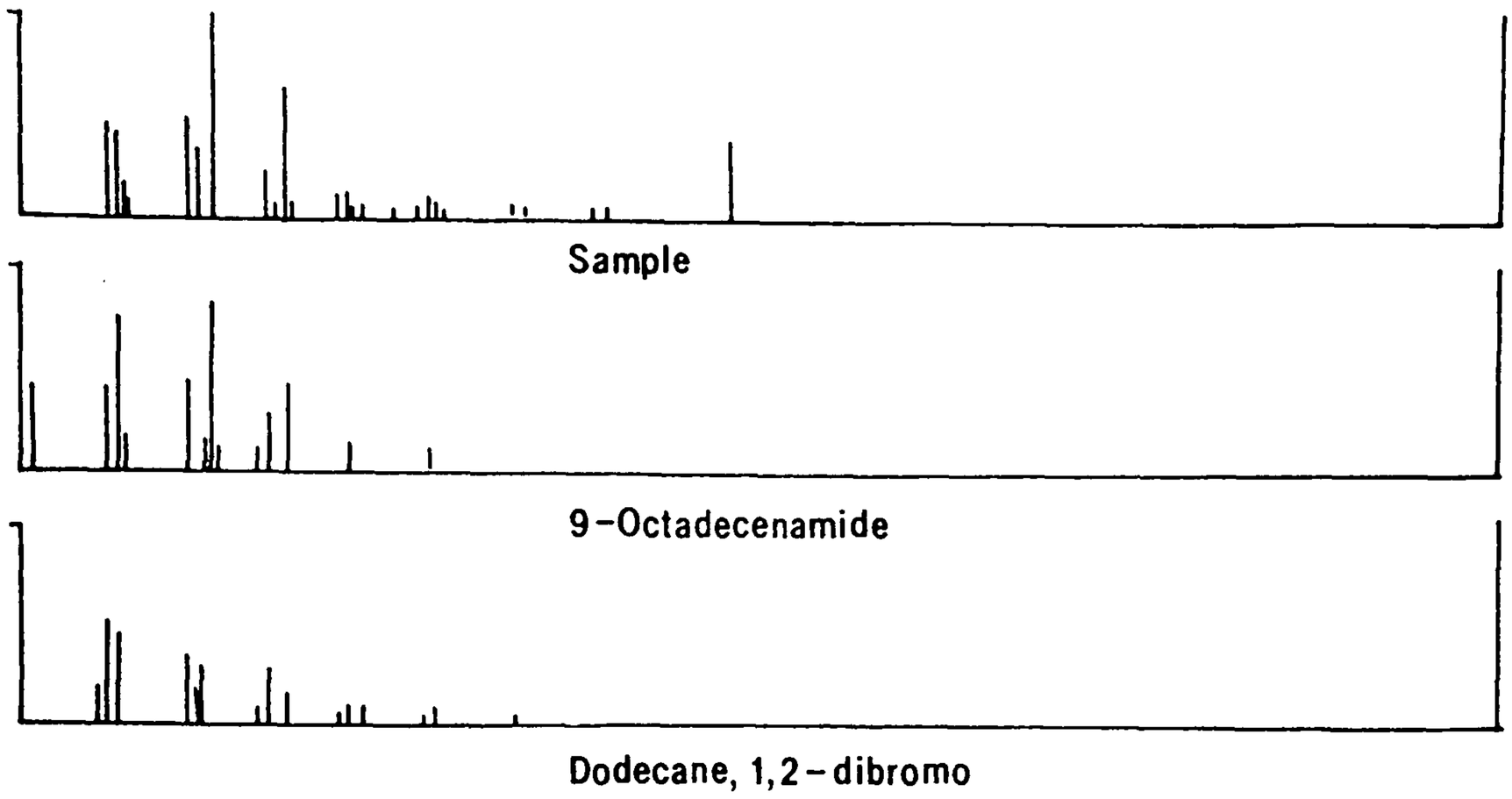

Fig.3.14 Library search of T130 peak D

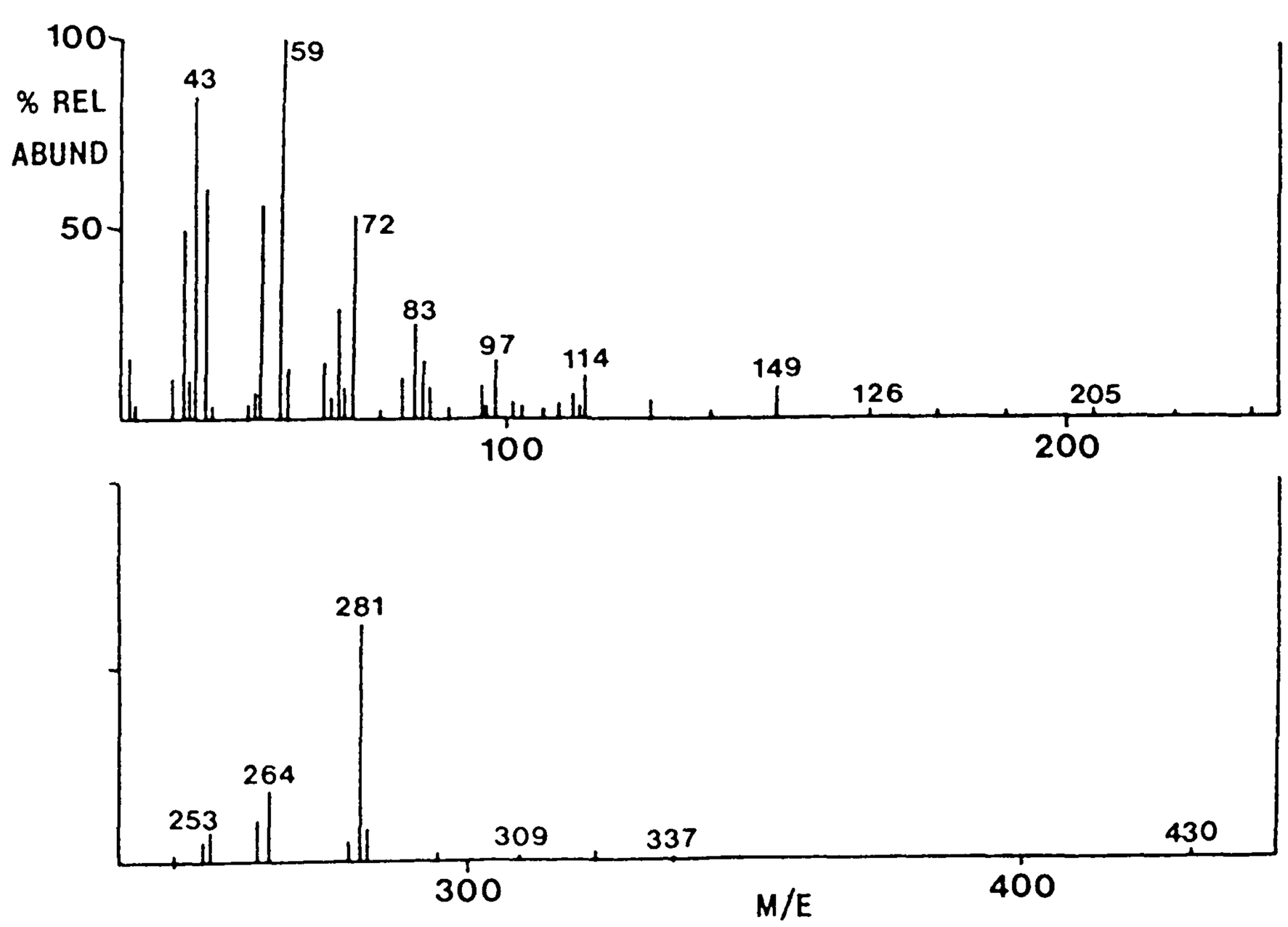

Fig.3.15 Mass spectrum of T180 peak E.

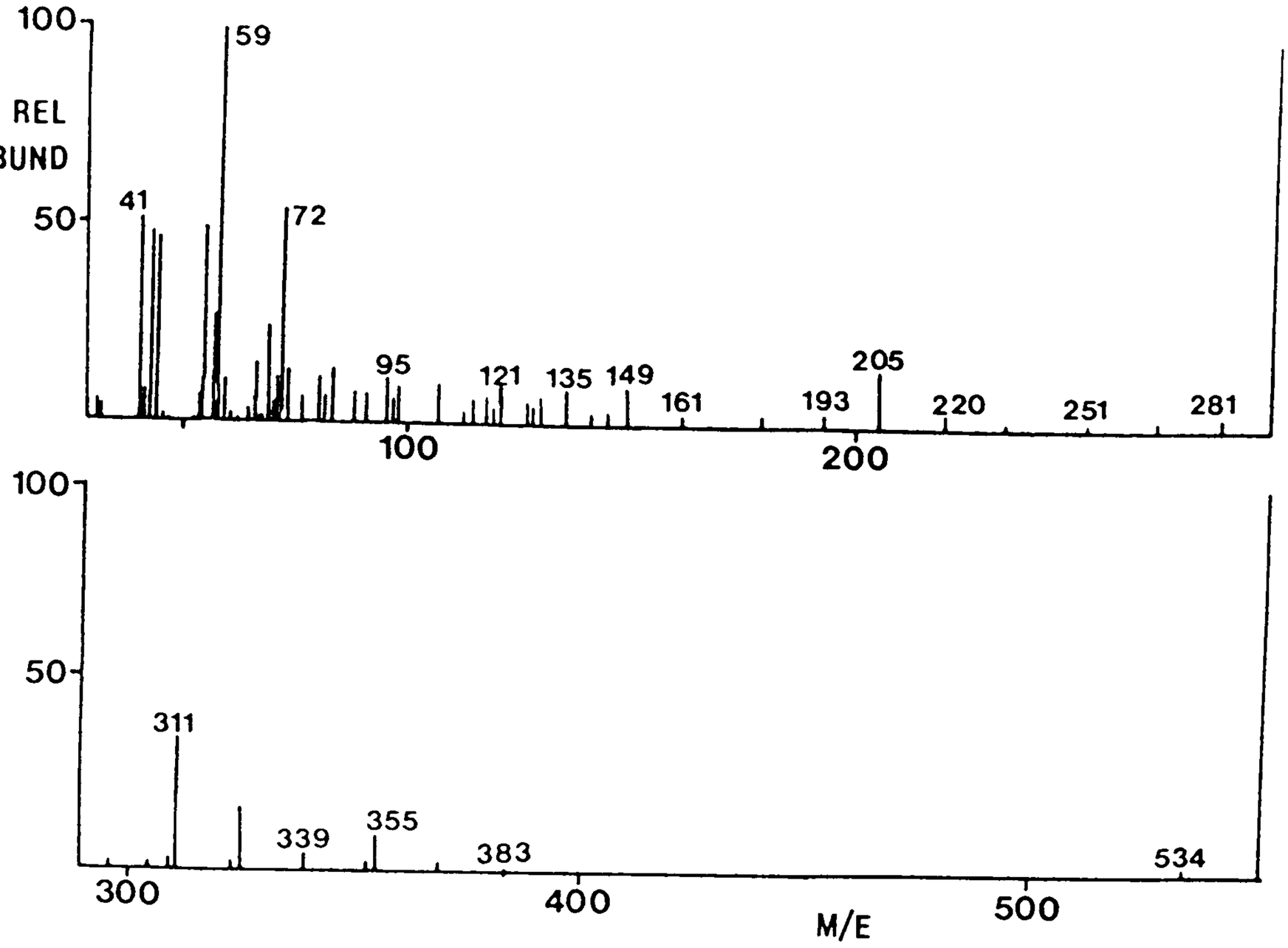

Fig.3.16 Mass spectrum of T180 peak F.

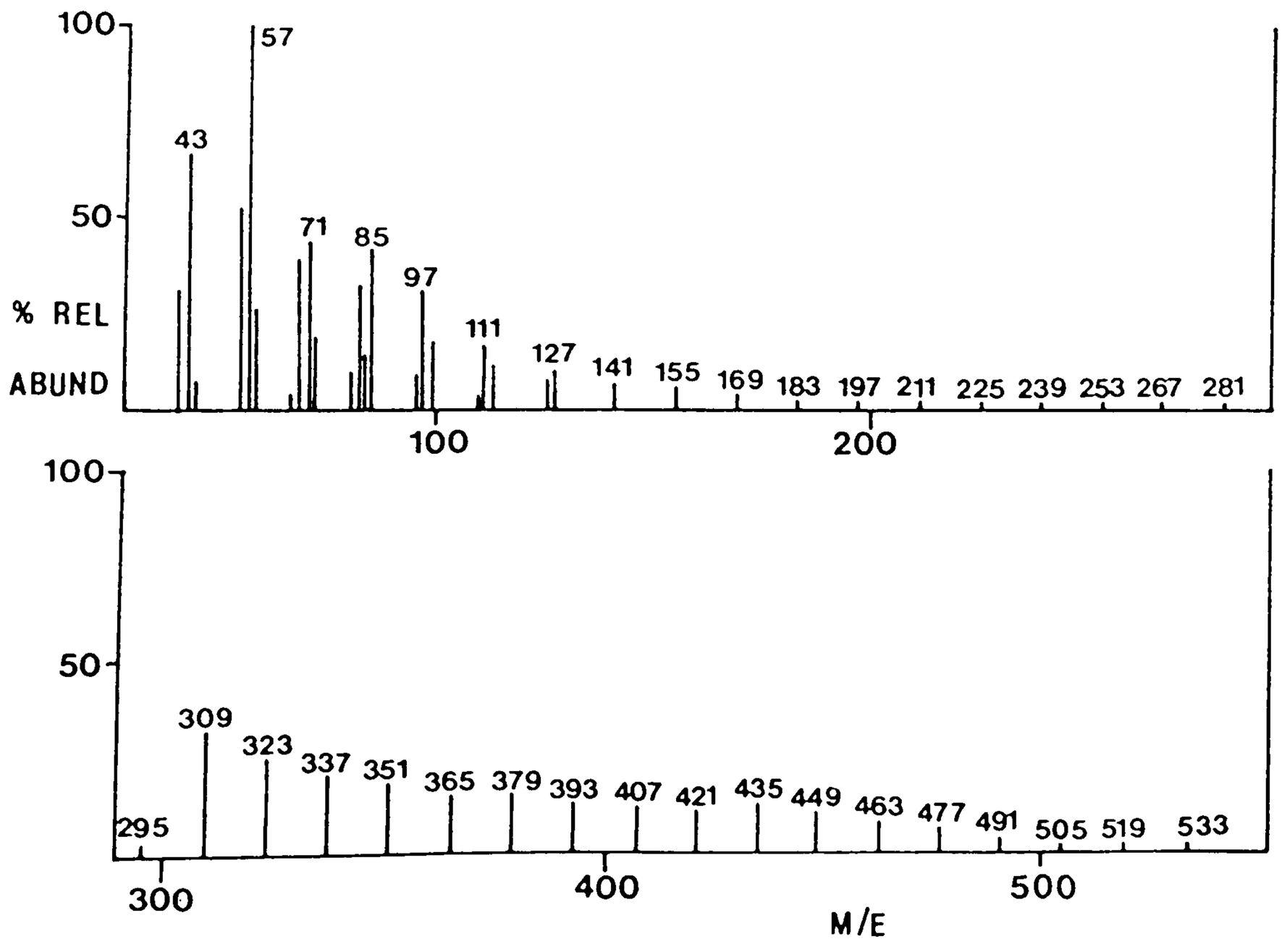

Fig.3.17 Mass spectrum of T180 peak G

Obviously, there is some contamination which has obliterated the surfactant component. This is not proved, but it appears likely that this peak is a hydrocarbon.

It was expected that the mass spectra of T180 would be similar to that of T130. The spectra in Figs.3.15 and 3.16 (peaks E and F in 3.9) are similar only to peak D of T130 (Fig.3.13) from which no evidence of a surfactant can be seen. The highest mass fragment in Fig.3.15 is 430, which would correspond to an EO chain length of only about 4 units. The molecule appears to be fragmenting to an extent such that a molecular ion is not seen. The difference in mass numbers tends to imply the loss of small groups of atoms. The library search for this spectrum is not shown since it suggests the same compounds as for T130 peak D.

Fig.3.16 shows the spectra corresponding to peak F in Fig.3.9. The molecular ion (534) again is too low to be an ethoxylated surfactant. Even at the beginning of the chromatograph the first few peaks should have at least 10 EO units, which would give a molecule ion of around 700. The library search again suggests the presence of an amide.

Peak G in Fig.3.17 produces a very similar spectra to peak C on Fig.3.8. The pattern shown in Fig.3.17 shows a continual loss of 28 mass units due to C_2H_4. The protonated molecular ion at 533 corresponds to a hydrocarbon having 38 CH_2 groups.

3.3.5 The Poisson Distribution

The ethoxylation of ethylene glycol (1,2-dihydroxyethene) has been well documented. It has been shown that the reaction products should vary in molecular size in proportions that conform to a Poisson function. Mayhew and Hyatt (66) demonstrated that a similar effect is seen in the ethoxylation of phenols to produce surfactants. Von Tischbirck (67) concluded that the distribution of adducts was largely dependant upon the catalyst employed. It is also a function of the molar ratio of ethene oxide to, say, fatty acids, (68) used in the reaction. The mass spectroscopy analysis positively identified two consecutive peaks in T130 and, assuming that each major peak is an exthoxylate increasing by one unit, a Poisson curve can be drawn. The area under each peak when plotted against the number of EO units should produce a Gaussian shape. The peak areas were determined by the "cut-and-weigh" method. The chromatogram was photocopied and each peak cut out and weighed. These weights were plotted against its corresponding EO number and the result is shown in Fig. 3.18. The percent peak area for each chain length is listed in Table 3.2

The curve follows the Gaussian pattern and shows the major chain length to be slightly less than 13. Generally, there appears to be a greater abundance of surfactant molecules with smaller chain length. Ideally, a theoretical Gaussian curve should be constructed for comparison with the experimental result. For this, information is required from the synthesis procedure which was unavailable here.

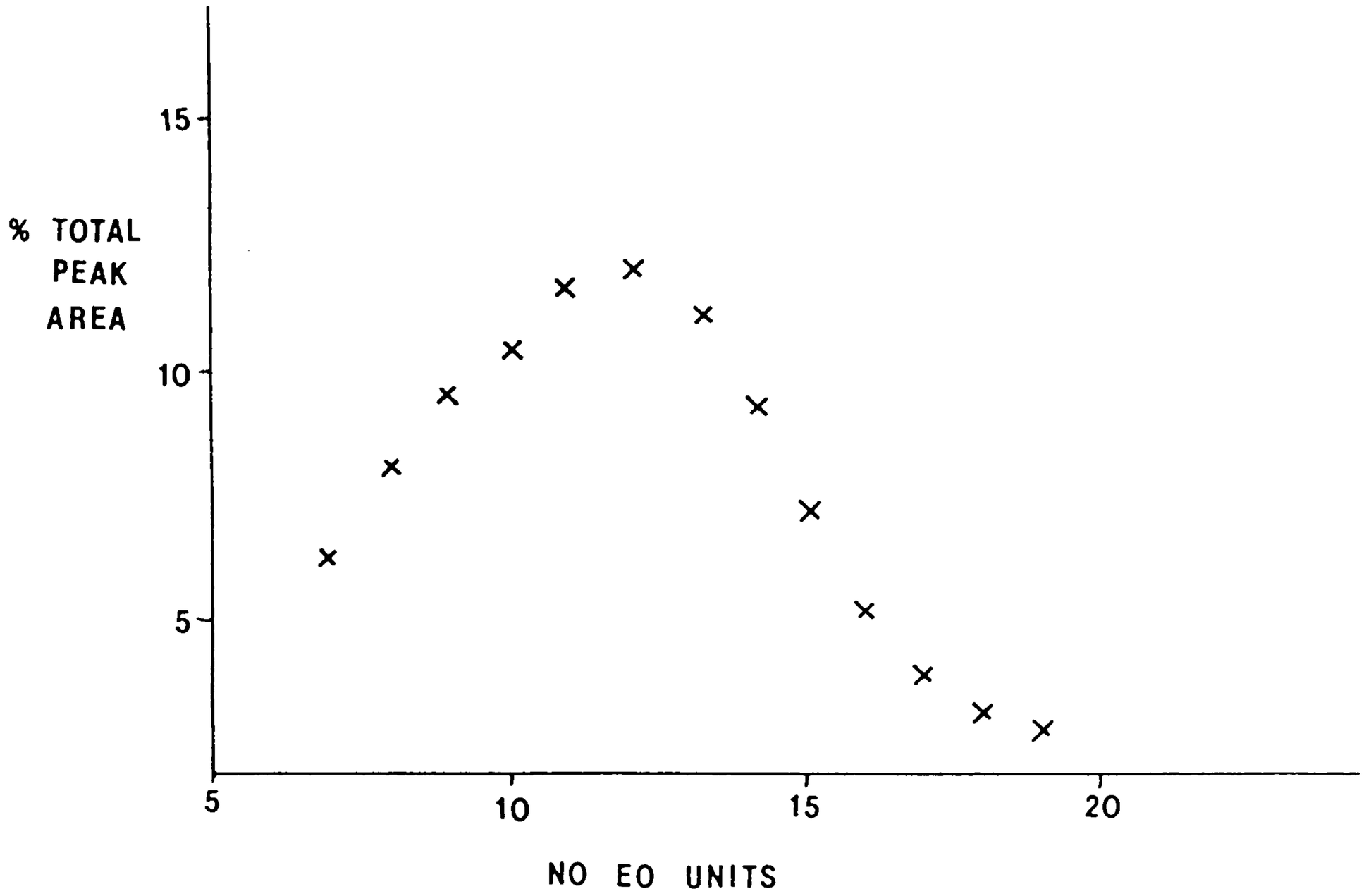

Fig.3.18 The Poisson distribution of the EO chain lengths for T130.

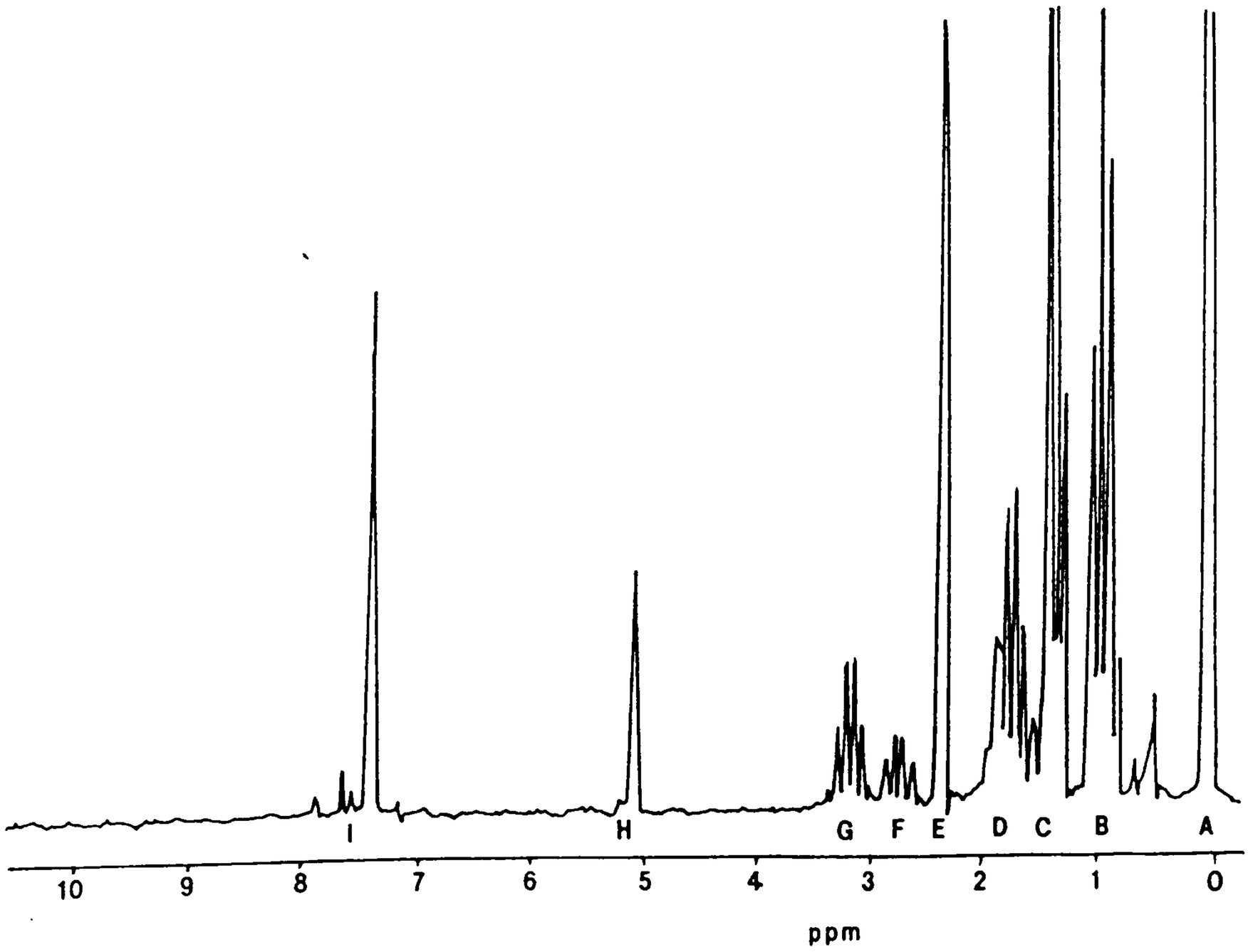

Fig.3.19 NMR spectrum for tributylphenol.

EO Number	Weight of Peak g	% Weight of total
7	0.0229	6.14
8	0.0297	7.97
9	0.0351	9.42
10	0.0386	10.36
11	0.0432	11.59
12	0.0435	12.07
13	0.0414	11.11
14	0.0348	9.34
15	0.0288	7.20
16	0.0194	5.21
17	0.0145	3.98
18	0.0119	3.19
19	0.0109	2.92
	0.3727	100.41

TABLE 3.2. Fraction of each chain length as a percentage of the total sample.

		1H	13C
Pulse Width (30° Pulse)	us.	6.00	3.00
Pulse Delay	s.	15.00	2.50
Frequency	Hz.	4000	6000
Filter at	Hz.	2000	3500
Aquisition time	s.	2.0480	1.3640
Observation Frequency	MHz.	199.50	25.05
Irradiation Frequency	Hz.	57.20	99.50

TABLE 3.3 Conditions for 1H and 13C NMR analysis.

3.4. Nuclear Magnetic Resonance Spectroscopy

3.4.1. Introduction and Theory

The HPLC and MS analysis provides information predominantly only on the ethene oxide chain. However nuclear magnetic resonance spectroscopy is also capable of analysing this group to support the previous results. Furthermore, it can be used to determine the substituents on the aromatic ring and complete the analysis of the whole molecule.

In nuclear magnetic resonance (NMR), the characteristic absorption energy of certain spinning nuclei allows the identification of atomic configurations in the molecule. Every nucleus with spin possesses a magnetic moment, which, under the influence of an external magnetic field, can take up different orientations with respect to that field. Absorption occurs when these nuclei undergo transitions from one alignment to an opposite one. The amount of energy required to cause a nucleus to realign depends on its chemical environment, and is proportional to the strength of the applied field. Magnetic nuclei that have been studied extensively apart from ^{1}H and ^{13}C are ^{3}H, ^{19}F and ^{41}P.

Nuclear magnetic resonance (NMR) became of interest to chemists only recently when Knight (69) reported in 1949 that the precise frequency of energy absorption by protons depends on the chemical environment of the hydrogen atoms. Since then, NMR has progressed to become one of the most useful analytical techniques. It is a

rapid and non-destructive method, but there is little in the literature published on its use in the study of surfactants.

The NMR analysis of the surfactants was carried out by ICI Petroleum and Plastics Division (Wilton, Cleveland, U.K.). The spectra from this analysis is unavailable. The NMR analysis of tributylphenol was performed at Brunel University.

3.4.2. Experimental

The HPLC analysis of tributylphenol (Fig. 3.6(b)) produced 4 peaks. It was reasonable to assume that they were due to various positions on the ring of the butyl groups. This was confirmed using proton magnetic nuclear resonance (^{1}H NMR) on a Varian CFT-20 NMR Spectrometer.

The conditions for the experiment are similar to those given in Table 3.3. The surfactants analysed by proton NMR at ICI were T040, T060, T130, T180, T040S, T060S, T150S and B712. The object was to determine the aromatic to EO number ratio. It was performed on a JEOL FX 200 NMR spectrometer and the conditions are given in Table 3.3.

^{13}C NMR was also carried out on T060S, T150S and B712 using a JEOL FX 100 NMR spectrometer. The conditions are also given in Table 3.3. Insufficient sample was available to analyse T040S by ^{13}C NMR.

T150S contained a large amount of solvent which was

removed prior to analysis. The remaining non-volatile fraction was analysed for the aromatic to EO ratio.

3.4.3. Results

The proton NMR spectrum of tributylphenol is shown in Fig. 3.19. The assignments for each peak are given in Table 3.4.

Fig. 3.20 shows four aromatic rings labelled A-D, which correspond to the HPLC chromatogram. This is included in the figure for easier cross-reference.

Table 3.5 lists the aromatic to EO ratio obtained and also the previously assumed values. For T040S and T060S, this ratio was unobtainable due to the high proportion of volatiles present in the samples

3.4.4 Discussion.

Proton NMR confirms the rather impure nature of the tributyl phenol. The four aromatic rings in Fig.3.20. correspond to the peaks labelled A-D in the HPLC chromatogram. Since the least bulky and least polar molecules will be eluted first from the column, the assignment using the NMR data agrees with the chromatographic results.

The NMR results carried out by ICI showed all the samples to be of a similar nature except B712. The B712 result was found to be a long chain linear alcohol which has not been ethoxylated. There is some evidence of branching on the alkyl chain.

Peak	Chemical Shift	Peak Type	Assignment
A	0.62	singlet	Unassigned
B	0.87	quartet	ortho tertiary butyl groups
C	1.30	quartet	para tertiary butyl groups
D	1.67	quartet	meta tertiary butyl groups
E	2.28	singlet	ether by products
F	2.72	quartet	impurities mainly tetra and penta substituted
G	3.10	quartet	phenols
H	5.10	singlet	hydroxyl groups
I	8 to 7	singlet	aromatic hydrocarbons- symmetrical signal shows that the trisubstituted isomer is preferentially formed

TABLE 3.4 Assignments for the NMR peaks.

Surfactant	Aromatic:EO Ratio	Assumed Ratio
T040	1:3.9	1:4
T060	1:5.8	1:6
T130	1:13.1	1:13
T180	1:17	1:18
T150S	1:14	1:15

TABLE 3.5 Number of EO units detected by NMR.

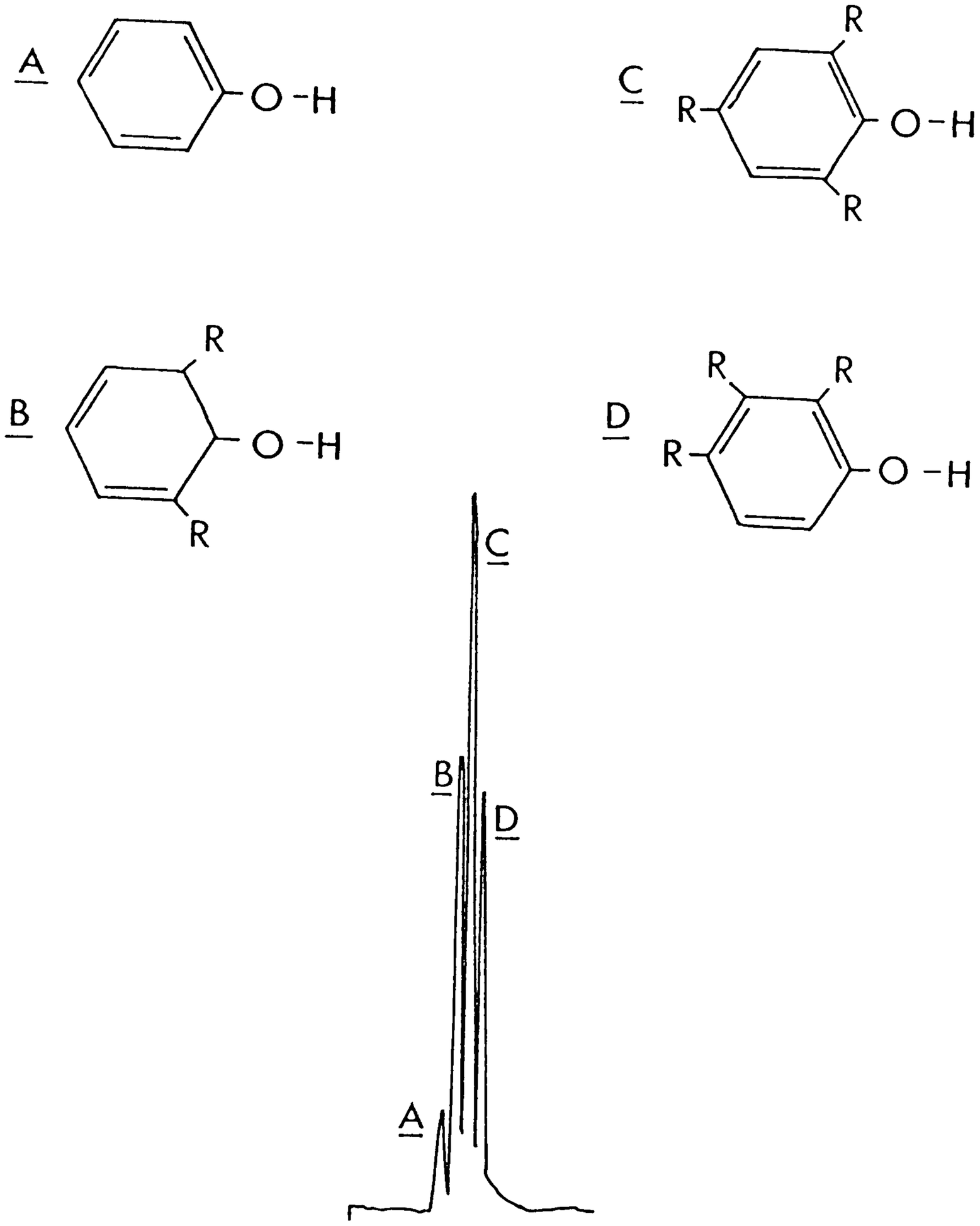

Fig.3.20 Compounds assigned to the NMR spectrum.

The substituents on the Sapogenat ring were originally assumed to be tri-tertiarybutyl groups. Proton NMR confirms the structure to be a secondary butyl group. It is likely that these molecules were prepared by Hoechst via the acid catalysed phenol alkylation with but-2-ene (70).

The volatile component in the sulphonates was suspected to be propan-2-ol. The presence of a methyl ester (type undetermined) was also detected in the sulphonated samples. This may arise if methanol is used in the preparation (71).

The values given in Table.3.5. show good agreement with the original values when calculated from the method of preparation. The true figures are all slightly low.

Overall, the NMR analysis provides some surprising and reliable results. The knowledge that the substituents on the ring are secondary and not tertiarybutyl groups has little, if any, effect on their use for enhanced oil recovery purposes. Now that the structure of the surfactants has been well defined, it is necessary to learn something about their conformations. It is known that the ethene oxide chain is able to assume various shapes depending on the chain length, temperature and possibly added materials.

3.5. The Study of the Confirmation of Surfactants by Raman Spectroscopy.

3.5.1. Introduction.

Surfactants have many properties which have been studied by a wide variety of techniques to determine their micellar size and shape and the extent of hydration, e.g. by molecular weight and viscosity data (72), X-ray diffraction (73) and by ^{1}H and ^{13}C NMR (74). The application of laser Raman spectroscopy to the analysis of surfactants provides more detailed molecular information. A broad study of cationic, anionic and nonionic surfactants using Raman Spectroscopy is given by Kalyanasundaram and Thomas (75). The peaks are assigned using information from earlier Raman studies of polymers such as polyethene glycol (76) or infra-red and Raman spectra of polyethene (77).

They show that aqueous micellar structures have a liquid-like core and that rod-shaped micelles are more ordered than sphere-shaped aggregates. Studies (72) from Raman spectroscopy provide information on the length of the ethene oxide chain. Three basic forms are considered to exist:-

i) planar symmetrical extended zig-zag conformation (see Fig.3.21a));

(ii) meander confirmation (see Fig.3.21.b)) and

(iii) coiled or helical structure (see Fig.3.21.c)).

Taking Triton X100, as an example, the length of the ethene oxide chain (9.5 average EO units) varies from 3.4nm (the zig-zag form), to 1.7nm (meander) and to 1.6nm

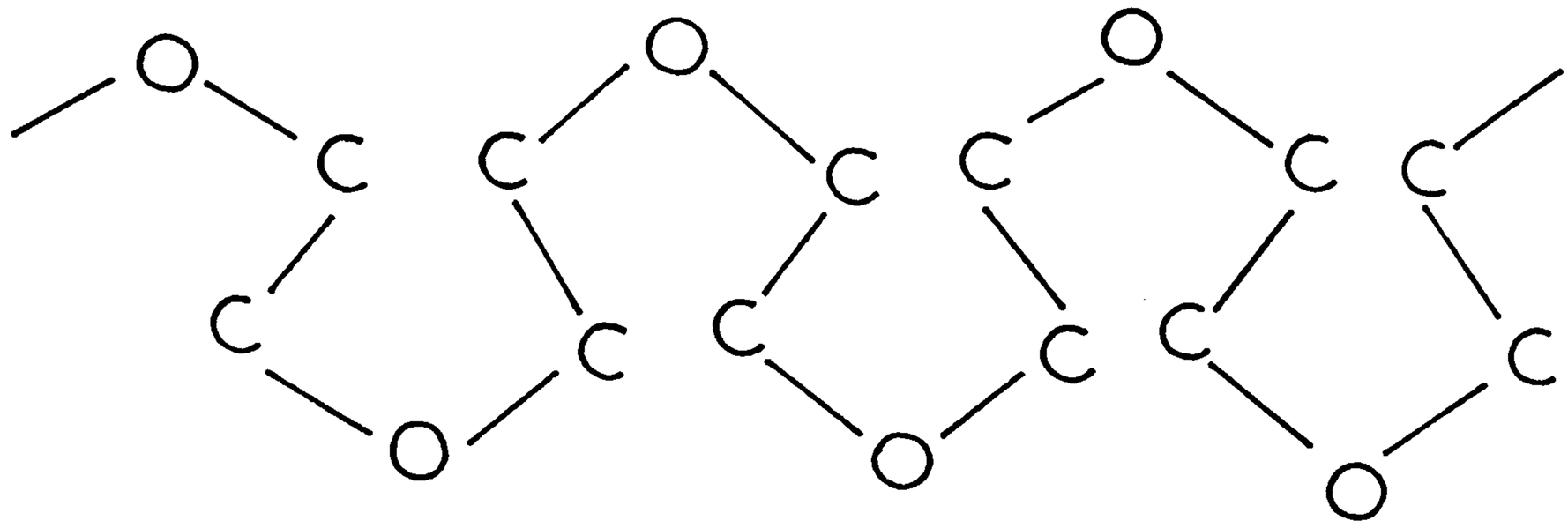

a) zig-zag

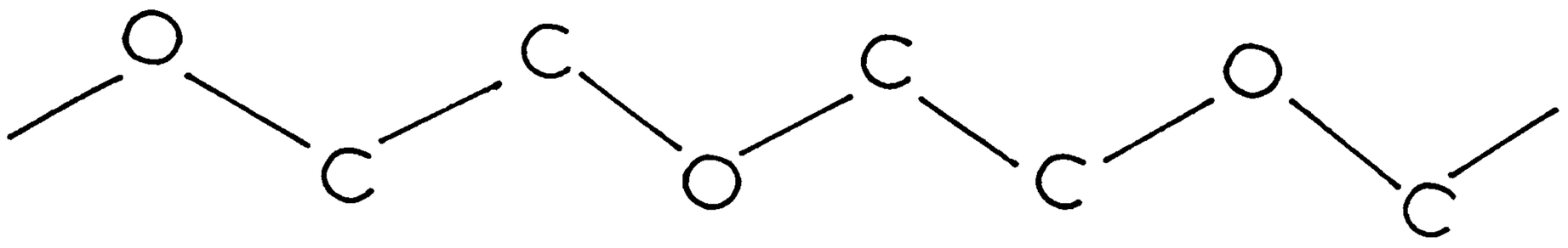

b) meander

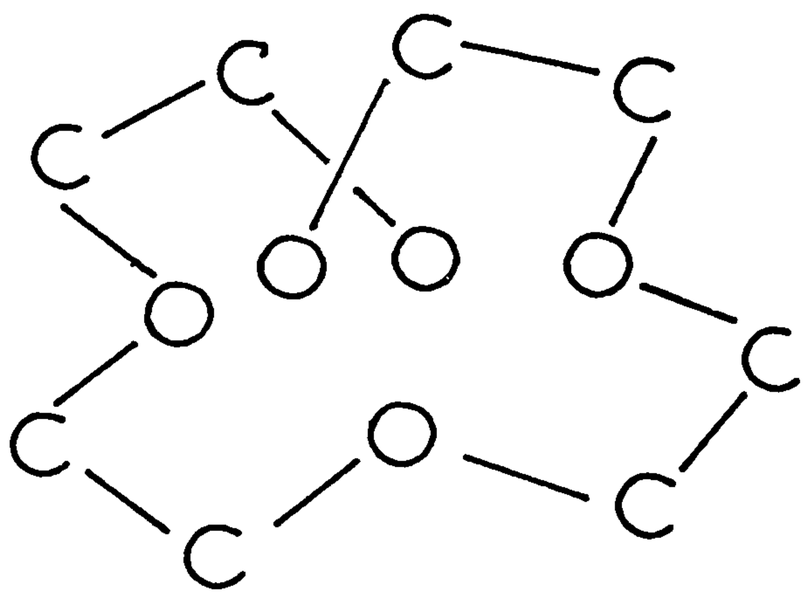

c) helix/coil

Fig.3.21 Conformations of the hydrophilic chain

(coiled or helical form), (78). These considerations lead to the conclusion that the frequencies of the meander forms would be intermediate in the characteristic regions between the frequencies of the other two forms.

The Theory of Raman Spectroscopy

The Raman effect arises when a beam of intense monochromatic light passes through a sample which scatters the light. If a photon interacting with a molecule in the sample is in an elastic collision, the observed light has the same frequency as the incident light and is called Rayleigh scattering. If the light is of a different frequency than the incident light due to an inelastic collision and there is energy transfer between the photon and the sample molecule, Raman scattering is observed. Both of the scattering effects are fairly weak. The light observed due to Rayleigh scattering is about 10^{-3} of the intensity of the incident light and that due to Raman is 10^{-6} or 10^{-7} of the intensity.

In order for a molecule to absorb in the infra-red, there must be a change in the dipole moment of the molecule with the vibration. By contrast, in Raman spectroscopy, the most intense vibrations involved are generally symmetric with less overall change in the dipole moment. Rather, for a vibration to be Raman active, there has to be a change in molecular polarisability. The Raman spectra provides complementary information to the IR spectrum. Certain vibrational modes are inherently stronger in Raman and weaker or absent from the IR

spectrum. Raman activity tends to be a function of the covalent character of bonds and can therefore reveal information regarding the structure of a molecule.

(i) Low Temperature Studies

Low temperature studies of surfactants were not carried out in this study, but can provide useful information. Using Triton X100, Cooney and Bartlett (79) show that at 77K, the surfactant takes on a more ordered structure in favour of the coiled, helical conformation. These low temperatures can pose problems. In particular, scattering of the laser beam increases and results in a loss of spectral quality.

(ii) Aqueous Solution Studies

In a recent study (78), it was shown that the addition of water to Triton X100 results in a reduction of the intensity of peaks which represent the presence of the zig-zag form. This result was confirmed and taken a step further (79). If the ratio of the zig-zag peaks to the helical peaks are plotted against weight % water addition to Triton X100, there is a decrease in the relative proportion of symmetrical zig-zag to the coiled forms, until a plateau is reached at about 33% water and corresponds to the amount of water necessary to hydrate the ethene oxide chain and a translucent gel forms of liquid crystals.

The information obtained here relates to the conformation of the polyoxyethene chain (which was originally reviewed by Rosch (80)). Concentrated surfactants have been used

at room temperature and at elevated temperatures.

3.5.2 Experimental

In the present study, Raman spectra were recorded on the following nonionic materials:

Triton -	X100 -	(octyl phenol polyoxyethene)
	N111 -	(nonyl phenol polyoxyethene)
Sapogenats -	T040 -	(tributyl phenol polyoxyethene)
	T060	"
	T130	"
	T180	"

The sulphonated Sapogenats, T040S and T060S, produced too much scattering of the laser beam to give a spectrum. Their liquids were slightly yellow in colour and contained minute air bubbles which could not be removed on centrifuging.

All the surfactants were used in their concentrated forms. Although the Raman scattering of water is weak, solutions below 20% (wt surfactant in water) were too weak to obtain a strong enough signal. A more powerful laser is required. Above this concentration, the structure of the surfactant changes as liquid crystal gels are formed.

The laser-excited Raman spectra reported in this study were recorded on a Spex Ramalab Raman Spectrometer system. A Coherent Radiation Laboratories argon-ion laser operated at 200 mW power of the 514.5 nm green line was used to excite Raman spectra. The samples were

contained in 1mm melting point capillary tubes. The scattered light was collected by a lens and focussed at the entrance slit of a double monochromator. A water-cooled EMI Type 9862B photomultiplier was used as a detector.

The spectra were run with a slit width of 160 μm, corresponding to a $5cm^{-1}$ band width. Hence the accuracy in the frequencies was estimated to be $+/-2cm^{-1}$. The Raman line positions were calibrated using the 314 cm^{-1} line of carbon tetrachloride.

The high temperature spectra were recorded using a brass heating block connected to a precision temperature controller (Oxford Instruments). The samples were heated up to the required temperatures (298K, 323K and 353K) and equilibrated for about 20 min.

3.5.3. Results

The room temperature studies of three of the surfactants are illustrated in Fig.3.22 (T040), Fig.3.23 (T180) and Fig.3.24 (X100); the others are nearly identical.

The two high temperature spectra are shown in Fig.3.25 (T040) and Fig. 3.26 (X100).

3.5.4 Discussion

The molecular structure of surfactants results in a complex spectrum such that it is not feasible to assign each vibration peak. However, clear evidence emerges for the two dominant conformations - the helix or coil and

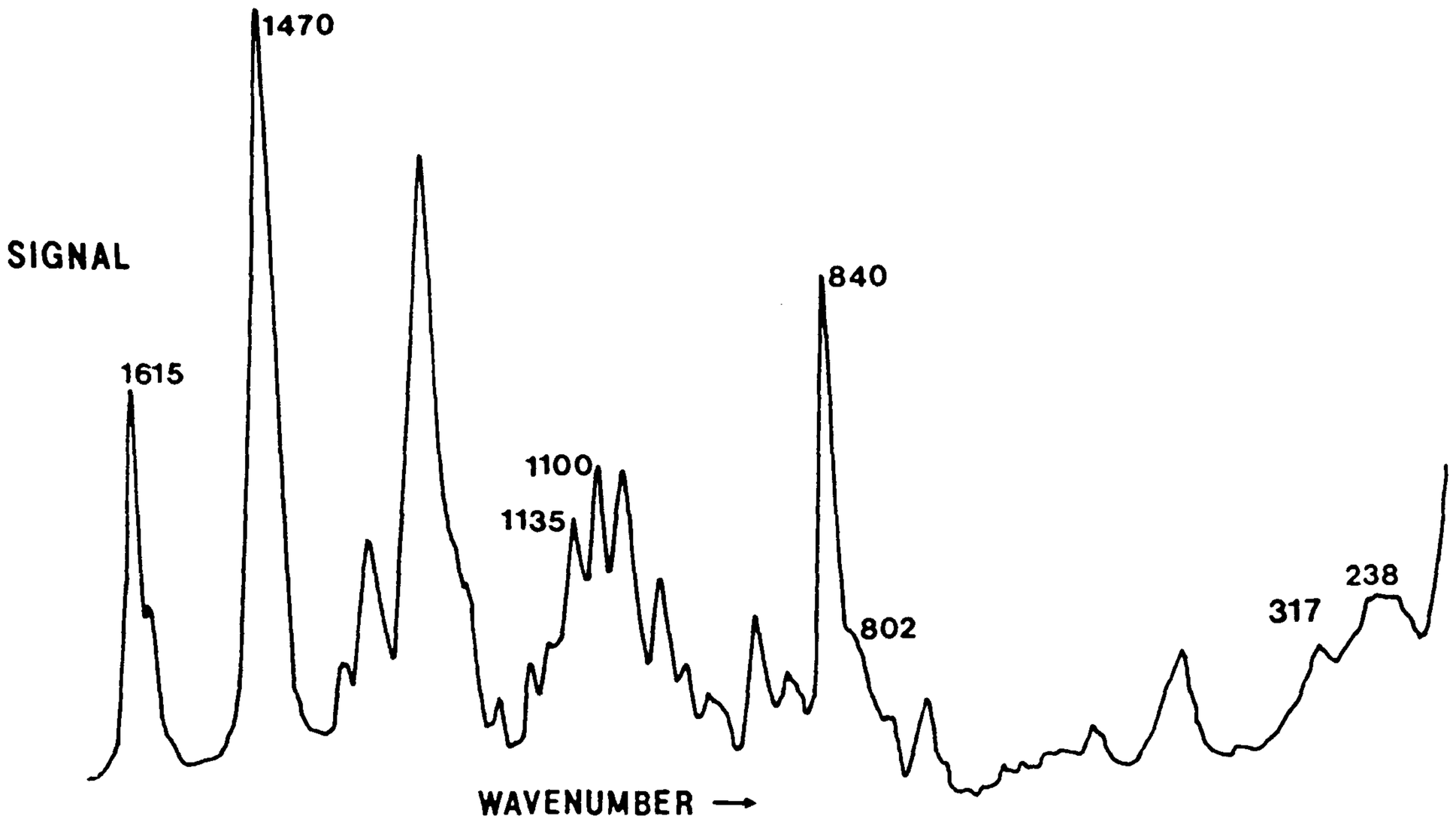

Fig.3.22 Raman spectrum of T040 at 297K.

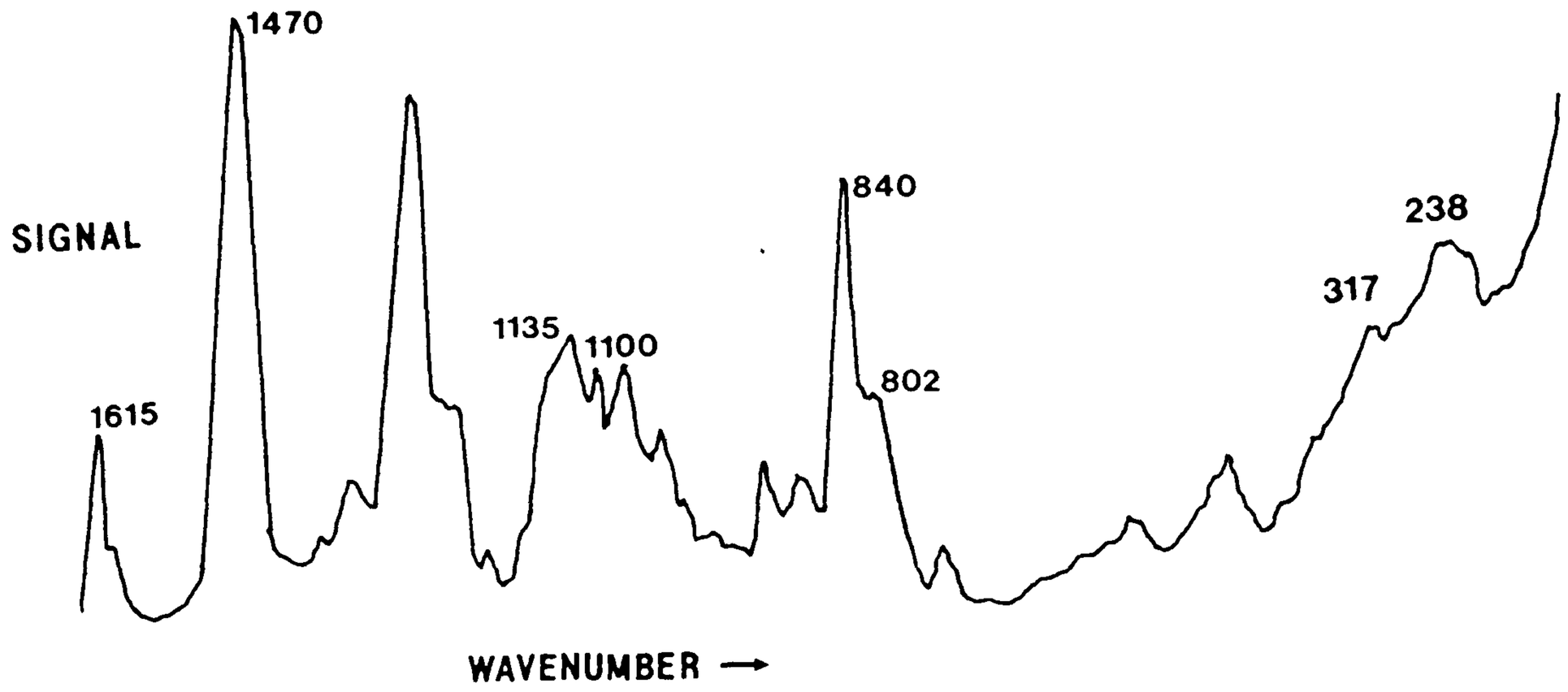

Fig.3.23 Raman spectrum of T180 at 297K.

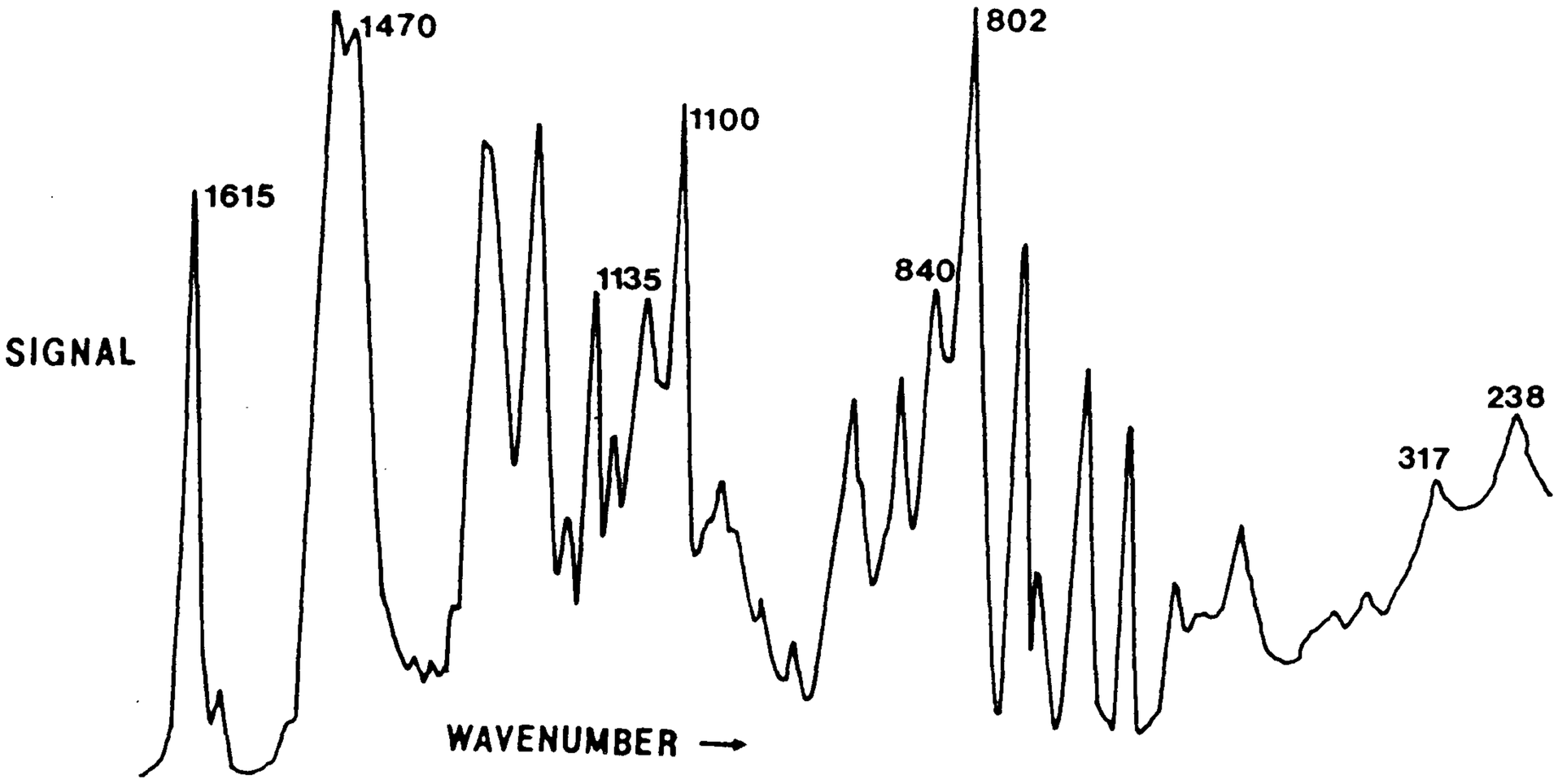

Fig.3.24 Raman spectrum of X100 at 297K.

the zig-zag (the latter is only for surfactants containing an aromatic ring between the alkyl and EO chain).

It is clear to see that all of the peaks of Triton X100 (Fig.3.24) are sharper than that of the Sapogenat (Figs.3.22 and 3.23). The Triton surfactant is pure in that it contains no impurities in the form of precursors, by-products and solvents. These components are probably responsible for the broadening of the peaks of the Sapogenats and leads to loss of resolution. Triton N111 produced a near identical spectrum.

The main band positions are listed in Table 3.6, together with their associated vibrations of the hydrophilic chain.

Ratio I_1 (238/1470)

The peak at 238cm^{-1} is dependent on conformation and is due to a concertina stretch of a methylene group. It is related to the peak at 1470cm^{-1} which is independent of conformation and is due to a bending of the methylene groups. The ratio, I_1, is a measure of the fraction of the zig-zag form; as seen in Fig.3.27, it decreases as the chain lengthens. The molecule favours a helicial structure as the EO number increases. The bands at 238 and at 317cm^{-1} are more pronounced in T040. This ratio, 238/317 is also related to the zig-zag structure; the higher the ratio, the more favoured is this form. They are ill-defined in T180, which suggest that a chain length of less than 18 units is required to obtain information from them.

Wave Number cm^{-1}	Vibration of EO Chain
800-811 1090-1105	Symmetrical zig-zag conformation
815-830 1124-1129	Intermediate meander form
840 1130	Helix/coil conformation

Table 3.6 Vibration and Corresponding Conformation.

		298K	323K	353K
T040	I_2(802/840)	0.356	0.370	0.404
	I_3^2(1100/1135)	1.160	1.279	1.17
X100	I_2(802/840)	1.587	1.539	1.513
	I_3^2(1100/1135)	1.520	1.573	1.652

Table 3.7 Ratios at 3 Different Temperatures.

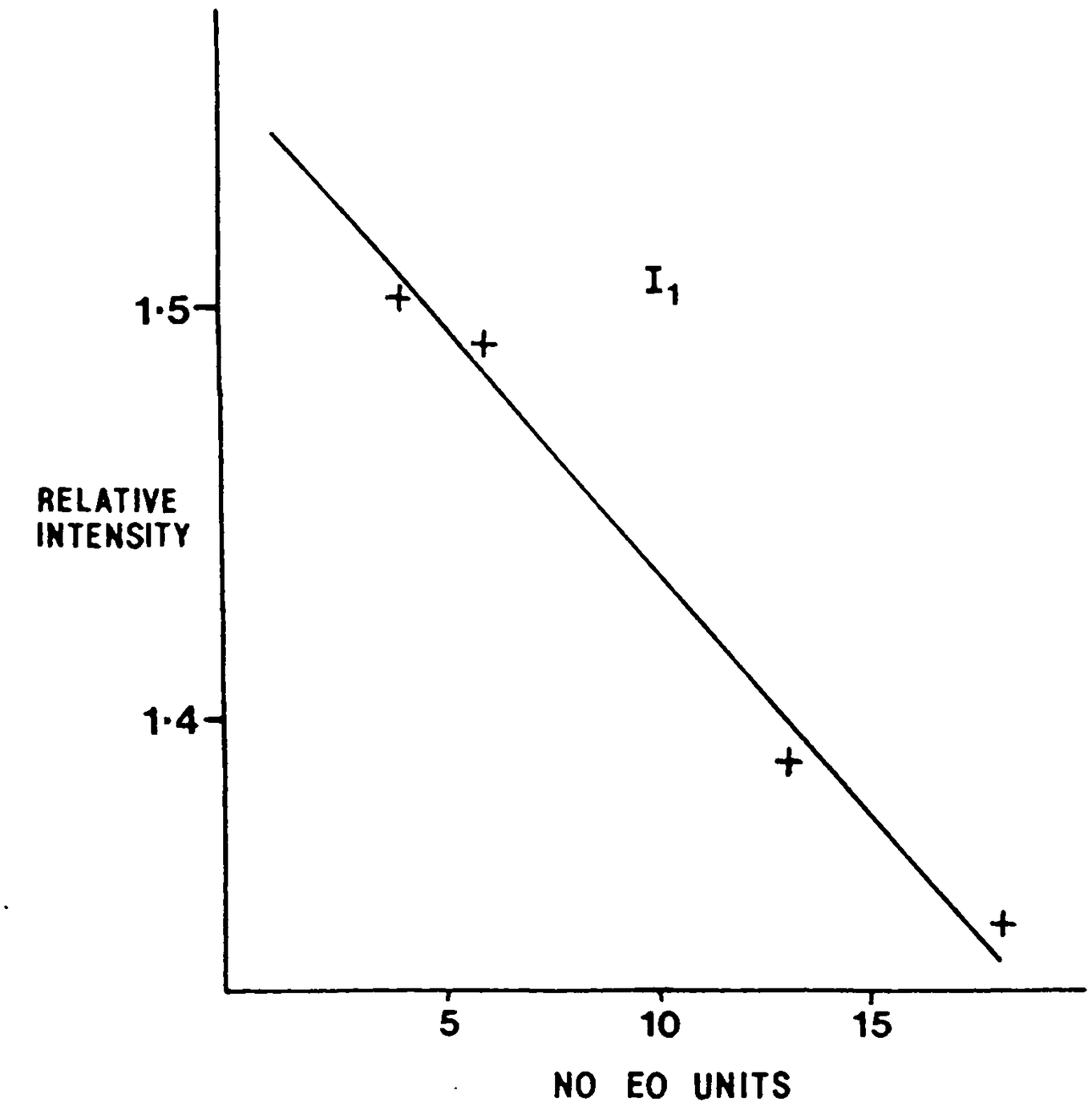

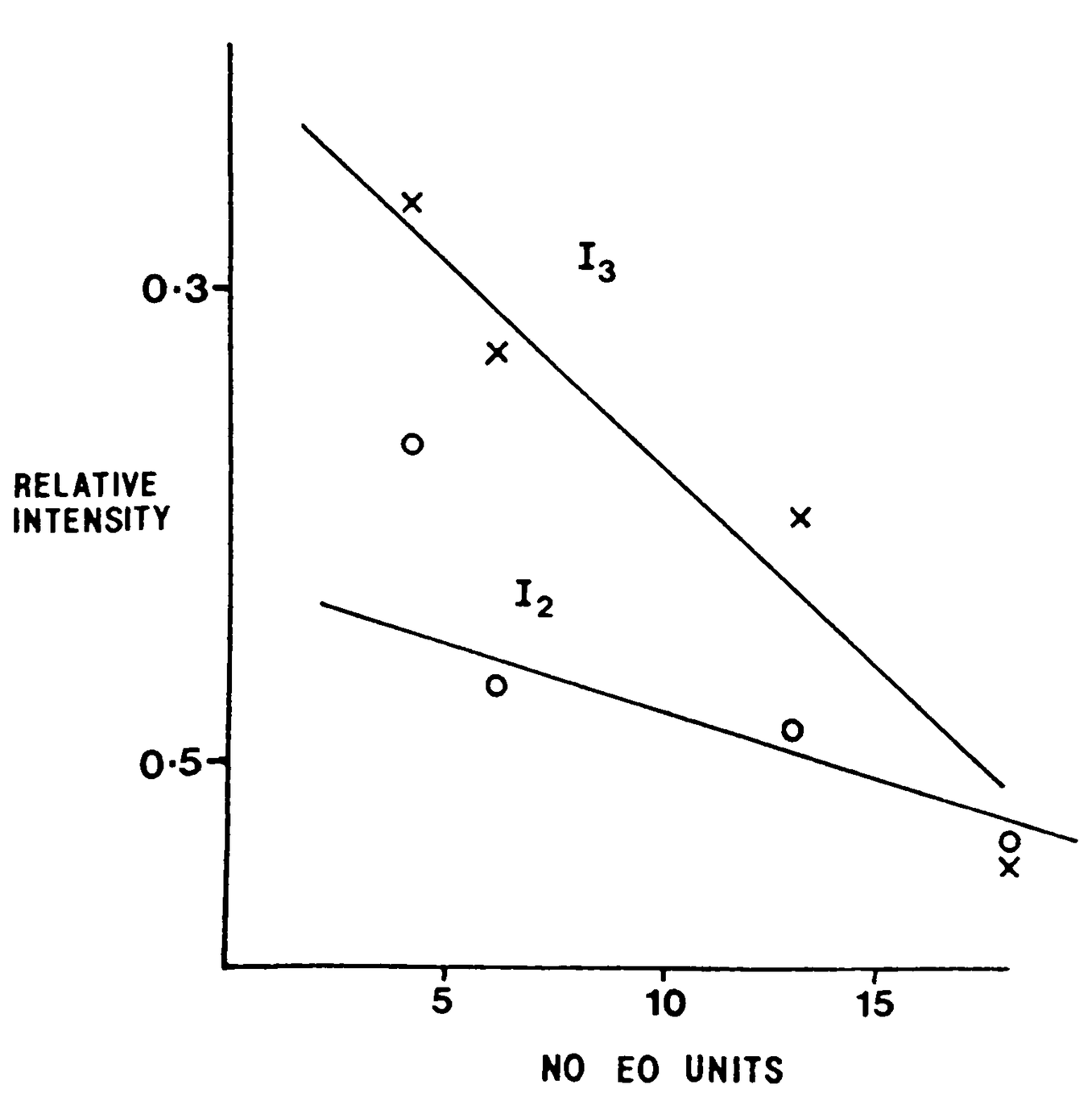

Fig.3.27 Changes in relative intensities with chain length

These peaks are stronger for the octylphenol Triton surfactant than for the Sapogenats. This is because the ring has a greater flexibility in the Triton, which in turn affects the EO chain. The butyl groups on the Sapogenat ring help to stabilise the whole molecule and thus the EO chain shows less movement.

Ratio I_2 (802/840)

The peak at 802cm^{-1} is due to the zig-zag form and that at 840cm^{-1} to the helical structure. This ratio also decreases as the chain increases and a helix form is preferred (see Fig.3.27). These peaks are only evident in surfactants containing an aromatic ring in the head group (78).

The 802cm^{-1} band contains shoulders which have been studied by sub-band analysis (81). It is suggested that aggregation or micellisation causes peaks at 788 and 814cm^{-1}.

Ratio I_3 (1100/1135)

This ratio decreases as the chain length increases (Fig.3.27). The peak at 1135cm^{-1} is due to the helical/coil, which the larger molecules prefer. The points on the graphs in Fig.3.32 show some scatter, but are similar to Cooney (79).

Ring Vibrations

The band at 1615cm^{-1} is due to the aromatic ring. It is more intense for the shorter chain length surfactants. As the chain lengthens, the chain vibrations mask the ring

vibrations. As stated above, the Sapogenats are more stable due to the ring substituents and show less vibration. Triton X100, therefore, will show a more intense peak. The unreacted precursors and also any by-products in the Sapogenats must also be considered and should contribute to this peak.

Intermediate Conformations

The wave number regions, 815-830 and 1124-1129cm^{-1}, are considered to be intermediate between the zig-zag and helical structures. They are attributed to an intermediate meander form or a mixture of ordered and disordered helical/coil forms.

The peaks are very similar in wavenumber to those of the helical/coil conformations and are difficult to distinguish. They are noticeable as small peaks or shoulders in between the pairs of peaks representing the zig-zag and helical forms (ie. between 802 and 840cm^{-1} and 1100 and 1135cm^{-1}).

Studies at Elevated Temperatures

The spectra of T040 and X100 at 353K are given in Figs.3.25 and 3.26.

Overall, the spectra at the lowest temperatures have better resolution than those at the raised temperatures. This is possibly due to the movement of tiny air bubbles which are always inherent in these samples. These scatter the laser beam leading to poorer resolution as less light is collected. At 353K there is poor

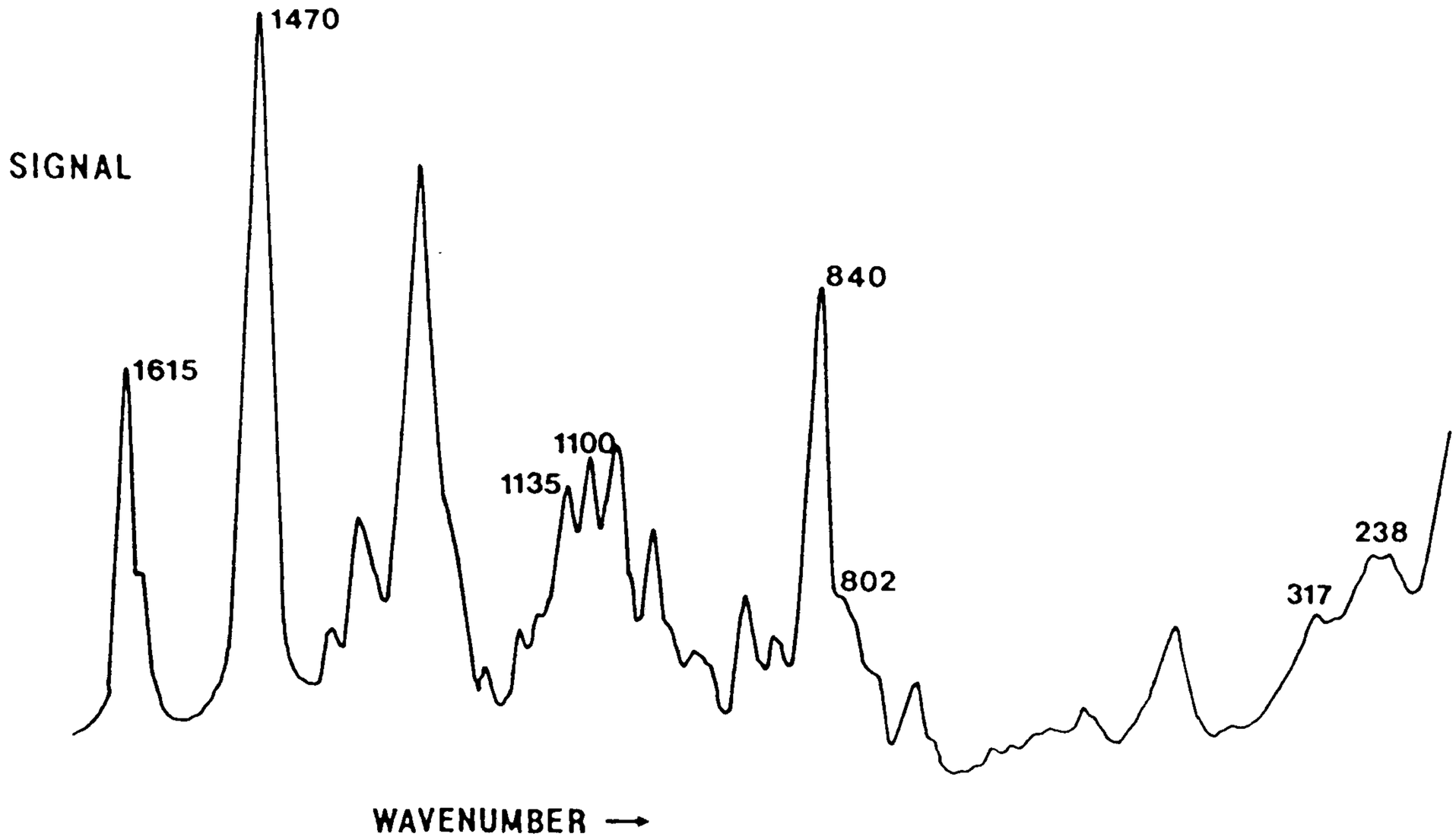

Fig.3.25 Raman spectrum of T040 at 353K.

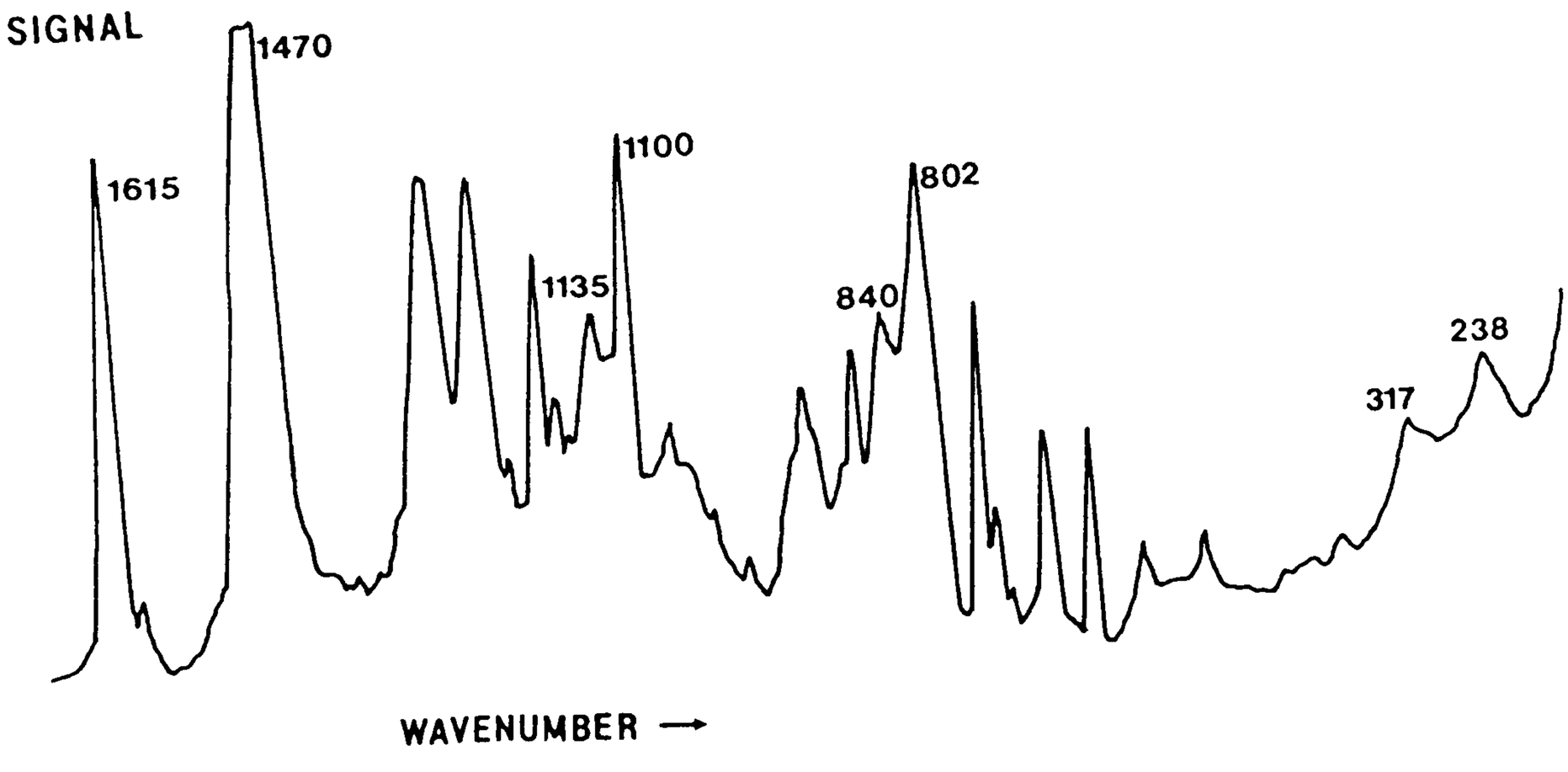

Fig.3.26 Raman spectrum of X100 at 353K.

resolution.

The ratios measured are I_2 (802/840) and I_3 (1100/1135), and the results are listed in Table 3.7.

For T040, both of the ratios increase (with the exception of I_3 at 353K), indicating that the zig-zag form is favoured at the expense of the helical or coil conformation.

In the spectra of X100, the I_3 ratio increases as the conformation takes on the zig-zag form, but the I_2 ratio decreases, as the helical form is prefered over the zig-zag form.

The data concerning the structure and conformation completes the analysis of the surfactants. It remains only to determine the extent of the impurities resulting from the method of synthesis.

3.6 Supplementary Analysis

Further analysis of the sulphonated surfactants T040S, T060S, T150S and B712 was carried out by ICI. The purpose was to determine (by weight %) the content of water, sodium chloride, propan-2-ol, sulphonic acid in the nonionic and anionic material.

3.6.1 Experimental

(i) Water Content:- The Karl Fischer Titration

The Karl Fischer reagent was a pyridinium methyl sulphate which was added to a solution of the surfactant

sample dissolved in dry methanol. This mixture was titrated against a standard Karl Fischer reagent to an electrometric end point.

(ii) Sodium Chloride Content:- Volhards Method

The surfactant was acidified with nitric acid, and pentanol, excess silver nitrate and Ferric Alum indicator added. This solution was titrated with potassium thiocyanate until a permanent brown colour was obtained. This was due to the iron indicator.

(iii) Propan-2-ol Content Using a Gas Chromatographic Method

A standard sample of propan-2-ol was run on a gas chromatograph using a Porapak Q column. Knowing the sample size, retention time and peak area, the presence and weight % of propan-2-ol was calculated.

(iv) Sulphonic Activity By Ion Exchange

The surfactant sample was eluted through a Dowex ion-exchange resin column. The eluate was titrated with sodium hydroxide to a phenolphthalein (pink) end point.

(v) Nonionic Material Content

The surfactant was shaken with an ion-exchange resin and methanol. An aliquot of this was diluted and chloroform, Hyamine (benzethonium chloride, an indicator used in the determination of surfactants) was added. After shaking and having allowed the chloroform to settle, the solution was filtered, the residue dried and weighed. This weight

as a percent of the initial sample weight gave the amount of nonionic material.

(vi) Anionic Material Content

The sample was diluted with distilled water and chloroform and an acid indicator added. This solution was titrated with hyamine until a turquoise-blue colour is obtained.

3.6.2. Results

The results of the suplementary analysis are summarised in Table 3.8

3.6.3. Discussion

All the surfactants contain almost half their weight as water and very little sodium chloride. T150S contains the highest proportion of propan-2-ol but since the other three sulphonates have been used more frequently, it was thought that most of the alcohol had already evaporated and initially they all contained similar amounts.

The anionic material content is not particularly high (30%) except for the B712 surfactant. The results for sulphonic acid are very similar to those of the anionic material, hence, the anionic activity can be assumed to be due to this acid.

The nonionic material is present as unreacted precursor and is not especially prominent in any sample. It is in the greatest concentration in the long chain sulphonate,

	T040S	T060S	T150S	B712
(i) water	49.0	48.0	49.0	48.0
(ii) sodium chloride	4.1	3.6	2.7	Neg.
(iii) 2-propanol	Insufficient sample	<0.1	7.2	<0.1
(iv) sulphonic acid	31.0	35.0	27.0	130.0
(v) nonionic material	Insufficient sample	7.4	11.7	0.3
(vi) anionic material	30.0	31.0	25.0	130.0

Table 3.8 Supplementary Analysis by ICI

(all values are %wt/vol)

T150S, since it is chemically more difficult to sulphonate the molecule as the EO chain lengthens.

CHAPTER 4

4. Physical Properties of Surfactants

4.1 Introduction

A single surfactant or surfactant blend for enhanced oil recovery use must meet several requirements to be successful in recovering residual oils, including:

(i) low interfacial tension between the crude oil and the microemulsion (i.e. to mobilise the residual oil);

(ii) low interfacial tension between the microemulsion and the drive bank (i.e. to prevent trapping of the microemusion in small droplets like the residual oil);

(iii) lower microemulsion mobility than that of the oil bank;

(iv) lower drive bank mobility than that of the microemulsion;

(v) low surfactant retention which determines the minimal amount of chemicals, and;

(vi) maintainance of favourable conditions throughout the flood (i.e. under the range of thermal and salinity conditions prevailing.

Points (iii) and (iv) are required to prevent the microemulsion channeling or fingering through the oil-water bank and the surfactant drive water through the microemulsion bank. The most demanding requirement is to maintain the necessary conditions (i)-(vi) over a long period of time as fluid flows through the heterogeneous reservoir and the phases begin mixing with each other.

With a vast array of commercially-available nonionic and anionic surfactants, those with little or no potential use for EOR in the North Sea were eliminated from this work. The general screening procedures for all of the surfactants evaluated here were:

(i) Solubility and stability in distilled water, BDH brine and Mobil sea water.

(ii) Thermostability 275-370K.

(iii) Viscosity. At ambient and raised temperatures in distilled, BDH and Mobil sea water.

(iv) Surface and interfacial tension at ambient and raised temperaures in distilled, BDH and Mobil sea water.

Other useful information (which is often available from the manufacturers) included:-

hydroxyl value (number of sites available for derivitisation)
water content
active agent content
pour point
density
flash point
pH

Further tests which have been carried out on the promising surfactants are:-

(1) adsorption

(2) phase behaviour

(3) microcapillary de-oiling

(4) laboratory flooding of (a) sand packs and (b) sandstone (core)

These last 4 points will be dealt with in Chapters 5 and 6.

These selection criteria impose constraints on the chemicals used. First, they must meet the basic operation requirements, i.e. reduce the interfacial tension and solubilise the relevant oil. Secondly, they must function under conditions encountered in the reservoir which may vary in temperature, salinity and composition of oil and rock. Mechanical stability is also important, particularly if shear-degradable polymers are included in the surfactant bank for mobility control. This will effect the surface equipment and the ability to inject the fluids but will not be considered here.

Overall, the surfactant system must be compatible with the oil, reservoir fluids and rock matrix. The following chapter discusses the properties of surfactants and their potential for EOR.

4.2 Cloud Point

4.2.1 Introduction

A distinctive feature of surfactant solutions, particularly the nonionics, is the sensitivity to temperature changes. A micellar solution will often turn turbid and precipitate the surfactant out of solution as the temperature is raised beyond a critical point called the Cloud Point or Cloud Temperature. It is also the minimum temperature at which a surfactant completely dissolves in a hot solution as it is cooled. The cloud point marks the condition where a surfactant-rich liquid

begins to form in equilibrium with the micellar solution. This property is an example of thermotropy, or a phase change caused by a temperature change, and usually reaches a limiting value soon after the cmc.

The water solubility and surface activity of surfactants are dependent on the hydrophilic nature of the ether linkages in the ethoxy chain. At room temperature, it is assumed that the ethoxy groups are hydrogen bonded with water, and the water solubility is dependent on the number of hydrated ether linkages. An increase in temperature reduces the forces of hydration and the surfactants begin to form liquid crystal-like phases out of the aqueous solution (82). As this happens, the surfactant becomes less soluble in water and exhibits a cloud point (except for very dilute solutions).

Cloud points place a limit on the surfactant type, concentration and temperature which can be used for EOR. Although nonionics can be used above their cloud points, this increases their adsorption onto reservoir rock which is undesirable (see Chapter 6).

4.2.2 Krafft Point

Now it is worth mentioning the Krafft point, although no experiments were carried out to determine this property.

Surfactants are not very soluble as monomers, but can be in micellar form. The Krafft temperature, T_k, is the temperature above which there is a rapid increase in the solubility of an ionic surfactant. Also, it is the

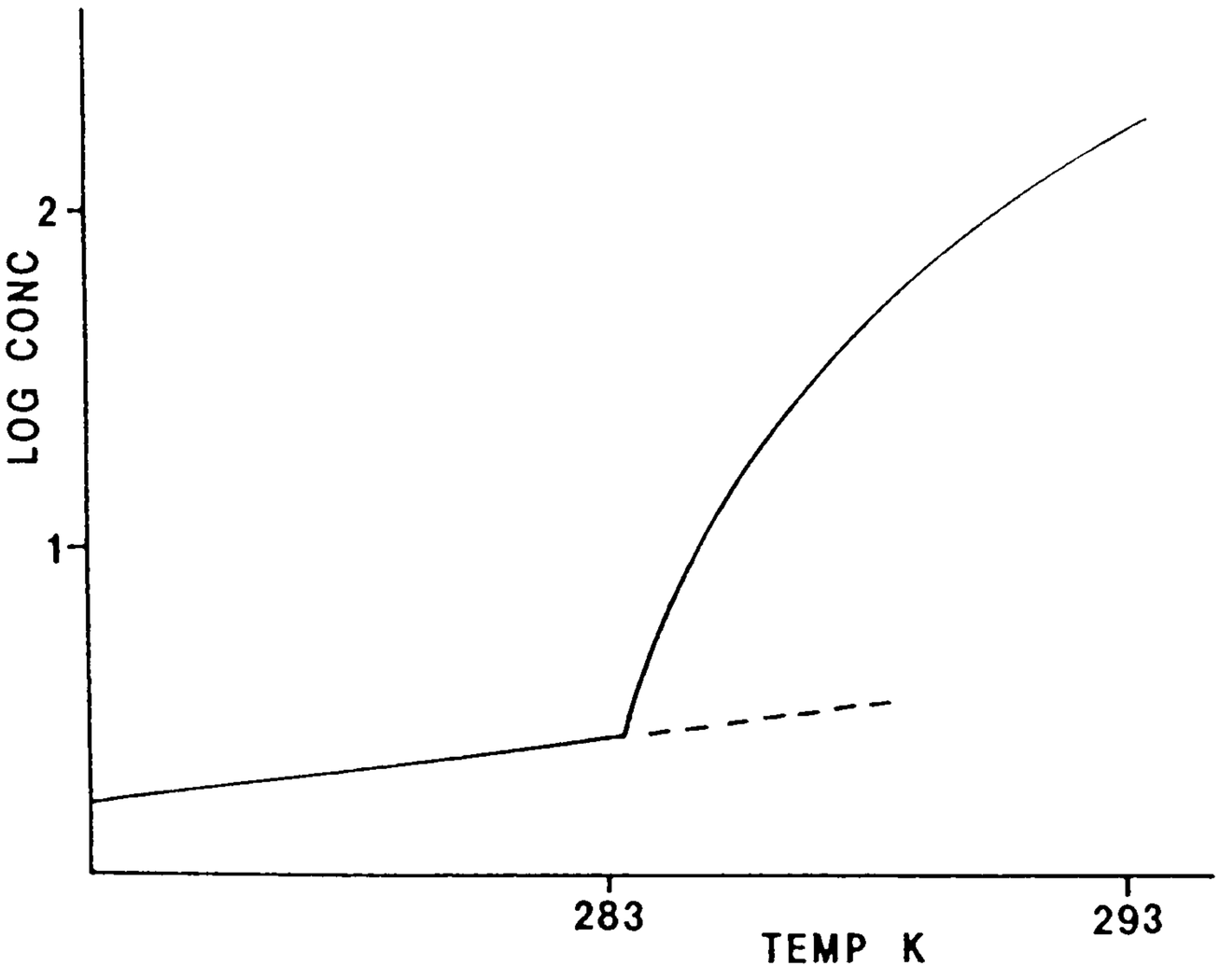

Fig.4.1 Solubility of sodium dodecyl sulphate in water showing the Krafft point.

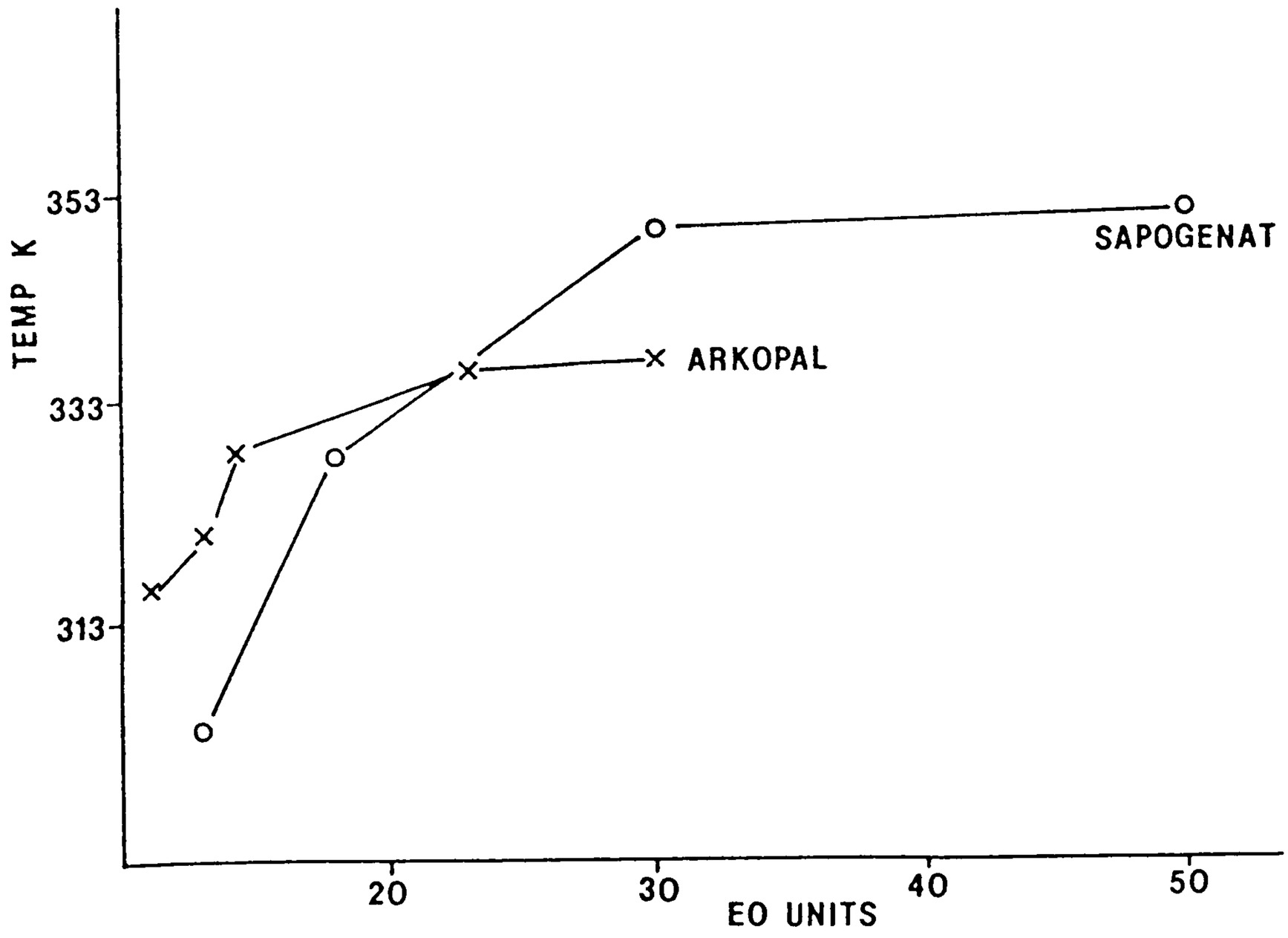

Fig.4.2 Cloud points as a function of chain length.

Surfactant	Water	BDH	MCW
N110	344-345	328-329	318
N130	356-357	338-339	323
N150	365-368	348-349	331
N230	>373	>373	339-341
N300	>373	>373	349-351
T130	335	323	305
T180	357	352-353	330
T300	>373	365-364	350-351
T500	>373	365-364	353-354
T040S	>373	cloudy at r.t	cloudy at r.t
T050S	>373	"	"
T080S	>373	"	"
T100S	>373	347-349	309-308
T150S	>373	>373	345-344
N101	327	315-318	
N111	345	323-331	
N150	368	345-352	
N114	275	-	
N100	338	321-325	
N102	361	333-337	

TABLE 4.1 Variation of Cloud Point (All 1% solutions With Salt Concentration) in (K).

temperature at which the solubility of a surfactant coincides with its cmc. Below this temperature, increasing concentration of the ionic surfactant leads to precipitation. The effect is illustrated in Figure 4.1.

4.2.3 Experimental

Surfactant solutions of varying concentration and salinity were heated slowly (at a rate of 1K min^{-1} near the cloud point) with constant stirring. The temperature was monitored to within 0.1K until the cloud point was observed or the solution boiled. The solution was allowed to cool and the temperature noted when the solution gained its original clarity.

Two concentrations were used, 1% and 0.1% (wt/vol), in distilled water, BDH brine and Mobil reservoir brine. For very accurate measurements, a temperature-programming unit connected to a spectrophotometer and a chart recorder should be used. This was considered to be unnecessary and the results that followed were measured visually.

4.2.4 Results (See Table 4.1)

For the majority of cases, the cloud point (as measured by raising the tempterature) coincided with the value obtained by decreasing the temperature. Where this was not the case, the range of temperatures is given. Changing surfactant concentration caused small (or negligible) depression of the cloud point (i.e. < 1K). A few surfactants from the Triton Series were studied to compare their properties as pure surfactants with those

of the non-purified samples of the Arkopals and Sapogenats.

4.2.5 Discussion

From Table 4.1, two trends are clear. Firstly, the cloud point increases as the ethene oxide chain length increases. With an increasing number of EO units, the molecule becomes slightly more polar and therefore has a greater solubility in water. A plot of cloud points versus EO chain length is shown in Fig. 4.2 for 1% (wt/vol) solutions in synthetic Mobil reservoir brine. The results suggest that greater than 50 EO units are required in surfactants for solution stability at reservoir temperatures of 370K. However both series appear to show a plateau and any further increase in chain length will not significantly raise the cloud point.

Products with a high degree of ethoxylation such as N230, T300 do not show a cloud point in water up to the boiling point at atmospheric pressure. By the addition of salts, it is possible to depress the cloud point so that it can be determined. Table 4.1 also shows the effect of using solutions of BDH brine and Mobil sea water. The cloud point decreases sharply as the salinity increases. This is due to a salting-out process.

Secondly, the effect of dissolved inorganic salts on the water-solubility of surfactants is similar to that of increasing the temperature. The salts have a greater affinity for water than do the ether linkages (in nonionics) and the salts dehydrate the surfactants. The

more soluble inorganic ions will precipitate the surfactant molecules out of solution. The water moleules will preferentially solvate the inorganic ions leaving fewer to solvate the surfactant. Hence the cloud point will be depressed.

The sulphonated surfactants appear turbid only when dissolved in BDH brine or Mobil sea water. The action of these surfactants is not adversely influenced by the cloud point. Therefore they can, to an extent, be used even at temperatures above the cloud point.

It is interesting to note that the Arkopal N150 and the Triton N150 have the same structure and, in spite of the difference in their purity, their cloud points are very similar.

4.3 Viscosity

4.3.1 Introduction

Most standard methods employed for the measurement of the viscosity of liquids are based on experimental application of either the Stokes or Poiseuille equations. The latter was used here and the Poiseuille equation for the coefficient of viscosity of a fluid is:

$$n = \frac{pr^4t}{8lv} \qquad \text{Pa.s}$$

where
v	= volume of liquid	m^3
p	= pressure at head of capillary tube	Pa
r	= radius of capillary tube	m
l	= length of capillary tube	m

It is not always necessary to measure all these quantities as, in practice, the viscosity may be determined by a comparison of a sample with a standard reference (water was used in this instant). When using a standard, the Poiseuille equation now becomes:

$$\frac{n_1}{n_2} = \frac{\rho_1 t_1}{\rho_2 t_2}$$

where ρ = density and was approximately equal to 1 for all samples (as shown in the following results)

t = time for meniscus to move between two measured points.

The equation used for calculating the viscosity was:

$$n = kt$$

where t is the time (in sec) and k is the calibration constant for a particular viscometer.

For enhanced oil recovery, it is necessary to use a surfactant system which has a similar viscosity to the residual oil. The reasons for this are explained in the introduction to this chapter.

4.3.2 Experimental

The experimental measurement of the viscosity of surfactant solutions was carried out using an Ostwald viscometer. Two sizes of viscometer were employed to check for reproducibility of results. In each case, the viscometers were calibrated against water at a chosen

temperature.

Two concentrations of surfactant were used, 1% and 0.1% (wt/vol) at 298K and 323K. The temperatures were maintained by a water bath accurate to ±0.5K.

The samples were dissolved in distilled water and also in a solution containing 10% sodium chloride to simulate the injection water and formation brine mix.

4.3.3 Results

Table 4.2 shows the variation of viscosity with concentration and chain length. Table 4.3 illustrates the effect of temperature on viscosity. Table 4.4 shows the variation when the surfactants were dissolved in a 10% sodium chloride solution.

4.3.4 Discussion

The viscosity decreases (see Table 4.2) as the concentration decreases. For the Sapogenat surfactants, an increase in chain length causes a reduction in viscosity, but there appears to be a minimum value between 18 and 30 EO units. Lengthening the chain further increases the viscosity. This trend is less marked for the lower concentration. The change in viscosity is less constant for the Arkopals but it can still be deduced that there is a minimum viscosity between 15 and 23 EO units.

Viscosity decreases by about 50% in all cases as the temperature is raised to 323K (see Table 4.3). Two

Surfactant	1%	0.1%
T110	1.0400	0.9414
T130	0.9521	0.8914
T180	0.9007	0.8804
T300	0.9888	0.8841
T500	1.0833	0.9299
4EOS	0.9439	0.9018
6EOS	0.9285	0.9041
N090	0.9909	0.8849
N100	0.9569	0.9090
N110	0.9934	0.9326
N130	0.9694	0.953
N150	0.9467	0.9199
N230	0.9495	0.9096
N300	1.0014	0.9198

TABLE 4.2 Viscocity (mPa.s) variations with Concentration
Concentrations are percent weight per volume of
distilled water at 273K.

Surfactant	298K	323K
T110	1.0408	0.6289(cloudy)
T130	0.9521	0.5951
T180	0.9888	0.5583
T300	0.9007	0.5673
T500	1.0833	0.6163
T040S	0.9439	0.5371
T060S	0.9285	0.5460
N090	0.9909	0.6457(cloudy)
N100	0.9569	0.5708
N110	0.9934	0.5595
N130	0.9694	0.5662
N150	0.9467	0.5538
N230	0.9494	0.5703
N300	1.0014	0.5495

TABLE 4.3 Variation of Viscosity(mPa.s) with Temperature.
All are 1% w/v solutions in distilled water

Surfactant	298K (mPa.s)	323K (mPa.s)
T110	1.1320	0.7505(cloudy)
T130	1.1423	0.6368(cloudy)
T180	1.0515	0.5937
T300	1.0684	0.6183
T500	1.1115	0.6205
T040S	1.1001	0.6196(cloudy)
T060S	1.0183	0.6155(cloudy)
N090	1.4009	0.6248(cloudy)
N100	1.1131	0.6332
N110	1.0328	0.6190
N130	1.0328	0.6581
N150	1.0491	0.6005
N230	1.0274	0.6201
N300		

TABLE 4.4 Variation of Viscosity with Temperature.
All 1% w/v solutions in 10% w/v NaCl solution

surfactants, T110 and N090, have reached their cloud points (indicated by an asterisk). The solutions are turbid and the viscosities are abnormally high. This table does not show the same consistency of results as Table 4.2. The Sapogenats show an increase in viscosity at high chain lengths (T300) but the Arkopals do not.

The effect of salt addition (see Table 4.4) is to increase the viscosity. A number of the surfactants have now attained their cloud point since the presence of sodium chloride reduces the surfactant solubility.

The two sulphonates T040S and T060S do not form clear solutions with salt. This does not mean that they have reached their cloud points as they are soluble surfactants but, however, even in distilled water, their solutions are turbid. Their viscosities are not increased greatly by sodium chloride and they can still function (at least for EOR purposes) as cloudy solutions.

4.4 pH

4.4.1 Introduction

The measurement of pH is the basis of monitoring a wide variety of processes using acid-base titrations, rates of reaction etc.. The determination of pH is simple in principle, based on the measurement of the potential of a hydrogen electrode immersed in the sample solution.

pH is defined by the concentration of hydrogen ions in aqueous solution. Water dissociates according to the following equation:

$$H_2O \;<\!\!-\!\!-\!\!>\; H^+ + OH^-$$

using activities, the pH is usually defined as:

$$pH = -\log_e a[H]^+$$

where $a[H]^+$ is the activity coefficient of the hydrogen ion.

For a nonionic surfactant, the dissociation will be very weak:

$$ROH \;<\!\!-\!\!-\!\!>\; RO^- H^+$$

The anionic sulphonated surfactants will be strongly dissociated and should be fairly acidic:

$$RSO_3Na + H_2O \;<\!\!-\!\!-\!\!>\; NaOH^- + H^+SO_3$$

4.4.2 Experimental

The pH of the solutions were measured by a PTI-15 Model pH meter precalibrated with standard buffers of pH 4.00 and 7.00 at the beginning of the measurements and then after about every 10 readings. The temperature was varied using a thermostatted water bath and was accurate to $\pm$0.5K. The parameters varied were temperature, salinity and concentration.

Three surfactants of the Triton series were also studied to observe any trends with purer amphiphilic compounds.

4.4.3 Results

Table 4.5 shows the variation of pH with temperature using surfactants dissolved in distilled water.

Table 4.6 illustrates the variation with salinity using distilled water and BDH brine. Clearly a change in

Surfactant	293K	313K	328K
T040	-	-	-
T060	-	-	-
T100	-	-	-
T110	6.64	6.70	6.76
T130	6.60	6.71	6.89
T180	6.33	6.58	6.82
T300	6.83	7.25	6.55
T500	6.81	6.93	6.44
T040S	6.93	7.14	6.93
T060S	3.65	3.70	3.81
N090	5.02	5.28	5.35
N100	6.64	6.77	6.49
N110	6.35	6.49	6.60
N130	6.60	6.15	6.16
N150	5.65	5.74	5.82
N230	6.57	7.55	-
N300	5.46	5.65	5.43
X100	6.99	6.49	6.55
X102	6.66	6.22	6.29
X114	6.44	6.23	6.29

TABLE 4.5 Variation of pH with Temperature in Distilled Water.

Surfactant	Dist. Water	BDH
T130	6.60	5.96
T180	6.33	5.81
N110	6.35	5.62
N130	6.60	6.12
N150	5.65	5.83
X100	6.99	6.29
X102	6.66	6.03
X114	6.44	6.63

TABLE 4.6 pH variation with Salinity.
Temperature = 328K

concentration from 1% to 10% (wt/vol) did not produce any significant variation in pH.

4.4.4 Discussion

Generally, the Sapogenat nonionic surfactant classes are similar to the Triton series and both have higher pH values than the Arkopal series.

Table 4.5 illustrates an increase in pH as the temperature is increased with a few exceptions (e.g. particularly at 328K, when they tend to decrease; at which temperature some of the surfactants will be at, or approaching, their cloud point).

Addition of ions to the solvent (see Table 4.6) causes a marked lowering of pH since this promotes dissociation. The values do not appear to follow any strict trends, even allowing for experimental error due to fluctuation in solution preparation and instruments. However, the Triton series show less variation. The Sapogenats and Arkopals contain varying amounts of impurities. The presence of solvents will alter the pH but evaporation of these will differ considerably between samples.

The pH results offer little discussion as a criterion for EOR; the operating pH of the Mobil reservoir is 6.5-8.0 and all the surfactants conform to this condition.

4.5 Interfacial Tension

4.5.1 Introduction

One of the major requirements of a surfactant system for

EOR is to generate an ultra-low interfacial tension at the oil-water interface in order to mobilise residual oil. Figure 4.3 shows an oil ganglion trapped by capillarity and pore constriction. The pressure of the curved interface between the two phases sets up a pressure difference which obeys the Laplace equation:

$$\Delta p = \gamma\left(\frac{1}{R_1} + \frac{1}{R_2}\right)$$

where Δp is the pressure difference across the pore and R_1, R_2 are the principle radii of curvature and γ the interfacial tension.

Δp, the capillary pressure opposing flow, is often approximated to:

$$\Delta p = \frac{2\gamma}{R}$$

Mobilisation of the oil drop will occur when Δp is exceeded by the pressure gradient over the length of the drop. The interfacial tension is also related to the contact angle, by Youngs relationship (83):

$$\gamma_{o/s} = \gamma_{w/s} + \gamma_{o/w}\cos$$

where is the interfacial tension for the oil-solid, water-solid and oil-water (see Fig. 4.4).

From the above equations, it can be deduced that a reduction in the interfacial tension will be necessary to mobilise any residual oil. There are various experimental techniques for studying and measuring

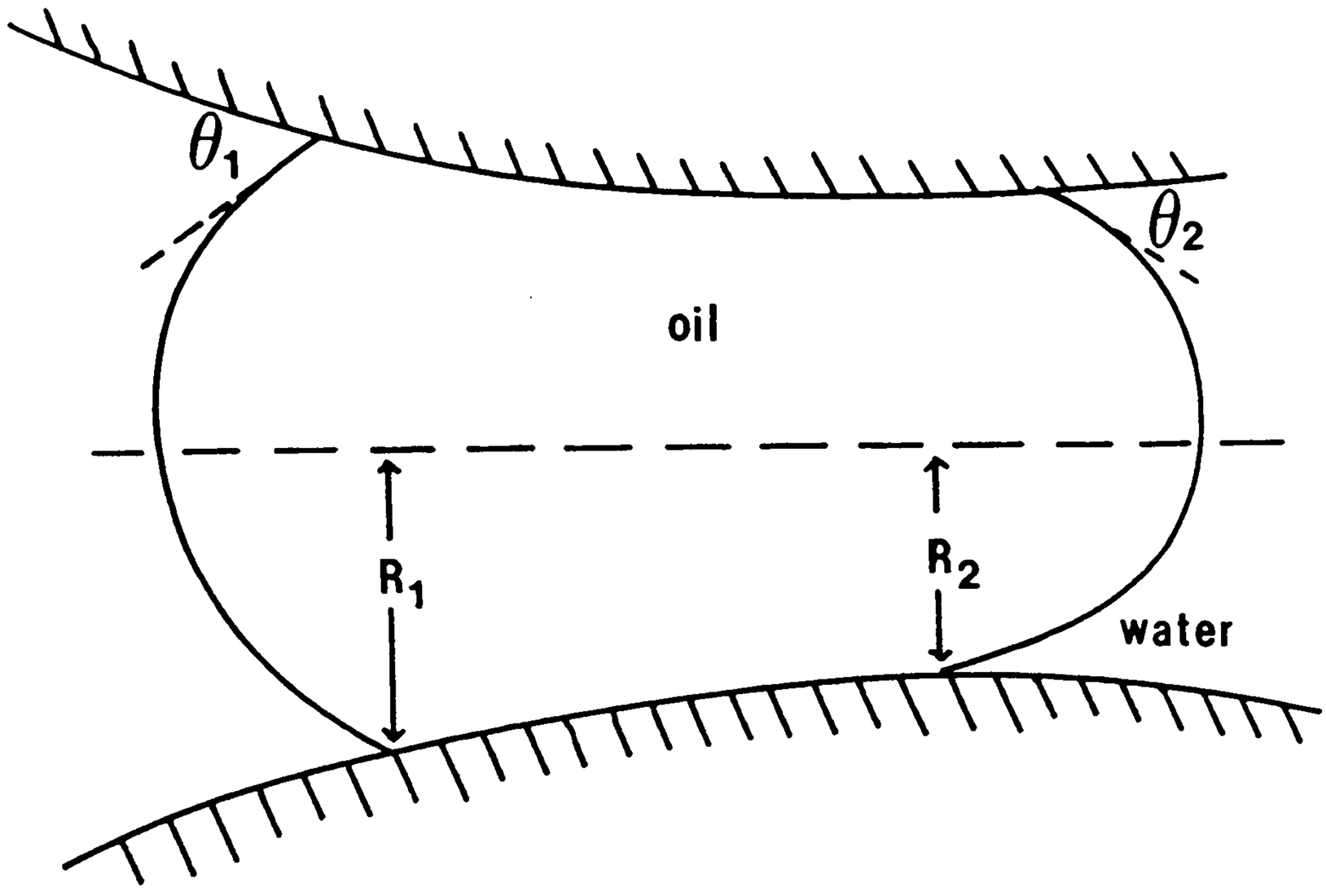

Fig.4.3 Model of an oil ganglion showing the relationship to the Laplace equation.

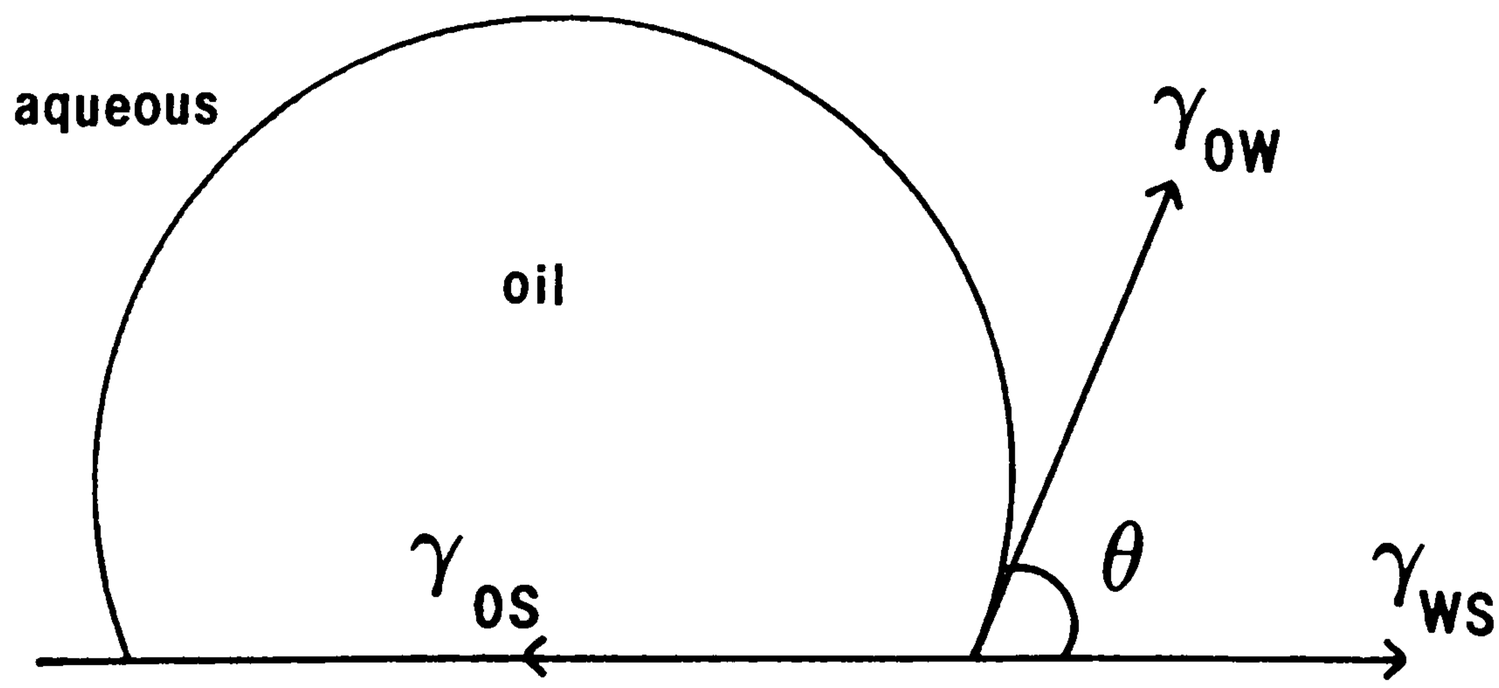

Fig.4.4 Forces on an oil drop in water on a solid surface.

interfacial tension. A few are briefly described below. A classical technique is the capillary rise method. A capillary tube of small diameter is partially inserted into the liquid. It will rise up the tube, opposed by gravity, and an equilibrium height is reached where the overall free energy of the system is minimised. In the pendant drop technique, a drop of the denser fluid is suspended from a capillary tube. Gravity acts to elongate the drop while interfacial tension forces oppose this due to the increase in interfacial area.

Measuring low values of IFT have been revolutionised by the development of the spinning drop apparatus. This was first suggested by Vonnegut in 1942 (84) and was called the rotating bubble method. Modifications (85) on this have since made this to be the most common and reliable technique. It depends on a drop of the oil surrounded by the more dense aqueous phase being spun until equilibrium is reached. In the resulting centrifugal field, the drop elongates along the axis of rotation. Interfacial tension opposes elongation because of the increase in area and a condition whereby the system has minimal free energy is reached. The analysis is similar to the pendant drop with the gravitational acceleration replaced by an acceleration term for a centrifugal field.

The spinning drop technique was employed for this surfactant work, but also the drop weight was initially used. This method is simple and requires little equipment but the results are not considered to be reliable as discussed later, however the theory is now

described.

As a slowly forming drop detaches itself from a capillary tip, the gravitational pull equals the interfacial tension. A secondary, minute bubble, known as Plateaus spherule, can also be seen to detach itself. At this point, the mass of the drop is proportional to the IFT.

$$Mg = Vg\rho = 2\pi R\gamma$$

where	M	=	combined drop masses	g
	V	=	combined drop volumes	g
	R	=	radius of tip	m
	g	=	acceleration due to gravity	ms^{-1}
	γ	=	interfacial tension	Nm^{-1}
	ρ	=	density of drop	Kgm^{-1}

This is a simplified equation and correction factors need to be applied (86). However, assuming the correction factors to be the same for all the solutions studied, the equation can be reduced to:

$$\frac{\gamma_1}{\gamma_2} = \frac{\rho_1 V_1}{\rho_2 V_2} = \frac{M_1}{M_2}$$

where the subscripts 1 and 2 refer to a standard and unknown solution.

4.5.2 Experimental

(i) Drop Weight

Solutions of varying concentration of the 2 surfactants studied; T180 and T300 were added dropwise (about 1 drop per 4 seconds) into decane as shown in Fig. 4.5. The weight increase after a certain number of drops (approx. 60) was noted using a top-pan balance accurate to 0.01g. Using the above equation, the interfacial tension could

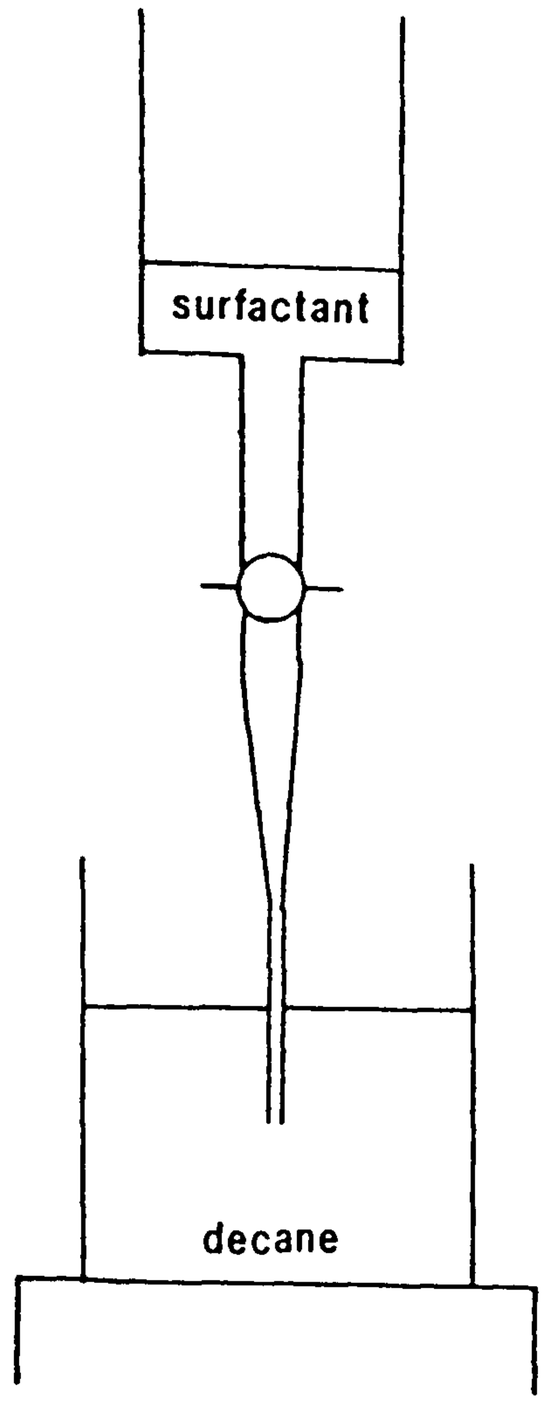

Fig.4.5 Apparatus for the drop-weight interfacial tension method.

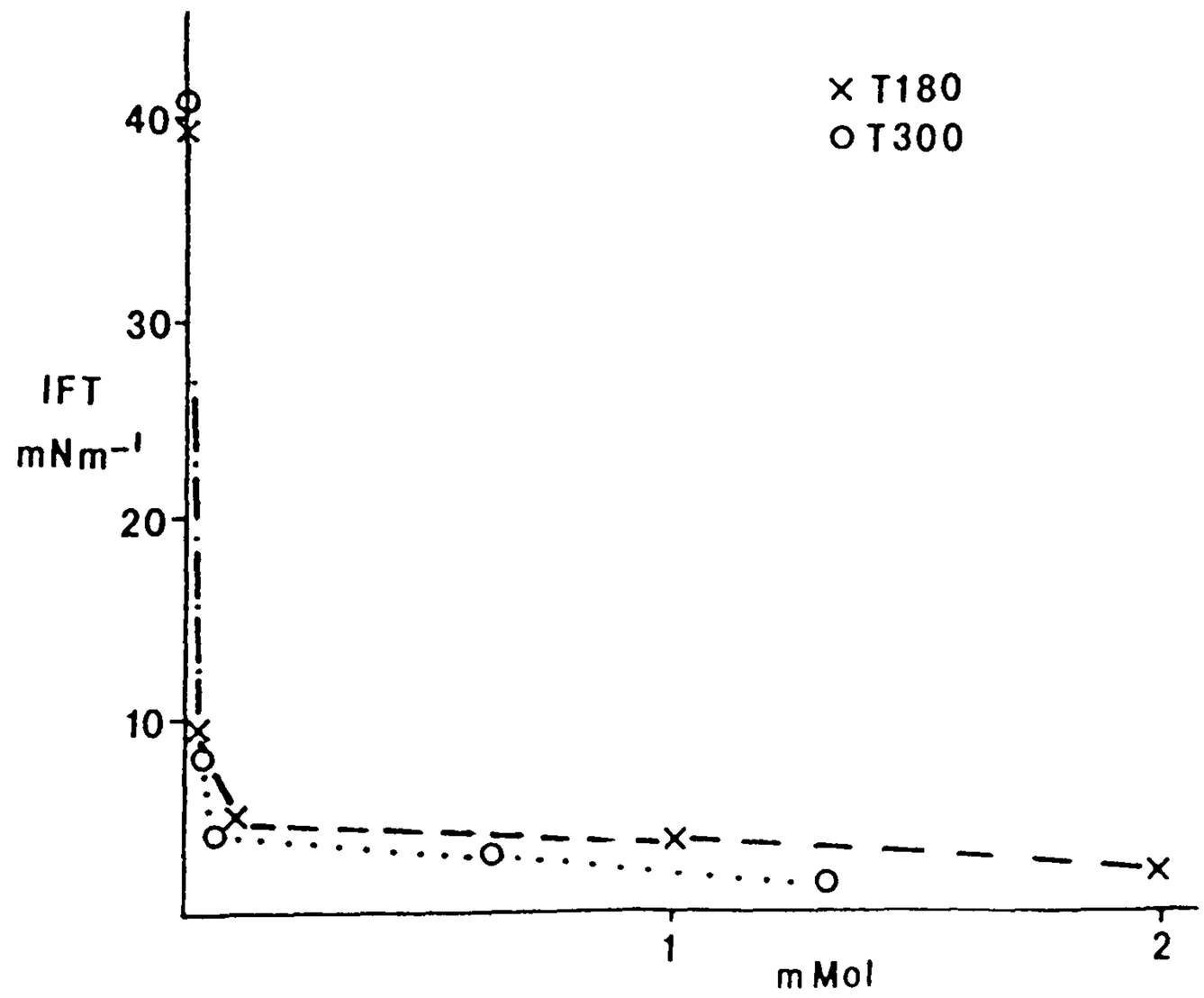

Fig.4.6 Reduction of IFT with surfactant concentration:

be measured. Water was used to calibrate the apparatus. Decane (BDH - HPLC grade) was chosen as the oil since it is pure and simple to work with.

(ii) Spinning Drop Method

The Spinning Drop Tensiometer (SDT) was manufactured by Bailey Engineering Company (Windsor, UK) and was supplied with high temperature facilities.

The surfactant/oil solutions were prepared as follows. A solution of the surfactant was left in contact with the oil (Mobil North Sea Oil) at a surfactant to oil ratio of 9:1 for about 15h with slight agitation. This allowed the 2 layers to come to equilibrium. A sample of the lower aqueous layer was injected into the sample tube of the SDT (about $0.5cm^3$). A $2mm^3$ drop of oil from the upper layer was injected into the SDT tube, which was inserted into the instrument. The tube was spun at about 8000 rpm. along its horizontal axis and the droplet adopts a stable elongated state.

Using the following equation, the interfacial tensions could be calculated:

$$\Gamma = \rho_1 - \rho_2 \ (\text{rpm})^2 \ 2R^3 . (1.5306 \times 10^{-6})$$

where Γ = interfacial tension (Nm^{-1})
ρ_1 = density of aqueous phase (kgm^{-3})
ρ_2^1 = density of oil phase (m)
R = radius of drop (m)
rpm = average reading for rotation

The factor, 1.5306×10^{-6} includes a conversion factor

for rpm to radians per second, and mm to cm. The majority of the experiments were carried out at 296K. Using a circulating oil bath, the temperature was increased to 330.5K (measured by inserting a thermocouple into the sample cavity).

The effect of an electrolyte was studied by using solutions containing 10% (wt/vol) sodium chloride.

4.5.3 Results

The values obtained by the drop weight method are illustrated in Fig. 4.6. The results for the spinning drop tensiometer are shown in Table 4.7.

4.5.4 Discussion

(i) Drop Weight Method

Fig. 4.6 illustrates how the IFT decreases with increasing concentration; the curve obtained being part of the Gibbs adsorption isotherm (see Fig. 4.7). From these curves, an approximate value for the cmc can be obtained. Whilst more points would be desirable, they both have values between 0.01 and 0.1%. Differences in ethene oxide chain length appears to have very little effect on the decrease in IFT. This is due to changes in surface activity achieved by a molecule, depending on both hydrophilic and hydrophobic group characteristics.

The errors involved have been calculated to be of the order of $\pm$10%, and primarily arise in weighing and surface ageing. The additional weight of the secondary bubble formed after each main drop (Plateaus Spherule)

All values mNm^{-1}		296K water	296K 10% NaCl	296K BDH Brine	330.5K
1%	T040	2.5			
0.1%	"	27.9			
1%	T060	8.2			
0.1%	"	50.6			
1%	T130	9.9			
0.1%	"	STICKING			
0.01%	"	15.25			
1%	T180	15.85	11.7		
0.1%	"	20.8	17.7		
0.01%	"	33.1	36.8		
1%	T040S	1.9	UNSTABLE		
0.1%	"	40.5	0.8		
0.01%	"	29.7	22.2		
1%	T060S	22.1	STICKING		
0.1%	"	28.9	"		
0.01%	"	STICKING	"		
0.1%	T060S:IPA	UNSTABLE	UNSTABLE		
0.01%		16.5		39.2	
1%T040S:IPA:SAS60		21.5			
0.1%		45.3		45.2	4.6
0.01%				46.7	
1%T040S:IPA:B712		16.3		STICKING	
0.1%		32.1		38.07	19.9
0.01%		36.8		40.4	31.3

TABLE 4.7 Spinning Drop Interfacial Tension Results.

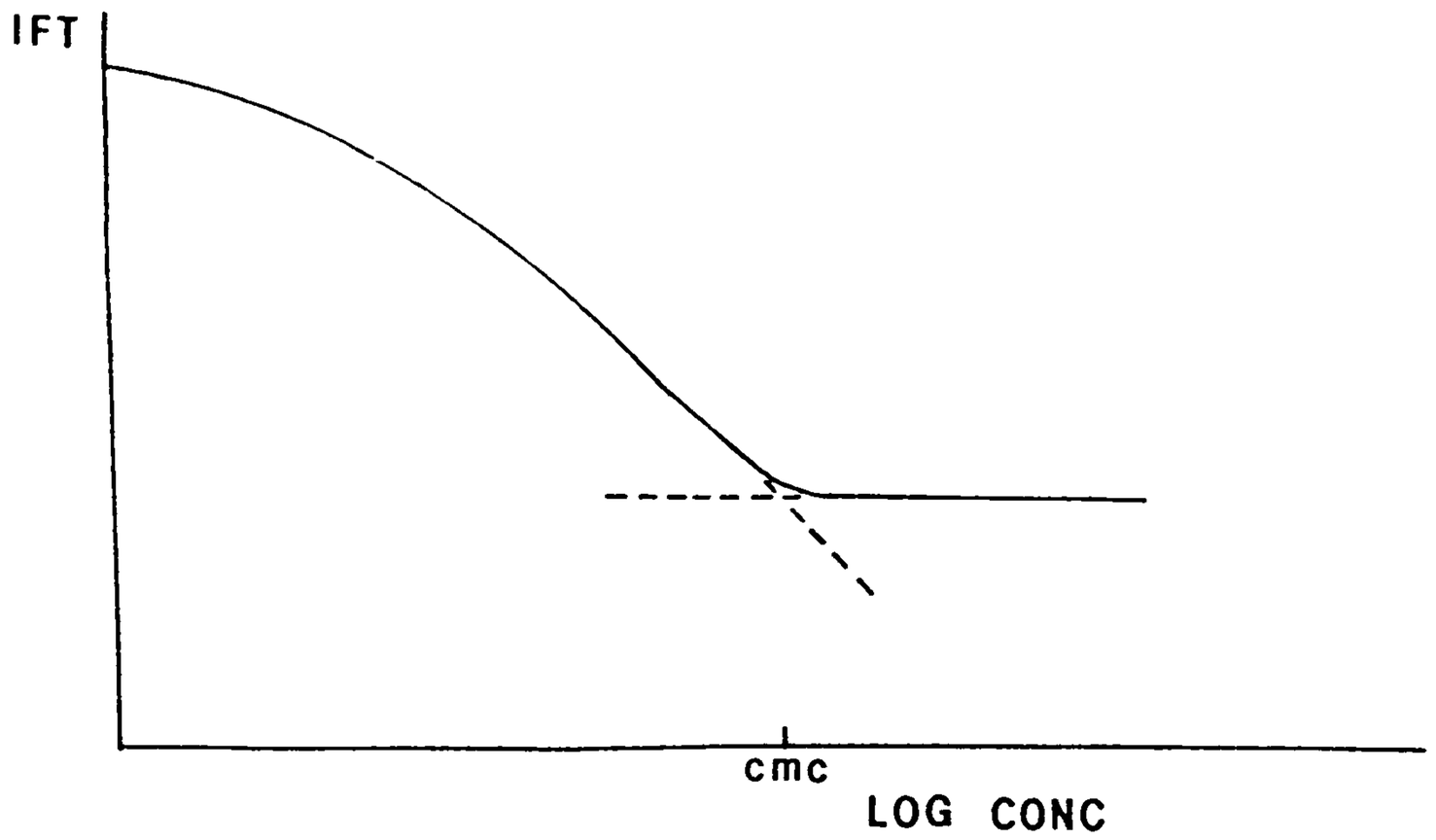

Fig.4.7 The Gibbs adsorption isotherm.

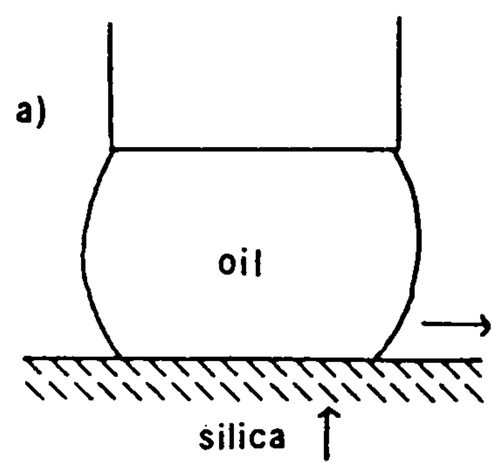

Fig.4.8 Distinction between the a) advancing and b) receding contact angles.

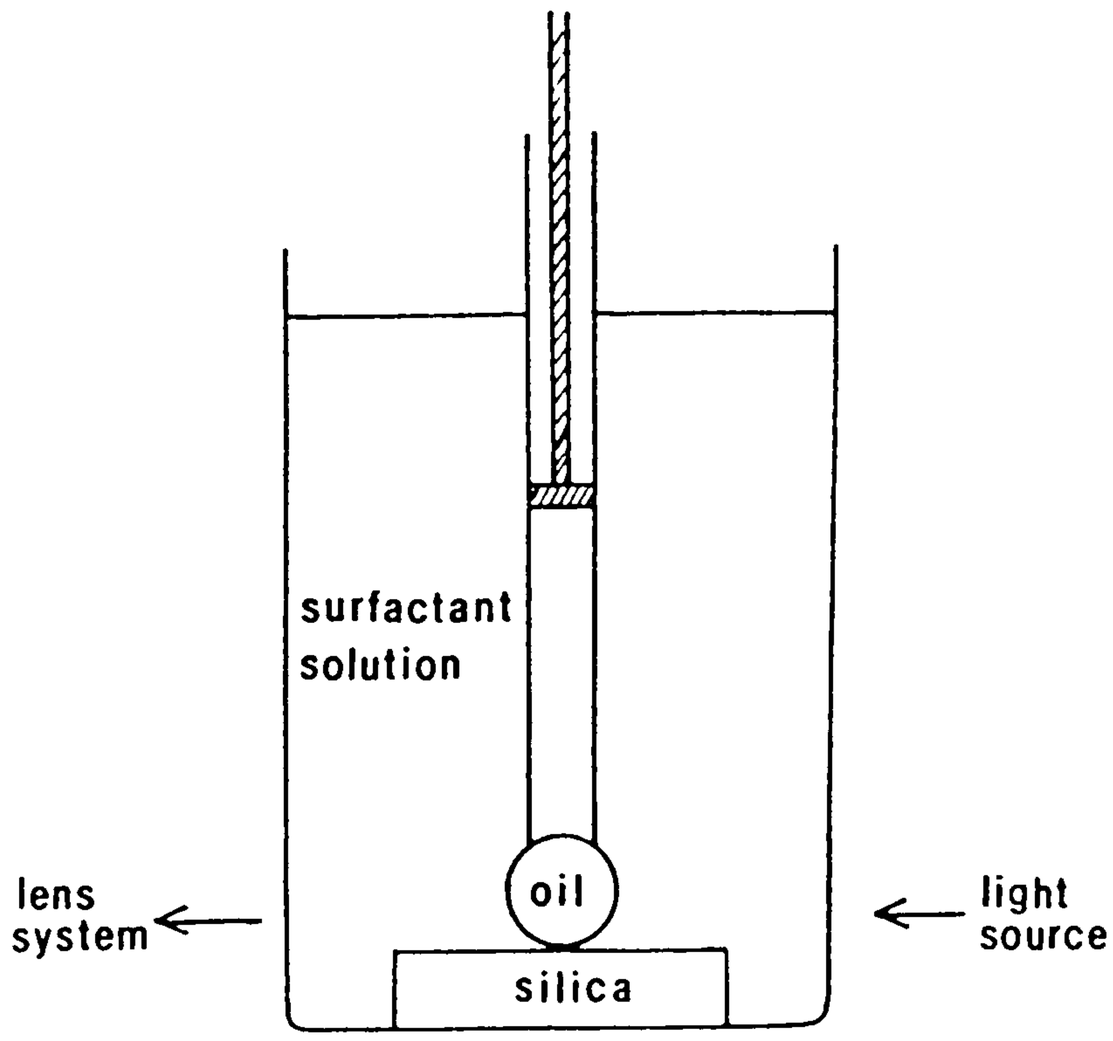

Fig.4.9 Apparatus for contact angle measurements.

was ignored, but over a number of drops, this weight could be significant. The drop should be formed, ideally, over 4-5 min, allowing the surface to come to equilibrium; taking into account any ageing effects. However the drops formed in this study could only be held at the capillary tip for a maximum of 10s.

(ii) Spinning Drop Technique

These experiments were conducted at ICI Petroleum and Plastics Division (Wilton, Cleveland, UK). Since this equipment was only available for a limited time, only 2 or 3 different concentrations were used for each surfactant, which did not allow cmc determinations as in the drop weight. This technique is more reliable, accurate and enables measurements to be taken at high temperatures.

In order to realise the contribution of a surfactant to interfacial tension reduction, blank experiments were run. Oil characteristics were measured against both distilled water and BDH brine at 296K and 330.5K. In all cases the oil drop stuck to the side of the sample tube and so the measurements would not have been of a "free" rotating bubble. Nevertheless, considering this error, interfacial tension calculations gave values of around $6mNm^{-2}$.

Generally, the interfacial tension is reduced as the concentration is increased. This was particularly noticeable with those marked "unstable" in Table 4.8. Here, the oil drop was disintegrating as it remained

stationary in the sample tube. Other oil drops disintegrated as they spun. Some drops stuck to the side and were flattened as they spun and so would not allow any valid measurements to be made.

The results show that the shorter chain length surfactants are more efficient in reducing the IFT than the larger molecules. The addition of 10% (wt/vol) sodium chloride produced a reduction, particularly in the case of 0.1% T040S. However, on making the surfactant solutions up in BDH brine, a slight <u>increase</u> in IFT was noticed.

At the bottom of the table, there are 3 blends of surfactants using a cosolvent (propan-2-ol denoted as IPA for brevity in tables and figures) and cosurfactants (SAS60 and B712). These systems are promising mixtures for enhanced oil recovery and are dealt with in Chapter 5. These blends are less efficient than using the shorter chain compounds on their own. In all cases it must be remembered that the surfactants SAS 60 and B712 are not pure compounds (like the main surfactants) and their impurities, however minute, may adversely affect interfacial behaviour.

The main error of this method is the placing of the oil drop into the surfactant-filled sample tube. It is imperative that the size of the oil drop is the same in all cases. In practice, this was difficult since some oil remained on the syringe needle, and in other cases it was difficult to inject one drop and several were

produced. These were then not all of a consistent size and it is then not valid to compare these surfactant systems.

4.6 Contact Angles and Wetting

4.6.1 Introduction

Defining a reservoir as water-wet or oil-wet refers to an average behaviour and it should be noted that wettability may vary considerably in a reservoir due to chemical or geometrical in homogeneities. Wettability effects on oil recovery were recognised long ago and the basic concepts and equations have been reviewed by Melrose and Brandner (87). Part of the function of the surfactant is directed towards reversing the wetting characteristics of the medium, at some cost in terms of chemical adsorption. It has been suggested that reservoir matrices of intermediate wettability offer the greatest potential for displacement efficiency.

The contact angle θ, that the liquid makes when it is at equilibrium wih the other phases it is in contact with (see Fig. 4.4) is related to the interfacial free energies of these phases. From the diagram, Youngs equation can be written as:

$$\gamma_{ow} \cos\theta = \gamma_{ws} - \gamma_{os}$$

where γ is the interfacial tension between the solid, s, the oil drop, o, and the aqueous surfactant phase, w.

Hysteresis

Hysteresis of the contact angle is defined as the difference between the advancing and receding angle. If the air/oil bubble maintains a spherical shape (see Fig. 4.8a), a value for the receding angle is obtained. This is the angle between the liquid and a solid surface which has already been water-wet and liquid phase is receding from the point of three-phase contact. If the bubble is "squashed" (Fig. 4.8b) and left to equilibrate for, say, 20 min, the advancing angle can be calculated. This is the angle between the liquid and a fresh non-wetted solid surface where the liquid is advancing towards the point of three-phase contact. In this study, the advancing contact angle is measured as the system is allowed to assume an equilibrium value.

It is difficult to examine the influence of wettability in oil recovery using reservoir rock because of the nature of the complex forces involved and the roughness of the surface. This type of study is, therefore, usually measured on macroscopic smooth planar substrates with known liquids. The angle can then be determined by a variety of techniques (88).

4.6.2 Experimental

To examine wettability behaviour, contact angle measurements have been made using drops of crude oil (decane, however, is the usual standard oil) held against an optically flat silica plate under aqueous sufactant solutions.

A small disc of silica (approximate dimensions 2 x 2 x 0.5cm) was fixed onto a microscope slide. The surface was polished using graded particle sizes of corundum and then thoroughly washed with acetone and distilled water. The mounted sample was placed in the trough (see Fig. 4.9) and a solution of surfactant ($100cm^3$) added. An oil bubble was introduced from the syringe and brought into contact with the silica surface by raising the level of the trough. A series of lenses allowed a magnified image of the bubble to be reflected onto a set of drawn concentric circles. Adjustments were made until the best fit was made for the bubble with a circle. The chord, c, (Fig. 4.10) and diameter, d, were measured and the contact angle was calculated from the equation:

$$\text{Sin}\,\theta = c/d$$

The variation of contact angle with pH was studied by adding drops of 1M HCl. Initially, very low concentrations of surfactant were used (e.g. 10^{-2}-10^{-6}M), but these produced negligible contact angles, even after an equilibrium time of 30min. Therefore, higher concentrations were used, beginning at 0.0001% (wt/vol).

4.6.3 Results

Table 4.8 shows the effect of concentration on contact angle. After the addition of acid, the reduction in pH and the effect of the angle is shown in Table 4.9.

4.6.4 Discussion

Generally, the contact angle increases with increasing surfactant concentration until the oil bubble becomes too

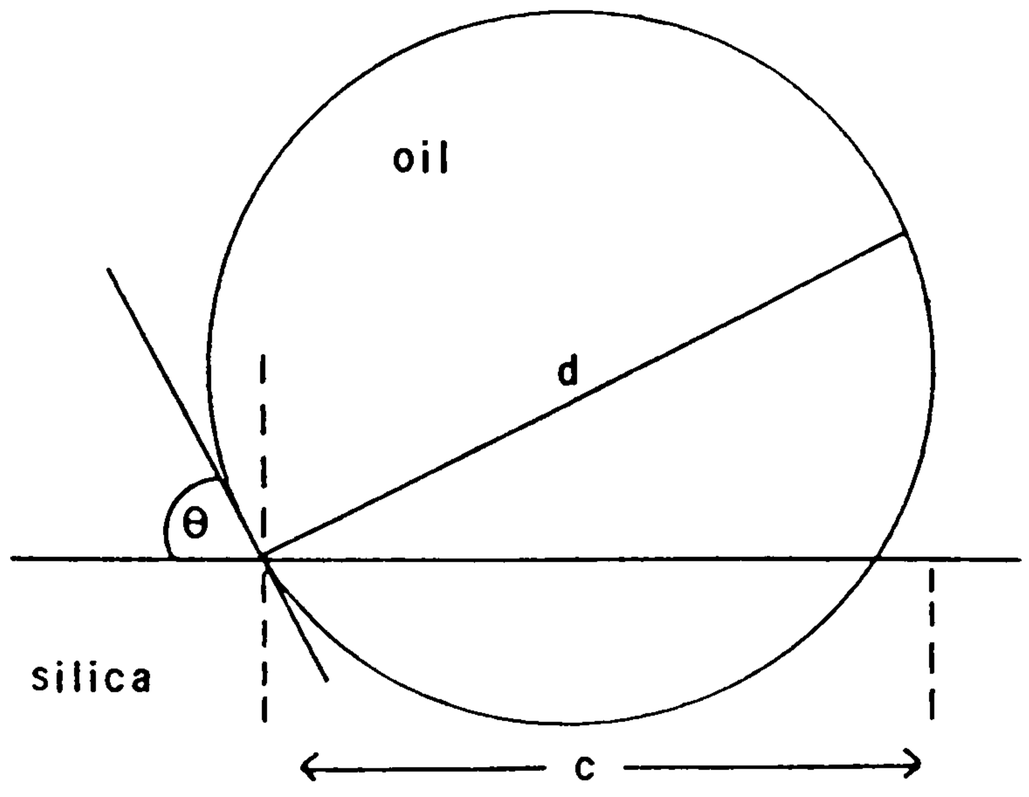

Fig.4.10 Measurements of the bubble for contact angle determination.

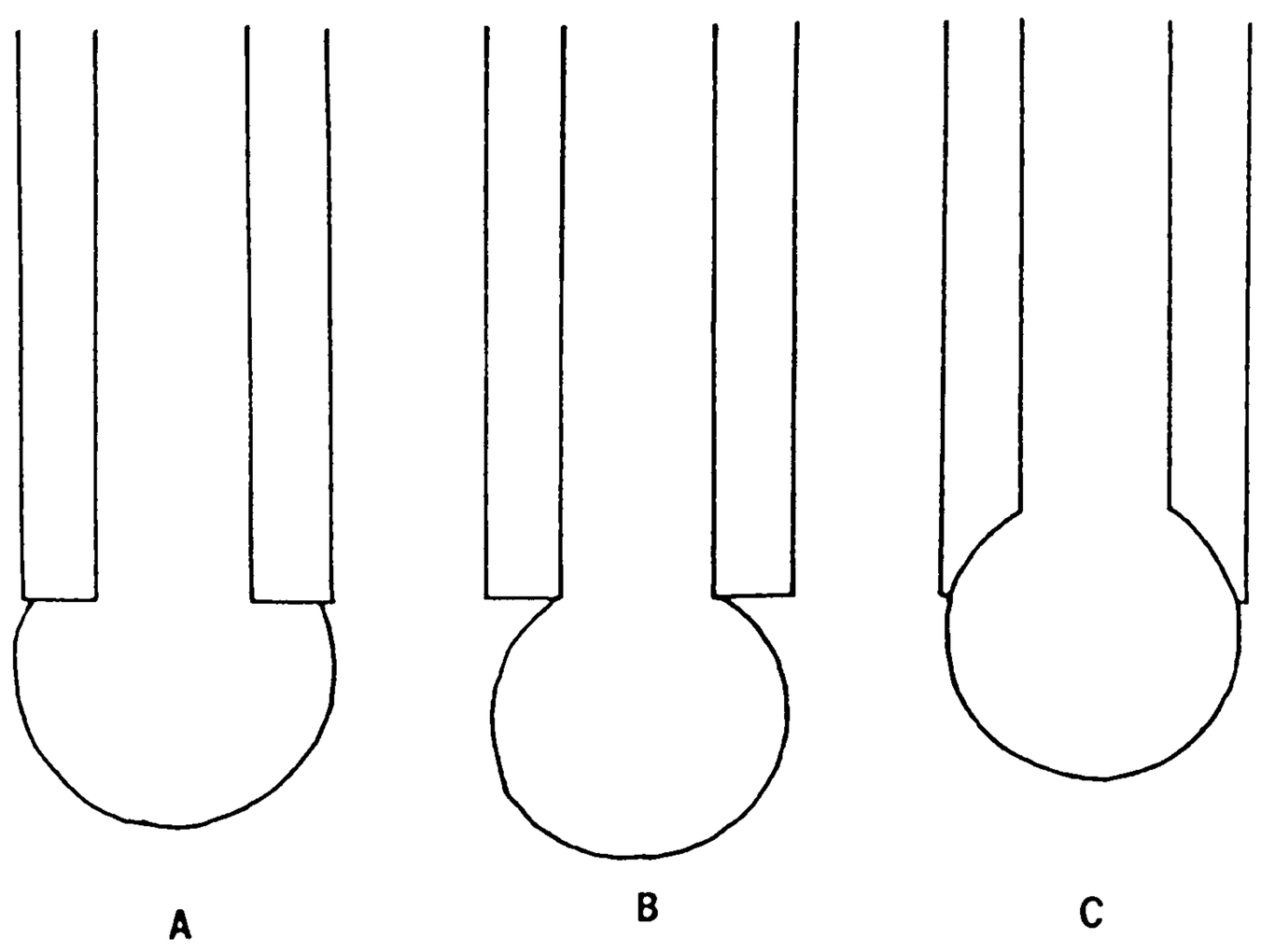

Fig.4.11 Shaping of the capillary to accommodate the bubble.

Surfactant	Contact Angle ^{o}	pH
0.001% T040S	1.7	6.5
0.01	2.4	5.9
0.1	4.4	6.23
1	3.7	5.7
0.001% T060S	5.7	5.6
0.01	11.9	5.6
0.1	23.6	5.8
T040S/SAS60/IPA/BDH		
0.0001%	7.5	5.9
0.001	9.8	6.2
0.01	NO BUBBLE	
T040S/SAS60/IPA/MRB		
0.0001	11.5	6.0
0.001	12.9	5.7
T040S/B712/IPA/MRB		
0.0001	4.8	6.7
0.001	5.7	5.6
0.01	6.8	5.7

TABLE 4.8 Variation of Contact Angle with Concentration.

Surfactant	Contact Angle °	pH
T040S		
0.001%	3.1	3.39
0.01	1.9	3.23
0.1	NO BUBBLE	
T060S		
0.01%	19.0	2.8
0.1	23.6	3.0
T040S/SAS60/IPA/BDH		
0.0001	10.5	2.75
0.001	9.0	2.5
T060S/SAS60/IPA/MRB		
0.0001	8.3	2.9
0.001	5.9	2.8
T040S/B712/IPA/BDH		
0.0001	10.8	2.5
0.001	7.9	2.4
0.01	19.6	3.3

TABLE 4.9 Variation of contact Angle with pH.

unstable, thereby preventing further measurements to be made. In some cases, this occurs after concentrations of 0.01% (wt/vol) are reached.

A decrease in pH tends to increase the wetting and thus the contact angle is reduced. This behaviour can be explained by considering the charge on the oil drop's surface and the silica. At high pH, there is a charge repulsion between the silica surface and the crude oil surface. This stabilises an intermediate water film between them. At low pH, there is an attraction between the negatively charged silica surface and the positively charged crude oil surface which causes strong oil wetting. The charge at the crude oil-aqueous interface is associated with naturally-occuring crude oil surfactants.

Obtaining valid, reproducible contact angles is more complicated and difficult than it appears. Although certain trends can be seen, there are many exceptions, possibly caused by:

(i) Contamination of the droplet by adsorption of impurities from the aqueous phase or from the oil droplet, which alters the surface; usually reducing the angle and producing hysteresis.

(ii) Surface heterogeneity; a solid surface, even when apparently smooth, may have impurities and defects that vary from place to place.

(iii) The shaping of the capillary to accommodate the bubble would allow better results. Fig. 4.11, situation a) was frequently observed and was used since it was difficult to reproduce the ideal shape in Fig. 4.11 b). If the capillary had been shaped as in Fig. 4.11 c), the measurements would be more accurate.

(iv) The sulphonated surfactants also contained solvents and precursors and the presence of these impurities affects wettability. The addition of a nonionic surfactant increases wetting power and so may produce a larger angle than is true.

4.7 Surface Tension of Surfactant Solutions in Contact With Air

4.7.1 Introduction

This property is not normally considered important when evaluating surfactants for oil recovery. However, it was studied here as it provides useful information about surfactant behaviour.

Molecules near the surface of a pure liquid have a different environment from those in the bulk fluid. A molecule in the interior of the fluid will experience forces in all directions due to the surrounding molecules. Molecules near the surface of the liquid will experience a weaker force from the gaseous region above the fluid than if this area was occupied by a denser medium. Such molecules will experience a force pulling

them back into the bulk of the fluid which has the effect of reducing the density in the region of the surface.

A variety of techniques for the measurement of surface tension of liquids are available. Some early methods include the bubble pressure method (89), the drop weight method (90), and the pendant drop (91).

The dynamic surface tension of a pure liquid is practically identical with static surface tension. However, in solutions of surfactants, the dynamic tension is usually found to be higher than for the static value because of a finite time required for equilibrium while the surfactant diffuses to the freshly-formed surface. The (Du Nouy) ring method has been adapted to the measurement of dynamic surface tension. By continuously overflowing the vessel with solution from which the ring is pulled, the surface is kept fresh and the pull on the ring measures the dynamic surface tension.

The technique adopted in this study was a static method.

4.7.2 Experimental

The experimental method chosen for surface tension measurement was the Du Nouy ring torsion balance (White Electrical Instrument Company Ltd., Malvern, Worcs), fitted with a platinum ring. The ring was lowered until it just touched the surface of the liquid. The surface was lowered until the ring broke free from the surface. The surface tension is read directly from the instrument. All measurements were conducted at room temperature and

the surface was allowed to come to equilibrium for 5 min. Surfactant solutions were prepared in distilled water and also in a 5% (wt/vol) sodium chloride solution.

The drop volume method was experimented with initially since this method appeared simple and quick, however the results were not as reproducible as expected. These are now discussed.

4.7.3 Results

Figure 4.12 illustrates the change in surface tension as a function of concentration. The effect of introducing an inorganic salt is shown in Table 4.10. The results obtained using the drop weight method are compared with the Du Nouy ring in Table 4.11. Values for the cmcs of the surfactants have been calculated from the two figures and are listed in Table 4.12.

4.7.4 Discussion

The surface tension rapidly decreases with increasing concentration (see Fig. 4.12) and reaches a point of inflection followed by a gradual increase or constant levelling. The break corresponds to the cmc. As explained earlier in Chapter 2, after these concentrations, the addition of surfactant produces no increase in monomer concentration but only in the micelle concentration. The maximum reduction in surface tension is achieved with the lowest chain lengths for each series. As the degree of ethoxylation increases, so the action on the surface tension of water is reduced. The Sapogenat series is more effective than the Arkopals.

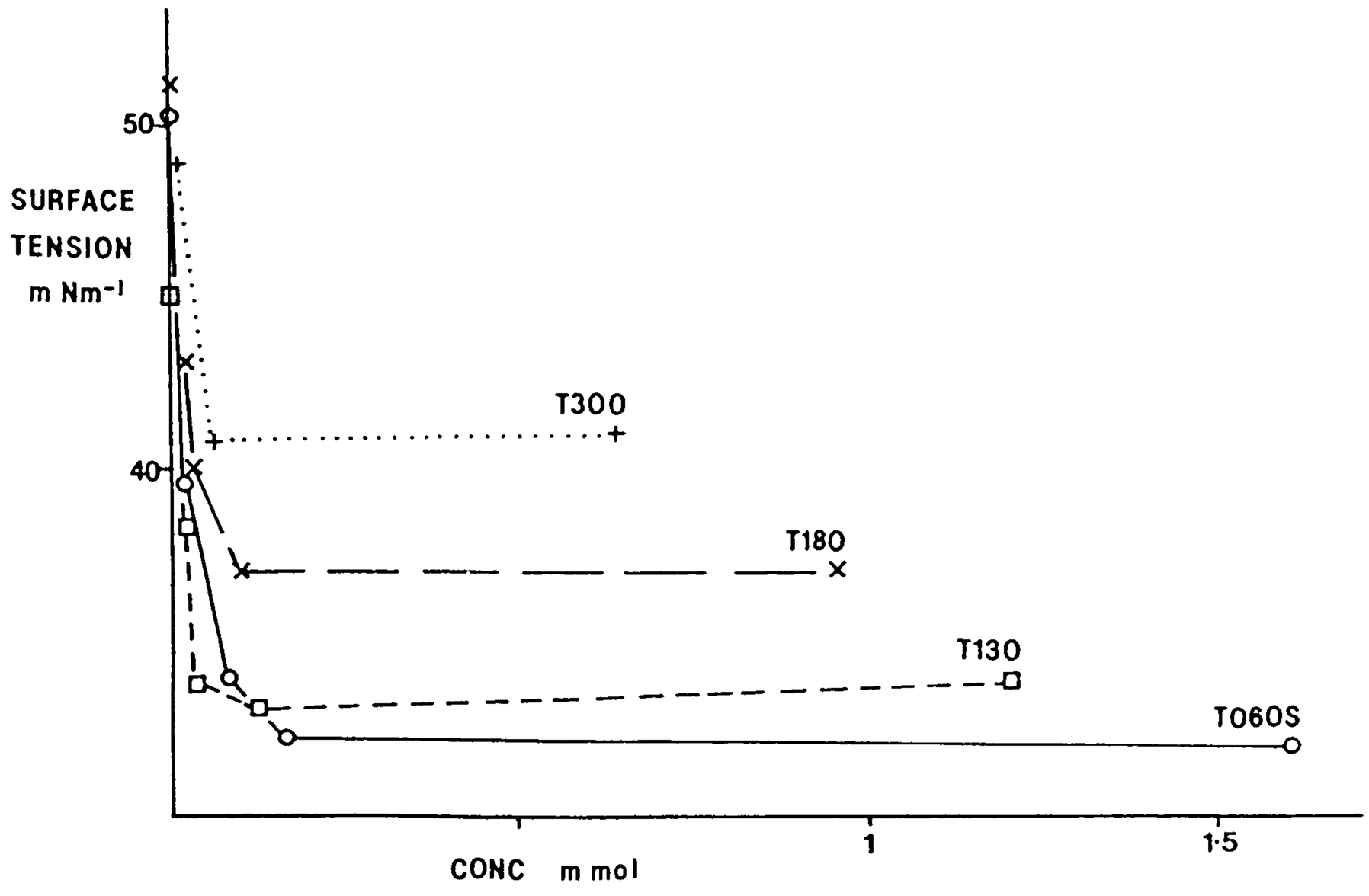

a) Sapogenats,

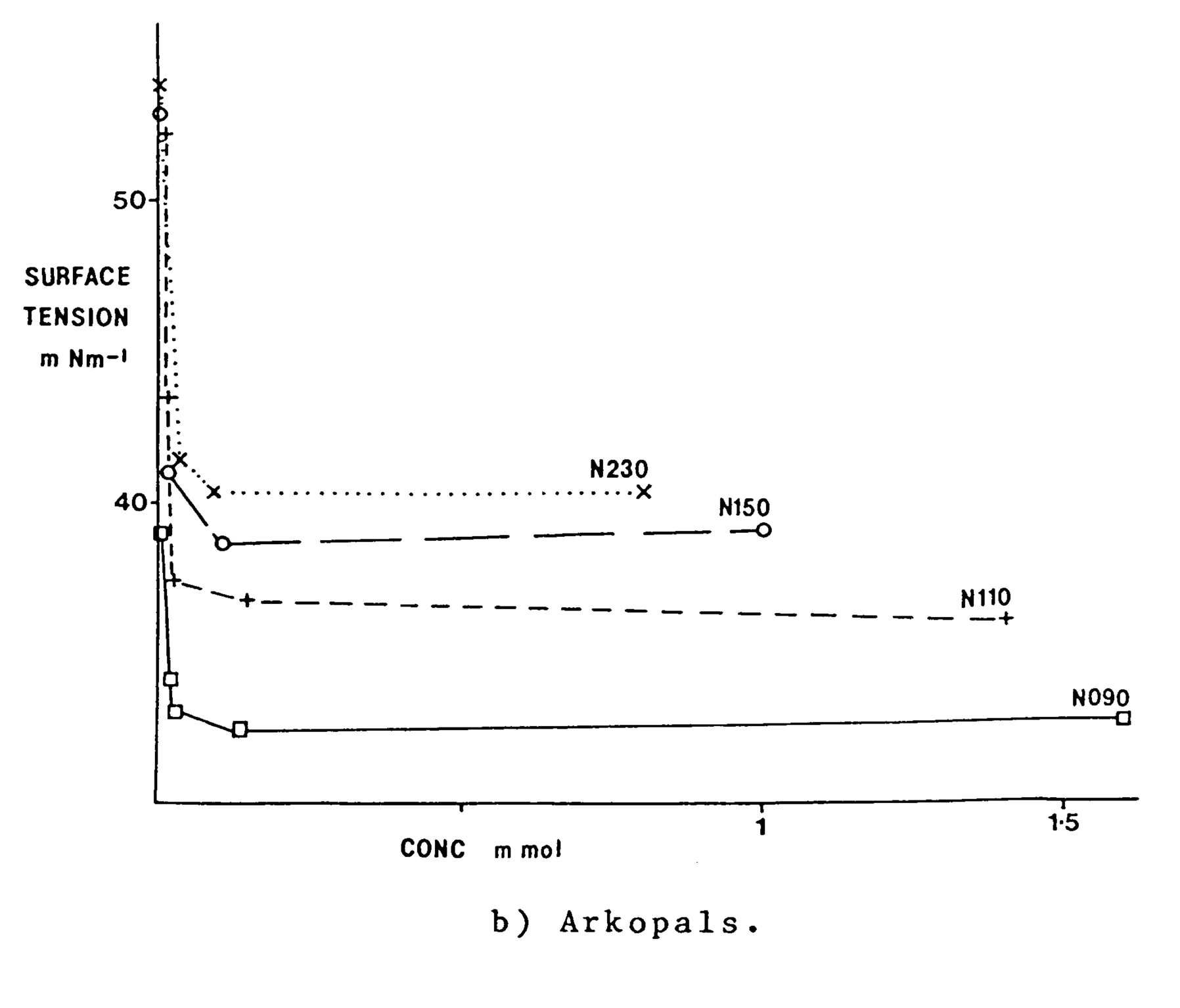

b) Arkopals.

Fig.4.12 Reduction of IFT with surfactant concentration

Surfactant	Surface Tension (mNm^{-1}) Distilled Water	5% NaCl solution
T110	31.2	30.1
T130	33.9	30.7
T180	37.2	33.6
T300	40.0	39.0
N110	39.1	37.0
N130	36.2	34.0
N150	36.1	35.5
N230	39.2	38.8

TABLE 4.10 Variation of Surface Tension with Electrolyte.
All 1% w/v solutions

Surfactant	Surface Tension(mNm^{-2}) Drop Weight	De Nouy Ring
T110	50.2	31.2
T130	50.2	33.9
T180	61.6	37.2
N090	52.5	32.5
N150	62.75	36.1
N300	76.45	40.02

TABLE 4.11 Comparison of Surface Tension Values using 2 methods.

Surfactant	C.M.C (μM.)
T040S	14.4
T060S	13.1
T110	14.2
T130	14.4
T180	11.4
T300	12.6
N090	11.7
N100	13.6
N110	13.4
N150	17.0
N230	14.1

TABLE 4.12 CMC values derived from Surface Tension Measurement.

The increase in the hydrophilic nature of the surface has caused surface tension to increase after the cmc until a limiting composition of surface is attained (92).

Table 4.11 illustrates the inaccuracy of the drop weight method. The drop at the end of the glass capillary tip should be suspended until equilibrium had been reached. At least 2 min is required and here the maximum time the drop was held before it detached itself was about 10 s. Longer equilibrium times are needed if adsorption of the solute is slow. This situation is analogous to measuring the surface tension by a dynamic method when equilibrium is not allowed to be attained and the results are higher.

The addition of sodium chloride ions to surfactant solutions reduces the surface tension with the reduction less marked as the chain length increases. If further measurements had been made to ascertain the cmc, the plots would probably show a sharper break at the cmc minimum. The cmc of a surfactant increases as its hydrophilicity increases. Conversely, the less soluble a surfactant is, the lower its cmc. Thus, in Table 4.12, the cmc of the sulphonates is approximately a tenth greater than the nonionic surfactants. Comparing the two surfactants having the same EO chain length but different hydrocarbon groups, the more hydrophilic tributyl Sapogenat (T110) has a higher cmc than the Arkopal (N110). The Arkopals show an increase in cmc as the EO chain length increases with the exception of N230.

The Sapogenats do not show such a clear trend and it is

difficult to draw any sound conclusions from this group. It is to be expected that they behave in a similar manner to the Arkopals, but errors included in the experiment (arising mainly from the lack of data points) have produced lower values than predicted.

CHAPTER 5

5 Solubilisation

5.1 Introduction

It is well known that alkanes and water do not mix, but that if a micelle-forming surfactant is added, a small amount of the oil may be solubilised in the micelles. This most important property of surfactants is directly related to micelle formation. Solubilisation is defined as the spontaneous dissolution of a substance (solid, liquid or gas) by interaction with the micelles of a surfactant to produce a thermodynamically-stable isotropic solution. If the solubility of a normally insoluble material is plotted (as in Fig.5.1) against the concentration of the surfactant in solution that is solubilising it, the solubility is very slight at concentrations below the critical micelle concentration (cmc). It then rises abruptly once the cmc is reached and indicates that solubilisation is a micellar phenomenon, since it occurs to a negligible extent at concentrations where micelles exist (if at all) in insignificant numbers.

The exact method of micellar solubilisation varies with the nature of the surfactant and the oil. Data on the sites of solubilisation are obtained mainly in studies of the surfactant before and after solubilisation. X-ray diffraction studies (93) have measured the changes in micellar dimensions while U.V. (94) and N.M.R. (95) spectroscopy indicate changes in the environment of the oil on solubilisation. As a result of these studies, solubilisation is believed to occur at a number of

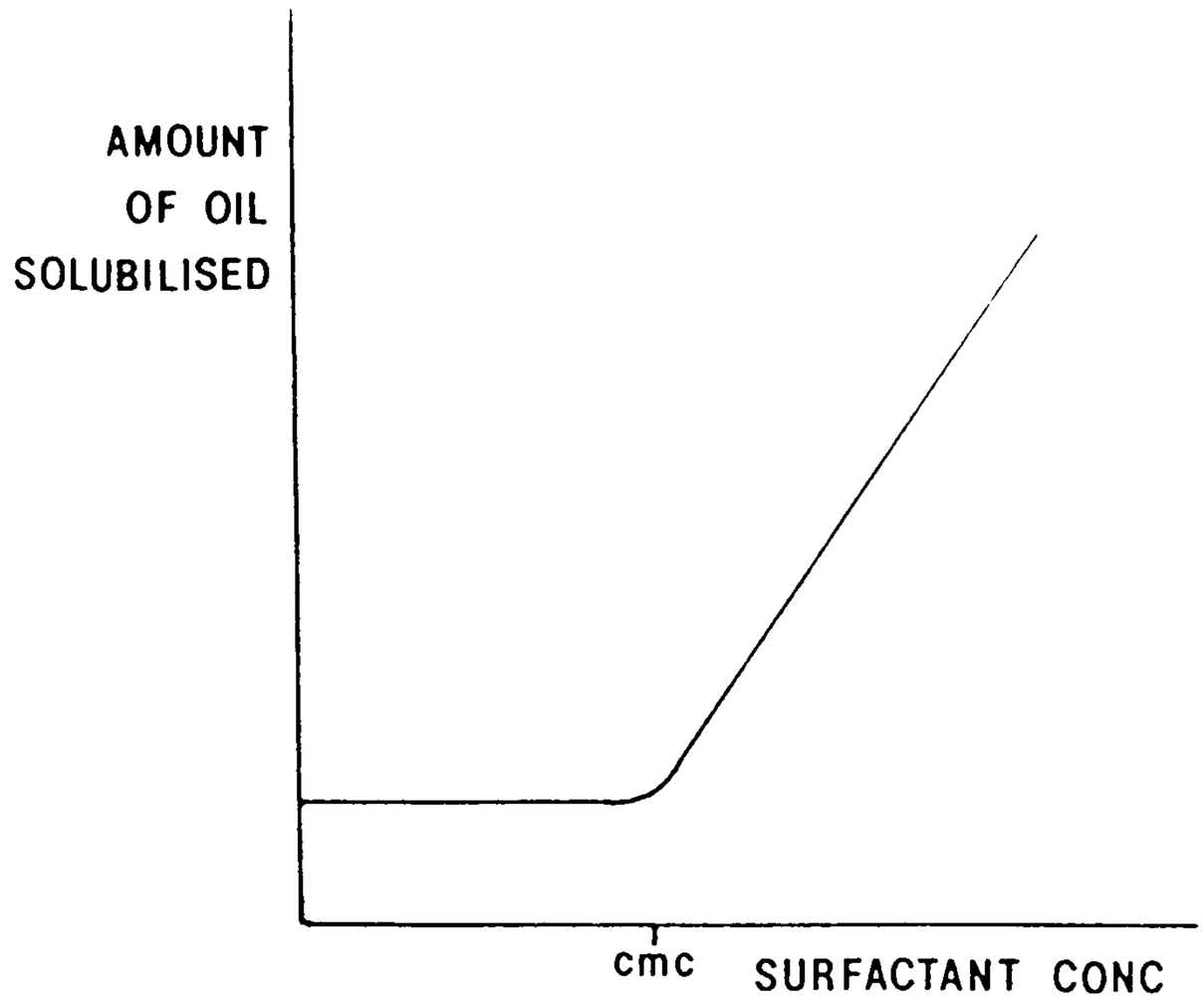

Fig.5.1 Amount of oil solubilised as a function of surfactant concentration.

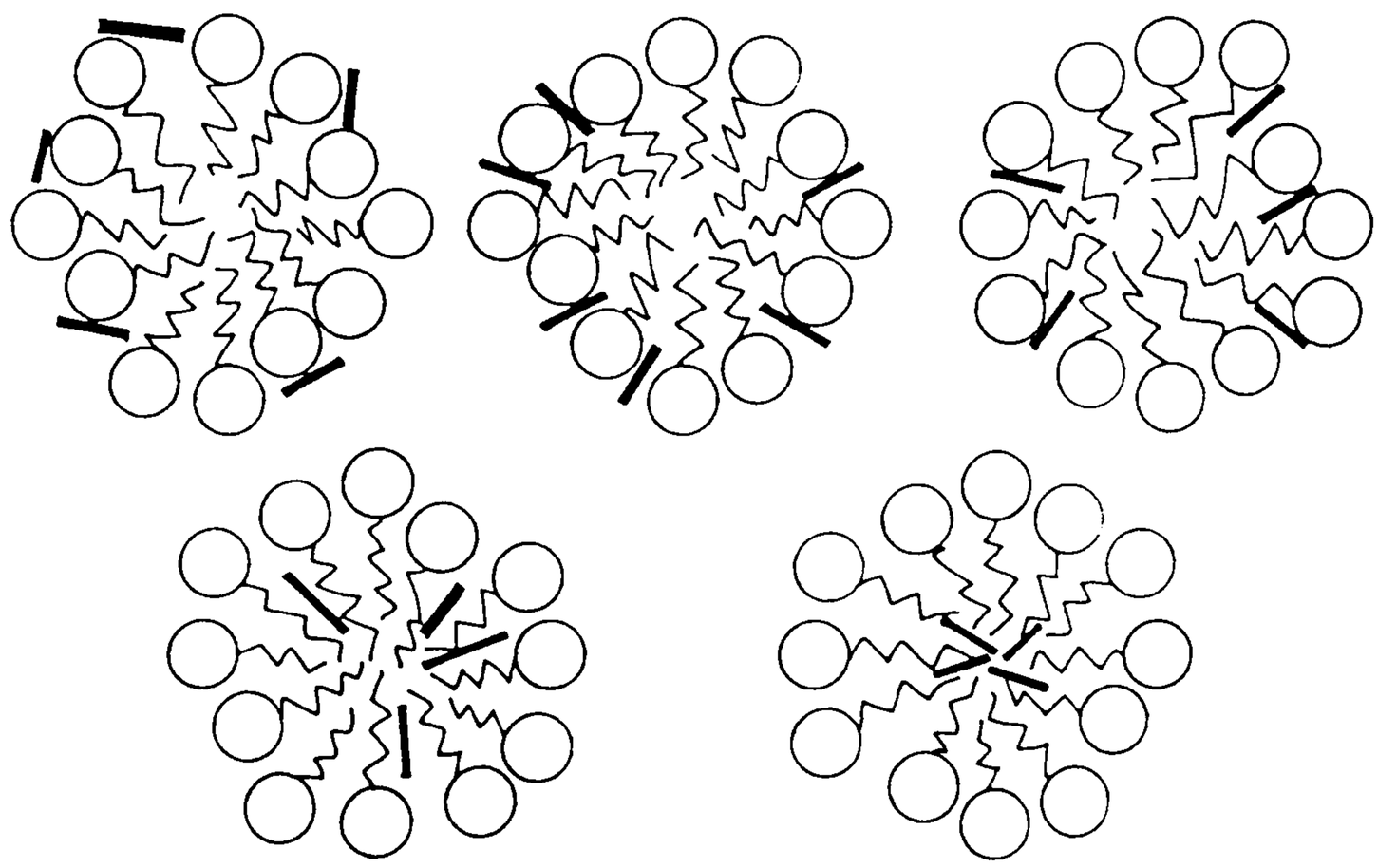

Fig.5.2 Possible locations of solubilisation sites.

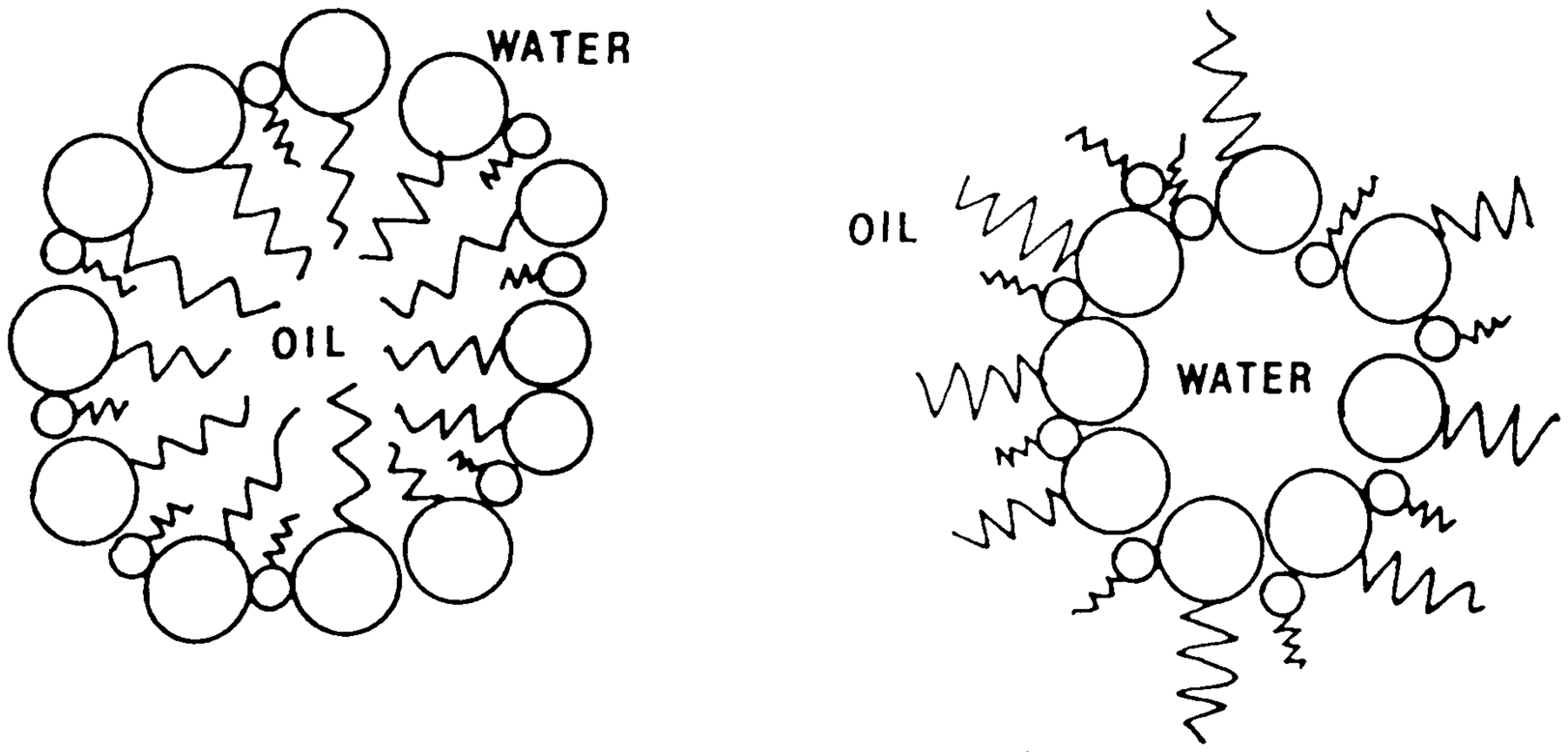

a) Hydrophilic Micelle

b) Hydrophobic Micelle

Fig.5.3 Types of micelle:

different sites in the micelle:

a) on the surface of the micelle (i.e. at the micelle-solvent interface);

b) between the hydrophilic head groups;

c) between the hydrophilic groups and the first few carbon atoms of the hydrophobic outer core, known as the "palisade" layer";

d) more deeply into the palisade layer and

e) in the inner core of the micelle.

(see Figure 5.2 (a-e)).

In concentrated aqueous surfactant solutions, the shapes of the micelles may be different from those in dilute solution, but the site of solubilisation is essentially the same.

5.1.1. Factors Affecting Solubilisation

(i) Structure of the Surfactant

Hydrocarbons are solubilised in the interior of a micelle and the amount of material solubilised generally increases as the size of the micelle increases. The greater the dissimilarity between the solvent and surfactant, the larger the aggregation number of the micelle. Thus an increase in the chain length of the hydrophobic portion of the surfactant generally results in increased solubilisation of hydrocarbons in the inner core in aqueous media. Bivalent metal surfactants appear to show greater solubilising power than the corresponding sodium salts for hydrocarbons (96). This is probably a reflection of the larger aggregation number (average

number of monomers per micelle) and therefore volume of the micelle. Branched chain surfactants appear to have less solubilising power than the straight chain compounds. This is due to their shorter effective chain length and also explains why unsaturated surfactants have less solubilising power for hydrocarbons than the corresponding saturated ones.

In general, the order of solubilising power for oil that is solubilised in the inner core appears to be:

nonionics > cationics > anionics

for surfactants with the same hydrophobic chain length. Nonionic surfactants may have greater solubilising potential than ionics in dilute solutions due to their lower cmc. Cationics are better than anionics due to their looser packing of molecules in their micelles.

(ii) Structure of the Solubilisate

For aliphatic or alkylaryl hyrdocarbons, the extent of solubilisation is less for the longer chain lengths but it increases with unsaturation or cyclisation. Branched chain compounds appear to have approximately the same solubility as their straight chain isomers. Polar compounds are solubilised close to the micelle-water interface and to a greater extent than nonpolar solubilisates that are sited in the inner core. Generally, the less polar the solubilisate, the weaker is its interaction at the micelle-water interface. This, coupled with an increase in its chain length reduces the degree of solubilisation (97).

(iii) Effect of Electrolyte

The addition of small amounts of neutral electrolyte to solutions of ionic surfactants appears to increase the extent of solubilisation of oils that are located in the inner core of the micelle. However, it decreases that of polar compounds that are solubilised in the outer portion of the palisade layer. The effect of the electrolyte is to decrease the repulsion between the like-charged ionic head groups which causes closer packing and thus less volume for solubilisation of polar compounds. However, it also increases the aggregation number, the volume of the inner core of the micelle and so hydrocarbon solubilisation is greater(98).

The addition of a neutral electrolyte to solutions of nonionic surfactants increases the extent of solubilisation of hydrocarbons. As above, it causes a closer packing of the hydrophilic head groups which increases the aggregation number.

(iv) Effect of Temperature

For ionic surfactants, an increase in temperature generally results in an increase in the extent of solubilisation for both polar and nonpolar solubilisates. This is due to the thermal agitation which increases the space available for solubilisation in the micelle(99).

In the case of nonionic surfactants, the effect of temperature depends on the nature of the solubilisate. Nonpolar materials which are located in the inner core of the micelle show increased solubility as the temperature

is increased, particularly as the cloud point is neared. This reflects the large increase in micellar aggregation number.

However, the solubility of polar materials passes through a maximum as the temperature is raised to the cloud point. A further increase in temperature causes dehydration and thus a tighter coiling of the ethene oxide chains. The volume in the micelle is decreased and so is the amount solubilised.

5.1.2. The Cloud Point

In general, long-chain nonpolar solubilisates which are solubilised in the inner core of the micelle appear to cause an increase in the cloud point. The volume of the micelle is generally increased, allowing more area at the micelle-water interface for hydration of the ethene oxide chains. For polar and polarisable compounds which are solubilised in the outer regions of the micelle, the cloud point is suppressed. This is due to the polar (or polarisable) compounds competing for the water molecules sites and dehydrating the chains (100).

5.2. Emulsification

5.2. Introduction

If a small amount of oil is solubilised within surfactant micelles and the resulting solution shaken, an emulsion (i.e. a relatively stable suspension of particles of a certain size within an immiscible medium) can be formed. Two types of emulsions based on the size of dispersed particles are recognised: opaque macroemulsion (used

synonymously with emulsion) having a particle size range 0.2-50nm which are easily visible under a microscope, and (ii) a microemulsion with particles between 0.01-0.20 nm which appears to the eye transparent or semi-transparent.

Microemulsions scatter little light (since for small particles light scattering is proportional to the square of the volume of the scattering particle) and are not turbid but are important in enhanced oil recovery (101).

Emulsions can also be classified into two types based on the nature of the dispersed phase caused by the emulsifying agent and to some extent on the process used in preparing the emulsion (see Fig. 5.3):

a) oil-in-water (o/w; where the oil is the "discontinuous" inner phase and the outer "continuous" phase is water/aqueous phase).

b) water-in-oil (w/o; where there is a dispersion of water or an aqueous solution in a water-immiscible liquid).

In general o/w emulsions are produced by emulsifying agents that are more soluble in the aqueous phase than the oil phase; the reverse is true for w/o emulsions and is suggested by the Bancroft rule (102).

5.2.1 Stability of Emulsions

Emulsions are not very stable due to the free energy contained in the interfacial area between the droplets and the surrounding area. If this interfacial energy is decreased, spontaneous emulsification can be reduced.

$$4/3\,\pi r^3 . \delta L = 4\,\pi r^2 . \gamma = \text{total free energy}$$

where L = latent heat per g

γ = interfacial surface energy

r = limiting radius

However, microemulsions are thermodynamically stable. Normally, they are formed spontaneously when oil and water are mixed with a surfactant and a cosurfactant. The surfactant, acting as the emulsifying agent, must stabilise the system to make it useful in this context. It does this by adsorption at the liquid-liquid interface as an oriented film. This reduces the interfacial tension between the two liquids and decreases the rate of coalescence of the dispersed particles.

(i) Effect of a Cosurfactant

Highly purified surfactants generally produce weak interfacial films that are not closely packed. Successful emulsifying agents are usually a mixture of two or more surfactants and a useful combination is an oil-soluble surfactant combined with a water-soluble one. Thus the addition of an alcohol to a sulphonate surfactant increases the lateral interaction between the surface active molecules in the interfacial film. The stability of the emulsion is increased as the packing is condensed to a stronger film.

(ii) Electrical Interactions

The presence of a charge on the dispersed particles constitutes an electrical barrier to the approach and coalescence of droplets. The source of this charge is in the adsorbed layer of surfactant with its hydrophilic end oriented towards the aqueous phase and is a significant factor in oil-in-water emulsions. In water-in-oil emulsions, there is very little charge, if any, on the particles. In emulsions stabilised by nonionic surfactants, the charge on the dispersed phase arises either from adsorption of ions from the aqueous phase or from frictional contact between droplets and the aqueous phase.

(iii) Droplet Size

An emulsion with a fairly uniform particle size distribution is more stable than one with a wide distribution of sizes. Larger particles have less interfacial surface per unit volume than smaller droplets and tend to grow at the expense of the smaller ones. If this process continues, the emulsion eventually breaks and the droplets coalesce. Short chain length surfactants have a smaller chain length distribution than that of the larger molecules and will thus produce a more limited range of droplet sizes.

(iv) Temperature

A change in temperature causes only slight changes in the interfacial tension between the two phases due to the relative solubility of the emulsifying agent in them. It may invert the emulsion (o/w to w/o or vice versa) or

cause it to coalesce.

5.2.2 Hydrophobic - Lipophobic Balance

In general for a surfactant to act as an emulsifier it must have a tendency to migrate to the interface and not remain dissolved in one phase or the other. It must not be too soluble but a mixture of a preferentially water-soluble surfactant (for oil-in-water emulsions) and preferentially oil-soluble (water-in-oil emulsion) will produce a better and more stable emulsion than an individual surfactant. Also, the more polar the oil phase, the more hydrophilic the emulsifier should be, the more non-polar the oil is that is to be solubilised the more hydrophobic should be the surfactant. The above discussion is usually the basis for selecting the most suitable emulsifying agent for a particular EOR system, and is known as the hydrophobic-lipophobic balance (HLB). There have been numerous attempts to determine HLB numbers from fundamental properties of surfactants such as cloud points (103), cmcs (104) and gas chromatography retention times (105). In other cases, it has been calculated from the structure of the molecule and emulsification data.

A major disadvantage of the HLB method of selecting surfactants as emulsifying agents is that it makes no allowance for a change in HLB value with temperature. At low temperatures, the hydrophilic part is dominant, as the temperature is raised there is a point where a change over occurs and the surfactant becomes hydrophic and so the HLB value decreases. As a consequence, phase

inversion may occur; therefore an o/w emulsion at room temperature may invert to a w/o emulsion at a higher temperature. At this temperature the hydrophobic and lipophobic tendencies of the surfactant balance and this is known as the phase inversion temperature. This is a recent and more reliable basis for selecting emulsifiers (106). Unlike the previous method, this method is indicative of its efficiency (the concentration required), its effectiveness (stability of the emulsion), and of course, the type of emulsion that can be expected from the system.

Another method to determine the HLB value is called the cohesive energy ratio (CER) (107). This involves matching not only the HLBs of oil and emulsifying agent but also their molecular volumes, shapes and their chemical natures. It also includes the ratio of intermolecular attraction between the oil phase and aqueous phase molecules.

5.3 Microemulsions

The term microemulsion was first introduced by Hoer and Schulman (108) to describe the transparent systems formed spontaneously when oil and water are mixed with an anionic surfactant using a medium chain alcohol as a cosurfactant. The nature of a microemulsion is well understood as a special type of micellar solution, but others have proposed that micelles and microemulsions are fundamentally different (109). In either case, the emulsifying agent is oriented so that the hydrophobic groups are facing the oil phase and the hydrophilic

groups the aqueous phase as shown in Figure 5.3.

In preparing a microemulsion with ionic surfactants, it is necessary to include a more hydrophobic cosurfactant. The ionic surfactant by itself is not sufficiently hydrophobic to allow for a large enough degree of solubilisation of the oil. Larger chain ionic surfactants require less cosurfactant than shorter chain lengths (110). The interaction between surfactant and cosurfactant is weak but its presence increases the aggregation number.

Surfactants do naturally lower the interfacial tension (to allow the spontaneous formation of an emulsion) but in most cases, the limit of solubility, or the cmc, is reached before it is sufficiently low. The addition of a cosurfactant of a different nature can lower the IFT further, even to a negative value (see Fig. 5.4 where a, b and c represent additions of cosurfactant), which cannot be realised with the main surfactant alone. The concentration of a surfactant in the aqueous phase is at or below the cmc. Most of the surfactant is at the interface. Nonionic surfactants often require no cosurfactants to produce an emulsion even with a pure sample of nonionic (ie. no mixture, or very little, of chain lengths, (111)).

5.3.1 The Winsor Scale

Winsor (112) recognised the three structures shown in Figure 5.5 to be present in an immiscible two-phase system (oil and water), containing a third surfactant

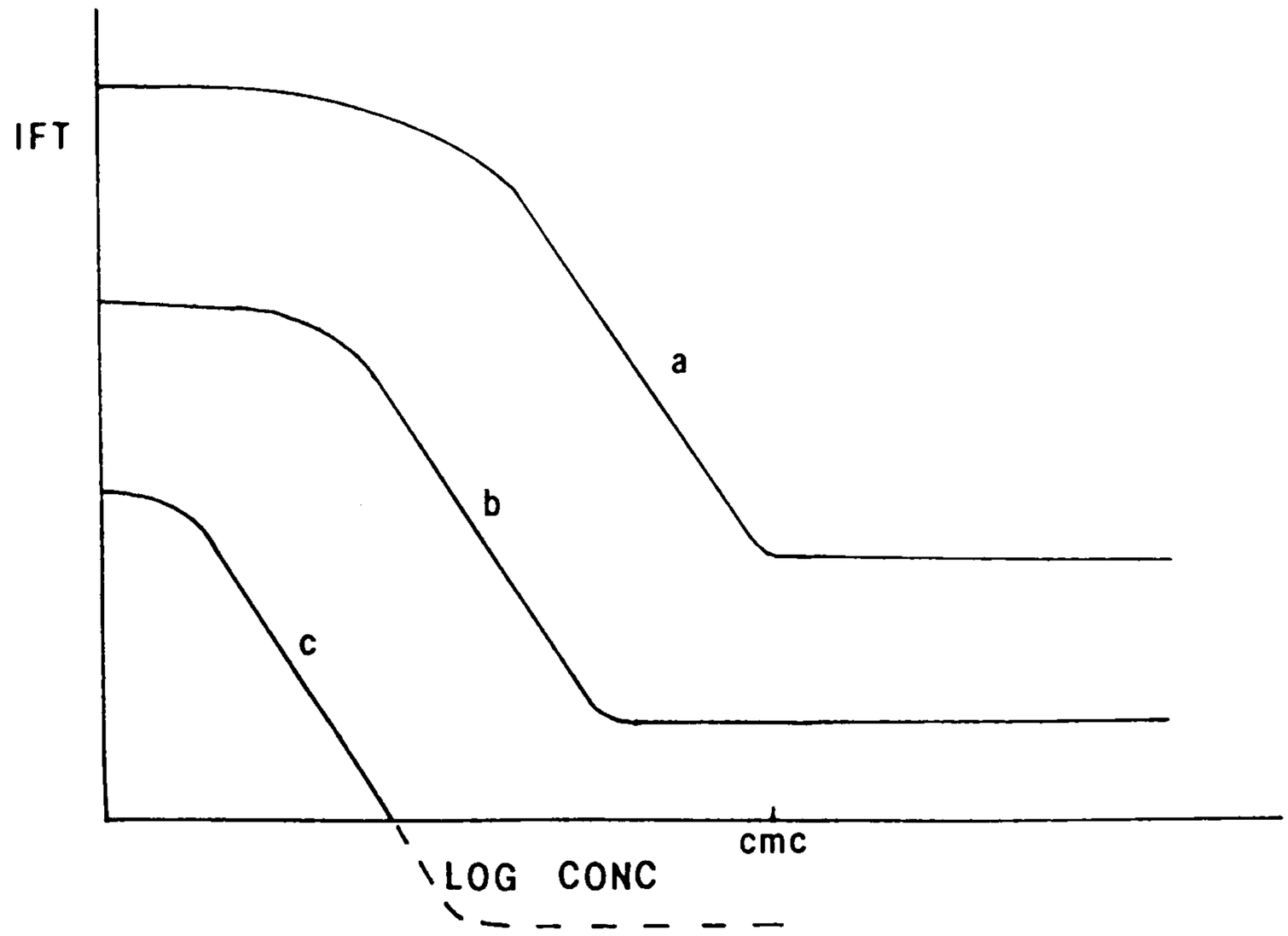

Fig.5.4 Effect of cosurfactant on the interfacial tension.

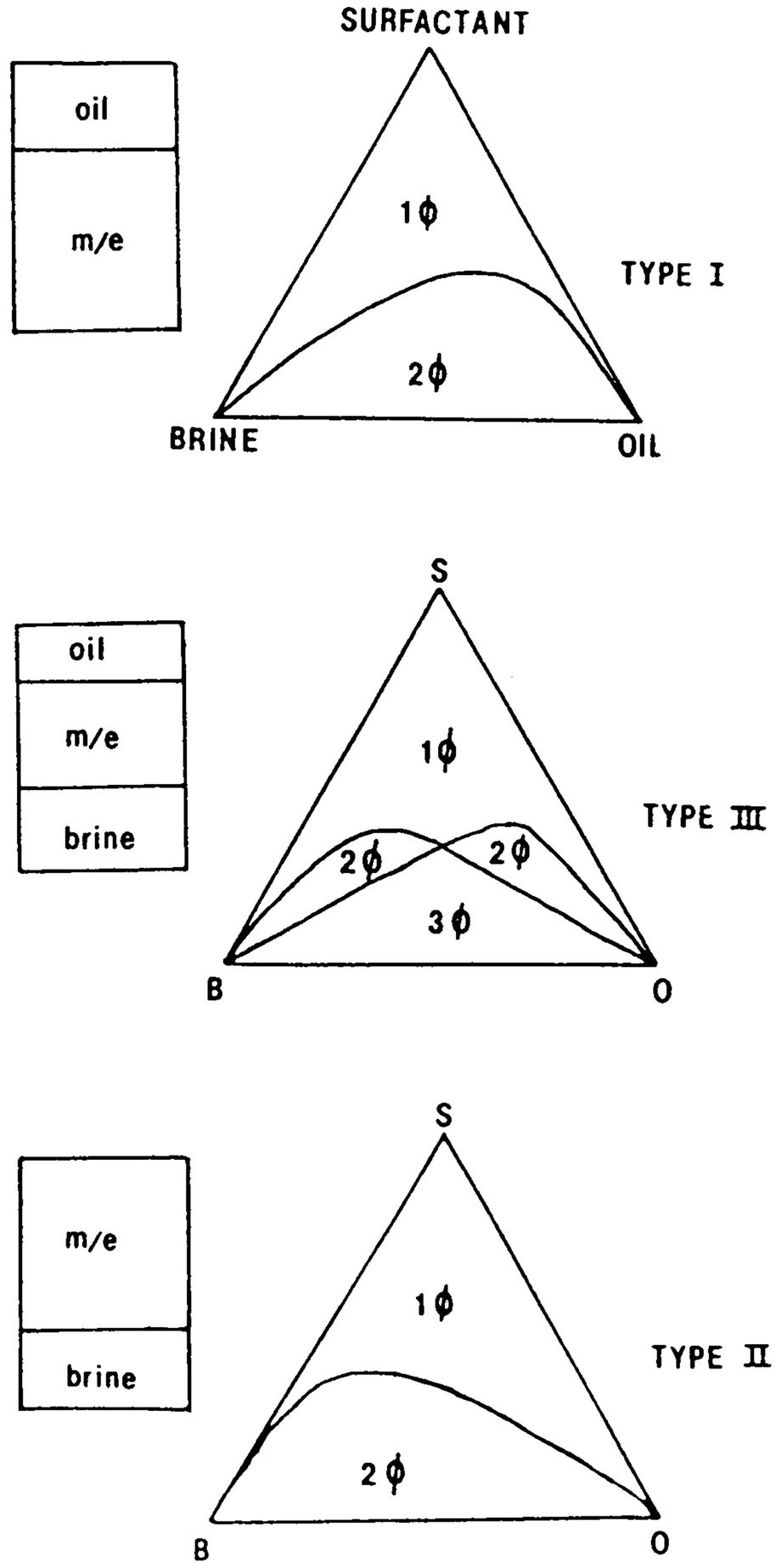

Fig.5.5 The Winsor three-phase system.

component with partial solubility in both phases:

(i) type I systems in which the surfactant is in the aqueous phase and the microemulsion is in equilibrium with excess oil.

(ii) type II systems in which the microemulsion is in equilibrium with excess water.

(iii) type III systems in which the microemulsion forms a stable middle phase in thermodynamic equilibrium with both excess oil and water.

Furthermore, type II can be positive or negative. The oil phase diminishes as the alcohol concentration decreases at the leading edge. Here, the oil saturation in the bank falls below the normal residual oil saturation and much of this oil becomes trapped as in waterflooding. This is termed a type II(-) or "under-optimum" and is a shrinking oil phase. In an expanding oil phase the slope of the tie lines is positive. This is in the region of increasing alcohol concentration as the system approaches miscibility and has greater oil recovery.

5.3.2. Microemulsions and Enhanced Oil Recovery

The action of a surfactant in mobilising the oil to be recovered depends on its solubility and interaction with the water and oil in the reservoir. It determines the type of microemulsion formed. It is apparent from the large volume of papers published on the phase behaviour of surfactants effective in displacing oil that a middle

phase, or type III, is required (113). This middle phase should contain virtually all of the surfactant. The salinity and temperature should be in the optimum range and the interfacial tension at a minimum between both the water and oil phases. It is therefore able to displace the oil effectively and can then itself be readily displaced by the water injected afterwards. However, Nelson (114) and Larson (115) recommend that the recovery from type II(+) - expanding oil phases - was equally good.

An essential step in the design of a microemulsion flood is to test the proposed system under reservoir conditions, fluids and rock. However, particularly when the pressure and the temperature are high and there is gas in solution, the testing can be very complex. It is therefore preferable to minimise any troublesome parameters.

Although for phase behaviour studies and core floods in the laborarory, the reservoir brine can be duplicated easily, the oil and pressure, however, present a different problem. Phase studies and core floods are more convenient to study under atmospheric pressure and with synthetic oils (stock tank and live crude). Most "live" crude oils contain a substantial quantity of gas that is absent from stock tank oil. Hence errors can arise in formulating a surfactant system if the oil exhibits a different viscosity and solvency from the live crude. Ideally, phase studies should be conducted at the pressure of the reservoir, but in most cases this is not feasible. Some researchers have studied the effect of

pressure (116) and concluded that there was only a marginal difference in equilibrium phase behaviour at the reservoir pressure (18 MPa) and atmospheric pressure using live and synthetic oils.

Diluting the stock tank crude with hydrocarbon solvents (e.g. 2-methyl heptan-1-ol, iso-octane) to approximate the viscosity of the live crude does not ensure that the diluted oil has the same solvency as the live crude oil for the surfactant. This synthetic oil also attempts to mimic the equivalent alkane number (for simplicity, one hydrocarbon with a carbon number equivalent to the average number of carbons in the oil) and is described more thoroughly elsewhere (50).

The phase type is expected to change from type III to type II(+), ie. the "optimal" system with stock tank oil becomes "over-optimal" with live crude oil. Such a change in phase behaviour should increase the amount of surfactant retained by the micelle core. Pressurising the stock tank crude oil with methane apparently causes little shift in phase behaviour. There is a small but insignificant, change towards type II(+) with methane. Using synthetic oil, the phase behaviour was considerably different. The presence of methane caused the phase environment to shift from type III to type II(-).

Using the original reservoir fluids where possible, it is necessary to produce ternary diagrams showing all the volume ratios of water, oil and surfactant. The solubilisation parameters can be deduced from these phase

volume diagrams. They are a measure of the volume of water and oil that is solubilised per volume of surfactant in the emulsion. A large volume of middle phase microemulsion indicates a large volume of a displacing phase with very low interfacial tension between it and the oil to be recovered. The value at which the microemulsion shows identical solubilisation for water and oil defines the point of optimum salinity. At this point, the interfacial tension between all the phases assumes a minimum value.

5.3.4 Techniques for Studying Microemulsions

Microemulsions have been studied with a wide variety of techniques, including:

(i) interfacial tension measurements (117) where low IFT is a typical property of microemulsions.

(ii) light scattering techniques, which identify the average particle size and interactions (118).

(iii) electrical conductivity, which is able to distinguish between o/w (exhibiting high conductivity) and w/o (showing low conductivity) emulsions (119).

In the following study, phase diagrams were used to study the microemulsions. The boundaries of the phase regions were found by visual observation. There is usually little

driving force towards equilibrium (e.g. differences in density) therefore, equilibration times were fairly long, normally a matter of weeks.

5.4 Experimental

Preliminary experiments (see Chapter 4) carried out on the nonionic surfactants showed them to be unsuitable for enhanced oil recovery at high temperature and high salinity (i.e. the Beryl reservoir conditions) because of their relatively low cloud points. The addition of an alcohol usually improved the behaviour of all surfactant classes but it could not prevent the precipitation of nonionic surfactants in high salinity brines. Hence, it was decided that anionic surfactants would probably be the most practical for EOR use in the Beryl field due to their higher stability.

Many surfactants and surfactant/alcohol mixtures were tested in order to determine their phase behaviour. Initially, the hydrocarbon phase used was n-decane and brines corresponding to seawater, reservoir brine and 50/50 seawater/reservoir brine formed the aqueous phases. The systems were studied in the presence and absence of short chain alcohols (i.e. propan-2-ol or isopropanol (IPA) with a b.pt. of 370.4K and 2-methyl propan-1-ol isobutanol(IBA) with a b.pt. 383K) cosolvents. They are reasonably inexpensive materials and remain stable liquids over the range of operating and reservoir conditions of 273-370K.

Into screw-topped sample tubes ($15cm^3$) was placed equal

volumes of the oil phase and aqueous surfactant solution. These tubes were shaken and left to equilibrate at various temperatures for 2-3 weeks. Evaluation of the phase behaviour is taken from the relative volumes of the separate phases observed and their characteristic appearance.

The following section combines results and discussion. It describes the reasoning and progress behind the route to promising surfactant blends. Illusstrative tables and figures are given throughout; each one discussed and explanations given for the next stages. Too many tables of results were produced to be included and so only a few are given as examples to illustrate the procedure.

5.5 Results and Discussion

5.5.1 Preliminary Experiments

Equilibrium phase studies carried out at 298K on simple solutions of T060S, T080S, T100S surfactants (Hoechst anionic) showed T080S to possess the best phase behaviour. Later, however, they were all found to exhibit poor behaviour in reservoir brine and formed II(+) systems in temperatures above 318K.

The system T080S appeared to be the most promising with the addition of an alcohol as a cosolvent resulting in improved phase behaviour; type III phases being produced. Figs. 5.6 and 5.7 show two different methods to illustrate the results. The former is the familiar triangular phase diagram. Surfactant concentrations of up to 10% (wt/vol) were used in various oil and brine

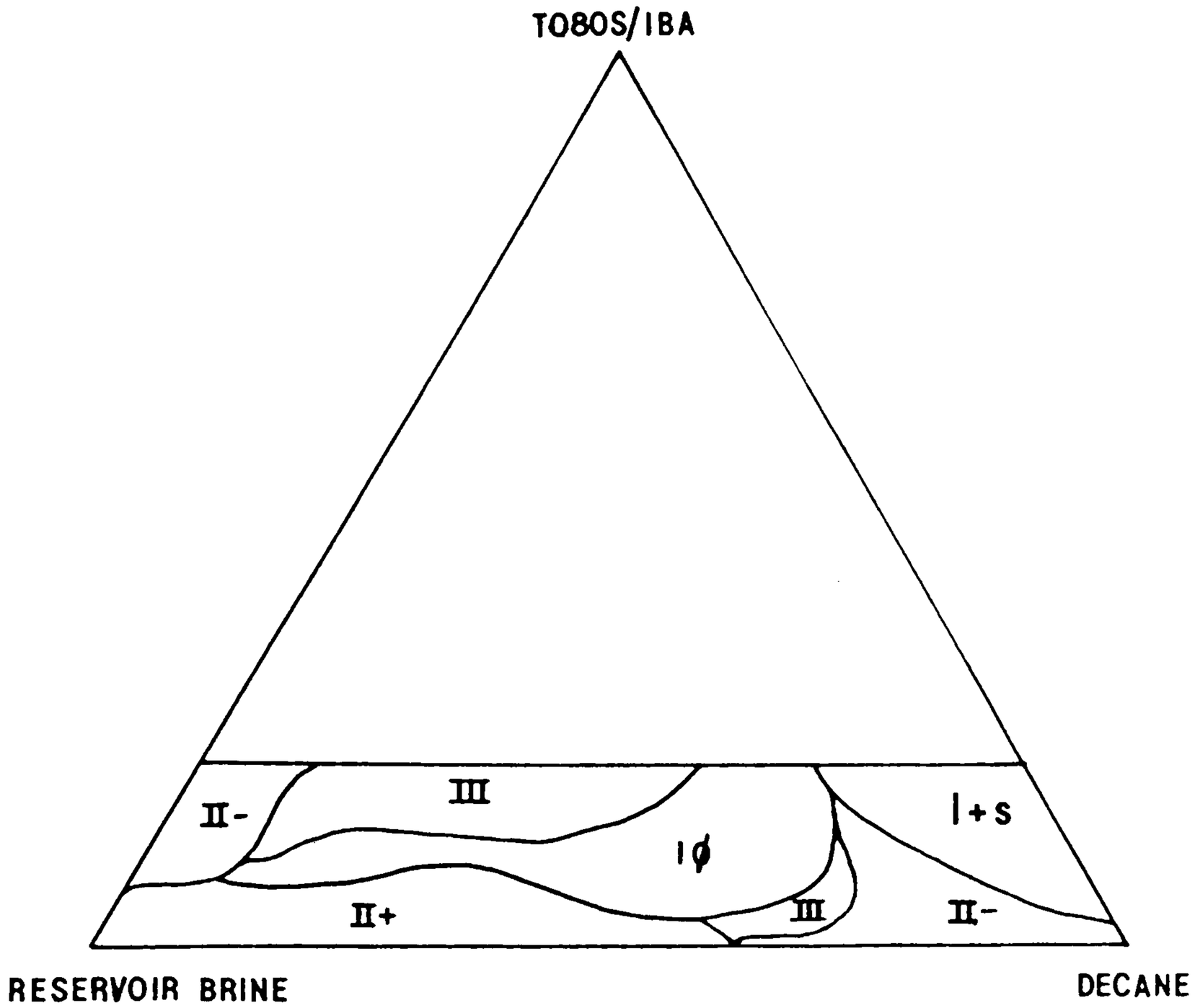

Fig.5.6 Phase behaviour of TO80S.

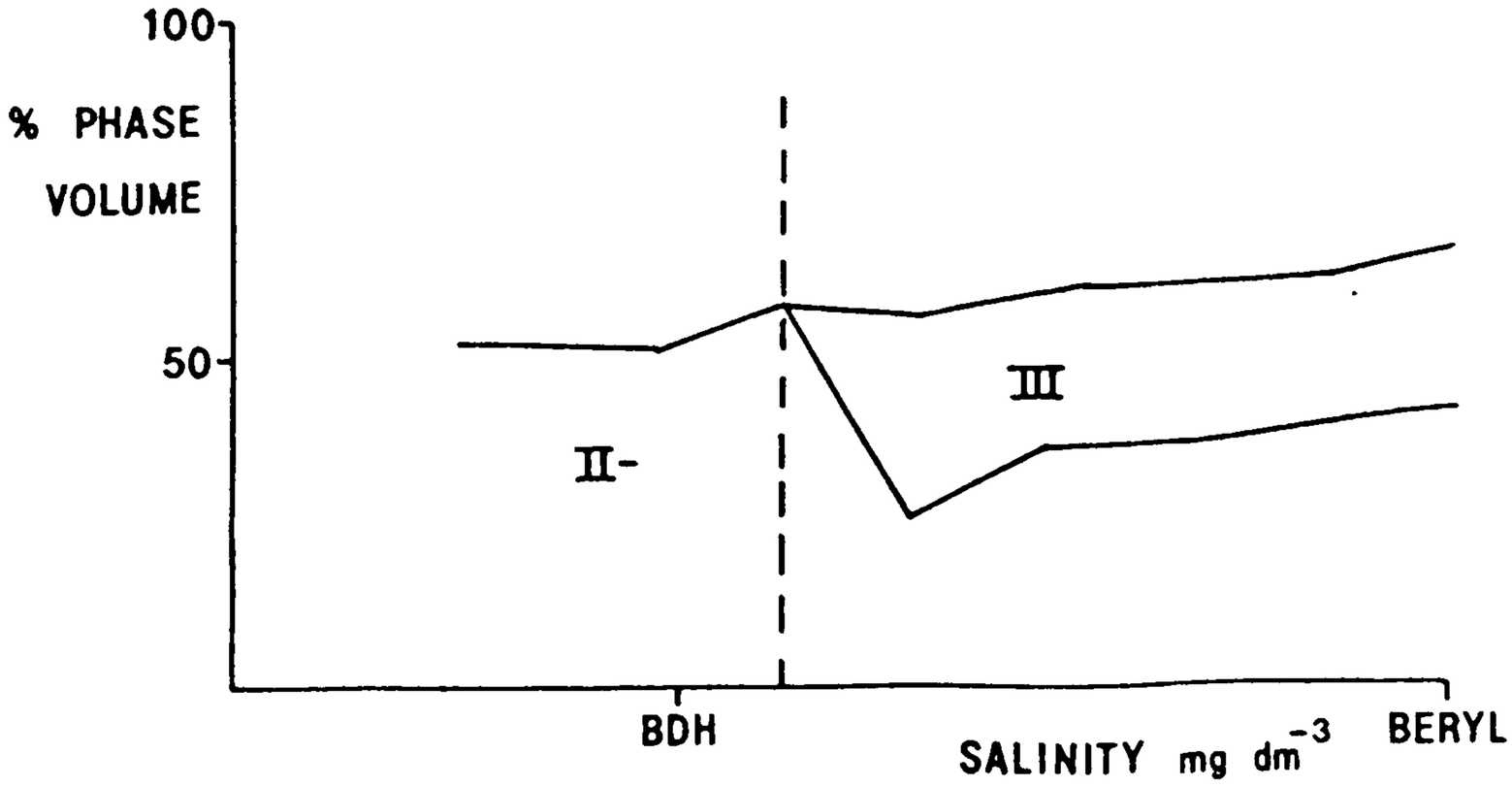

Fig.5.7 Phase behaviour of TO80S.

ratios. T080S was used with isobutanol as the cosolvent. These proportions represented equi-distant points in the lower third of the diagram and after analysing the experiments the regions of phases could be plotted. The other (see Fig.5.7) shows how the two main phases were produced as a function of salinity. The dotted line represents the meniscus between the microemulsion and the oil phase.

5.5.2 The Use of Novel Surfactants

It was clear that in their present form, the surfactants are unsuitable for oil recovery. Also, it was already known that the greater the number of ethene oxide units in nonionic species, the greater is their tolerance to the effects of heat and salinity in aqueous solutions. Also, surfactants with the sulphonate linkage exhibit the best phase behaviour in brine/decane systems. Thus it was deduced that a surfactant was required that contained the sulphonate linkage and had a chain length of 15 EO units or more. This type of surfactant was not commercially available and so it was necessary to synthesise it at Brunel. This work has already been described in Chapter 2.

Six nonionic surfactants(Sapogenats T180, T300; Arkopals N130, N150, N230, N300) were so sulphonated.

5.5.3 Effect of Structure

The extent to which the hydrophobic end of a surfactant is able to control the properties of the molecule is well understood in work carried out by Hoechst (71). Three

different types of sulphonated surfactants differing only in the hydrophobic chains attached to the aromatic nucleus were studied:

(i) tributyl (EO) - SO_3Na

(ii) nonyl (EO) - SO_3Na

(iii) dinonyl (EO) - SO_3Na

The results quoted by Hoechst from microcapillary deoiling and interfacial tension measurements, show the surfactants with the tributyl structure (i) to be the optimum for EOR applications.

The results of the Brunel sulphonates agreed in that the nonyl group is the least stable when dissolved in brines of high salt content and the dinonyl is intermediate between (i) and (iii). The nonyl group possesses almost free rotation about the aromatic nucleus and is able to orientate itself in such a way as to occupy the least possible hydrophobic configuration. The molecule therefore has a greater difficulty in forming micelles and stabilising oil-brine emulsions. The tertiary groups on the surfactants (i) are not subject to this free rotation and so the properties of the surfactant molecules are retained in brine.

5.5.4 Phase Studies on the Novel Sulphonates

Phase studies carried out on the sulphonated surfactants initially showed excellent phase behaviour with larger volumes of type III appearing than for T08OS/IBA (see Table 5.1). However, after a few weeks at temperatures in excess of 333K a sharp deterioration in the phase properties occurred. Precipitation was also noticed

Surfactant	Media	Temperature in K			
		290	318	328	343
N300S	Distilled Water	III	II+	II+	II+
	Sea Water	III	II+	II+	II+
	Seawater/Res.Brine50:50	III	II+	II+	II+
	Beryl Res. Brine	III	II+	II+	II+
N150S	Distilled Water	III	II+/III	II+ III	II+/III
	Seawater	III	II+/III	II+ III	III
	Seawater/Res.Brine50:50	III	II+/III	III	III
	Beryl Res. Brine	III	III	III	III/II-

TABLE 5.1 Phase behaviour of sulphonated surfactants N300S and N150S

which is a common occurrence. There is a decrease in the sulphur content that is thought to be due to hydrolysis of the sulphonates:

$$R\text{-}SO_3\text{-}Na + H_2O \rightarrow R\text{-}OH + NaHSO_4$$

FTIR analysis carried out on samples of the surfactant before and after equilibrium showed that hydrolysis had occured. A shift towards a type II(+) phase equilibrium was also observed.

5.5.5 Phase Studies on Commercial Sulphonates

In the previous studies described, all phase equilibrium measurements used decane as the oil phase. Some experiments would be of greater value in an EOR sense if the surfactants were tested against dead (or topped) crude oil. This is "live" crude oil minus the gaseous and very light volatile components. At this stage Mobil North Sea oil was unavailable and so the oil used was a sample of topped crude oil from the BP Forties field. Heochst had provided a series of low and high molecular weight nonionic surfactants with their sulphonated homologues.

The phase results for these are given in Tables 5.2 and 5.3. The results on these commercial surfactants show that sulphonates with long ethoxylate chains give favourable phase behaviour with decane but are less successful with the crude oil. The shorter ethoxylate chains perform better with the crude oil. The cosolvent IPA or IBA improves the hydrophilic character of the surfactants which promotes II(-) phases. From the

1. T040S / BDH BRINE
2. T040S / IPA / BDH BRINE
3. T040S / IBA / BDH BRINE
4. T040S / BDH:MOBIL BRINE (50:50)
5. T040S / IPA / BDH:MOBIL BRINE (50:50)
6. T040S / IBA / BDH:MOBIL BRINE (50:50)
7. T040S / MOBIL BRINE
8. T040S / IPA / MOBIL BRINE
9. T040S / IBA / MOBIL BRINE
10. T040S / BDH / BP CRUDE
11. T040S / IPA / BDH / BP CRUDE
12. T040S / IBA / BDH / BP CRUDE
13. T040S / BDH:MOBIL BRINE (50:50) / BP CRUDE
14. T040S / IPA / BDH:MOBIL BRINE (50:50) / BP CRUDE
15. T040S / IBA / BDH:MOBIL BRINE (50:50) / BP CRUDE

TABLE 5.2.1 Key of components used on TABLE 5.2.2.

SYSTEM	TYPE	PHASES % LOWER	% MIDDLE	%UPPER
1.	II-	43	0	57
2.	III	40	5	55
3.	Iϕ	---------- turbid ----------		
4.	II-	45	0	55
5.	III	37	10	53
6.	III	37	15	48
7.	2ϕ	45	0	55
8.	2ϕ	45	0	55
9.	2ϕ	45	0	55
10.	II-	43	0	57
11.	II-	44	0	56
12.	II-	44	0	56
13.	III	40	7	53
14.	III	34	24	42
15.	III	9	68	23

Table 5.2.2.

1. T080S / BDH BRINE
2. T080S / IPA / BDH BRINE
3. T080S / IBA / BDH BRINE
4. T080S / BDH:MOBIL BRINE (50:50)
5. T080S / IPA / BDH:MOBIL BRINE (50:50)
6. T080S / IBA / BDH:MOBIL BRINE (50:50)
7. T080S / MOBIL BRINE
8. T080S / IPA / MOBIL BRINE
9. T080S / IBA / MOBIL BRINE
10. T080S / BDH / BP CRUDE
11. T080S / IPA / BDH / BP CRUDE
12. T080S / IBA / BDH / BP CRUDE
13. T080S / BDH:MOBIL BRINE (50:50) / BP CRUDE
14. T080S / IPA / BDH:MOBIL BRINE (50:50) / BP CRUDE
15. T080S / IBA / BDH:MOBIL BRINE (50:50) / BP CRUDE

TABLE 5.3.1 Key of components used for TABLE 5.3.2.

SYSTEM	TYPE	PHASES % LOWER	% MIDDLE	% UPPER
1.	II+	44	0	56
2.	II+	44	0	56
3.	II+	45	0	55
4.	II-	55	0	45
5.	III	20	39	41
6.	III	37	24	39
7.	II+	43	0	57
8.	2Ø	43	0	57
9.	IØ	----------turbid----------		
10.	II+	43	0	57
11.	II+	44	0	56
12.	II+	43	0	57
13.	II+	42	0	58
14.	II+	41	0	59
15.	II+	40	0	60

Table 5.3.2.

results, IPA appears to be a more effective cosolvent than IBA due to the more hydrophilic character of the former.

5.5.6 Introduction of a Cosurfactant

At a salinity of about 1.5% in aqueous solutions, petroleum sulphonates tend to form precipitates as previously described. In the case of the Hoechst secondary alkane sulphonate SAS 60, precipitation does not begin until a salinity 2.5 or 3.0%. If too much cosurfactant is used, then the sulphonate is rendered so soluble in water that its effectiveness for reducing the interfacial tension is reduced. Moreover, the cost of the cosurfactant is generally 2-5 times as great as the primary anionic surfactant.

Hoechst trials on SAS 60 show the interfacial tension is dependent to some extent on temperature and is also markedly influenced by the salinity of the solution. An IFT of 0.6 Nm^{-1} was detected in demineralised water but with addition of 5g of salt per dm^3, the value was 0.8 mNm^{-1}. Good salt compatability and interfacial tension reduction of this surfactant is not sufficient for its use alone in an oil reservoir. It is therefore logical to experiment with this surfactant combined with others.

Hoechst tested a combination of SAS 60 with a series of nonionic surfactants since these are stable, inexpensive and readily available. The two surfactants were highly compatible but gave a poor decrease in the IFT than with the nonionic alone and unsatisfactory flooding results.

This is attributed to the greater adsorption of the nonionic ethoxylated surfactant on a packed sandstone column which destroys the mixed ratio. Hoechst then tested various ratios of SAS 60 with sulphates, sulphonates and carboxylates (all prepared from the tributyl phenolethoxylates). The sulphonates used with SAS 60 as a cosurfactant exhibited considerable compatibility with salt and produced low IFTs. This was true across a range of temperatures from ambient to above 333K (when the sulphates hydrolyse) and also across a broad salinity range of 75-150g.dm^{-3}. Another advantage is that their adsorption on quartz is comparable in magnitude, thus separation of the surfactant mixture during the flooding process is less likely.

Another possible cosurfactant supplied by Hoechst is B712. Very little is known about this compound and it is not (at the time of writing) available on the market. As described in Chapter 2, it is also a secondary alkane sulphonate but contains higher carbon numbers than SAS 60. Hoechst had conducted no trials on this surfactant but, considering its similarity to SAS 60, it appeared to be a promising cosurfactant.

At this stage, Mobil North Sea oil was available and the remaining phase studies were carried out using this. So far, the most promising system investigated (with decane, and BP Forties crude oil) is a combination of the two Hoechst sulphonates T040S and B712 with IPA. Further work was carried out using blends of short chain sulphonates T040S and T060S and a cosurfactant of B712 or

SAS 60. The results are tabulated in Tables 5.4 and 5.5, and the following blends gave the most promising results (in order):-

1.	T040S/B712/IPA	ratio - 80:10:10
2.	T040S/SAS 60/IPA	80:10:10
3.	T040S/IPA	90:10
4.	T040S	100
5.	T060S/IPA	90:10
6.	T060S	100

The results show that the phase behaviour of T040S and T060S are markedly enhanced by the addition of IPA and a cosurfactant (B712 or SAS 60). The behaviour of blends 1,2, and 5 (above) was found to be fairly tolerant of slight changes in surfactant composition. The addition or removal of a few percent of one component of the surfactant mixture did not appear to be detrimental to phase performance.

5.5.7 Experiments with Synthetic Mobil Oil

The results reported in Table 5.6 with synthetic hydrocarbon phases do not give good correlation with results obtained from similar experiments carried out with stock tank crude diluted with iso-octane.

The precipitation of the surfactant systems out of solution was a problem and in general, oil solubilisation was found to be low (i.e. less than 50% volume of oil and 50% volume of surfactant). In addition, many systems show no phase mixing of the oil and water layers at all, even after standing to equilibrate for 6 weeks at 343K.

BRINE	TEMP(K)	TYPE	PHASES LOWER	MIDDLE	UPPER
Seawater	293	IØ	----no phase boundary----		
50/50 Brine	"	IØ		"	
Formation	"	IØ		"	
Seawater	318	III	15	47	38
50/50 Brine	"	"	10	41	49
Formation	"	"	6	85	9
Seawater	338	II-	53	0	47
50/50 Brine	"	III	40	10	50
Formation	"	III	37	23	40
Seawater	336	II-	53	0	47
50/50 Brine	"	III	41	8	51
Formation	"	III	2	93	5

TABLE 5.4 Phase Results for the Surfactant System T040S (40%), B712 (10%), IPA (50%) -10% solution.

BRINE	TEMP(K)	TYPE	PHASES LOWER	MIDDLE	UPPER
BDH	318	III/Ppt	44	7	49
BDH/MFB	"	"	44	7	49
MFB	"	"	44	7	49
BDH	338	III	32	40	38
BDH/MFB	"	III	40	35	25
MFB	"	- precipitation of surfactant blend			
BDH	353	II-	52	0	48
BDH/MFB	"	- precipitation of surfactant blend			
MFB	"	- " " " "			

Phase Results for Surfactant System
T040S (80%), B712 (10%), IPA (10%) - 10% solution

BDH	318	- precipitation of surfactant blend			
BDH/MFB	"	- " " " "			
MFB	"	- " " " "			
BDH	338	II+	40	0	60
BDH/MFB	"	- precipitation of surfactant blend			
MFB	"	- " " " "			

Phase Results for Surfactant System
T040S (80%), SAS60 (10%), IPA (10%) - 10% solution

TABLE 5.5

BRINE	TEMP(K)	TYPE	PHASES LOWER	MIDDLE	UPPER
BDH	318	N.O.M.	50	0	50
BDH/MFB	"	N.O.M.	50	0	50
MFB	"	III	37	15	48
BDH	338	- precipitation of surfactant blend			
BDH/MFB	"	-	"	"	"
MFB	"	-	"	"	"
BDH	353	N.O.M.	50	0	50
BDH/MFB	"	N.O.M.	50	0	50
MFB	"	N.O.M.	50	0	50

Phase results for T060S (100%)

BDH	318	N.O.M.	50	0	50
BDH/MFB	"	II-	42	0	48
MFB	"	III	40	20	40
BDH	338	N.O.M.	50	0	50
BDH/MFB	"	II-	52	0	48
MFB	"	III	32	26	32
BDH	338	III	23	35	42
BDH/MFB	"	III	2	62	36
MFB	"	III	47	20	33
BDH	353	II-	53	0	47
BDH/MFB	"	III/Ppt	27	25	48
MFB	"	- precipitation of surfactant blend			

Phase Results for Surfactant System
T040S (90%), IPA (10%) - 10% solution

TABLE 5.5 (cont.)

BRINE	TEMP(K)	TYPE	PHASES LOWER	MIDDLE	UPPER
Seawater	313	II-	56	0	44
50/50 Brine	"	II-	55	0	45
Formation	"	II-	56	0	44
Seawater	338	II-	55	0	45
50/50 Brine	"	III	42	30	28
Formation	"	III	40	25	35

TABLE 5.6 Phase Results for the Surfactant System T040S (80%), SAS60 (10%), IPA (10%) - 10% solution.

BRINE	TEMP(K)	TYPE	PHASES LOWER	MIDDLE	UPPER
Seawater	313	II-	52	0	48
50/50 Brine	"	II-	51	0	49
Formation	"	II-	51	0	49
Seawater	338	II-	52	0	48
50/50 Brine	"	II-	52	0	48
Formation	"	II-	52	0	48

TABLE 5.6 Phase Results for the Surfactant System T060S (80%), SAS60 (10%), IPA (10%) - 10% solution.

BRINE	TEMP(K)	TYPE	PHASES LOWER	MIDDLE	UPPER
BDH	318	N.O.M.	50	0	50
BDH/MFB	"	II-	52	0	48
MFB	"	Ppt			
BDH	338	II-	51	0	49
BDH/MFB	"	II-	51	0	49
MFB	"	- prcipitation of surfactant blend			

Phase Results for Surfactant System
T080S (80%), IPA (20%) - 10% solution

TABLE 5.6 (cont.)

The effect of adding iso-octane (to mimic the viscosity of live crude oil) was to change the phase behaviour from II- towards III and finally II+. The blends of T040S/B712/IPA or T040S/SAS 60/IPA with iso-octane/stock tank crude showed the best phase behaviour. For systems which used synthetic hydrocarbons, the T060S/IPA blend gave the best behaviour.

Overall, using the stock tank crude results, the blend of T060S/IPA appears to be the most tolerant to different types of oil phases. It unfortunately offered fairly poor oil solubilisation.

In comparison, the blends of T040S/B712 or T040S/SAS 60 (both with IPA) displayed good oil solubilisation, but only for a limited range of hydrocarbon blends.

5.6 Microcapillary Deoiling Studies

5.6.1 Introduction

Capillary deoiling was used as a rapid method of determining the deoiling efficiency of surfactant solutions. These studies are not necessarily a strong indication of the performance of the surfactant blends. Nevertheless, it was thought that these tests would give a good guide to the success of the blends. The results are discussed on a relative rather than on a quantitative basis.

5.6.2 Experimental

The results were obtained on measurements of the ability of the surfactant systems to deoil a glass capillary tube

of 1mm diameter and 25mm in length. They are sealed at one end and filled completely with Mobil oil. The capillaries were placed in a tube containing the surfactant blend and the time is recorded for the capillaries to empty completely of oil.

5.6.3 Results

The deoiling times are listed in Tables 5.7 and 5.8. The primary anionic surfactant was always present and the concentrations of IPA, SAS 60 and B712 altered.

5.6.4 Discussion

The addition of IPA was found to improve the deoiling behaviour of all surfactant systems studied. The addition of a cosurfactant apparently impaired the action of T060S but markedly improved the performance of T040S where SAS 60 was prefered to B712; too much IPA obviously results in longer deoiling times since this is added at the expense of a surfactant. Overall, it is clear that the presence of a cosurfactant in a low concentration is not detrimental to the blend. The times for T040S are noticeably longer than for T060S.

5.7 Viscosity Measurements

The results of the viscosity measurements carried out on surfactant formulations in brine and on the hydrocarbon phases are given in Tables 5.9 and 5.10 respectively.

From Table 5.9, it is clear that for a type of sulphonated surfactant, the measured viscosity at a particular temperature varies little with surfactant

Surfactant Blend			Deoiling Time (Min) --------293(K)---------				--------338(K)--------			
T060S	B712	IPA	8.0	4.0	2.0	0.8	8.0	4.0	2.0	0.8
100	0	0	1.2	2.2	4.4	6.8	1.2	3.5	4.8	5.0
90	10	0	7.0	6.0	7.0	16.0	2.4	9.5	11.8	25.0
80	20	0	38.0	56.5	64.5	73.5	11.0	13.0	13.0	15.0
50	0	50	1.1	1.3	1.4	2.8	0.4	0.7	1.2	2.1
45	45	10	17.0	72.5	134.0	231.0	18.5	79.0	85.0	296.0
45	5	50	4.0	4.0	7.0	10.0	0.7	1.3	1.6	2.0
40	10	50	9.2	8.8	29.5	59.4	0.8	3.0	5.3	6.7
25	25	50	31.0	28.5	28.5	6000.0	0.8	4.5	6.5	7.5

TABLE 5.7 Microcapillary Deoiling Trials on T060S.

Surfactant Blend			Deoiling Time (Min)							
			--------293(K)----------				----------338(K)-------			
T040S	B712	IPA	8.0	4.0	2.0	0.8	8.0	4.0	2.0	0.8
100	0	0	9.2	17.7	25.1	135.0	2.1	12.4	14.4	52.0
90	10	0	5.5	8.0	31.5	102.0	3.5	5.5	30.0	79.0
80	20	0	7.0	12.0	18.5	48.7	2.5	4.0	8.5	130.0
50	0	50	3.0	77.0	720.0	10000.0	1.2	4.3	57.0	90.0
45	45	10	6.0	14.5	153.0	1900.0	1.0	1.6	6.0	37.0
45	5	50	3.6	63.5	7200.0	14400.0	1.6	3.0	28.0	480.0
40	10	50	1.5	5.5	11.5	120.0	0.8	3.0	5.3	6.7
25	25	50	2.5	7.5	240.0	308.0	1.0	1.5	3.8	75.0
80	10	10	5.0	16.0	73.0	500.0	1.7	5.0	9.5	94.5
T040S	SAS60	IPA								
80	10	10	2.5	4.5	15.0	50.0	1.8	2.3	5.6	9.7
90	10	0	6.1	8.2	42.0	120.0	3.0	6.1	19.7	43.0

TABLE 5.8 Microcapillary Deoiling Trials on T040S.

Surfactant Composition	Temperature(K)	Viscosity(mPa.s)
T060S(100%)	293	1.19
@ 2% in Seawater	343	0.64
T060S(90%) + IPA(10%)	293	1.23
@ 2% in Seawater	343	0.62
T040S (99%) + IPA (10%)	293	1.24
@ 2% in Seawater	343	0.62
T040S(80%) + B712(10%) + IPA(10%)	293	1.24
@ 2% in Seawater	343	0.67
T040S(80%) + SAS60(10%) + IPA(10%)	293	1.23
@ 2% in Seawater	343	0.63

TABLE 5.9 Viscosity Measurements on Surfactant Solutions in Brine.

Oil Phase	Temperature(K)	Viscosity(mPa.s)
Iso-Octane	293	0.541
Synthetis STC*	"	2.019
Synthetic Live	"	0.768
STC(Beryl B)	"	8.030
STC(Beryl)50% : Iso-Octane50%	"	1.882
Synthetic Live	348	0.513
STC(Beryl)90% : Iso-Octane10%	"	1.720
STC(Beryl)80% : Iso-Octane20%	"	1.519
STC(Beryl)70% : Iso-Octane30%	"	1.286
STC(Beryl)60% : Iso-Octane40%	"	1.029
STC(Beryl)50% : Iso-Octane50%	"	0.916

* - STC =Stock Tank Crude

TABLE 5.10 Viscosity Measurements on Hydrcarbon Phases.

composition. For example - at 293K for a 2% (wt/vol) solution, the viscosity will be 1.19 mPa.s to 1.24 mPa.s and at 343K, the range is 0.62-0.67 mPa.s.

The viscosities of the hydrocarbon phases reported in Table 5.10 show a blend of 50% iso-octane and 50% stock tank crude to represent the best working formulation for simulating "live" crude oil in experimental trials.

5.8 Laboratory Flooding Trials

5.8.1 Introduction

Flooding trials are the only complete and final method for determining the effects of the proposed injection fluid upon the permeability of the formation reservoir. There are many such tests illustrated in the literature (116) but this type of research could not be carried out at Brunel. Hoechst AG. in Frankfurt agreed to carry out preliminary trials on 3 blends (labelled A,B,C) which they prepared. Brunel sent the oil which was to be used. This was a blend of 50% iso-octane with 50% Mobil stock tank crude oil.

The experimental conditions and results were forwarded in a report from Hoechst and this is included in appendix 1.

Other tests were also carried out - solubility, microcapillary deoiling, lowering of the interfacial tension, phase behaviour and adsorption measurements. These results are also provided with the report, which is discussed in the final chapter.

CHAPTER 6

6.1 Introduction

6.1.1 Adsorption at the Solid-Liquid Interface

Adsorption is always important with surfactant-based enhanced oil recovery methods and high adsorption is a major drawback to their use. Adsorption can affect:

(i) the cost effectiveness of the EOR process as chemicals are lost (as a result of selective adsorption and chromatographic separation);

(ii) the chemical balance of the slug;

(iii) the permeability of the rock matrix; and

(iv) the wettability of the reservoir rock.

Besides adsorption onto reservoir rock, surfactant loss can occur by dissolution into the oil phase resulting in surfactant being trapped in residual oil. Various methods have been proposed for reducing the loss including the use of different salts and sacrificial adsorbates such as short chain alcohols or surfactants having a broad range of chain lengths. It has been reported (120) that the adsorption of petroleum sulphonates is selective or that the high equivalent weight sulphonates are adsorbed preferentially while the useful low chain lengths show almost no adsorption at all.

For some surfactant solutions, the loss reaches a minimum value if the reservoir is preflushed with brine or a sodium chloride solution (121). For low concentration surfactant floods, surfactant adsorption is the critical factor affecting the efficiency of the operation. With widely spaced production wells (5 spot pattern), a

strongly adsorbing surfactant in a dilute aqueous solution would provide little or no surfactant at the flood front to release the oil or the time lag would be intolerably long. Further, if surfactant adsorption rendered the formation oil-wet, this would add to the delay in production; rapid oil production being associated with water-wet pores.

Commercial polyethoxylated surfactants are usually mixtures of homologues with a Poisson distribution of ethoxy groups (122). This problem requires the measurement of adsorption of each species. The total adsorption of mixtures of surfactants can be higher than that of the individual species of which they are composed. Some adsorption studies have utilised single-component systems (123), but most have used mixtures, sometimes with a narrowed distribution (124). Most isotherms measure the total adsorption of a mixture.

One of the earliest sets of adsorption measurements reported is that of Hsiao and Denning (125) using ill-defined commercial nonionic surfactant mixtures. McCracken and Datyner (126) subsequently re-analysed this data and concluded that the calculated area per adsorbed molecule for a heterogeneous surfactant is close to that expected for the equivalent homogeneous surfactant. Even if selective adsorption occured, the apparent adsorption maximum does not differ significantly from the mixture to the single-component surfactant.

6.1.2 Mixed Micelles

Mixed micelles are formed by mixtures of similarly structured ionic or nonionic surfactants. They can show large deviations from ideal solution theory because the micellar composition of these solutions will differ from the bulk composition of the surfactant mixture. For example, the cmc of these mixtures is often much less than predicted and in some cases is less than the cmc of either of the surfactant components. This is due to a reduction in the electrical repulsions of the charged head group of the ionic surfactant as the nonionic molecules intrude between them. Above and below the cmc, the amount adsorbed in equilibrium with the bulk solution will vary with surface/solid ratio through fractionation of the differing components in the mixture.

6.1.3 The Adsorption Isotherm

A number of attempts to model surfactant adsorption have been reported, for example the finite-layer BET model (127) with the Langmuir adsorption isotherm and the Tempkin model (128). Scamehorn (129) and Cases (130) believed that none of these represents the characteristic isotherm shapes and so developed theoretical based models which represent real isotherm shapes. The model used here for simplicity is based on the Langmuir concept.

6.1.4 Adsorption Equation

At the solid-liquid interface, it is necessary to determine:

(i) the amount of surfactant adsorbed per unit mass or area of the solid adsorbent;

(ii) the equilibrium concentration of the surfactant in the solution/liquid phase;

(iii) the concentration of the surfactant at the surface of the adsorbent and

(iv) the orientation and therefore mechanism of the adsorbed surfactant.

The fundamental equation for calculating the amount of one component (component 2) of a binary solution adsorbed onto a solid adsorbent is (131):

$$n_o \, {}_m\Delta X_2 = n^s{}_2 X_1 - n^s{}_1 X_2$$

where

n_o = the total number of moles of solution before adsorption

ΔX_2 = $X_{2,0} - X_2$

$X_{2,0}$ = the mole fraction of component 2 before adsorption

X_1, X_2 = the mol fractions of components 1 and 2 at adsorption equilibrium

m = mass of adsorption (g)

$n^s{}_1$, $n^s{}_2$ = the number of moles of components 1 and 2 adsorbed per gram of adsorbent at equilibrium.

When the liquid phase is a dilute solution of a surfactant (component 2) that is more strongly adsorbed onto the solid than the solvent (component 1), then:

$$n_o \, \Delta X_2 \approx n_2$$

where

n_2 = the change in the number of moles of component

$n^s{}_2 = 0$ and $X_1 = 1$

therefore

$$n^s{}_2 = \frac{n_2}{m} = \frac{C_2.V}{m}$$

where

$C_2 = C_{2,0} - C_2$

$C_{2,0}$ = molar concentration of component 2 before adsorption;

C_2 = molar concentration of component 2 at adsorption equilibrium;

V = total volume of liquid phase, litres.

Then n^s_2, the amount adsorbed, is plotted against C_2, the equilibrium concentration to give the adsorption isotherm.

The isotherm can be plotted in terms of surface concentration C^s_2 in moles.g^{-1} as a function of C_{eq2}. The surface area per unit mass of the solid adsorbent is as;

$$C^s_2 = \frac{C_2 \cdot V}{a_s . m}$$

The Langmuir isotherm (127) is commonly expressed as:

$$C^s_2 = \frac{C^s_m \cdot C_2}{C_2 + a}$$

6.1.5 General Features of the Isotherm

The adsorption isotherms of nonionic surfactants are generally Langmuirian and thus of the type shown in Fig.6.1 reversible with little hysteresis. The first plateau, A, has been found in only a few systems but this may be explained by lack of experimental data in this region of very low concentrations which may obscure the presence of the plateau. The inflection and sharp increase at B occur at concentrations which are close to the cmc. This is followed by a second plateau region at C and a further, usually very marked increase at D is sometimes observed at higher concentrations.

Occasionally, plateau C is absent from such systems and the isotherm takes on a sigmoidal shape (131).

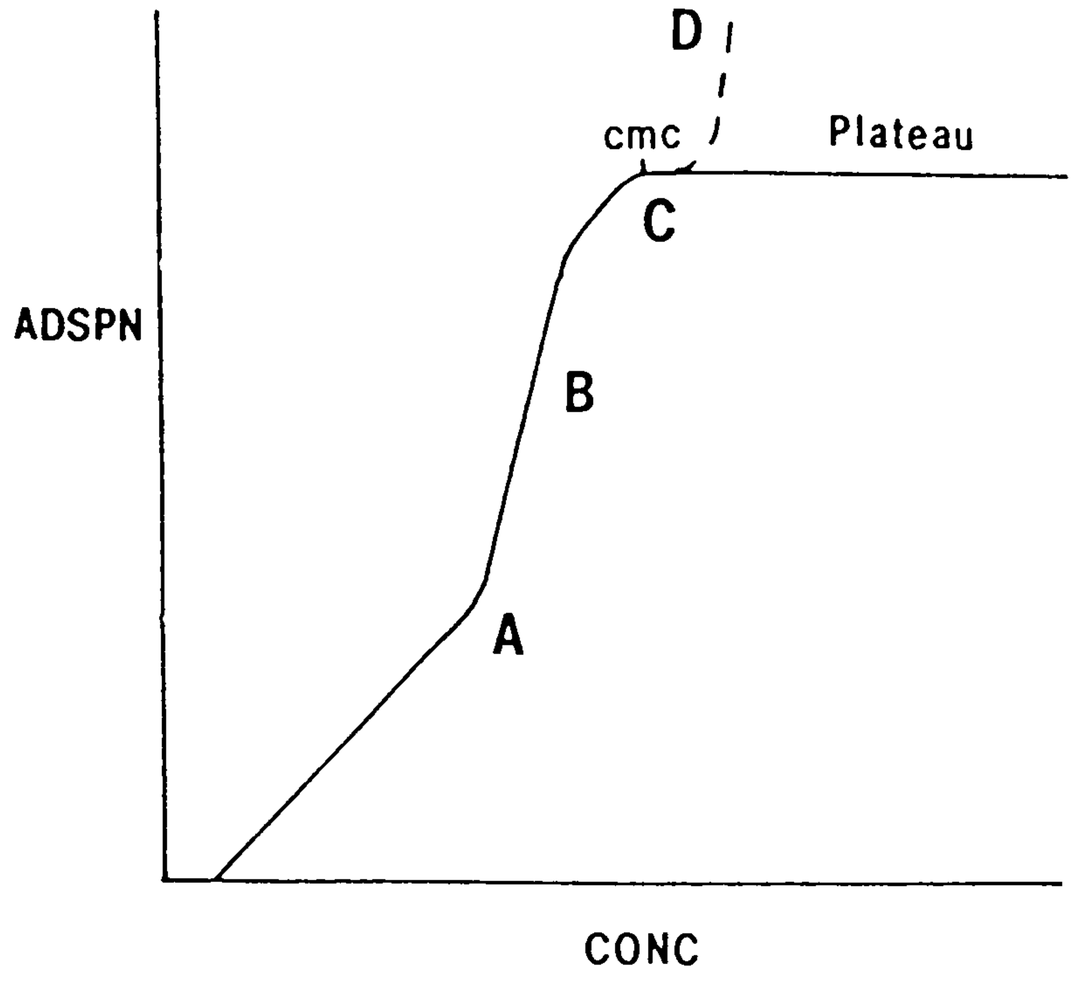

Fig.6.1 Idealised Langmuir isotherm for adsorption of surfactants at the solid/liquid interface.

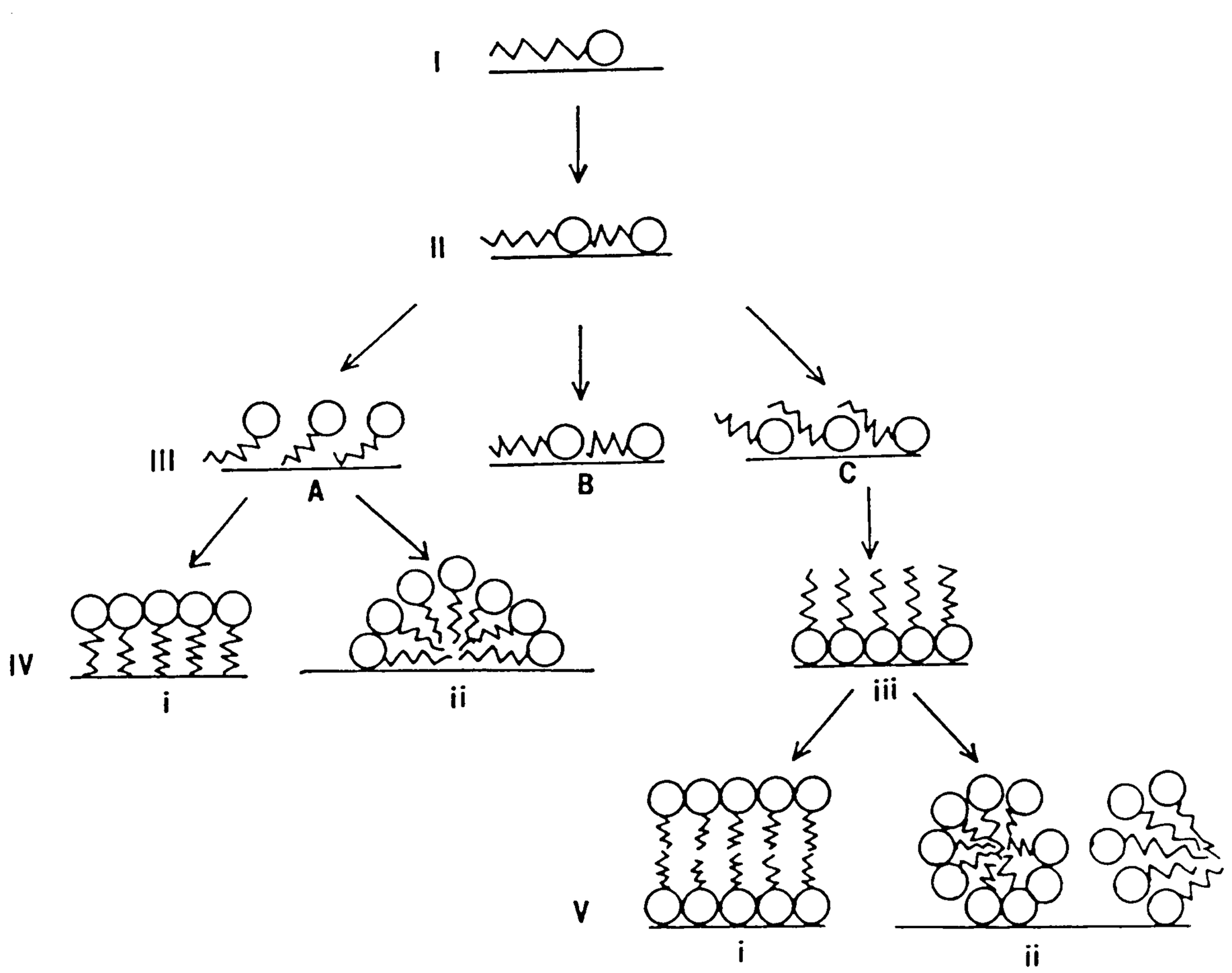

Fig.6.2 Changes undergone by adsorbed nonionic surfactants.

The molecular structure of the surfactant influences the shape of the isotherm. Within a homologous series, it is found that increasing the length of the hydrocarbon chain generally increases the magnitude of adsorption at the plateau C. Increasing the size of the polar group by adding ethene oxide units tends to decrease adsorption and also the cmc. The initial slope of the isotherm tends to increase with increasing alkyl chain length but changes in the hydrophilic group varies according to the effect of adsorbate structure. As the adsorbate becomes more polar, the first plateau occurs at lower adsorption values and in some studies adsorption appears to occur only at concentrations above the cmc.

6.2 Theory of Nonionic Surfactant Adsorption.

Nonionic surfactants are physically adsorbed, rather than chemisorbed. The adsorbate-adsorbate and adsorbate-solvent interactions (due to hydrogen bonding) cause aggregation in bulk solution which lead to changes in orientation and packing of surfactant at the surface. Fig.6.2 shows the most likely changes undergone by nonionic surfactants adsorbed from aqueous solution.

Stage I. At very low concentrations, monomer-monomer interactions are negligible. Adsorption occurs because of van der Waal's forces and the surfactant adsorbs onto a surface where there are very few other molecules. In this region, the individual molecules are unassociated and exist as sparsely adsorbed species lying flat on the surface. Henry's law is also obeyed.

Stage II. A gradual increase in the slope of the isotherm occurs as monolayer saturation is approached. Most of the solvent molecules will have been displaced from the surface, although the surfactant itself will probably still be hydrated, (see Fig.6.2(II)).
The subsequent stages of adsorption are dominated by adsorbate-adsorbate interactions. These interactions determine how the adsorption will progress which depends on the nature of the adsorbent and the hydrophobic-lipophilic balance (HLB), which has been explained fully in Chapter 5, in the surfactant.

Stage III. If the hydrophilic group is only weakly adsorbed it will be displaced from the surface by the alkyl chains of adjacent molecules, Fig.6.2(III)A is favoured if the surface is nonpolar or the surfactant has a low HLB (ie. short rather than long EO chain).
However, with a polar surface, there is a strong interaction between the hydrophilic group and the surface, and the alkyl chain is displaced. Fig 6.2(III)B, occurs when neither type of displacement is favoured and the molecule lies flat on the surface. In this case adsorption is not expected to change with any further increase in concentration since there is little evidence for the existence of layers of nonionic molecules at high bulk concentrations lying flat on a surface.

Stage IV. The change in the amount adsorbed in the third stage is unlikely to be great but as the concentration of the surfactant in the bulk solution approaches the cmc

(C_{eq} <cmc) there will be a tendency for the alkyl chains of the adsorbed molecules to aggregate. The molecules will become vertically oriented and a large increase in adsorption will be observed. The lateral forces due to the alkyl chain interactions tend to lead to an uncoiling of the ethene oxide chain, thus reducing the surface area occupied per molecule. Therefore, the longer the (surfactant) alkyl chain (and the shorter the polyethene oxide chain), the greater the extent of adsorption. With nonpolar adsorbents, the surface aggregation process can occur at concentrations below the cmc. With polar adsorbents, the head group may be strongly bound to the (hydrophobic) surface and not until the surfactant concentration is above the cmc will the alkyl chains pack closely, (see Fig.6.2(IV)(iii)). For non-polar adsorbents, Fig.6.2(IV)(i) or (ii) represents the final adsorption state, but for polar adsorbents, Fig.6.2(IV)(iii) is only an intermediate stage.

Stage V. Increasing the surfactant concentration causes further adsorption, promoted by alkyl-alkyl attraction. The surface micelle model for adsorption on polar solids above the cmc is shown in Fig. 6.2(V)(ii). The changes taking place are similar in the adsorption layer (but slightly distorted) as in the bulk solution. With comparable aggregation numbers the surface regains its hydrophilic character. The plateau reached is usually twice the value as in the monolayer and can be increased by raising the temperature as the hydrophobic chains become less solvated and more compact. Lengthening the alkyl chain and decreasing the ethoxy chain increases

adsorption since lateral compression is increased.

The absence of adsorption below the cmc in certain nonionic surfactant-polar surface systems may indicate a process whereby the van der Waal's attraction between surfactant and surface is opposed by a repulsion from a relatively thick surface solvation layer. Adsorption is prevented until Stage IV, when surfactant aggregation effects dominate. However, most nonionic surfactants contain polar groups which are likely to be adsorbed quite strongly on polar surfaces by hydrogen bonding to surface hydroxyls. Any apparent absence of adsorption below the cmc is more likely to be due to lack of detection at very low concentrations.

Klimenko (132) suggested that above the cmc, adsorbed surfactants form micellar or hemi-micellar aggregates on the surface, as described above. Data on the kinetics of adsorption indicate that the micelles on the surface are not deposited from bulk solution but result from the association of previously adsorbed monomer.

6.3 Anionic Surfactants

6.3.1 Adsorption of Anionic Surfactants

The original theory of an adsorption mechanism was first expounded by Gaudin and Fuerstenau in 1955 (133) and it was likened to a bulk micellisation process. The development of this concept has been based mainly on studies on silica (in the form of quartz) and alumina, but these substrates are usually considered to represent surface chemical behaviour of typical oxides. Extensive

electrokinetic data (134) provides a hemi-micelle concept and discusses the effect of pH, chain length and surface charge. Further evidence for the hemi-micelle theory comes from parallel adsorption studies on alumina (135), thermodynamic data (136) and heats of immersion studies (137).

6.3.2 Theory and Isotherms

The binding of surfactant ions on a polar surface occurs in two steps:

(i) at low surface coverage, there is polar adsorption of surfactant ions into the first layer (see Fig.6.3(i)). The surfactant ion binds mostly as a substrate for a like-charged OH^- in the electrical layer. The completed adsorption layer has apolar character. Adsorption has occured as a result of electrostatic attraction between surfactant ions and the surface.

(ii) at higher surface coverage, there is attraction of surfactant ions at the first adsorption layer as a result of van der Waal's forces between the hydrocarbons of the surface chains. (see Fig.6.3(ii)). The layer has polar character and its electrical charge is compensated with anions or cations from the solution.

Irregularities occur when there is:

(i) Non-homogeneity of the solid which contributes various binding forces.

(ii) Formation of hemi-micelles at higher surface concentration of the surfactant.

(iii) Adsorption of surfactant ions into the second layer before the first layer is complete.

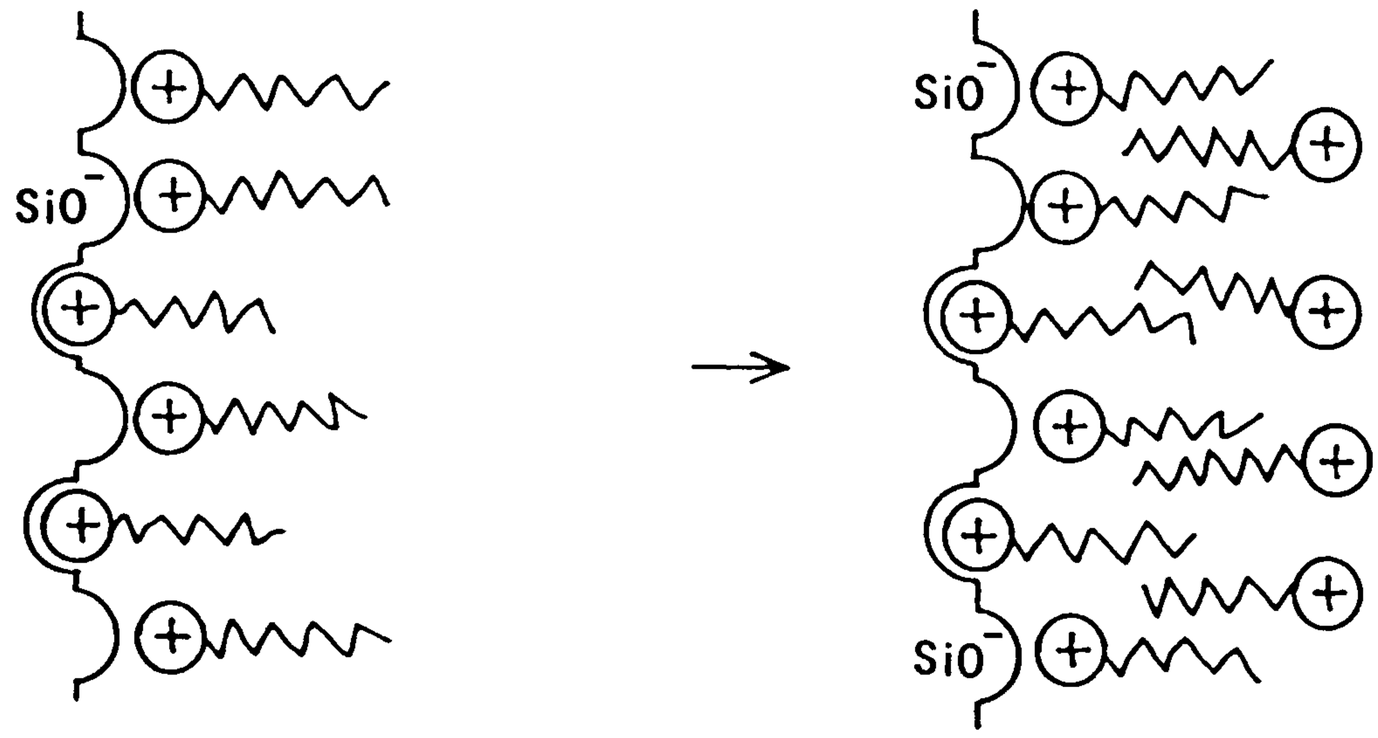

(i) (ii)

Fig.6.3 Adsorption of anionic surfactants.

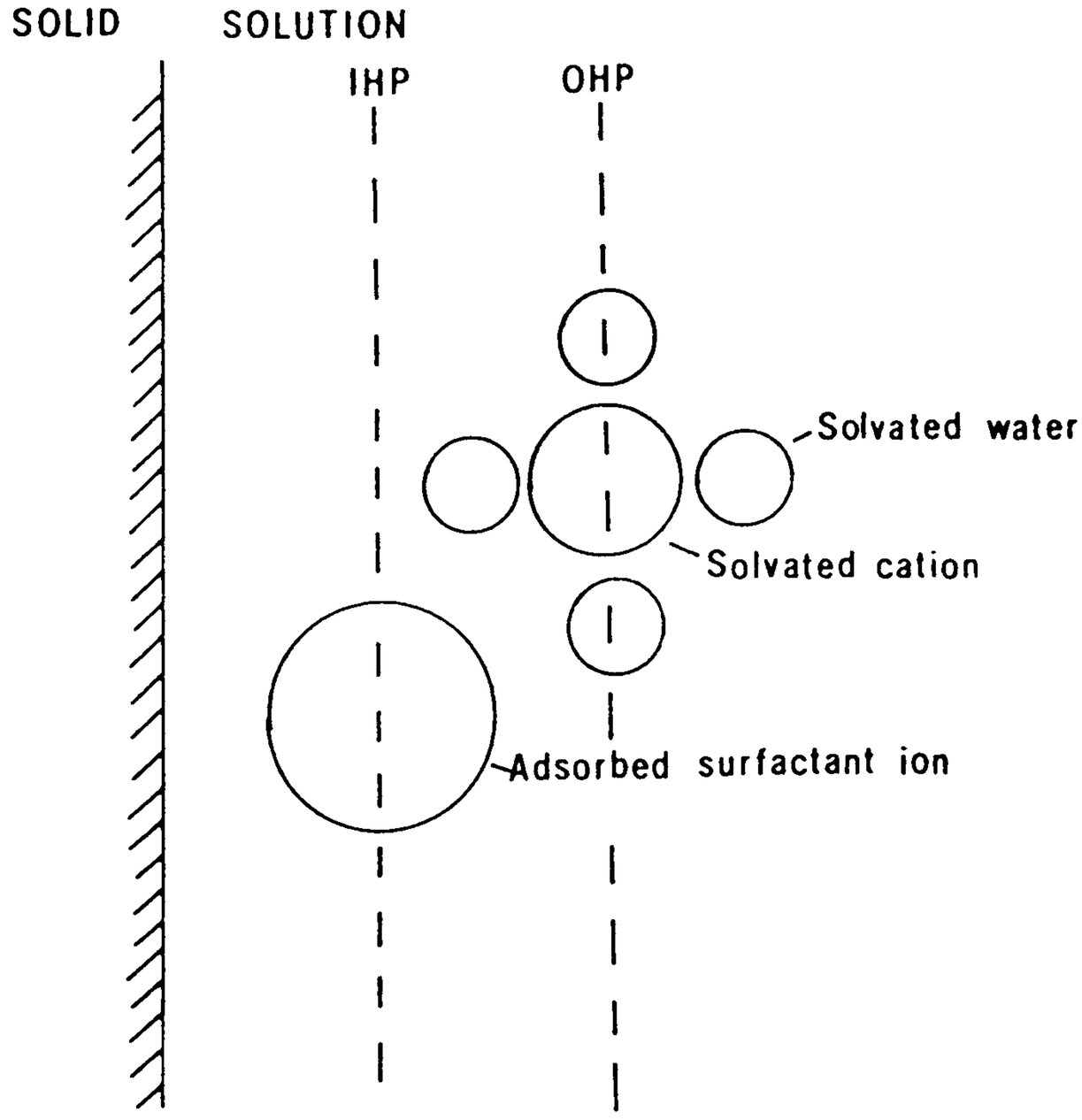

Fig.6.4 Grahames' double layer.

In Fig.6.3, a plateau is attained around the cmc with the charged heads pointing towards the surface. A second plateau can be seen as the bilayer forms. Support for this theory stems from:

(i) calculated areas occupied per molecule at complete coverage,

(ii) the existance of two plateau regions, and

(iii) the hydrophobicity of the surface.

Somasundaran studying the adsorption of monosulphonates (138) has proposed that after stage (ii) in Fig.6.3, the surface has acquired a negative charge. Further adsorption of ions is retarded by electrostatic repulsion between the surface and sulphonate ions in solution.

The adsorption of surfactant ions is considered as a special case of the adsorption of ions referred to in Grahame's treatment of the electrical double layer (138). See Fig.6.4. It is the electrical interaction within this layer that influences adsorption. The inner Helmholtz plane (IHP) corresponds to the locus of centres of specifically adsorbed ions, in this case, the ionic head group. At very low coverage, it is assumed that the IHP and OHP (outer Helmholtz plane) coincide.

The generation of surface charge occurs when a solid is in contact with an aqueous solution. Under certain pH conditions, the net surface charge will be zero, ie. at the point of zero charge (p.z.c.). The charging mechanism of inorganic oxides such as SiO_2 and Al_2O_3

relies on the presence of ionisable groups on the solid surface. The hydrogen and hydroxyl ions are considered to be potential-determining. In aqueous solution, the surface is fully hydroxylated and the adsorption and dissociation of H^+ from surface hydroxyls accounts for the surface charge (139):

$$MOH_{(surf)} \text{ <--> } MO^-_{(surf)} + H^+_{(w)}$$

$$H^+_{(w)} + MOH_{(surf)} \text{ <--> } MOH_2{}^+_{(surf)}$$

where surf = from the surface

w = from water

These two equations are characterised by an equilibrium constant

$$K = \frac{a_{MOH_2}{}^+}{(a_{MO^-})\ (a_{H^+})^2}$$

although this charging mechanism is idealised, it provides an acceptable model for oxide surfaces.

6.3.3 Effect of Surface Charge

A distinction has been drawn between the physical mechanisms of adsorption of ionic surfactants on hydrophilic surfaces such as oxides and on surfaces possessing some hydrophobic character (carbon, polymers). This difference is due primarily to a reduction in attraction between the hydrophobic moiety of the surfactant ion and the (hydrated) oxide surface. Adsorption data of Tamamushi and Tamaki (140) for sodium dodecyl sulphate (SDS) on alumina shows that adsorption does not occur when the surfactant and surface are of

similar charge. However, Doss (141) found that dodecyl ammonium ions adsorbed on positively-charged alumina surfaces. Also, Balzer and Lange (142) stated that for a series of alkyl benzene sulphonates on alumina, adsorption still occurs to a small extent when the surface is negative. In the case of highly polar surfaces, there should be little attraction for hydrocarbon chains to be adsorbed.

6.3.4 Mechanism of Adsorption

Much attention has been devoted to defining the various contributions to the adsorption process for a wide variety of surfactants and adsorbents. ΔG_{ads} (the adsorption free energy) is usually assumed to comprise of additive contributions, mainly electrostatic interactions and specific (non-electrostatic) interactions.

$$\Delta G_{ads} = \Delta G_{elec} + \Delta G_{spec}$$

where:

ΔG_{ads} refers to a mean adsorption energy;

ΔG_{spec} is the chemical free energy referring to chemical bonding between the adsorbate and the adsorbent and

ΔG_{elec} subdivides into electrostatic and chemical terms.

(i) Electrostatic Interactions

Usually ΔG_{elec} is ascribed to coulombic interactions. A dipole term is included which arises through an exchange process occuring between the surfactant ion in bulk solution and in the adsorbed state. Water (n molecules) is also desorbed and its dipole moment is accounted for

in the equation:

$$\Delta G_{dip} = \sum_{j} \Delta n_j \mu_j Es$$

where Δn_j is the change in number of adsorbed dipoles j of moment μ_j and Es is the electric field strength across the plane of adsorbed species.

In Stern's original equation ΔG_{dip} is neglected and the interpretation of ΔG_{elec} is simplified.

(ii) Specific Interactions

The subdivision of ΔG_{spec} into interactions can be made according to interactions between particular species:

$$\Delta G_{spec} = \Delta G_{cc} + \Delta G_{cs} + \Delta G_{hs} + \ldots$$

The first term, ΔG_{cc} is identified as the free energy change due to chain-chain interactions between the hydrophobic parts of the adsorbed ions. ΔG_{cs} also involves hydrophobic interactions but with the chain-substrate. It is also highly dependent on the nature of the solid surface and any associated water.

(iii) Chain-Chain Interaction and Hemi-micellisation

One of the principal concepts that have been used to explain the adsorption of surfactants is hemi-micellisation. For strongly hydrated oxide surfaces, the dominant contribution to ΔG_{spec} is ΔG_{cc}. This term arises from the tendency of the hydrophobic moieties of the surfactant to remove themselves from an aqueous environment by forming aggregates on the adsorbent surface. The experimental data on which this theory

depends stems from the sodium dodecyl/sulphate/alumina system by plotting the amount adsorbed and zeta potential against surfactant concentration (135).

The initial rise in the extent of adsorption occurs with no accompanying change in zeta potential; indicating a simple exchange of ions between the surfactant and those in the double layer of the surface. At the hemi-micelle concentration, the adsorption rises steeply as hemi-micelles form on the adsorbent. A dramatic change in the zeta potential also occurs. Further discussions in support of this concept include electrokinetic (143) and contact angle data (144).

(iv) Chain-Solid Interactions

The ΔG_{cs} term has little significance for oxide surfaces but is important for less polar surfaces which do not generally attract water molecules above a first layer. Therefore ΔG_{cs} rather than ΔG_{cc} governs the first stages in adsorption and produces much higher initial slopes of the isotherm. For surfaces of hydrocarbon character, the ΔG_{cs} per CH_2 group is of the same order of magnitude as ΔG_{cc}. Rendall (143) confirmed this on studying chain-solid interactions with a series of anionic surfactants on Nylon sols.

(v) Headgroup Effects

The term ΔG_{hs} is introduced to cover all other contributions not accounted for in the other terms. It includes chemical interactions such as hydrogen or covalent bonding and solvate terms. The strong binding

of alkylaryl sulphonates, for example, proteins, has been attributed to charge delocalisation over the benzene sulphonate headgroup. For micellisation, and for adsorption, the benzene ring has been considered not as part of the headgroup but as contributing the equivalent of 3-4 CH_2 groups in the alkyl chain (146).

6.4 Kinetics of Adsorption

A study of the kinetics of adsorption of surfactants at an interface is essential to the understanding of interfacial phenomena such as solubilisation, emulsification, flotation and foam stability. It has been shown (147), that adsorption is proportional to the square root of time and is also a function of the chain length of the surfactant as well as the valencies and concentrations of added electrolytes. A simple diffusion theory approach does not adequately account for adsorption of surfactants since surface tension measurements as a function of time shows that equilibrium is not attained immediately. The concept of a surface energy barrier has also been introduced (148). This is called the potential barrier theory, which accounts for the repulsive electrical energy of the molecules at the surface and those in the bulk solution. It also predicts that the adsorption rate is accelerated by adding excess electrolyte since this will shield the surface charge. Only if the concentration of the electrolyte is large enough, adsorption may be explained by a simple diffusion theory and apparent diffusion coefficents for the surfactant molecules/ions.

At the instant a fresh surface is formed by a solution, the concentrations of solute near the surface should be the same as those of the bulk solution. Fick's law expresses diffusion as a function of concentration gradient and so it cannot account for the accumulation of solute at the surface of solution. The thermodynamics of adsorption requires that the more surface active the solute, the greater its adsorption potential. The forces near the surface can be regarded as being responsible for adsorption of surfactants at the interface. This is the diffusion-determining factor rather than the normal concentration gradient. Any factors increasing the surface activity of the surface activity of the surfactant will also increase adsorption.

Overall, taking into account all the possible factors involved, a higher value of adsorption will be achieved than if diffusion alone was involved.

6.5 Techniques for Adsorption Measurements

6.5.1 Introduction

A great deal of work reported recently is based on the traditional batch method, although a widening range of techniques is being employed for analysis of the equilibrium solution. This method is tedious and often difficult to apply over a range of temperatures. Improved techniques have been designed to obtain more precise data. For example, to remove the possibility of atmospheric contamination, Lavionov (149) has designed apparatus in which the outgassed solid is placed into a bulb closed with a glass membrane. The solution is injected through this with a microsyringe.

Another novel technique, the slurry technique, has been described (150). It requires the measurement of the increased amount of the component of interest in the separated solid rather than the depletion of the equilibrium solution. Another method proposed for static adsorption stems from Nunn and Everett (151) which used a "concentration null" method. After contacting a solid with a known solution, the amount of the adsorbed component is determined as being equivalent to the amount required to return the solution to its original composition.

Liquid chromatography techniques are increasingly used for the determination of isotherms. These can permit accurate adsorption measurements at low surface coverages and on low specific surface area materials. This method can be used with conventional HPLC equipment with only minor modifications. Overall, the sensitivity of the continuous flow chromatographic method is greater than the classic batch technique. Wang (152) give a thorough assessment of the use of frontal analysis in which the solution concentration is changed step-wise and the chromatogram recorded.

6.5.2 Direct Measurements

Direct measurements of adsorption are necessary where conventional solution depletion methods are of inadequate sensitivity. This is particularly true for measurements at high solution concentrations or low solid surface areas.

(i) Radiotracers Direct studies of amounts adsorbed have been attempted with isotopically-labelled compounds at the air-solution interface, by direct counting through a thin window. Using tritium, the concentration from the underlying solution can be significant and is considerably higher when using a "harder" radiation source such as ^{14}C or ^{35}S. This method could be applicable to surfactant adsorption at the solid-liquid interface, but the main problem is that radiation strong enough to penetrate the substrate would give rise to a count rate from the sub-solution as well as from the adsorbed layer.

An alternative approach is to count after the removal of the solid. However, the passage of the solid through the solution-air interface may cause fresh deposition or removal of surfactant. Additional surfactant may be deposited by evaporation of a finite amount of solution adhering to the solid. A review of this technique has been given by Muramatsu (153).

(ii) Infrared Studies The widely-used IR technique is unsuitable for aqueous surfactant solutions because of the high infrared adsorption by water. The technique of using a KBr disc equilibrated with a surfactant solution followed by a drying process has been used to study the mechanism of chemisorption. For adsorption studies, there are ambiguities which can occur particularly during sample preparation and drying.

(iii) Neutron Scattering This technique is not fully developed as far as surfactant adsorption is concerned,

but neutron scattering methods have recently been developed which allow detailed studies of the adsorbed layers. The scattering cross-sections for hydrogen and deuterium are very different, so by using appropriately deuterated molecules in H_2O - D_2O mixtures, the contrast may be varied in order that selected features may be studied. Other neutron scattering data concerning the micelle size, structure and aggregation numbers has been referred to in section 2.3.

6.5.3 Solution Depletion Methods

(i) Background The most widely-used approach is to study the depletion from solution in equilibrium with the adsorbent. The problem is in causing a measurable change in concentration and so the method is applicable only when the specific surface area of the substrate is not too small. Only an apparent adsorption isotherm is obtained by these direct methods. Some of the principal methods for measuring surfactant concentration are briefly discussed below.

(ii) Radiotracers Solution concentrations may be measured, providing a suitably labelled compound can be prepared, by using a Geiger-Muller tube or a liquid scintillation counter. The method is highly specific and sensitive and therefore particularly useful for very low concentrations or for the study of single components of a surfactant mixture.

(iii) Dye Extraction A number of techniques have been developed whereby a nonpolar complex of the surfactant is extracted into a solvent with a dye molecule. The

concentration is deduced visually, by titration or spectrophotometrically. Such methods are simple, quick but are not very specific.

(iv) Photometric Analysis When the surfactant contains a suitable chromophore such as alkylbenzene sulphonates or pyridinium ions, the concentrations may be determined by UV spectrophotometry.

(v) Interferometry There are a few reports of interferometric analysis applied to ionic surfactant adsorption. The refractive index of aqueous solutions is affected to a similar extent by surfactant ions as by electrolyte. Therefore, it is not generally useful for studies particularly in the presence of other ions.

(vi) Surface Tension As with refractive index, it is more widely used for nonionic surfactants. Although there are more sensitive methods it is a particularly useful method for identifying the cmc unless the equilibrated solution is diluted.

(vii) Ion Selctive Electrode Electrodes selective to surface active ions have been used in studies of surfactant binding to polymers and protiens.

Conventional ion selective electrodes have been able to determine the uptake of, for example Na^+ or Br^- ions in conjugation with positvely charged surfactant ions.

6.6 Experimental

6.6.1 Static Techniques

These were determined by the so-called 'batch', 'static' or 'immersion' method. These tests were conducted by equilibrating a known amount of oxide with a surfactant solution in a screw-topped glass tube. Random hand agitation served to ensure equilibration between the solid and the bulk solution. The samples were usually left for 2 or 3 weeks in a thermostatted oven to provide temperature regulation. Most of the samples were centrifuged and then decanted as near as possible to the test temperature. The surfactants all contain a benzene ring and exhibit strong absorption in the UV spectrum. The solutions were analysed by a Lambda 9 UV Spectrophotometer (Perkin + Elmer UK). An example of one of the UV spectra of the surfactants used is shown in Fig. 6.5. The wavelength at which the sample was run is marked and each surfactant was studied at the same frequency.

Equilibrium concentrations were determined by comparing measured values with calibration curves prepared from stock solution. An example is given in Fig.6.6. The accuracy of this static method is difficult to estimate. The main troublesome areas are the impurity of the surfactants and scattering due to the non-uniformity of size of the silica spheres, weighing the oxides, and preparation of solutions. An approximate calculation for the accuracy produces an error in the range of 10 to 15%. The errors are discussed fully towards the end of this chapter.

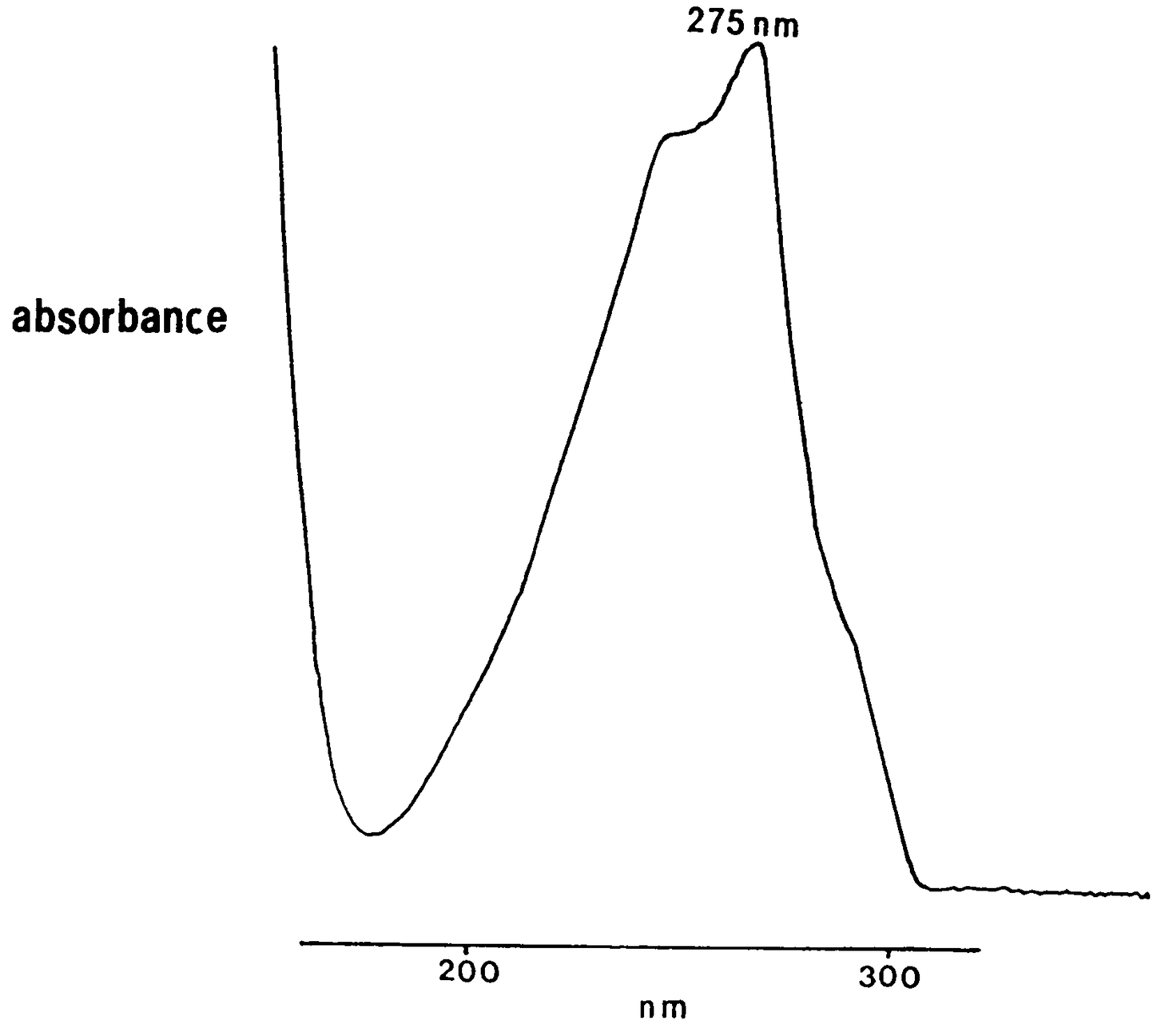

Fig.6.5 UV spectra of T180.

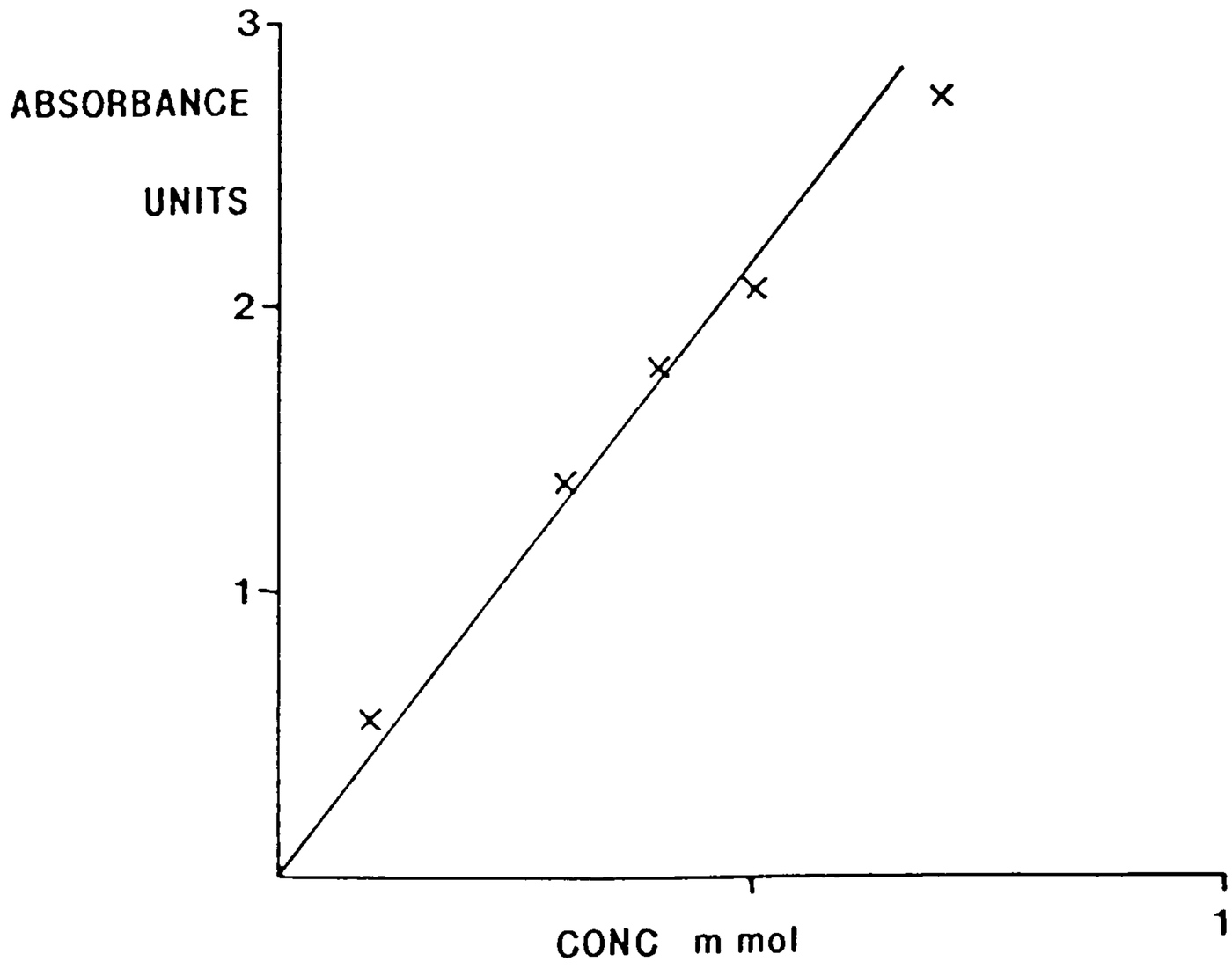

Fig.6.6 Calibration curve for T180.

The surface excess amount of surfactant solution at the solid-liquid interface is:

$$\Gamma = \frac{(C_i - C_f) \cdot V}{M \quad A_s}$$

where C_i = initial concentration

C_f = final equilibrium concentration

V = total volume

M = mass of adsorbent

A_s = specific surface area of the adsorbent

All the surfactants were used as received from their manufacturer and stock solutions were prepared from distilled water or brine. Aqueous solutions of each surfactant were prepared by diluting to the required concentration. They were all amenable to analysis by UV spectroscopy.

The adsorbents used were silica spheres of two sizes (1.5mm and 2.5-3mm), alumina, and the crushed Berea sandstone. Each sample tube contained 0.2g of the oxide, which, in the case of silica, amounted to 26 or 27 spheres for the smaller size and 10 spheres for the larger. Silica and alumina were the main oxides used and details of the characterisation of all the adsorbents has been given earlier (see section 2.2).

Using a series of surfactants, (i.e. T130, T150, and T100S), the effect of their chelation with aluminium ions was studied. A stock solution of each surfactant was

four weeks. The Al^{3+} ions were incorporated into the hydrophilic surfactant chain. The adsorption of this complex in aqueous solution over silica as compared to the uncomplexed nonionics and anionics was studied.

In both static and dynamic experiments, tests to evaluate the effect of brine were hampered by the poor solubility of surfactants in the brine on their own. The addition of a co-solvent, in this case propan-2-ol, alleviated the problem to an extent, but for simplicity, all adsorption tests were conducted using distilled water.

Studies on the adsorption of sulphonates in Berea cores (151) indicate that equilibrium was attained slowly and the higher the concentration of surfactant, the greater the equilibrium time required. After a few tests, it was decided that an equilibrium time of four weeks was necessary; with three weeks being sufficient at elevated temperatures.

6.6.2 Dynamic Technique

One of the major problems with the static technique is the difficulty of accurately measuring concentration changes, especially when the solution is very dilute or when the system contains only slightly adsorbing species. Accurate concentration measurements can be eliminated in a dynamic technique in which a step-concentration change is introduced into an adsorbent packed column. This chromatographic technique has been widely used in the determination of adsorption from gases, but very little work has been directed towards liquid systems. The

advent of high pressure liquid chromatography demonstrates that with only slight modifications, the chromatograph can be used to measure adsorption from solution. The mathematics of ideal equilibrium chromatography were first derived by Wilson (152). They deal with flow through a packed column rather than the adsorption process itself.

There are two alternative approaches to the theory of chromatographic adsorption measurement: namely microscopic and macroscopic.

a) Microscopic. This deals with ideal equilibrium chromatography and is based on a mass balance equation over a differential section of the column. It is concerned exclusively with constant volume.

b) Macroscopic. This is based on a mass balance over the entire column and can be applied in cases which include the effects of volume changes and dispersion. However, this approach is only applicable to the frontal analysis technique where the column is preflushed with a solution of known composition until equilibrium is established. Then a concentration-step change is introduced into the column and the effluent flow rate and composition are recorded. This was the approach used in this study.

An empty steel chromatography column (4.6 x 250mm) was packed with water-saturated adsorbent and mounted in a flow system similar to an HPLC set-up. The flow was

maintained at 1.5cm^3 min^{-1}. After temperature equilibrium had been achieved, 1mm^3 incremental injections of a 20% (wt/vol) aqueous surfactant solution were made. After equilibrium was maintained for at least 20min, further injections were added until the experiment was complete. The output from the column was monitored by a UV detector.

Measurement of Dead Volume

The dead volume of the equipment must be known as accurately as possible at each solution injection. This volume was calculated by adding together the volume of the tubing, fittings, reservoir and void volume of the column. To confirm the value, water was flushed through the system producing a steady baseline. A non-adsorbing solvent was injected and the time was noted until a signal appeared in the UV detector. Knowing the flow rate, the volume of the system could be calculated.

6.7 Results

6.7.1 Batch Experiments

(i) Effect of Chain Length

The variation of the EO chain length for the Sapogenat and Arkopal nonionics is shown in Figs.6.7 and 6.8 respectively, while Fig.6.9 illustrates the effect of EO chain length of the sulphonated Sapogenats.

(ii) Effect of Temperature

Using a series of nonionic Sapogenats (ie. T130, T150 and T180) the adsorption was studied a higher temperature (see Fig.6.10).

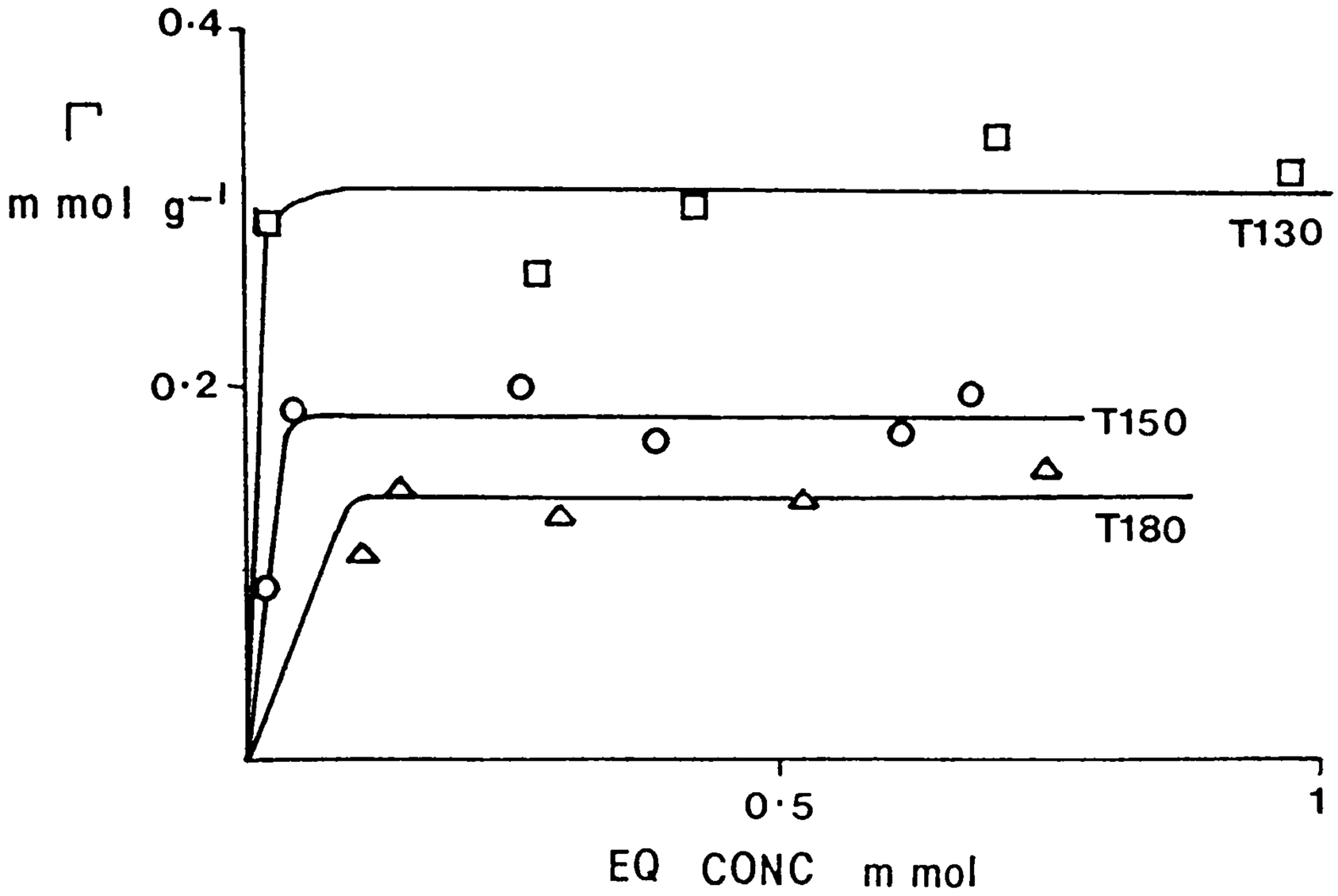

Fig.6.7 Effect of chain length on the extent of adsorption of nonionic Sapogenats

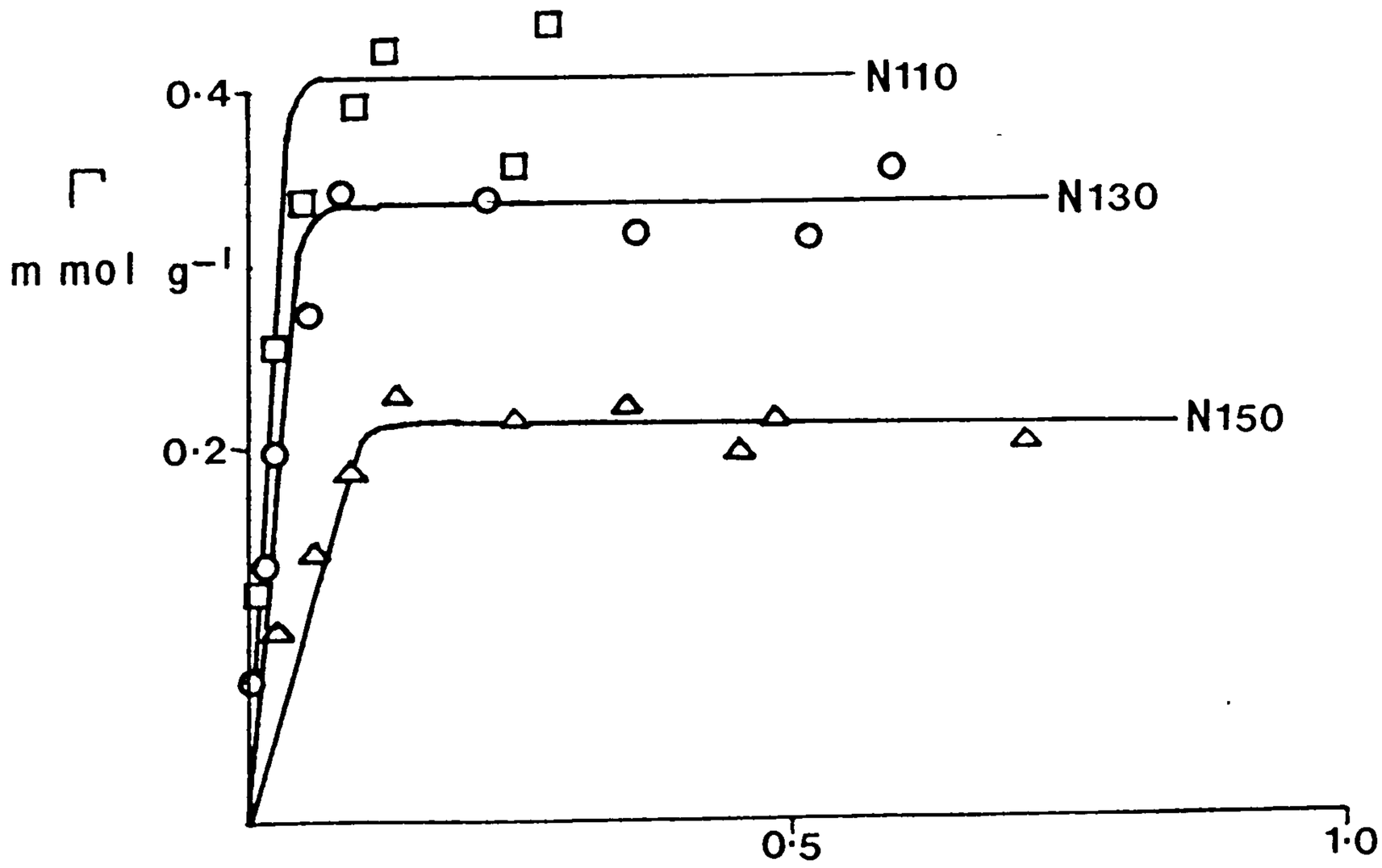

Fig.6.8 Effect of chain length on the extent of adsorption of nonionic Arkopals

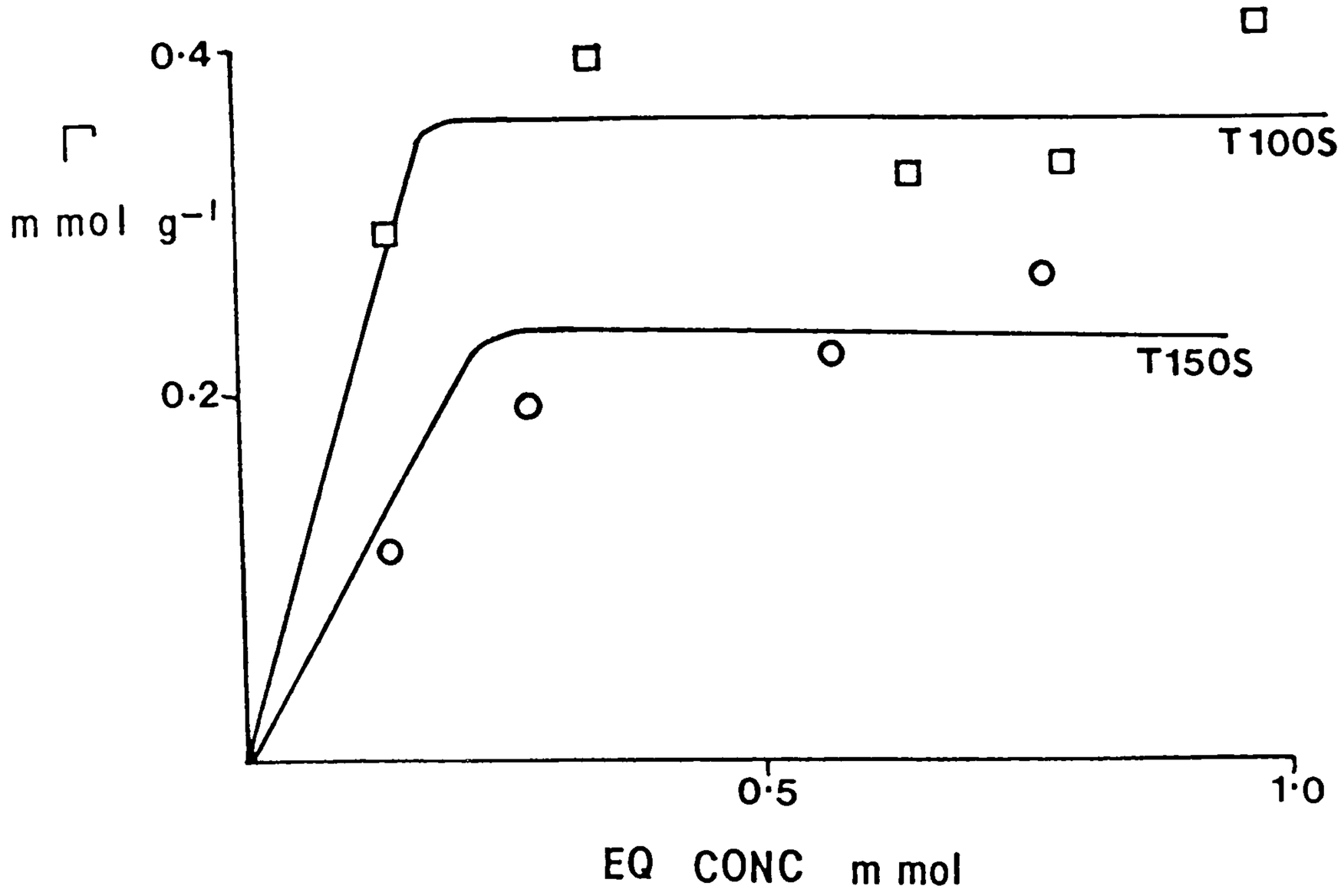

Fig.6.9 Effect of chain length on the extent of adsorption of anionic surfactants.

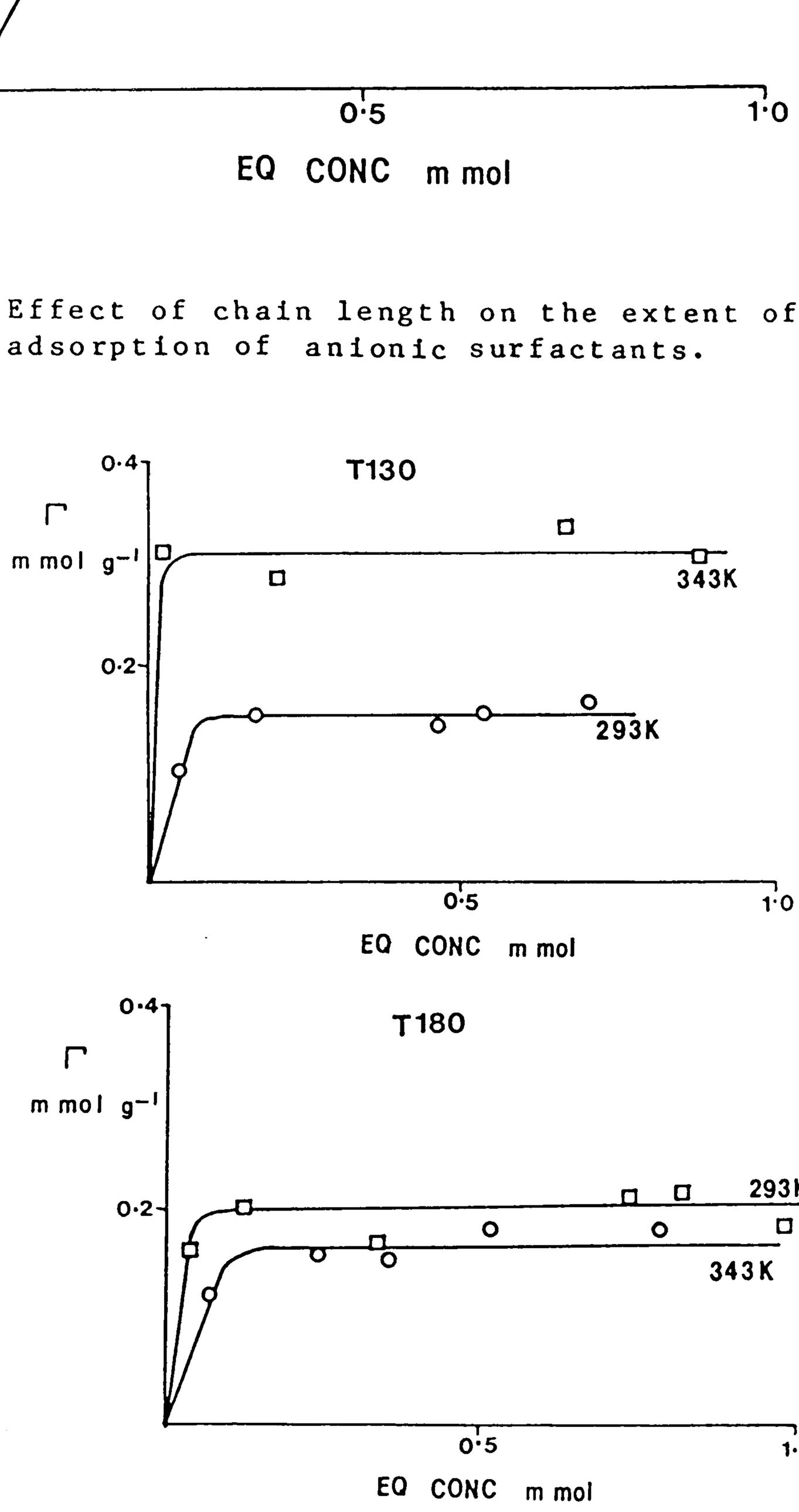

Fig.6.10 Effect of temperature on the extent of adsorption.

(iii) Effect of Sulphonation

Fig.6.11 shows the isotherms for one nonionic and one anionic Sapogenat, both having the same chain length of 15 EO units, and hence the effect of sulphonation on adsorption.

(iv) Effect of a Co-solvent

Fig.6.12 illustrates the effect on the extent of adsorption of propan-2-ol (10% wt/vol added) at 333K.

(v) Addition of Aluminium Ions

The effect of aluminium Al^{3+} ions complexing in solution with a nonionic, together with the original nonionic surfactant is revealed in Figure 6.13.

(vi) Effect of Adsorbent Pore Size

Silica spheres of size 1.5mm and 2.5-3.0mm were contacted with T130 at 333K and the isotherms shown in Fig.6.14. The other adsorbent used was alumina with the Arkopals N130 and N150. The results are shown in Fig.6.15 and may indicate the effect of Al^{3+} on the net surface charge of the oxide.

6.7.2 Dynamic Experiments

Using the long chain length Sapogenat T300, the adsorption was studied on Silica (2.5-3.0mm) at 323K (see Fig.6.16). Fig.6.17 shows the adsorption of a short chain (T040S) sulphonate onto reservoir rock at 353K. An experiment was also conducted on chromatographic alumina (N_2 BET surface area $14m^2g^{-1}$) with N150. The rate or extent of adsorption was too low to measure; other

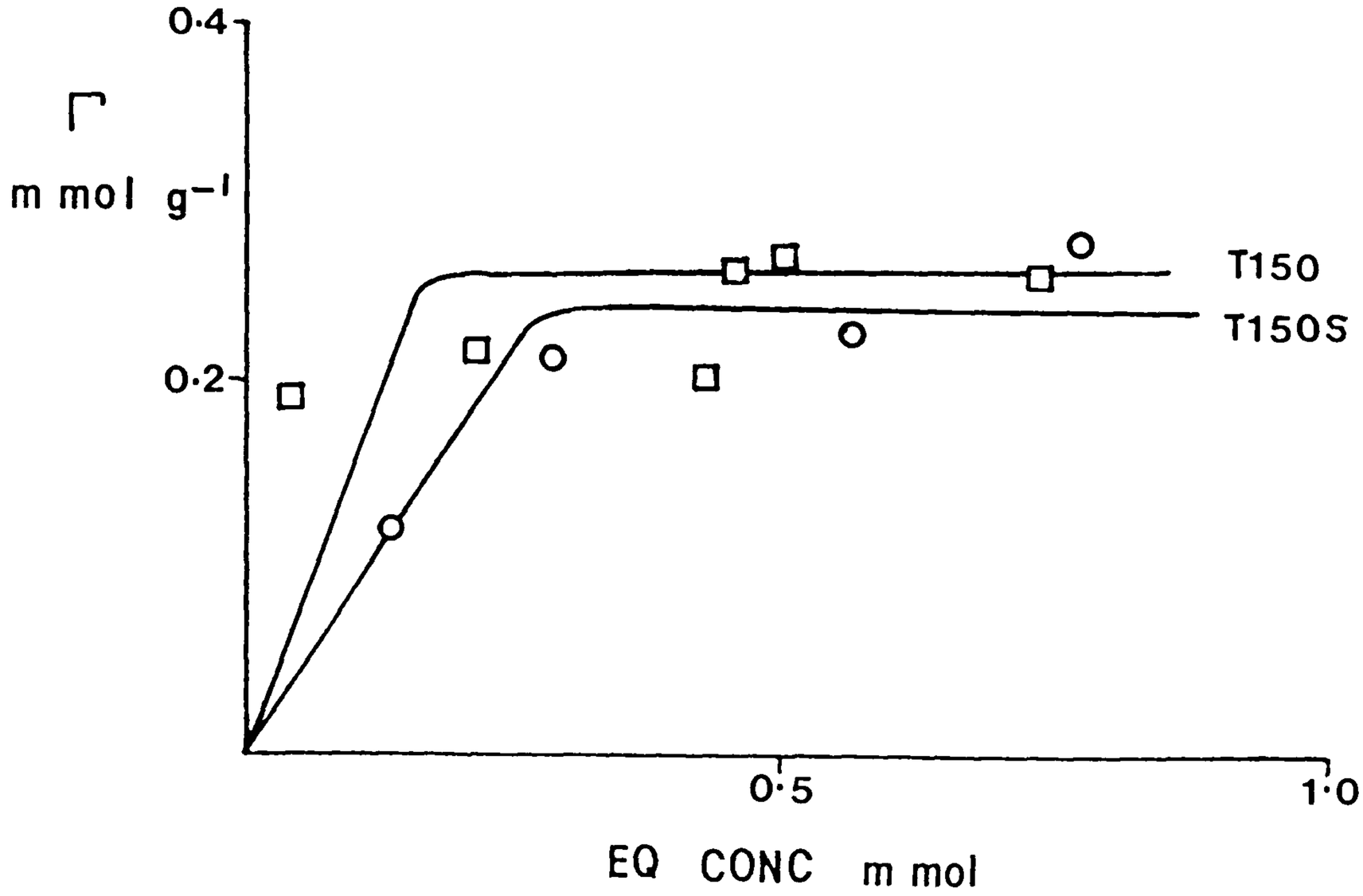

Fig.6.11 Effect of sulphonation on the extent of adsorption .

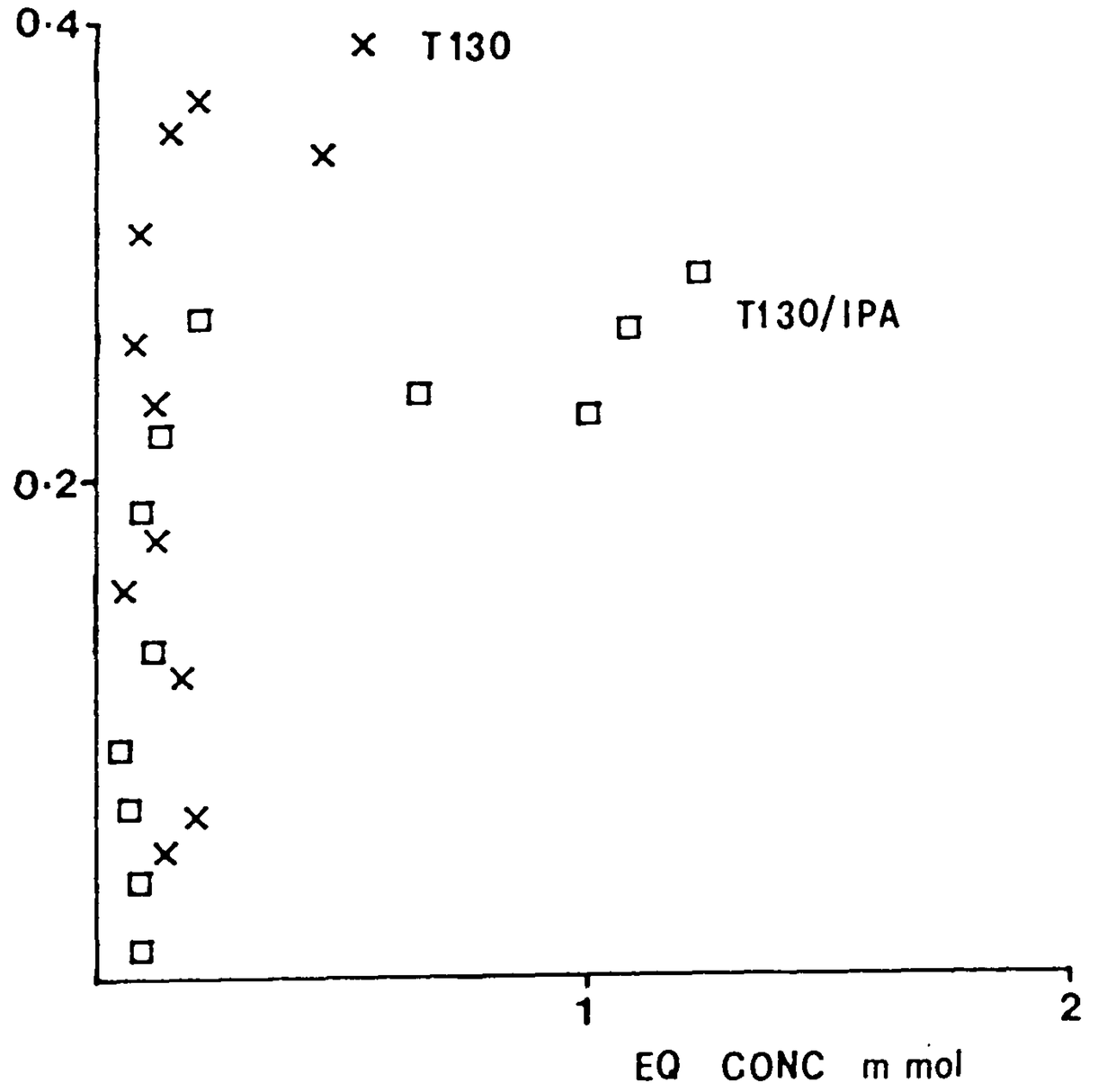

Fig.6.12 Effect of cosolvent at 333K on adsorption.

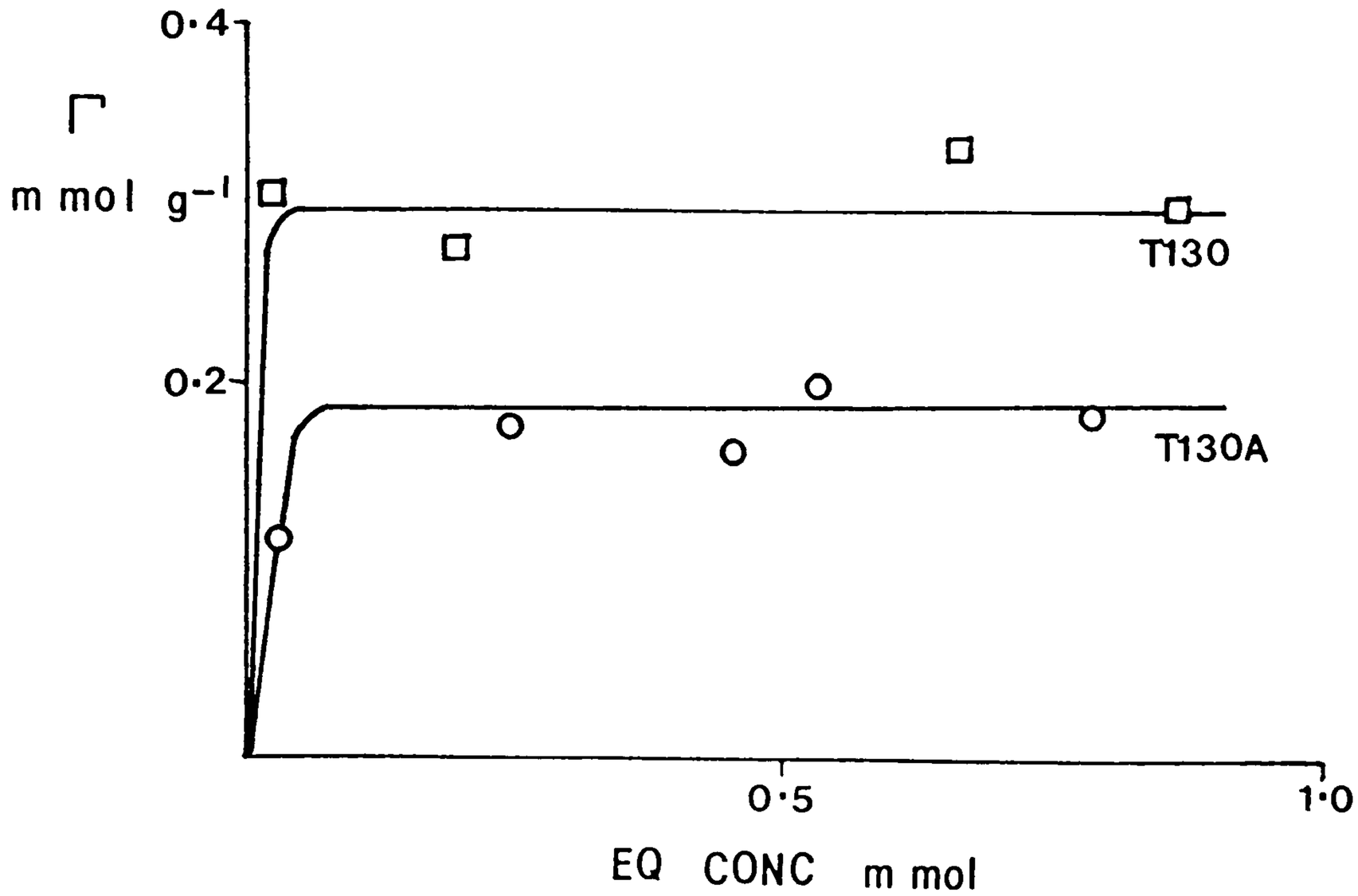

Fig.6.13 Effect of aluminium ions on adsorption.

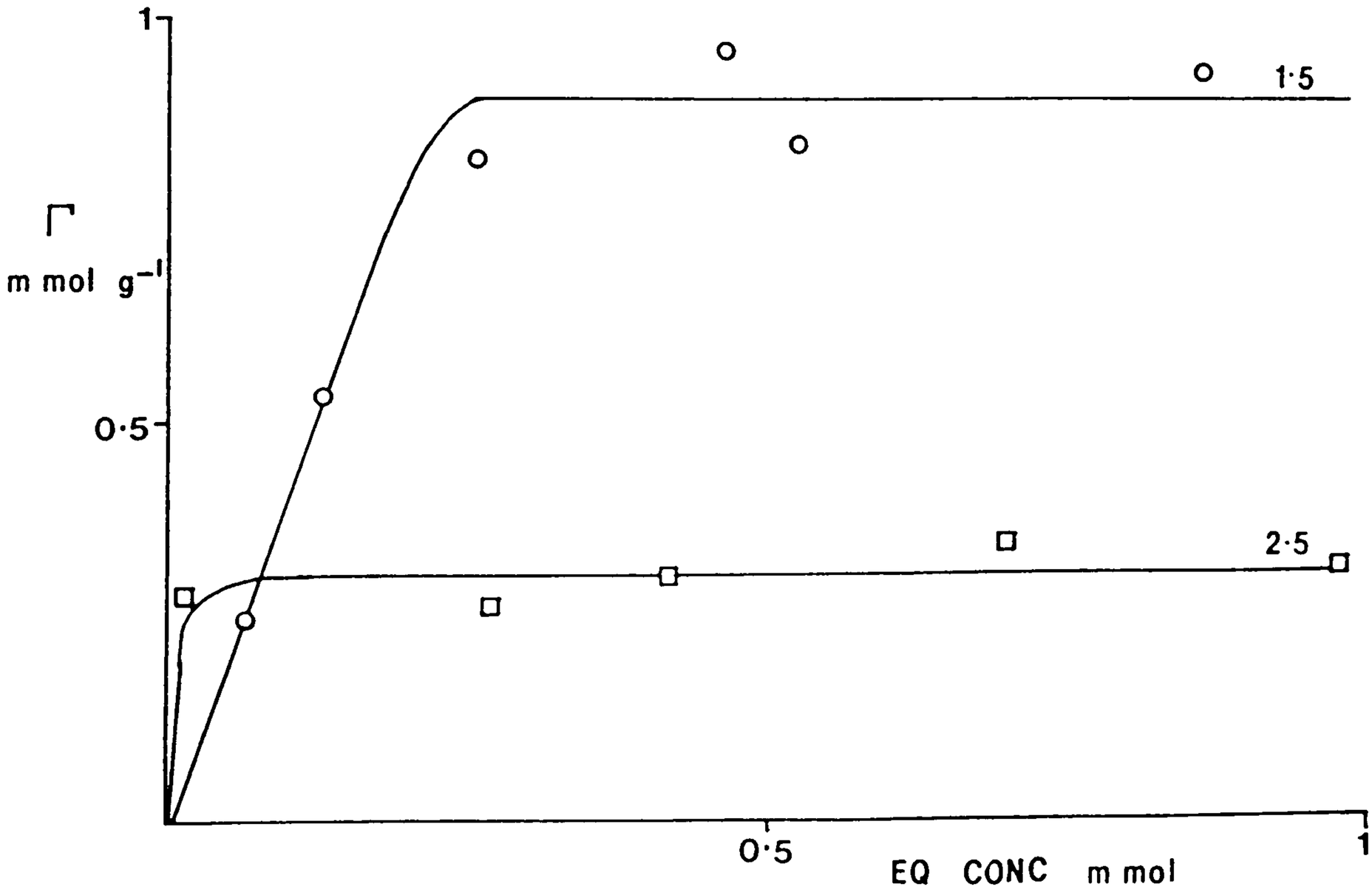

Fig.6.14 Effect of adsorbent size on adsorption.

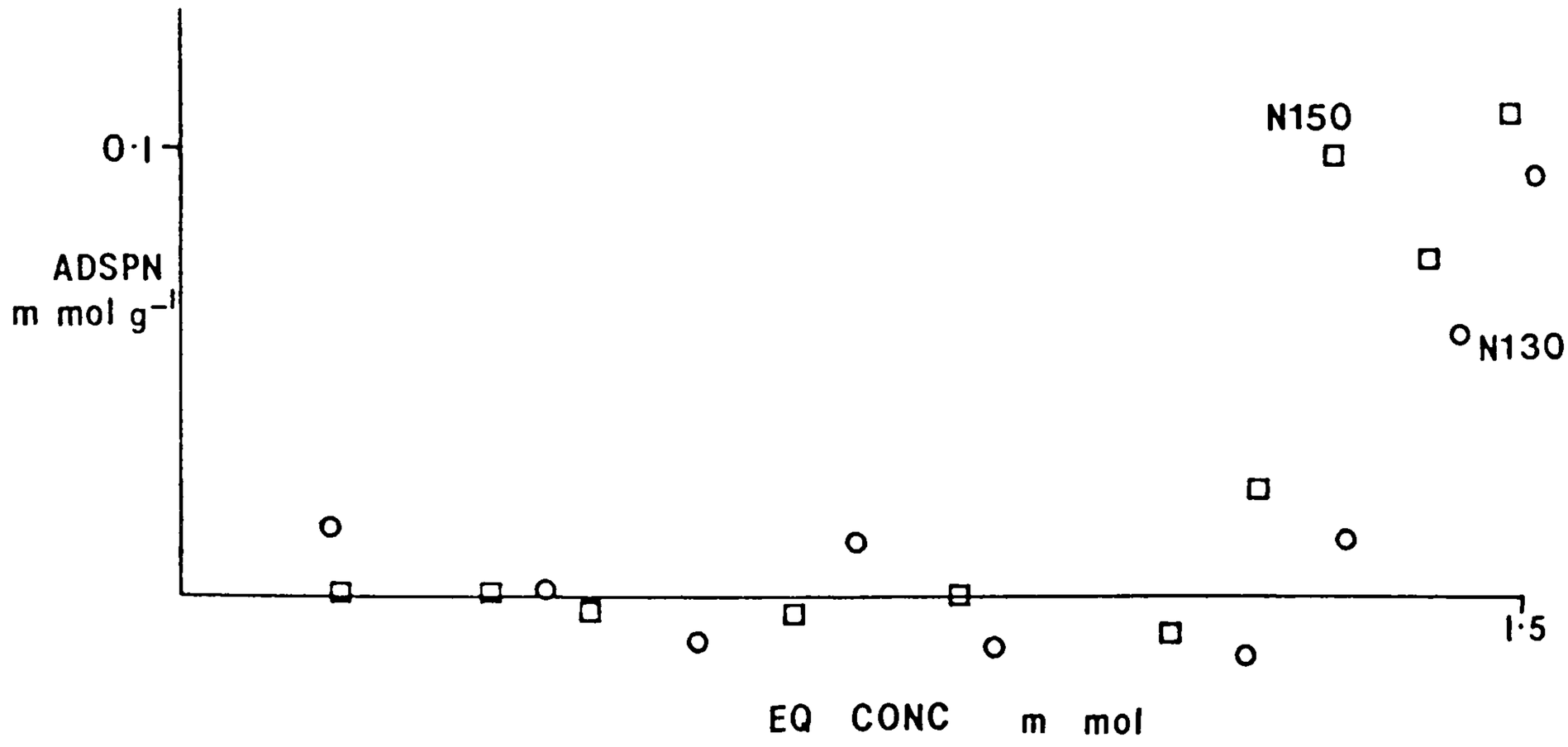

Fig.6.15 Adsorption of nonionic surfactants on alumina.

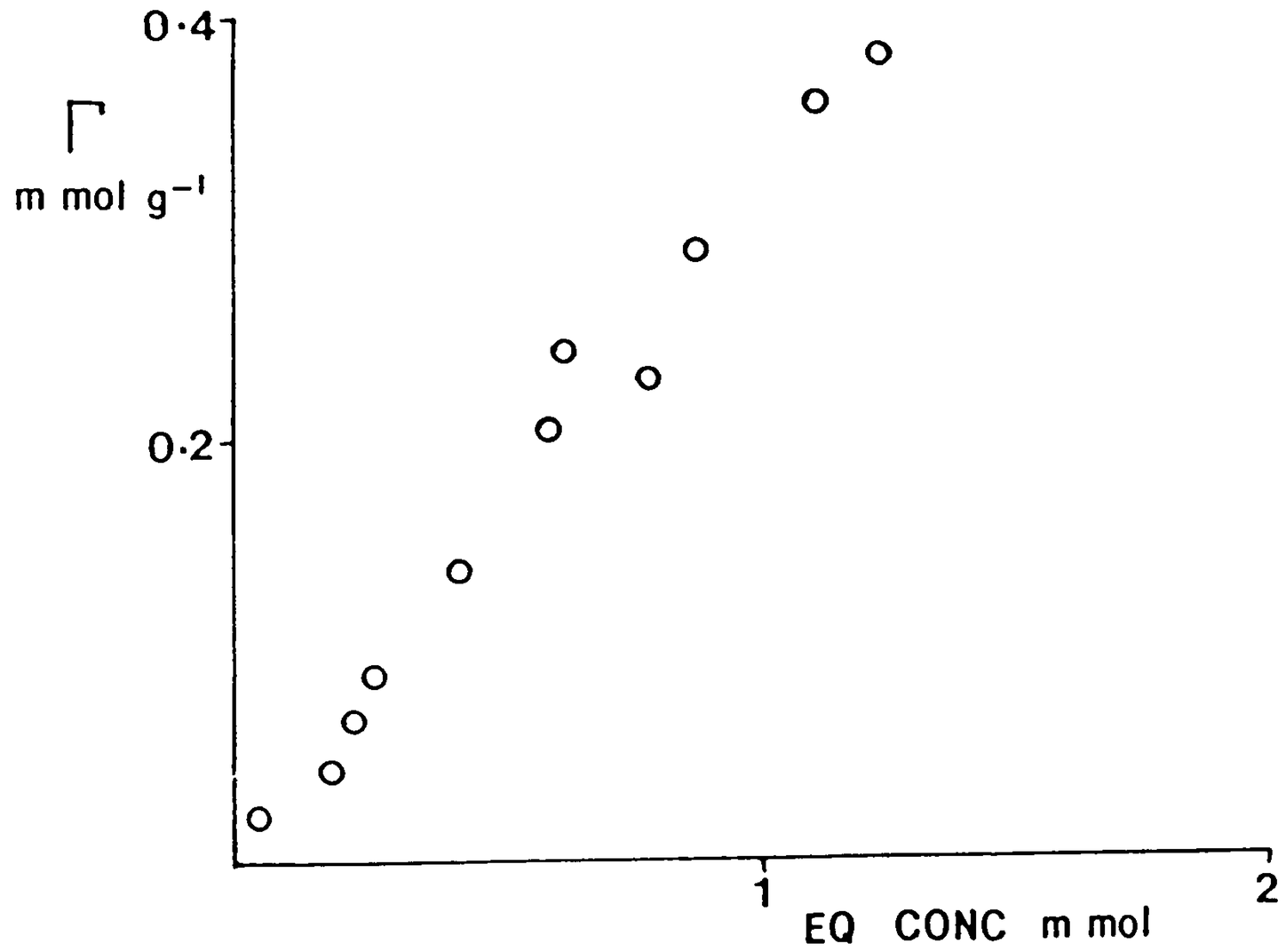

Fig.6.16 Flow adsorption of T300 on silica at 323K.

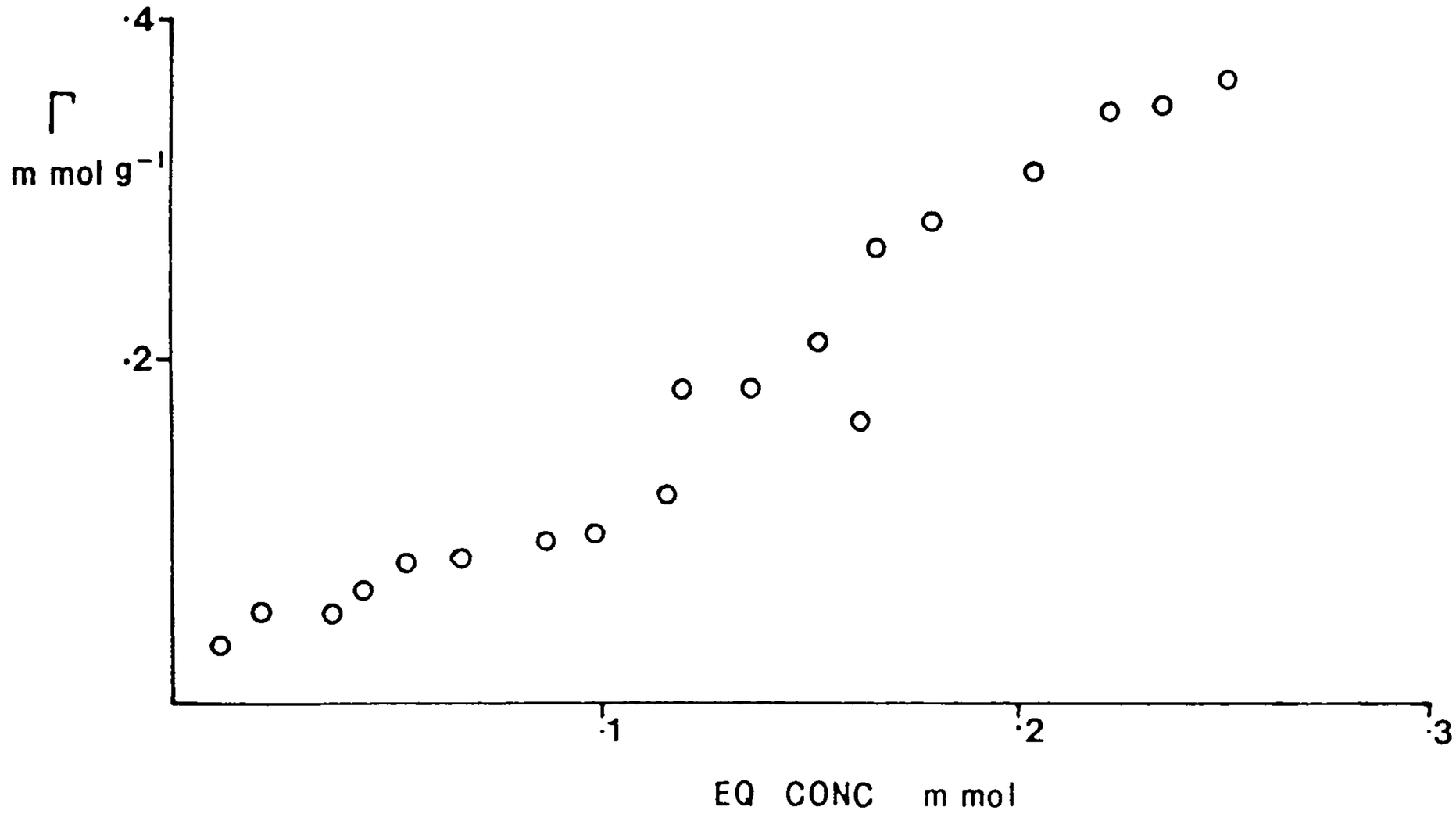

Fig.6.17 Flow adsorption of T040S on silica at 353K.

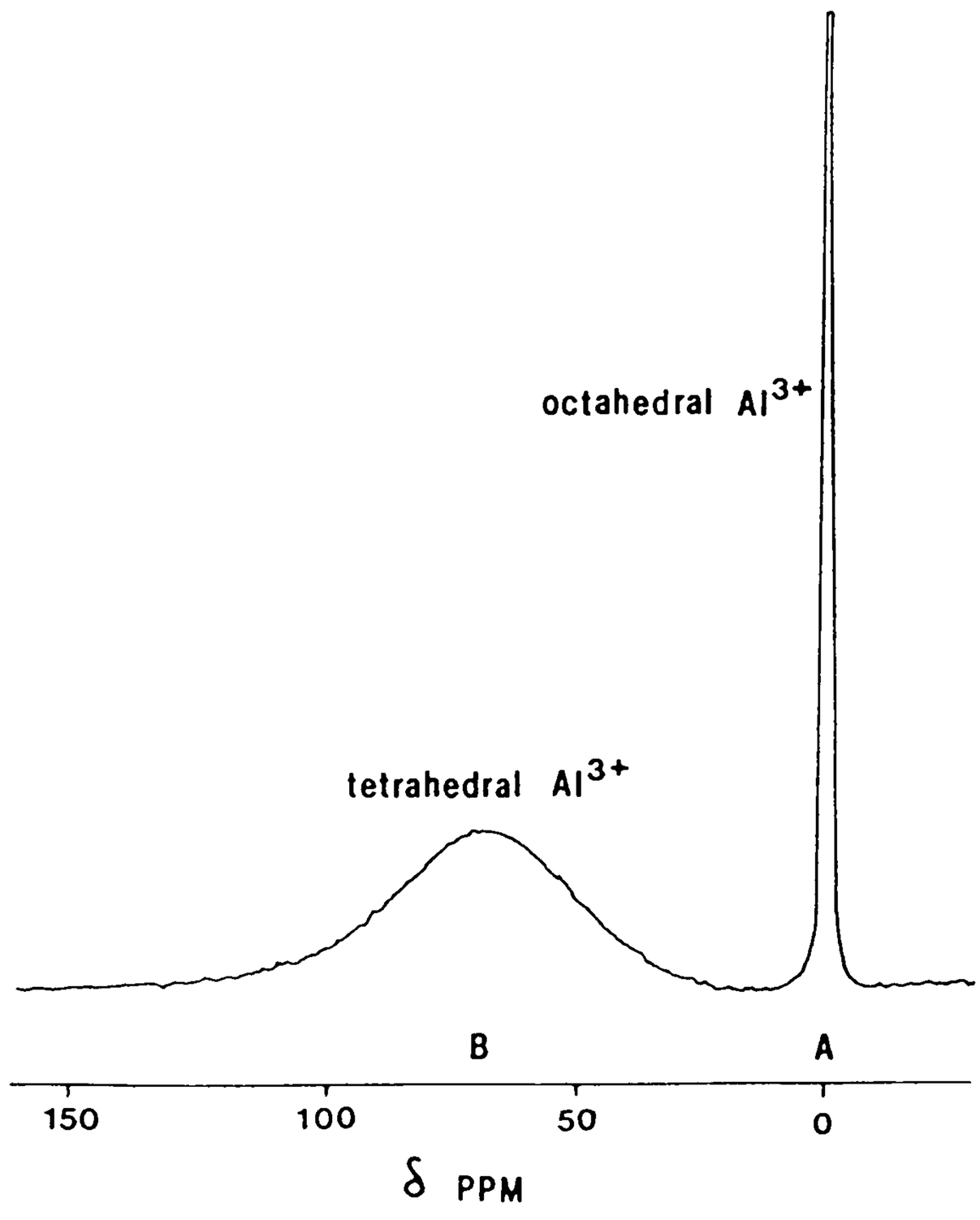

Fig.6.18 NMR spectrum of T130-aluminium ion

systems were studied but few reliable results were obtained due to reasons stated in the discussion.

6.8 Discussion

First, it is necessary to be cautious in the interpretation of the adsorption results presented. The types of surfactant and the adsorption methods (batch and flow) used here caused problems, and some of the isotherms were difficult to interpret. Aside from the systems illustrated in the following discussion, many other surfactant/oxide combinations were studied but interpretation of the results was problematical. The possible reasons for this are discussed in the last section of this chapter.

The results were deemed not to be accurate enough for highly quantitative analysis and so were used only semi-quantitatively. However, apparent maxima in the extent of adsorption of the surfactants are given in Table 6.1. Specific features of the isotherm discussed in the introduction cannot clearly be distinguished. Final plateau values are, overall, easily seen but the shape of the isotherms leading up to the plateaus is not so readily interpretable.

The lack of results for brine-surfactant systems was due partly to the poor solubility of the nonionic and anionic surfactants. Addition of an alcohol improved the problem but it was also found that the presence of ions discoloured the solutions and made analysis by UV difficult. Before the results are discussed, it is

Surfactant	$mmolg^{-1}$
T130	0.306
T150	0.175
T180	0.156
T100S	0.273
T150S	0.233
N110	0.420
N130	0.335
N150	0.215

TABLE 6.1 Approximate apparent maxima in the extent of adsorption at 273K.

necessary to ascertain whether it is possible for adsorption to occur. The surface areas and lengths of the surfactant molecules have been calculated using the isotherm plateau values and standard bond lengths. Considering these calculations together with surface area and pore size data, the adsorption processes discussed here can be better understood.

6.8.1. Calculation of Surface Area of the Surfactant Molecule T130

Mol. wt. = 834g

amount adsorbed at plateau = $26.5 mg.g^{-1}$

number of molecules present at the surface at the plateau = extent of adsorption

$$= \frac{26.5}{1000} \times \frac{6.023 \times 10^{23}}{834}$$

$$= 1.9138 \times 10^{19} \text{ molecules}$$

Surface area of silica (2.5-3mm) = $255 m^2.g^{-1}$

surface area of one T130 molecule

$$= \frac{255}{1.9138 \times 10^{19}} \quad m^2$$

$$= 13.3 \text{ nm}^2$$

The other average surface areas occupied per molecule for the surfactant molecules were calculated in a similar manner; the results are listed in Table 6.2.

This table also includes the lengths of the same molecules. They were calculated assuming that each molecule was "stretched out" to the greatest extent (ie. each bond angle was 180°. It was also assumed that the nonyl group on the aromatic ring (in the Arkopals) was

Surfactant	Average Surface Area per molecule nm^2	Approximate length of one molecule nm *
T130	13.3	6.6
T150	20.5	7.5
T180	24.8	8.7
T100S	16.2	5.8
T150S	28.9	7.9
N110	9.1	6.8
N130	11.8	7.7
N150	17.5	8.5

TABLE 6.2 Surface Area and Length of the Surfactant.

* Calculated assuming molecular linearity and using literature bond lengths (Handbook of Chemistry and Physics 1984).

molecule, is likely.

Values for the bond lengths were obtained from the literature. The reduction of area as the chain length decreases could be accounted for in terms of better molecular packing (with a shorter, less flexible hydrophobic tail) or smaller molecules fitting into pores more effectively.

The radius of the silica spheres are as follows:

size	% pores	of radius nm
spheres 2.5-3mm	83	6-10
	6	10-20
spheres 1.5mm	21	20-30
	70	30-60

When comparing the size of the molecules, it is clear that the larger molecules such as T150, T180, T100S and T150S will not have the total surface area of the silica accessible to the surfactant molecules. If there are errors in the adsorption experiment (from which the areas of the molecules are calulated) it is possible that these larger molecules are as much as 10% smaller in size. Therefore, the assumption that all of the surface area of the silica will be available to the surfactant molecules could be true. This is further substantiated by considering the maximum possible length of one surfactant molecule.

If the minimum radius of the 2.5-3.0mm silica spheres are taken, then the diameter will be 12nm. The longest

molecule is nearly 9nm and should have easy access to the smallest of the pores. Similarly for alumina where the pore radius was found to be 15nm (section 2.2) and the suface area 14nm^{2}g^{-1}.

6.8.2 Batch Experiments

(i) Effect of Chain Length

The effect of the number of EO units in the surfactants upon the extent of adsorption is shown in Figs.6.7, 6.8 (nonionic) and 6.9 (anionic). The extent of adsorption decreases with increasing chain length. This can be explained by the size of the molecule and therefore its accessibility to the pores. Although it is assumed and has been shown that the molecules are totally accessible to the pores, the decrease in adsorption is more likely to be due to the first molecules adsorbing. They will occupy an increasingly larger area as the chain length increases and restrict the approach of further molecules, and therefore, they cannot be fully close-packed. As the chain length increases, the change in the extent of adsorption is less although it has been shown (154) that a plot of EO chain length versus plateau values is linear.

Generally it has been stated that an increase in the non-polar chain length (the surfactants being constant in EO chain length) causes an increase in the extent of adsorption. The increase in the hydrophobic size renders the surfactant less soluble in water and it therefore will have a preference for the adsorbate. For anionics, the effect on the hydrophilic group is less marked than

for nonionics.

The effect of substitution around the benzene ring in the surfactant molecules used in this study is not so well defined. The surfactants depicted in Fig.6.8 contain a nonyl group which is less bulky than the tri-substituted Sapogenats used in Figs.6.7 and 6.9. The isotherms were drawn using a best fit method among the scattered points. This results in a loss in accuracy and obscures any differences in the plateaus.

(ii) Effect of Temperature

Fig.6.10 indicates a reduction in the extent of adsorption as the temperature is increased for the nonionic surfactants T130 and T180 as long as the cloud point is not approached. At the higher temperature, the surfactant becomes more soluble in aqueous solution and will have less preference for the solid surface and adsorb less. In the case of T130, the cloud point (~335K) is neared and the surfactant begins to precipitate out of solution onto the adsorbent. The shorter chain molecules are the first to lose their solubility as the temperature is increased and are thus adsorbed. A continued increase in temperature will dehydrate the surfactant molecules with greater chain lengths thereby increasing the extent of adsorption.

There is always a balance between the competitive processes of adsorption and solubility. Each surfactant class will have an optimum solubility for a particular chain length and this will vary with temperature.

(iii) Effect of Sulphonation of Nonionic Surfactants

For a surfactant with an average of 15 EO units (see Fig.6.11), the anionic derivative molecule has a lower extent of adsorption. The sulphonate group increases the solubility in aqueous solution and will thus have less preference for the oxide. The surface of silica has an overall negative charge, and will repel the ionic group, contributing to a decrease in the extent of adsorption. It is also a bulkier molecule. The cloud points are higher than for the corresponding nonionics and so the reverse effect in the extent of adsorption as seen with T130 in Fig.6.10 will not be seen.

(iv) Effects of Co-solvent

Fig.6.12 illustrates the addition of propan-2-ol (IPA) on adsorption. The adsorption is greater without the alcohol. T130 is only reasonably soluble in aqueous solution but its solubility is enhanced by the presence of IPA. The surfactant will remain in solution, even at an elevated temperature of 333K. It is also possible that the alcohol will preferentially adsorb onto the silica surface, thus inhibiting adsorption of the surfactant.

In other words, it must be considered that the silica surface now has coverages of:

$$\theta_{total} = \theta_{surfactant} + \theta_{IPA} + \theta_{H_2O}$$

and as a result, $\theta_{surfactant}$ is less than in the absence of propan-2-ol.

Therefore, there is less adsorption of the surfactant at high concentrations of co-solvent and more at lower

concentrations. The propan-2-ol may be considered to be acting as a sacrificial agent but its use in enhanced oil recovery is limited by the cost and flammability.

(v) Effect of Aluminium Ions in Solution

It has been shown that long chain surfactants can incorporate Al^{3+} ions into their structure by bonding with the oxygen atoms of the ethene oxide chain. The nuclear magnetic resonance spectra (see Fig.6.18) shows the presence of the hexa-hydrate aluminium ion (Peak A) in an octahedral configuration and the tetrahedral ion (Peak B) bonded to two of the ethene oxide groups via four oxygen atoms. There are still two water molecules bonded to the ion but are probably located further away. This has the effect of increasing the size of the surfactant molecules (and the micelle) and the stability relative to the adsorbed state. Therefore, the number of these coordinated molecules that will be attracted to the silica surface will be reduced and the extent of adsorption decreased. The positive charge of the aluminium ion is simultaneously reduced and will be less attracted to the negative silica surface. Any free Al^{3+} ions remaining in solution will be preferentially adsorbed which changes the net charge on the silica surface. Thus, the number of adsorption sites available to the surfactant molecules will be limited. The isotherms illustrated in Fig.6.13 for the surfactant T130 show that the reduction in adsorption appears to change as the chain length is altered. This suggests that chelation of the aluminium ion is encouraged with larger molecules and can be better accommodated. It seems

reasonable that there is an optimum chain length for this process considering the sizes of the ion and surfactant and charge compensation.

(vi) Effect of Adsorbate Size.

Using silica spheres of a smaller size, e.g. 1.5mm as in Fig. 6.14 rather than 2.5-3mm, the adsorption plateau is approximately twice as great. However, by normalising the adsorption by using equation:

$$\Gamma = \frac{\Delta C \,.\, V}{M \,.\, A_S}$$

where A_S is the surface area, the extent of adsorption per unit weight of adsorbate should be the same.

The plateau value for the 2.5-3.0mm silica (surface area $255 m^2.g^{-1}$), using T130 is ~$0.03 mmol.g^{-1}$ and ~$1.1 mmol.g^{-1}$ for the 1.5mm silica (surface area $58 m^2.g^{-1}$). However, substituting these values into the above equation does not produce similar results as expected.

The main reason is due to the method of measuring the surface area. The BET technique used here relies on the amount of N_2 that can enter the surface pores. This small molecule is not comparable in size to the large surfactant molecules. Hence, the surface area accessible to the gas molecule will be far greater than that to the surfactant.

The higher surface area oxide (2.5-3.0mm silica) has the narrower range of pore radius. This suggests that most

of the surface area is due to an internal area of "ink-bottle" shaped pores. This shape is readily able to accommodate N_2 molecules but cannot allow a surfactant molecule to enter. The apparent surface area, therefore, is less than that for the surfactants and the values should thus be used with care.

Alumina

Many experiments were conducted using alumina/surfactant systems. Only two results are presented here, which are combined in Fig. 6.15, since very little adsorption was detected. It can only be concluded from all of these results in the light of the accuracy in detecting such low adsorption, that adsorption in all cases was less than or about the same as the two nonionic Arkopals, N130 and N150 showed very little adsorption up to a 1%(wt/vol) solution concentration. The average pore radius of the adsorbent is 15nm and it is reasonable to assume that the surfactant molecules, whether nonionic or anionic, can enter the pores of the alumina. It is thought that the surfactant molecules in aqueous solution above an alumina surface assume a greater stability. As discussed earlier, the aluminium ions present in solution are complexed with the surfactant molecules. This stabilises the surfactant and it is then less likely to adsorb. Also, the surfactant molecules are small enough to enter the pores of alumina but in their complexed state they have increased their size and are now possibly too large for adsorption. (See section 2.2 for data on adsorbents).

This and further research on the low extent of adsorption on alumina has been published (155).

6.8.3 Dynamic Experiments

Fig.6.16 shows adsorption of T300 on silica spheres of diameter 2.5-3.00mm. Being a surfactant of long chain length (~30 EO units there should be a fairly low extent of adsorption value (see Fig.6.7) where T180 has reached a plateau by 0.1mmol.g^{-1} and T300 should already have reached this part of the isotherm. The isotherm in Fig.6.16 shows strong adsorption at low concentrations and no sign of approaching a plateau. This result is obviously erroneous and the main cause is believed to be detector drift. The equilibrium time for each injection of T300 (and the other surfactants tried with this method) appeared to be unusually long. It therefore appeared that adsorption was taking place to a greater extent than was true.

Another problem with this method is due to the equipment. Although the column was held at constant temperature, the rest of the apparatus remained at room temperature. Although the flow rate was low (1cm^3.min^{-1}) the surfactant was continually passing from a cool area to a heated zone and this must affect the solubility.

Fig.6.17 illustrates the adsorption of a short chain sulphonated Sapogenat (T040S) on crushed Mobil reservoir rock. The adsorption is higher than expected, probably for similar reasons as those given above for T300. Other sources of error for this technique are discussed in the following section.

6.9 Summary

(1). The temperature affects the solubility of the adsorbate on adsorbent. Generally, an increase in temperature increases the solubility and thus adsorption is reduced. However, the reverse is true for surfactants at, or nearing, their cloud point.

(2). With increasing ethoxy chain length, adsorption is reduced. An increase in hydrophobicity in the molecule will increase adsorption as solubility is reduced.

(3). Converting a nonionic to an anionic surfactant reduces adsorption due to greater solubility and less attraction for the like-charged surface.

(4). A co-solvent reduces adsorption by increasing the solubility of the surfactant and perhaps by preferential adsorption.

(5). Adsorption may also be reduced by preferentially adsorbing a positive ion onto a silica surface and also by increasing the size of the surfactant molecule by chelation. The reduction in adsorption is less for sulphonated surfactants than for the nonionics

6.10. Sources of Error

6.10.1. Batch Experiments

(1). Mineral dissolution (i.e. cation leaching) from the adsorbent, particularly at elevated temperatures, can cause sulphonate precipitation. It usually requires the addition of co-surfactant and sequestering agents to improve surfactant solubility. Nonionic surfactants are not as susceptible to salting out effects.

(2). Mineral dissolution can also cause particles from

the solid to remain in suspension even after centrifuging. This can result in apparent extra absorption or diffusion of the UV beam, leading to a spuriously large value for the surfactant concentration. This had the effect that the calculated equilibrium concentrations in solution being larger than the initial concentration and this produced unreal negative resuluts. Filtering the solutions might reduce this error, but then surfactant retention on the filter paper causes a problem.

(3). Surfactants can denature in the presence of air, particularly particularly at elevated temperatures. De-aerated water should thus be used for all solutions and the sample tubes air-tight.

(4). Surfactants can also de-nature in the presence of divalent cations leached from the adsorbent. These can catalyse oxidation of the surfactant and colourise the solution. This gave false UV absorption values, when using reservoir rock as the adsorbent, since the solutions were slightly yellow in appearance.

(5). It is vital to maintain the same solid/liquid ratio at all points in the isotherm. Variation in this parameter affects the final pH of the solution, which in turn can have an adverse effect on the adsorption equilibrium. In order to prevent evaporation, sealed ampoules for the samples should be used.

(6). The number of silica spheres (2.5-3mm) used in any experiment is relatively low (about 10). Therefore, the total surface area available to the surfactant may

vary by ±10% if one less or more sphere is present.

(7). Other errors are those associated with sufactant solution preparation, weighing of the spheres, UV measurements and calculation of equilibrium values from calibration graphs.

The accuracy of this batch adsorption method can be illustrated by comparing Figs.6.7 and 6.12. Here, the isotherm for T130 is shown, having been measured at different times. The plateau extent of adsorption value in Fig.6.7 is only slightly higher 8% than that in Fig.6.12. This seems reasonable.

6.10.2 Dynamic Experiments

(1). Care should be taken to avoid unduly long adsorption times as detector drift becomes a significant source of error. Since the detector signal depends on the solution concentration, with a higher concentration, the accuracy of measurements increases due to reduced detector drift.

(2). Detector volume (i.e. an equipment parameter) should be reduced as much as possible. This can be achieved by using a small inner diameter tubing, a minimum of fittings, and as small as possible distance between the column and detector. A tighter packing of the adsorbent in the column will reduce the void volume. However, too tight a packing requires excessive pump pressure and can lead to pump "cut-out".

(3). Adsorption on the walls of the column, tubing etc., is another possible error source. A calculation of the

surface area of the adsorbent and a rough measurement of the surface area of the equipment shows that approximately only 1% of the available surface area is due to the equipment.

(4). Any air in the system, particularly in the column, can cause the surfactant to decompose. This arises from not using de-aerated water and from any leaks in the system.

CHAPTER 7

7 DISCUSSION

The problems encountered in developing a potentially efficient surfactant slug are numerous. It is not technically feasible to satisfy completely all the problems outlined in the introduction to this thesis; therefore priorities and weightings must be given. It was decided that a great deal of importance lay in the understanding of the structure and properties of the surfactants (including the co-surfactants) used. The ability of the single, or blends of, surfactants to form a stable microemulsion was also to be given major attention. As far as the oil companies are concerned, the economics (cost and availability of the chemicals) of the process feature prominently and this is directly related to the extent of surfactant adsorption in the reservoir matrix. For example, in selecting a co-surfactant, the two main candidates were both secondary alkane sulphonates. These both adsorb to the same extent on most oxide surfactants but one is more readily available at a reasonable cost and far better characterised than the other. Similarly, in choosing a co-solvent that favoured microemulsion formation, the restrictions were its cost and flammability.

The fortunes of any oil company are tightly involved with movements in the oil price. Profits also depend on future reserves and down-stream activities, such as refining and marketing. Since 1979, oil consumption has fallen. European oil demand tripled between 1955 and 1964, but growth in world consumption of oil prices,

investment in oil is riskier than some other sectors, and this has an effect on the interest in EOR.

Oil companies are still recovering from the oil crisis of early 1986 when Saudi Arabia and the rest of OPEC raised their output substantially, causing prices to crash (the lowest $7.50 a barrel). They have, however, since cut back and this costraint, coupled with the continuing Gulf War between Iran and Iraq, is again raising prices. There are signs that consumption of oil is rising again, simulated by economic growth and low oil prices. The price of oil is expected to stabilise at $18 to $20 a barrel. The faster the world economic growth, the larger the rise in oil demand.

Since the earliest days oil recovery, the production techniques have been relatively poorly understood. Only recently has research provided the necessary information for a more efficient approach. This has been spurred on by the discovery and increasing use of natural gas in the late 1970's, the energy crisis caused by the miners strike in 1974 and the oil price increase in the early 80's. More recently, the blow to the oil companies due to the low price is aggravated by the knowledge that oil is an irreplaceable commodity and a non-renewable resource. The demand of the chemical companies, the future decline of natural gas resources, coupled with the success of enhanced oil recovery techniques to the oil reserves discovered and undiscovered, ensures a bright future for the oil industry provided present hydrocarbon reserves can be more efficiently extracted and used and ultimately

new routes to hydrocarbon fuels, feedstocks and intermediates can be devised.

One of the first physical tests carried out to eliminate surfactants with little or no EOR potential is their solubility. This simple experiment determines the maximum temperature at which the surfactants are soluble in aqueous and saline solutions and can therefore be used to solubilise oil. Although this temperature is marked by the cloud point when the solutions appear turbid, the sulphonated surfactants do not form transparent solutions but stable dispersions which are still useful for oil recovery. The nonionic surfactants on their own are too unstable, particularly in the presence of inorganic salts, when they readily precipitated out. This was certainly found to be true here (see section 4.2 on cloud point and Chapter 6 where the extent of adsorption was increased). However, the inclusion of a co-surfactant and/or oo-solvent dramatically improved the situation (see Fig.6.12 where propan-2-ol increases the surfactant solubility and reduces the extent of adsorption).

The high pressure liquid chromatograph analysis clearly detects only those components containing the aromatic ring (i.e. the surfactant and any remaining and unrecovered precursors). . The amounts of the other reactants and solvents were not determined but since only a small rise in the baseline of the refractive index recorder was observed (and this is due largely to the changing solvent gradient) it can be assumed that these components are not present in any great quantity.

The extent of ethoxylation revealed by NMR spectrometry and the subsequent analysis by mass spectometry of T130 has provided enough information to characterise these surfactants. The major chain lengths range from 7-20 EO units. This result is not surprising and it is unfortunate that there was not the opportunity to analyses the other surfactants likewise in the same detail.

The mass spectrometry analysis was interesting but it is difficult to explain those peaks which perhaps contained an amide or bromide (as suggested by the library search - Fig.3.14 but it must be remembered that these searches have limitations).

The nuclear magnetic resonance spectroscopy results completely characterised the surfactant molecules in terms of the aromatic substituents and the length of the ethoxy chain. It has been determined that these substituents are three secondary butyl groups which help to stabilise the molecule. If the groups were tertiary butyl (as originally assumed) they would increase the stability but the difference would be slight.

The size of these surfactant molecules allows them to take up various conformations (or intermediate surface phase). This aspect is particularly important when considering the extent of adsorption. It has been found here that:

(i) lower temperatures favour coiled and higher temperatures favour zig-zag conformation; and

(ii) larger EO chain lengths are coiled but only at lower temperatures, whereas shorter chains are zig-zag.

A particular pore on an oxide surface can only accommodate a certain number of linear (zig-zag) molecules, leaving part of the molecule to rotate and vibrate around the outside of the pore. If the surfactants are in a more compact state (coiled) then a greater number may be allowed in the pore. Thus the extent of adsorption will be lower in the zig-zag extended form when at higher temperature. The sufactants at higher temperatures will therefore have a greater energy than those at lower temperatures. Their structure will then cover a larger area, particularly as they will be given greater freedom of movement.

The supplementary analysis of impurities (water, sodium chloride content etc.) in the surfactants here shows that water is mainly (nearly 50%) present. The others are present in fairly low concentrations. They will not adversely affect adsorption, interfacial tension reduction, stability, microemulsion formation etc., since in a micellar slug there will be a large quantity of water and salts present. Since it has to be accepted that these surfactants are not pure, it is at least as important to consider the properties of mixtures as of simple single compounds.

The viscosity, pH, surface tension and contact angle experiments were conducted mainly to gain a better insight into surfactant behaviour. For enhanced oil

recovery purposes, these properties are not important since the viscosities and pH measurements come well within the range required. The contact angles and surface tension tests were performed to illustrate how surfactants modify the behavior of aqueous solutions. The cloud point and interfacial tension measurements are two of the main screening procedures for surfactants and their results eliminate certain classes.

Mobil Oil Company has outlined their priorities in selecting surfactants. Their emphasis lies in the cost of materials, stability, and reduction of interfacial tension. More attention though was devoted to their phase behaviour and extent of adsorption on reservoir rock.

The works published concerning the batch method of adsorption usually state the time of equilibration, it is highly dependent on the type of surfactant and temperature. These times can only be taken as an approximate guide since equilbrium times are dependent upon the individual surfactant used. For the system presented here, two surfactants (N130, N150) in the batch experiments were analysed after 1,2,3,4 and 5 weeks. After 3-4 weeks at ambient temperature, the difference in the plateaus was negligible. At an elevated temperature, 3 weeks was found to be sufficient.

It cannot be stated that after these times, true eqilibrium data points were reached. The insensitivity of the technique may mask an equilibrium plateau at an

earlier time and temperature show a lower extent of adsorption. There may also be another plateau after 5 or 6 weeks. However, the plateaus obtained after the chosen equilibrium times are clearly evident and this is taken as "apparent equilibrium".

The accuracy of these adsorption experiments is difficult to define since the results (eg. plateaus) varied, but some consistency was observed. For example in the isotherms obtained for T130 at various times, in determining the effect of sulphonation, and the presence of aluminium ions. This illustrates the difference in the values which was calculated to be approximately 10%. This is similar to the estimate made in Chapter 6 when taking into account size and shapes of the silica speres, errors in preparing solutions, UV instrument fluctuation etc.

The surface area of one surfactant molecule has been calculated from the experimental isotherms. The reduction in surface area of one molecule as the hydrophilic chain length decreases could be explained by a more efficient packing of the amphiphilic molecules. Also, the reduced size of the molecules means they can fit into the pores more effectively. This is one explanation of the increase in the extent of adsorption as the EO chain length decreases (the other main reason being the decrease in solubility at lower chain lengths and hence a preference for adsorption).

Although adsorption pore radii and pore volumes have been given, it must be remembered that these are average

values and that they were measured using nitrogen; a molecule whose average dimension is far smaller than a solvated species and so it can enter the "ink-bottle" shaped pores which are not accessible to a surfactant molecule. Consequently, the surface area of an oxide will be higher than if the adsorbate surface area was conducted using a molecule of larger size. This is the concept of fractality. For the present elementary calculations, imperfect though these are, it is assumed that all the surface area is available to the surfactant molecule. It is also likely that the effective average pore radii was less than stated. There may be water molecules adsorbed at the pore opening which will reduce the possibility further of surfactant molecules entering.

Although the study of the conformation of surfactants using Raman spectroscopy reveals that the molecules can become more extended as the temperature is increased. It does not show how "energetic" these molecules are. It is reasonable to assume that the ethoxy tails are not stationary but are capable of substantial movement. As the first few molecules of a layer are adsorbed they will not only occupy adsorption sites but will appear to have a bigger area than when immobile (at a low temperature). This will hinder the adsorption of molecules on neighbouring sites.

At ambient tempertures (298K) the surfactant molecules will have quite low kinetic energy but the larger the hydrophillic chain, the more mobile their tails will be. Even slight movements of the chains will help to restrict

the approach of further molecules.

Considering the assumptions made and the caution exercised in the batch method of adsorption, it would be interesting to compare the values for the surface area of one surfactant molecule with a literature value for a similar molecule. The fatty acid group of compounds was thought to be of a similar nature and certain data on this class of molecule is well documented. However, the shortest ethoxy chain surfactant used in the batch method was N110 which contains 11 EO units (i.e. 22 carbon and 11 oxygen atoms in the ethoxy chain). The longest common fatty acid is only 22 carbon atoms long, which is only two-thirds the length of N110 (assuming an oxygen atom to have a comparable C-O to C-C bond length and the atoms to be similar in size. There are longer fatty acids to be found in certain plants and animals, but these are rare and consequently have little published information.

The solubilisation and stability of the microemulsion formed was the major method of searching for an effective oil recovery blend. Although reduction of interfacial tension and low adsorption are also important, using these parameters, the search would have been tedious. By observing the microemulsion formed, this was a surer and more rapid approach.

Initially, trial and error eliminated many surfactants and potential blends. Sometimes, the route taken did not yield satisfactory results, (e.g. in the synthesising novel anionic surfactants of long EO chain lengths - the

emulsions formed were unstable). Finally using Hoechst surfactants with an alcohol, the best three blends possible in terms of microemulsion formation and stability were otained. These together with synthetic oils, were dispatched to Hoechst in Germany to carry out flooding trials.

Hoechst conducted a comprehensive review of the surfactant blends, predicted by the present fundamental work, whose results are in Appendix 1. The flooding trials were carried out at 353K at a rate of flooding of $8cm^3.h^{-1}$, against atmospheric pressure. After water flooding of a sand pack saturated with synthetic oil, about 70% of the oil was recovered. With surfactant and polymer (chosen by Hoechst) flooding the additional oil recovery was as high as 19.6%. Hoechst suggested that by changing the surfactant and concentration, and the flooded volumes, the degree of de-oiling can be improved. One of the sand packs (No.3) gave de-oiling values of only about 58%. This model was immediately flooded with water after surfactant flooding by which additional de-oiling values of about 17% were obtained. Another of the packs (No.4) showed a sudden unexplained rise in pressure after surfactant and water flooding.

In addition to the flooding trials, the solubility and micro-capillary de-oiling of the surfactant systems was studied over a concentration range of 0.1-0.2% (wt/vol) and a temperature range of 298-370K. Table 1 interprets the numbers used in the microcapillary de-oiling results in terms of capillary size and time for complete or partial de-oiling. The reduction of

interfacial tension was monitored using a spinning drop tensiometer at 333K and 353K.

Provisional adsorption tests and phase behaviour were undertaken. The parameters studied and the best surfactant blend for them are summarised below.

Solubility	all are soluble (298-370K)
Interfacial Tension	T040S/B712/IPA (80:10:10) (particularly at 1% and 2% concentration wt/vol)
Microcapillary de-oiling	T040S/B712/IPA (80:10:10) particularly at 333 and 353K)
Sandpack Flooding	T040S/SAS60/IPA (80:10:10) (T040S/B712/IPA did work equally well but there is an unexplained very high pressure increase
Adsorption	T040S/B712/IPA at 353K resulted in negligible adsorption but overall at 333K and 353K the system T040/B712/IPA was the most effective
Phase Studies	T040S/B712/IPA

It appears that the surfactant blend consisting of T040S, B712 and IPA is the most promising for enhanced oil recovery. The other blends also worked well and all could be improved upon.

The results of laboratory tests may well be difficult to reproduce in an oil reservoir; indeed the scaling of laboratory results in the oil field is troublesome with any recovery process. The displacement mechanism, associated adsorption, mobility control etc., with surfactant systems makes scaling particularly difficult. Nevertheless, a better understanding of the complex

interaction between the injection fluids and reservoir components (oil, brine and rock) is desirable for a successful application of various oil recovery processes. This can only come from a thorough understanding of the fundamental interfacial chemistry involved. It is hoped that the present work has contributed modestly in this way.

Appendix I

Hoechst Report

Surfactant Flooding Conditions

Temperature:	353K
Oil:	Stock Tank Crude oil/iso-octane (60:40)
Surfactant Systems: (2% surf. concn.)	A T060S/2-propanol (90:10)
	B T040S/SAS60/2-propanol (80:10:10)
	C T040S/B712/2-propanol (80:10:10)
Polymer:	Rhodoflood XR (A202)
Sand Pack 1:	1/2PV System A. 2% Surfactant conc. 1PV Polymer XR. 500ppm in sea water
Sand Pack 2:	1/2PV System B. 2% Surfactant conc. 1PV Polymer XR. 500ppm in sea water
Sand Pack 3:	1/2PV System B.
Sand Pack 4:	1/2PV System C. 2% Surfactant conc. 1PV Polymer XR. 500ppm in sea water

Injection Water:	KCl	0.764g.dm^{-3}
	$CaCl_2.2H_2O$	1.280 "
	$MgCl_2.6H_2O$	11.520 "
	$SrCl_2.6H_2O$	0.030 "
	Na_2SO_4	3.994 "
	$NaHCO_3$	0.186 "
	NaCl	25.845 "

Sand Pack 1 - 4

Sand	Crushed quartz sand
Particle size	0.03-0.15mm
Specific surface area	$0.15 m^2.g^{-1}$

	Sandpack 1	Sandpack 2	Sandpack 3	Sandpack 4	
Length	15.04	15.04	15.04	15.04	(cm)
Diameter	2.58	2.58	2.58	2.58	(cm)
Cross Section Area	5.23	5.23	5.23	5.23	(cm^2)
Porosity Approx.	49.90	49.90	51.90	48.50	(%)
Permeability	0.52	0.60	0.91	0.56	(D)
Oil in Place	29.00	29.50	29.00	29.50	(cm^3)
Residual Water	26.13	24.86	28.96	22.70	(%)
Pore Volumes	39.26	39.26	40.82	38.18	(cm^3)
Flow Rate	8.00	8.00	8.00	8.00	($cm^3 h^{-1}$)
Water Flooding	4.02	3.79	3.53	4.41	(PV)
Surfactant Flooding	0.50	0.50	0.50	0.50	(PV)
Polymer	1.00	1.00	-	1.00	(PV)
Water Flooding	6.06	5.70	5.20	6.79	(PV)
Oil Recovered by Water Flooding	70.60	70.10	57.50	69.80	(%)
Total Oil Recovered	81.40	87.10	74.40	89.40	(%)
Additional Oil Recovered by Surfactant Flooding	10.80	17.00	16.90	19.60	(%)

Oil Recovered by Surfactant Flooding

Amount injected	Sandpack 1	Sandpack 2	Sandpack 3	Sandpack 4
0.5 PV	0.0%	0.0%	0.0%	0.0%
Surfactant Flooding				
1.0 PV	0.4%	7.1%	3.5%	0.0%
1.5 PV	0.7%	11.5%	9.0%	7.1%
Polymer Flooding (sandpack 1,2,4)				
2.0 PV	10.0%	11.5%	11.4%	13.5%
2.5 PV	10.0%	14.6%	13.1%	14.9%
3.0 PV	10.4%	14.9%	13.5%	15.6%
3.5 PV	10.8%	16.0%	14.9%	15.6%
4.0 PV		16.0%	15.2%	16.9%
4.5 PV		16.3%	15.6%	16.9%
5.0 PV		16.6%	15.6%	17.3%
5.5 PV		16.6%	16.9%	17.3%
6.0 PV		16.8%		17.6%
6.5 PV		16.8%		17.6%
7.0 PV		17.0%		19.3%
7.5 PV				19.3%
8.0 PV				19.6%
Water flooding				
Total Oil Recovered	81.4%	87.1%	74.4%	89.4%
Additional Oil Recovered by Surfactant	10.8%	17.0%	16.9%	19.6%

Surfactant System A for Beryl Reservoir

T060S 90% : Isopropyl alcohol 10% in Sea Water

Surfactant Concentration	Solubility 298-370K	Microcapillary deoiling (mins) 298K	313K	333K	353K	363K	Interfacial tension (mNm^{-1}) Spinning-Drop-Tensiometer 333K	353K
2.0%	soluble	6	5	4	6	6	$4x10^{-2}$	$5x10^{-2}$
1.0%	"	5	4	3	4	6	$5x10^{-2}$	$5x10^{-2}$
0.5%	"	4	4	3	0	6	$6x10^{-2}$	$6x10^{-2}$
0.1%	"	2	0	2	0	0	$9x10^{-2}$	$8x10^{-2}$

Surfactant System B for Beryl Reservoir

T040S 80% : SAS60 10% : Isopropyl alcohol 10% in Sea Water

2.0%	Soluble	5	6	6	6	8	$3x10^{-2}$	$6x10^{-2}$
1.0%	"	5	6	6	8	6	$4x10^{-2}$	$5x10^{-2}$
0.5%	"	4	5	6	8	6	$5x10^{-2}$	$4x10^{-2}$
0.1%	"	2	3	6	6	6	$4x10^{-2}$	$3x10^{-2}$

Surfactant System C for Beryl Reservoir

T040S 80% : B712 10% : Isopropyl alcohol 10% in Sea Water

2.0%	"	4	6	6	6	9	$1x10^{-2}$	$2x10^{-2}$
1.0%	"	3	6	6	8	8	$3x10^{-2}$	$3x10^{-2}$
0.5%	"	4	4	6	8	9	$7x10^{-2}$	$2x10^{-2}$
0.1%	"	0	3	6	6	8	$5x10^{-2}$	$4x10^{-2}$

Table 1. Key to the Efficiency of Deoiling Values.

Value	
9	Empty (30mm) after 10min.
8	Empty after 1h.
7	Empty after 3h.
6	Empty after 20h.
5	16-25mm emptying after 20h.
4	9-15m emptying after 20h.
3	4-8mm emptying after 20h.
2	1-3mm emptying after 20h.
1	Trace emptying after 20h.
0	Unchanged after 20h.

Adsorption Behaviour of Surfactant System A,B,C

Model matrix:

Valentin-Busch-Quartz sand

particle size 0.03 - 0.15mm

spec. surface $0.51 m^2.g^{-1}$ sand (BET method)

SiO_2 99.6%, Al_2O_3 0.14%, Fe_2O_3 0.0012%

Feldspar 0.2%, K_2O 0.04%

Adsorption Conditions:

$80 cm^3$ 1% (100%) surfactant systems A,B,C in 100% sea water

24h 333 to 353K rotating in glass bottles two phase titration before and adsorption

333K	weight	area
A	0.2 $mg.g^{-1}$ sand	0.5 $mg.m^{-2}$ sand
B	0.4 $mg.g^{-1}$ sand	0.9 $mg.m^{-2}$ sand
C	0.5 $mg.g^{-1}$ sand	1.0 $mg.m^{-2}$ sand

353K

A	0.04 $mg.g^{-1}$ sand	0.07 $mg.m^{-2}$ sand
B	1.3 $mg.g^{-1}$ sand	2.6 $mg.m^{-2}$ sand
C	0.3 $mg.g^{-1}$ sand	0.6 $mg.m^{-2}$ sand

Adsorption Behaviour of Surfactant Systems A,B,C

Model matrix:

Valentin-Busch-Quartz sand

Particle size 0.03-0.15mm

Spec. Surface $0.51 m^2.g^{-1}$ sand (BET method)

SiO_2 99.6%, Al_2O_3 0.14%, Fe_2O_3 0.0012%

Feldspar 0.2%, K_2 0.04%

Adsorption conditions:

$80 cm^3$ 2% (100%) surfactant systems A,B,C in 100% sea water

24h at 333 and 353K rotating in glass bottles two phase titration before and after adsorption

333K	weight	area
A	0.6 $mg.g^{-1}$ sand	1.1 $mg.m^{-2}$ sand
B	0.9 mg/g^{-1} sand	1.8 $mg.m^{-2}$ sand
C	0.1 mg/g^{-1} sand	0.2 $mg.m^{-2}$ sand

353K

A	4.1 $mg.g^{-1}$ sand	8.0 $mg.m^{-2}$ sand
B	0.0 $mg.g^{-1}$ sand	0.0 $mg.m^{-2}$ sand
C	0.3 $mg.g^{-1}$ sand	0.6 $mg.m^{-2}$ sand

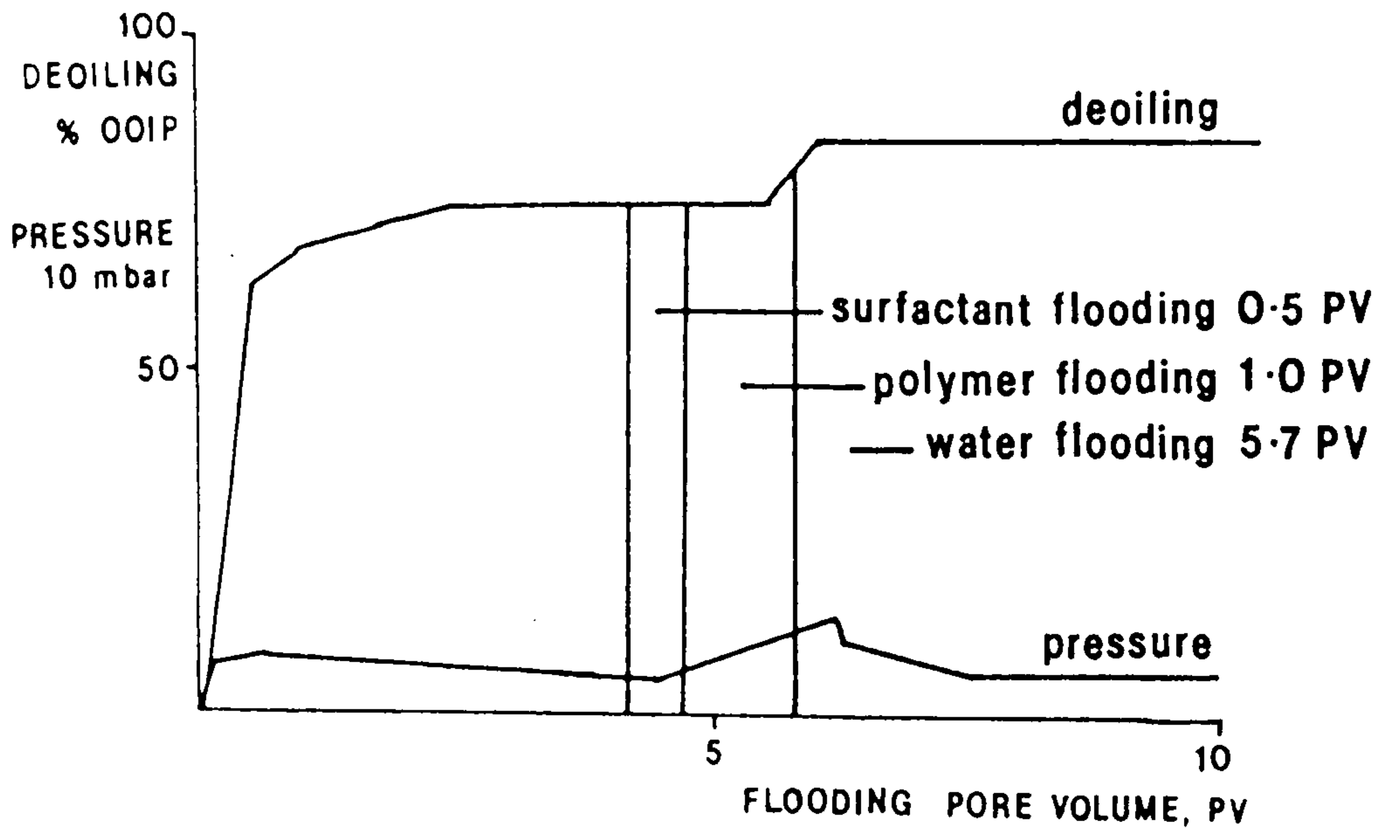

System A, sand pack 1

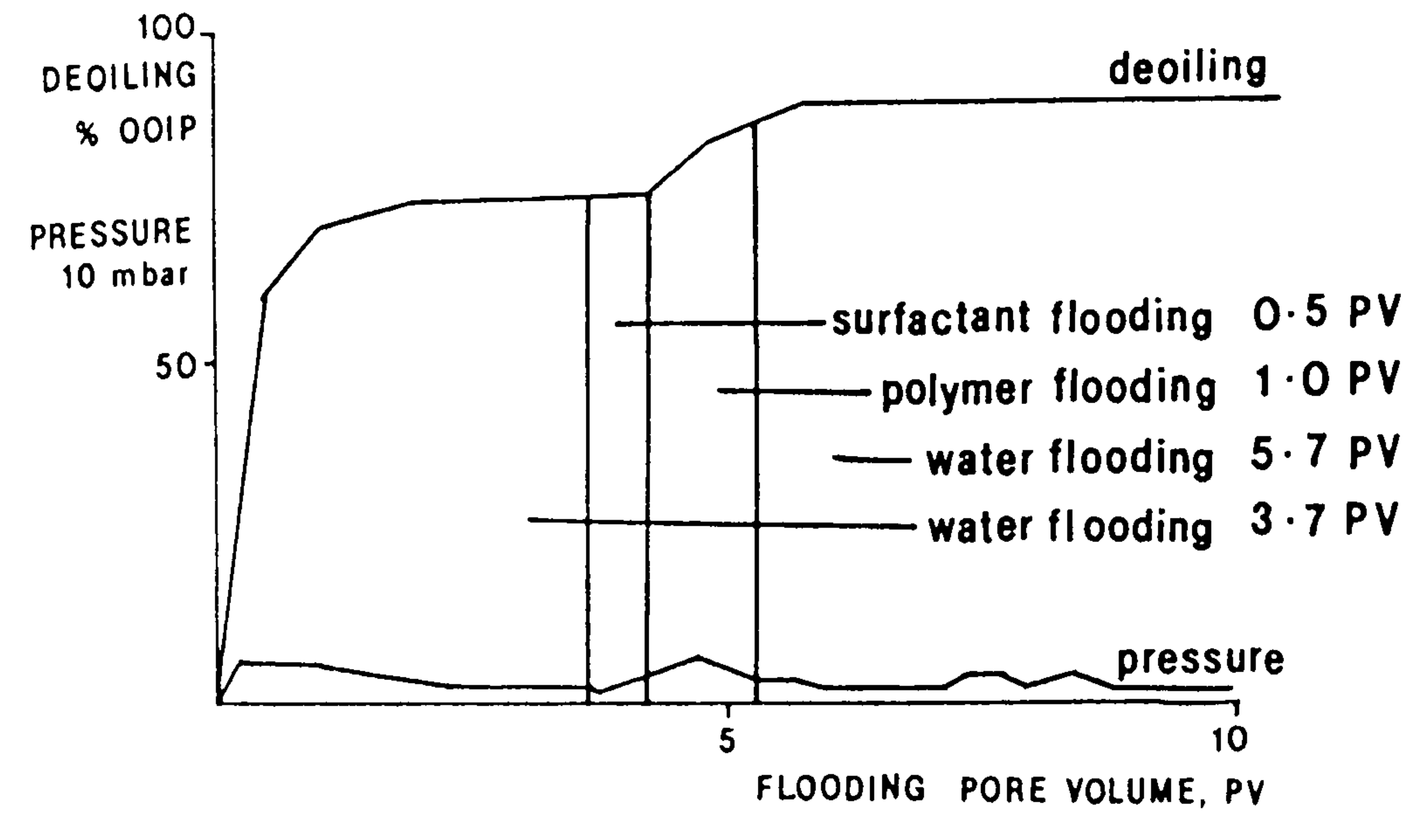

System B, sand pack 2

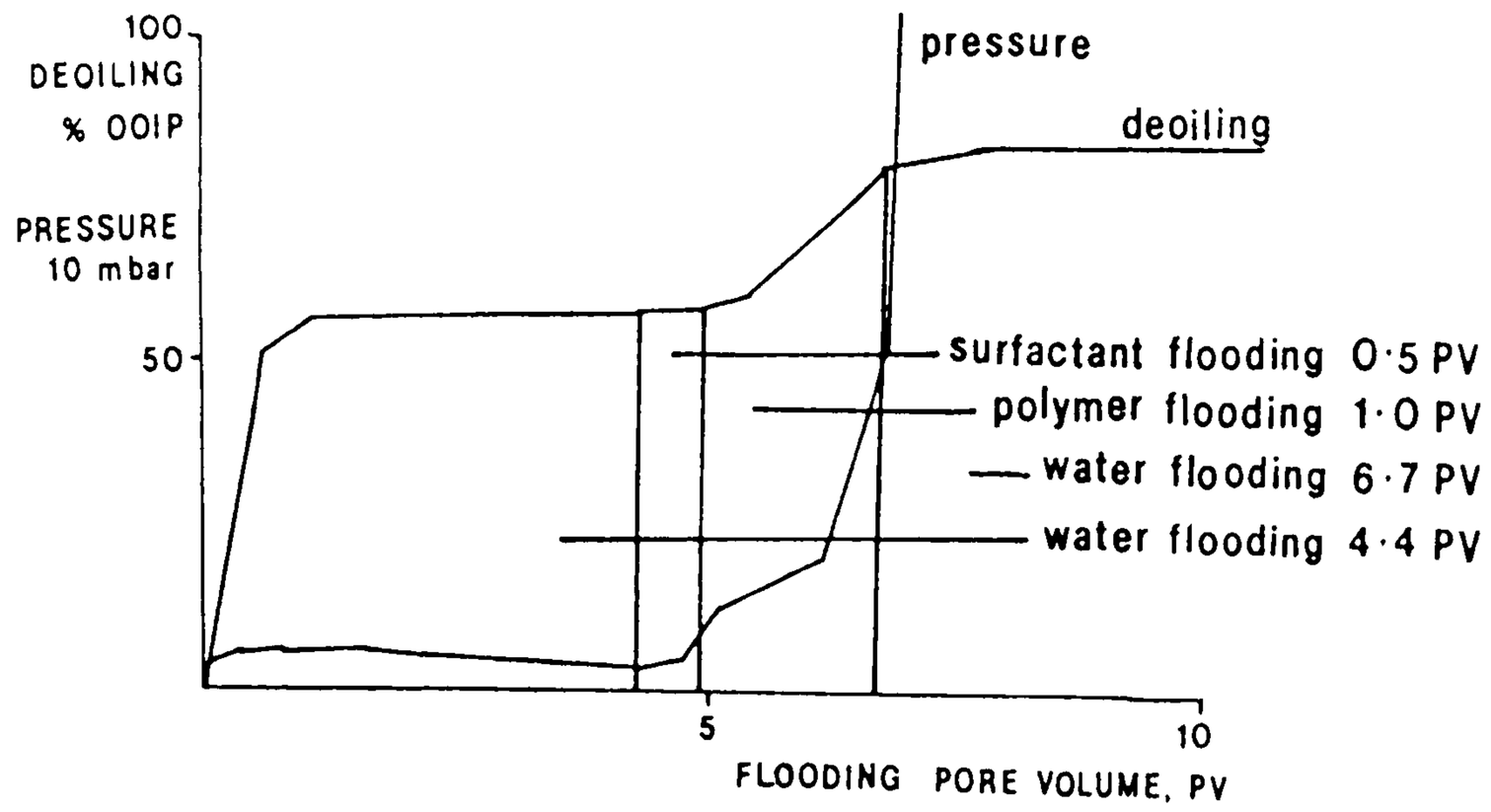

System C, sand pack 3

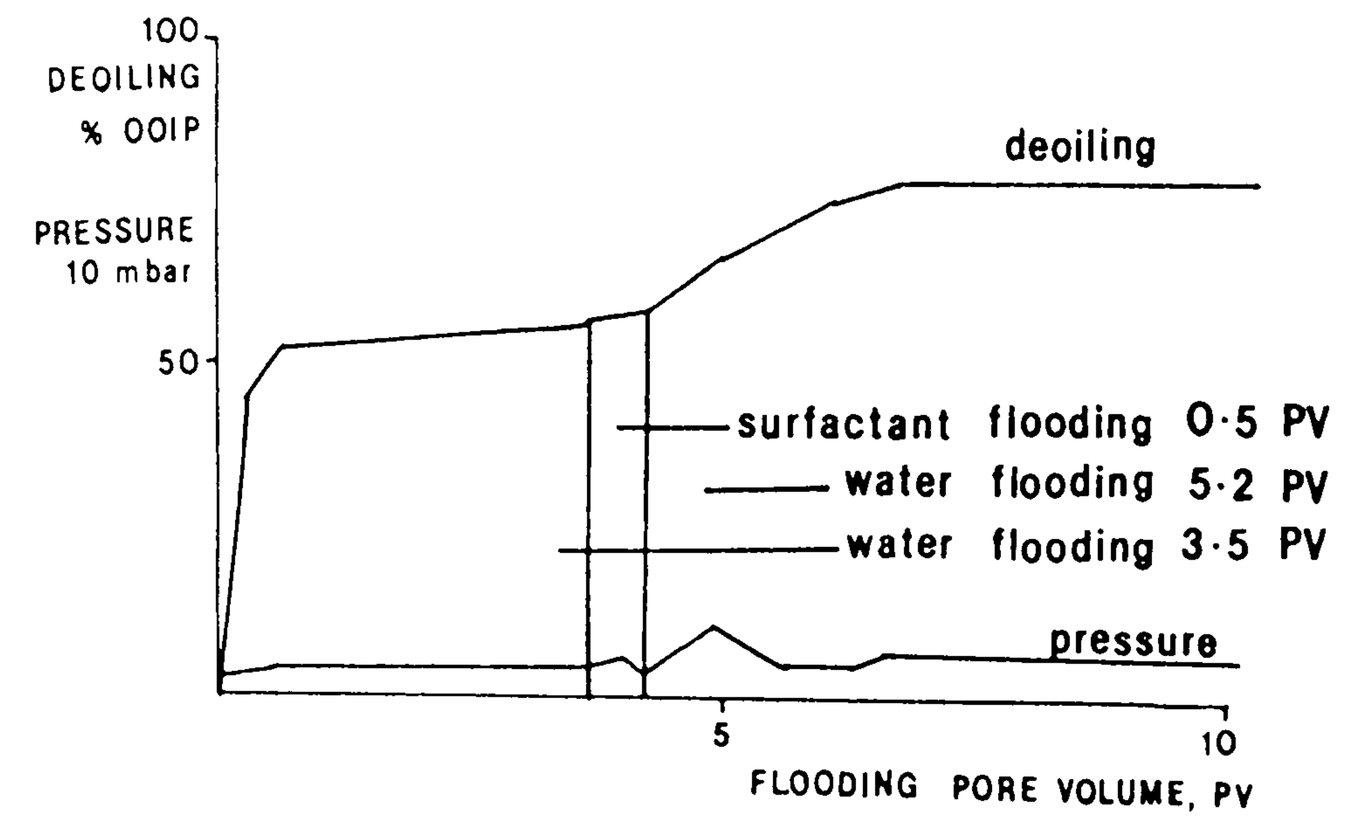

System D, sand pack 4

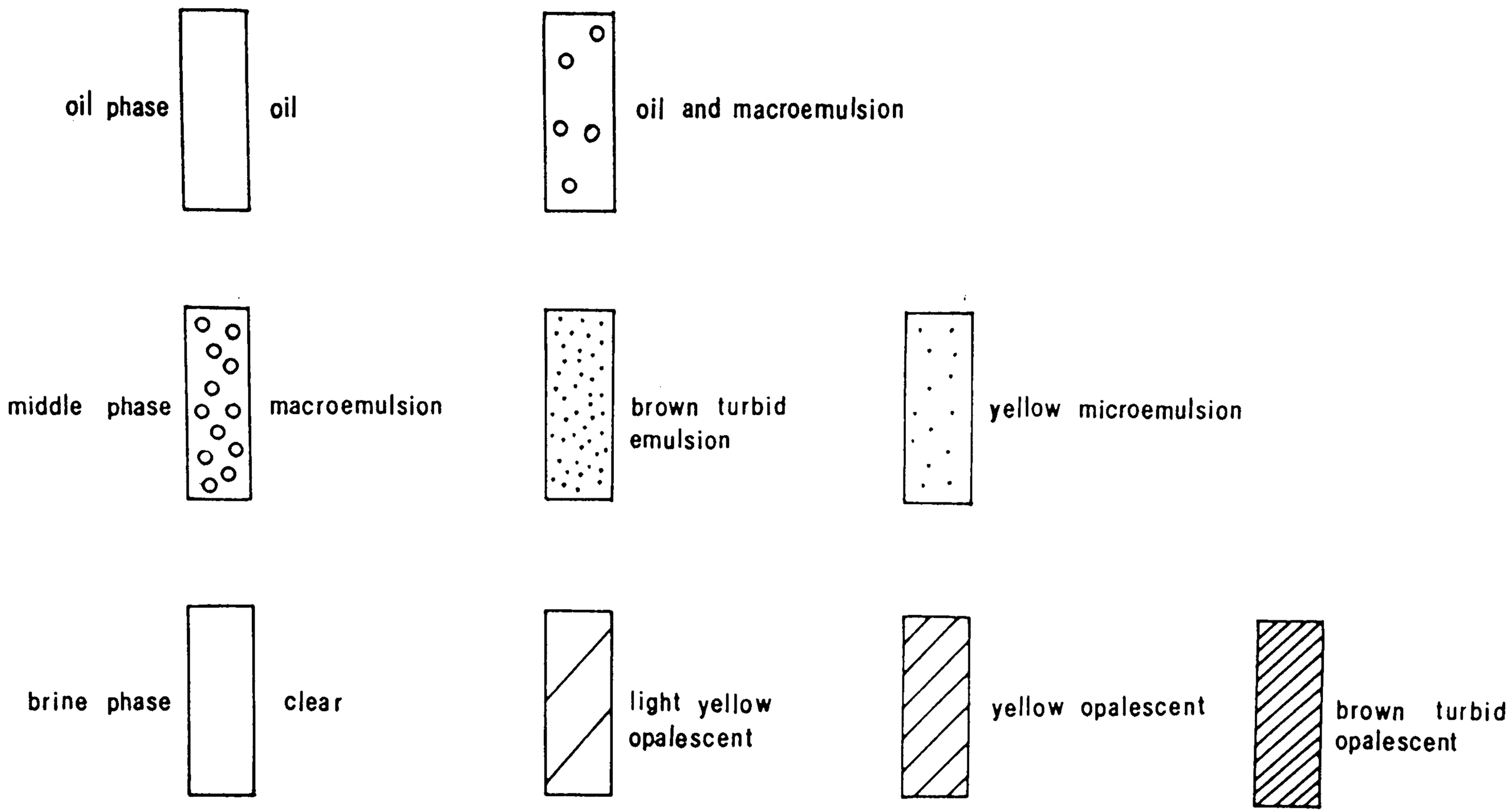

Fig.2 Key to phase behaviour formed.

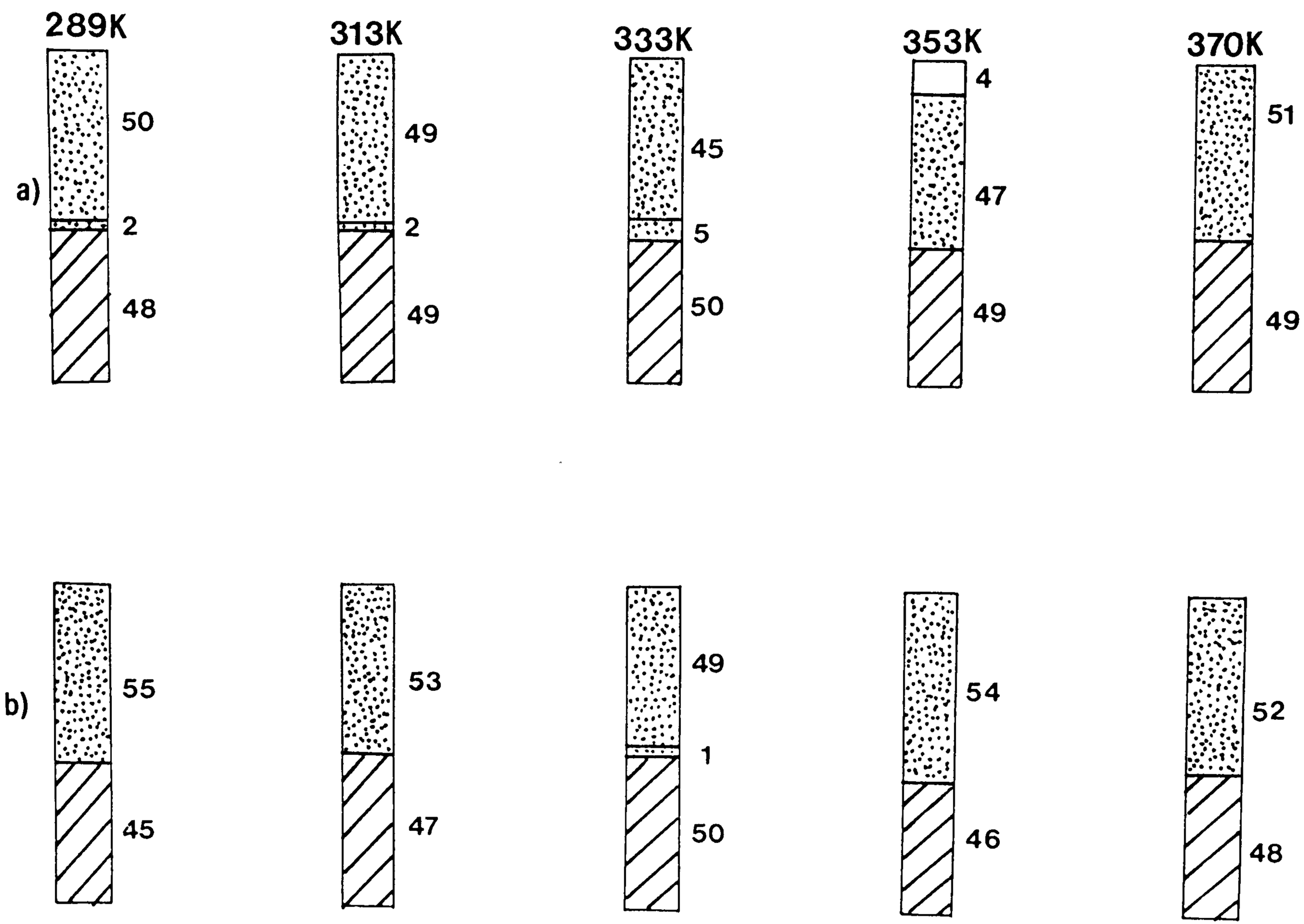

Fig.3 Phase behaviour of system A. Equilibrium time - 14 days.
a) 1% surfactant in brine; b) 2% surfactant in brine.

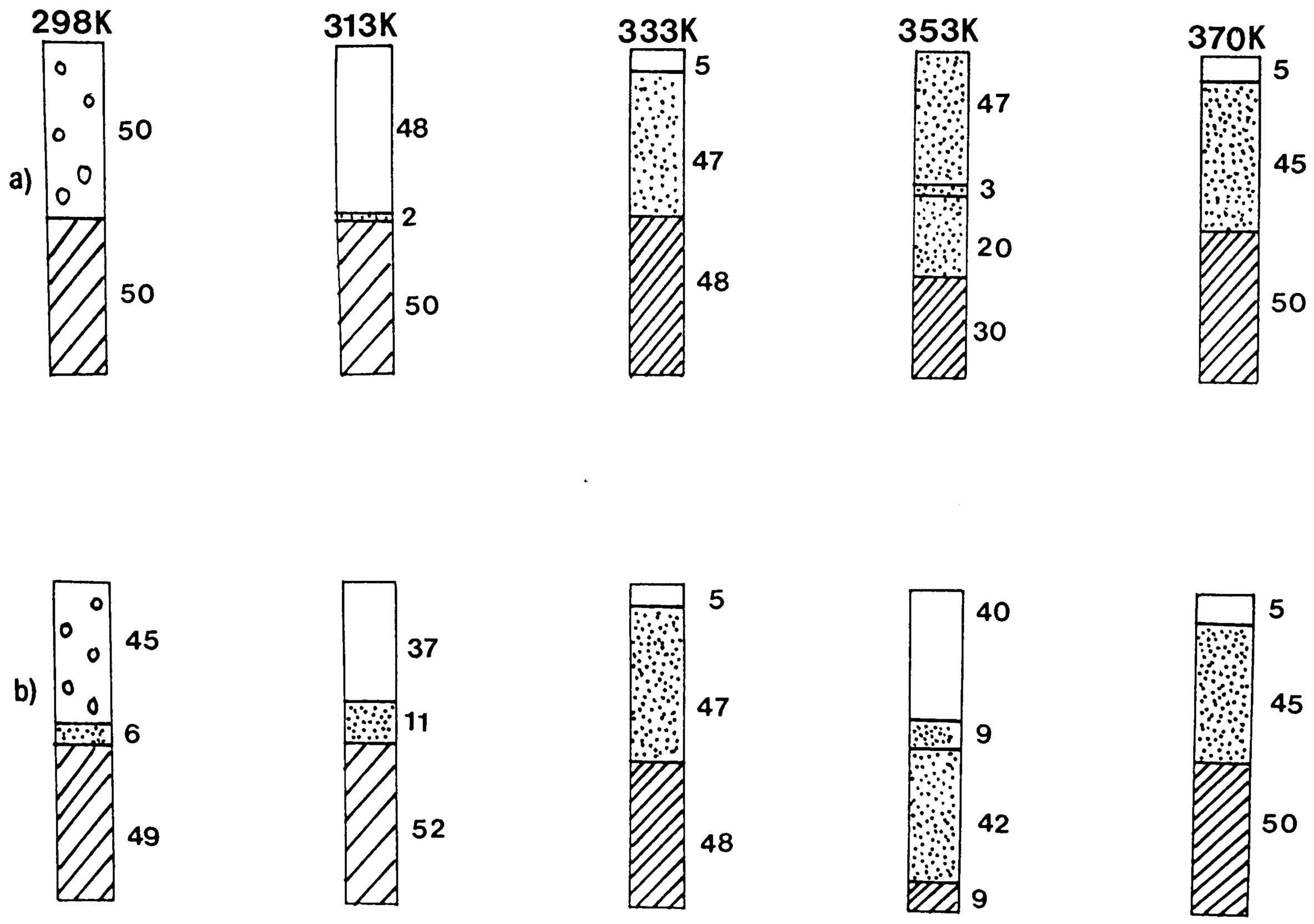

Fig.4 Phase behaviour of system B. Equilibrium time - 14 days.
a) 1% surfactant in brine; b) 2% surfactant in brine.

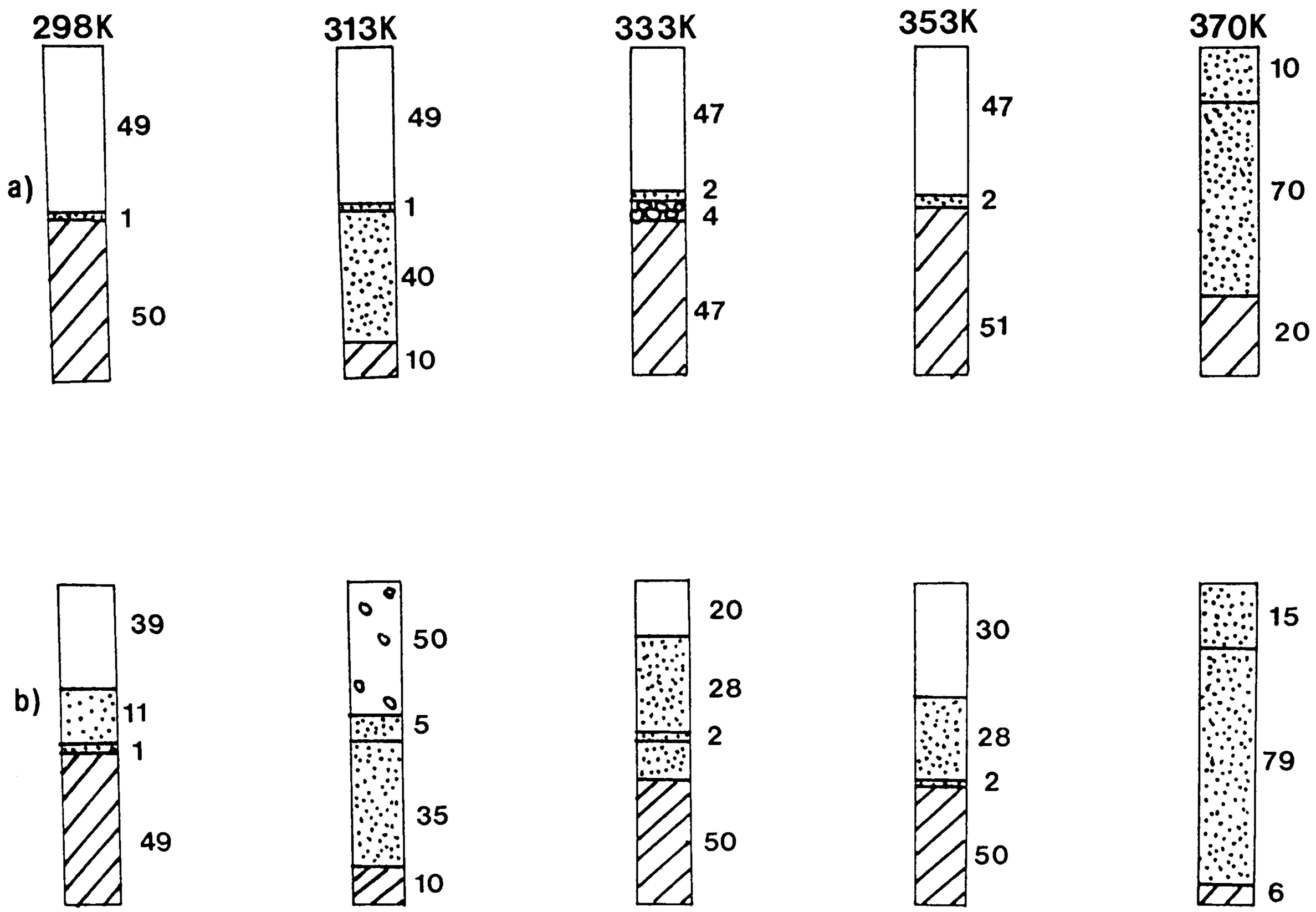

Fig.5 Phase behaviour of system C. Equilibrium time - 14 days.
a) 1% surfactant in brine; b) 2% surfactant in brine.

REFERENCES

1. Clark, N.J. Elements of Petroleum Reservoirs. Soc.Pet.Eng. of AIMMPE. (USA, 1969).

2. De Golyer, E.(ed.) 'Elements of the Petroleum Industry.' p289. AIME.(New York, 1940).

3. Tate, J.F. and Maddox, J. US Patent No. 4,094,798 (1978).

4. Holstein, E.D. Presentation to API Production Development Annual Meeting. April, 1982, San Antonio, USA.

5. Van Poolen, H.K. Fundamentals of Enhanced Oil Recovery. (Penwell Books, 1980, Tulsa, USA).

6. Martin, W.L., Dew, J.N., Powers, M.L. and Stevens, H.B. Results of a Tertiary Hotwater-flood in a Thin Sand Reservoir. p243, AIME. Trans. V. (1968).

7. Bursell, C.G. and Pittman, G.M. J.Pet.Tech. Aug, p997 (1975).

8. Gates, C.F. and Sklar, I. J.Pet.Tech. Aug, p981 (1971).

9. Parrish, D.R., Pollock, C.B. and Craig, F.F. J.Pet.Tech. June, p676 (1974).

10. Herbeck, E.F., Heintz, R.C. and Hastings, J.R. Pet.Eng. Feb, p58 (1976).

11. Herbeck, E.F., Heintz, R.C. and Hastings, J.R. Pet.Eng. March, p84 (1976).

12. Herbeck, E.F., Heintz, R.C. and Hastings, J.R. Pet.Eng. April, p66 (1976).

13. Holm, L.W. and Josendal, V.A. J.Pet.Tech. Dec, p1427 (1974).

14. Wang, H.L., Duda, J.L. and Radke, C.J. J.Coll.Int.Sci. 66, 15 (1978).

15. Giles, C.H., MacEwan, T.H., Nakhwa, S.N. and Smith, D. J.Chem.Soc. 3, 3937 (1960).

16. De Groot, M. US Patent No. 1,823,439 (1929).

17. De Groot, M. Us Patent No. 1,823,440 (1930).

18. Holbrook, W.B. and Olson, R.W. US Patent No. 3,006,411 (1958).

19. Blair, C.M., Groves, W. and Lehmann, S. US Patent No. 2,356,205 (1942).

20. Gogarty, W.B. and Olson, R.W. US Patent No. 3,254,714 (1962).

21. Widmyer, R.H. and Pindell, R.G. Proc. 2nd. Jnt. SPE/DOE Symp. on EOR. p301, SPE 9793. April 5-8. (Tulsa, USA 1981).

22. Holm, L.W. and Josendal, V.A. Oil Gas J. 70, 158 (1972).

23. Gogarty, W.B. J.Pet.Tech. 28, 93 (1976).

24. Leach, R.O., Wagner, O.R., Wood, H.W. and Harpke, C.F. J.Pet.Tech. Jan, p206 (1962).

25. Kuuskraa, V.O. and Hammershaimb, E.C. and Stosur, G. Proc. World Congr. Vol.2, p387 (1984).

26. Inks, C.G. and Lahring, R.I. J.Pet.Tech. 11, 1320 (1968).

27. Corkill, J.M., Goodman, J.F. and Walker, T. Trans.Far.Soc. 63, 759 (1967).

28. Dill, K.A. Surfactants in Solution. Vol.1, p307 (eds. Mittal, K.L. and Lindman, B. Plenum, 1984).

29. Russel, J.C. and Whitten, D.G. J.Am.Chem.Soc. 104, 5937 (1982).

30. Menger, F.M. Acc.Chem.Res. 12, 111 (1979).

31. Preston, W.C. J.Phys.Chem. 52, 84 (1948).

32. Durham, K.(ed.) Surface Activity and Detergency. Chap. 7. (MacMillan, London, 1961).

33. Cabane, B, Duplessix, R. and Zemb, T. Surfactants in Solution. Vol.1, p373 (eds. Mittal, K.L. and Lindman, B. Plenum, 1984).

34. Corkill, J.M. and Walker, T. J.Coll.Int.Sci. 39, 621 (1972).

35. Crook, E.H., Fordyce, D.B. and Trebbi, G.F. J.Phys.Chem. 67, 1987 (1963).

36. Dwiggins, C.W., Bolen, R.J. and Dunning, H.N. J.Phys.Chem. 64, 1175 (1960).

37. Mukerjee, P. Advan.Coll.Int.Sci. 1, 241 (1967).

38. Paradies, H.H. J.Phys.Chem. 84, 599 (1980).

39. Miller, S.A., Bann, B. and Thrower, R.D. J.Am.Chem.Soc. 4, 3623 (1950).

40. Gilbert, E.E. and Miller, S.A. US Patent No. 2,793,964 (1967).

41. Cerfontain, H. Mechanistic Aspects in Aromatic Sulphonation and Desulphonation. (Wiley, 1968).

42. Kirk-Othmer, R.E. Encyclopaedia of Chemical Technology. (Wiley-Interscience, 1979).

43. Stillson, G.H., Sawyer, D.W. and Hunt, C.K. J.Am.Chem.Soc. 67, 303 (1945).

44. Flory, P.J. J.Am.Chem.Soc. 62, 1561 (1940).

45. Fineman, M.N., Brown, G.L. and Myers, R.J. J.Phys.Chem. 56, 963 (1952).

46. Konishi, K. and Yamaguchi, S. Anal.Chem. 38, 1755 (1966).

47. Brunauer, S., Emmett, P.H. and Teller, E. J.Am.Chem.Soc. 60, 309 (1938).

48. Puerto, M.C. and Reed, R.L. Soc.Pet.Eng.J. Aug, p669 (1983).

49. Ritter, H.L. and Drake, L.C. Ind.Eng.Chem. Analyst Edn. 17, 782 (1945).

50. McClure, J.D. J.Am.Chem.Oil Soc. 59, 364 (1982).

51. Nakamuro, K., Morikawa, Y. and Matsumoto, I. J.Am.Chem. Oil Soc. 58, 72 (1981).

52. Nakae, A., Yamanaka, M. and Tsuji, K. Anal.Chem. 52, 2275 (1980).

53. Allen, M.C. and Linder, D.E. J.Am.Oil Chem.Soc. Oct, p950 (1981).

54. Aserin, A., Frenkel, M. and Garti, N. J.Am. Oil Chem.Soc. 61, 805 (1984).

55. Jandera, P. Liq.Chrom.Env.Anal. Chap.4, p115 (1984).

56. Garti, N., Kaufman, V.R. and Aserin, A. Sepn.Pur.Methods. 12, 49 (1983).

57. Liquid Chromatography Technical Report. HPLC Analysis of Surfactants. Du Pont, Delaware, USA. (1982).

58. Van der Maeden, F.P.B., Biemond, M.E.F. and Janssen, P.C.G.M. J.Chrom. 149, 539 (1978).

59. Pilc, J.A. and Sermon, P.A. J.Chrom. 398, 375 (1987).

60. Rothman, A,M. J.Chrom. 253, 283 (1982).

61. Nadeau, H.G., Oaks, D.M., Nichol, W.A. and Carr, L.P. Anal.Chem. 36, 1914 (1964).

62. Melander, N.R., Nahum, A. and Horvath, C. J.Chrom. 185, 129 (1979).

63. Levsen, K., Wagner-Redeker, W. and Schafer, K.H. J.Chrom. 323, 135 (1985).

64. Covey, T.R., Lee, E.D., Bruins, A.P. and Henion, J.D. Anal.Chem. 58, 1451A (1986).

65. Arpino, P.J. J.Chrom. 323, 3 (1985).

66. Mayhew, R.L. and Hyatt, R.C. J.Am.Oil Chem.Soc. 29, 357 (1952).

67. Von Tischbirch, G. Proceedings 3rd. Int. Congr. Surfactant Activity. A13, No.21, p126 (Cologne, W.Germany, 1961).

68. Goldsmith, H.A. Chem.Rev. 33, 257 (1943).

69. Knight, D.W. Phys. Rev. 76, 1259 (1949).

70. Hoechst A.G. US Patent No. 4,091,014 (1978).

71. Hoechst A.G. E. Patent No. 0,116,929. (1984).

72. Robson, R.J. and Dennis, E.A. J.Phys.Chem. 81, 1075 (1977).

73. Marsden, S.S. and McBain, J.W. J.Phys.Chem. 52, 110 (1948).

74. Ribeiro, A.A. and Dennis, E.A. J.Phys.Chem. 80, 1746 (1976).

75. Kalyanasundaram, K.and Thomas, J.K. J.Chem.Phys. 80, 1462 (1976).

76. Koenig, J.L. and Angood, A.C. J.Polym.Sci. Part A, 8, 1787 (1970).

77. Yoshihara, T., Tadokoro, H. and Murahashi, S. J.Chem.Phys 41, 2902 (1964).

78. Cooney, R.P., Barraclough, C.G. and Healy, T.W. J.Phys. Chem. 87, 1868 (1983).

79. Bartlett, J.R. and Coonet, R.P., J.Chem.Soc. Far.Trans. I. 82, 597 (1986).

80. Rosch, M. Nonionic Surfactants. p753. (ed. Schick, M.J. Arnold Dekker, 1967).

81. Painter, P.C., Coleman, M.M. and Koenig, J.L. The Theory of Vibrational Spectroscopy and its Application to Polymeric Materials. (Wiley-Interscience, 1982).

82. Rosen, M.J. Surfactants and Interfacial Phenomena. (Wiley, 1978).

83. White, L.R. J.Chem.Soc. Far.Trans. I. 73, 390 (1977).

84. Vonnegut, B. J.Am.Chem.Soc. 13, 6 (1942).

85. Cayias, J.L., Schechter, R.S. and Wade, W.H. Am.Chem.Soc.Symp. Series No.9, p235 (1975).

86. Harkins, W.D. and Brown, F.E. J.Am.Chem.Soc. 41, 503 (1919).

87. Melrose, J.C. and Brandner, C.F. J.Can.Pet.Tech. 13, 54 (1974).

88. Adamson, A.W. Physical Chemistry of Surfaces. 3rd. edn. (Wiley-Interscience, 1976).

89. Casel, H.M. US Patent No. 2,448,768 (1942)

90. Brown, R.C. and McCormick, H. Phil.Mag. 39, 420 (1948).

91. Fordham, S. Proc.Roy.Soc. A194, p1 (London, 1948).

92. Vold, R.D. and Vold, M.J. Colloid and Interface Chem. p663 (1983).

93. Hartley, G.S. Nature 163, 767 (1949).

94. Riegelman, S.N., Allawala, N.A., Hrenoff, M.K. and Strait, L.A. J.Coll.Int.Sci. 13, 208 (1958).

95. Eriksson, J.C. Acta Chem.Scand. 17, 1478 (1963).

96. Satake, I., Matsuura, K. Bull.Chem.Soc. Japan, 36 (1963) 813.

97. Mankowich, A.M. J.Am.Oil Chem.Soc. 37 (1960) 587

98. Klevens, H.B. J. Am. Chem. Soc. 72 (1950) 3780

99. Elworthy, P.H., Florence, A.T. and MacFarlane, C.B. Solubilisation by Surface-Active Agents. p90. (Chapman and Hall, London, 1968).

100. Nakagawa, T. Nonionic Surfactants. Chap17 (ed. Schick, M.J. Dekker, New York 1967) .

101. Bansal, V.K. and Shah, D.O. Microemulsions. p149 (ed. Prince, L.M., Academic Press, 1977)

102. Bancroft, W.D. J.Phys.Chem. 17, 514 (1913).

103. Schott, H. J.Pharm.Sci. 58, 1443 (1969).

104. Lin, I.J. and Lambrechts, J.C. J.Coll.Int.Sci. 45, 378 (1973).

105. Becher, P.and Birkmeier, R.L. J.Am.Chem.Soc. 41, 169 (1964).

106. Shinoda, K.and Arai, H. J.Coll.Int.Sci. 20, 93 (1965).

107. Beerbauer, A. and Hill, M.W. Am.Cosmet.Perfum. 87, 85 (1972).

108. Hoar, J.P.and Schulman, J.H. Nature 152, 102 (1943).

109. Shah, D.O. 48th.Natnl.Coll.Symp. p173. June, (Austin, Texas, 1974).

110. Rosana, H.L. and Gerbacia, W.E. Proc.Int.Conf. Surface Active Substances. (Zurich, 1972).

111. Hayes, M.E. and Bourrel, M. Interfacial Tension and Phase Behaviour of Nonionic Surfactants. SPE 7581.

112. Winsor, P.A. Solvent Properties of Amphiphilic Compounds. (Butterworth Sci. 1954).

113. Reed, R.L.and Healy, R.N. Improved Oil Recovery by Surfactant and Polymer Flooding. p383 (eds. Shah, D.O. and Schechter, R.S. Academic Press, 1977).

114. Nelson, R.C.and Pope, G.A. Soc.Pet.Eng.J. 18, 325 (1978).

115. Larson, R.G. SPE 6744. SPE/AIME 52nd. Annual Fall Meeting. Oct.9-12. (Colorado, USA, 1977).

116. Nelson, R.C. Soc.Pet.Eng.J. June, p501 (1983).

117. Chatenay, D., Langevin, D. and Meunier, J. J.Disp.Sci.Tech. 3, 245 (1982).

118. Vrij, A., Nieuwenhuis, E.A., Fijnaut, H.M. and Agterof, W.G.M. Disc.Far.Soc. 65, 101 (1978).

119. Bennett, K.E., Hatfield, J.C., Davis, H.T. and Macosko, C.W., Scrien, L.E. Microemulsions. p65 (ed. Robb, I.D., Plenum Press, 1982).

120. McCune, C.C. J.Pet.Tech. 1, 17 (1977).

121. Gogarty, W.B., Davis, B. SPE 3806. SPE/AIME. Improved Oil Recovery Smp. April 16-19. (Tulsa, USA, 1972).

122. Schat, N. and Greenwald, H.L. Nonionic Surfactants. p8. (ed. Schick, M.J. Dekker, 1967)

123. Corkill, J.M., Goodman, J.F.and Tate, J.R. Trans.Far.Soc. 63, 2264 (1967).

124. Schott, H. Koll.Zh. 199, 158 (1964).

125. Hsaio, L. and Denning, H.N. J.Phys.Chem. 59, 362 (1955).

126. McCracken,J.R., Datyner,A. J.Coll.Int.Sci. 60, 201 (1977).

127. Tamamushi, B. and Tamaki, K. Proc.2nd.Int Cong.Surface Activity. 3, 449 (1957).

128. Dobias, B. Coll.Polym.Sci. 256, 465 (1978).

129. Scamehorn, J.F., Schechter, R.S. and Wade, W.H. J.Coll.Int.Sci. 85, 463 (1982).

130. Cases, J.M., Goujon, G. and Smani,S. AIChE Symp. Series 71, (1975).

131. Langmuir, I. J.Am.Chem.Soc. 40, 1361 (1918).

132. Klimenko, N.A. Koll.Zh. 42, 561 (1980).

133. Gaudin, A.M. and Fuerstenau, D.W. Trans. AIME. 202, 958 (1955).

134. Ball, B. and Fuerstanau, D.W. Disc.Far.Soc. 52, 361 (1971).

135. Somasundaran, P. and Fuerstenau, D.W. J.Phys.Chem. 70, 90 (1966).

136. Roy, R. and Fuerstanau, D.W. J.Coll.Int.Sci. 26, 102 (1968).

137. Somasundaran, P. and Fuerstanau, D.W. Trans. AIME 252, 275 (1972).

138. Grahame, D.C. Chem.Rev. p41 (1947).

139. Fuerstenau, D.W. Pure Appl.Chem. 24,135 (1970).

140. Tamamushi, B. and Tamaki, K. Trans.Far.Soc. 55, 1007 (1959).

141. Doss, S.K. Inst.Min.Met. Trans.(C) 85, 193 (1976).

142. Blazer, D. and Lange, H. Coll.Polm.Sci. 257, 292 (1979).

143. Somasundaran, P., Healy, T.W. and Fuerstenau, D.W. J.Phys.Chem. 68, 3562 (1964).

144. Wakamatsu, T. and Fuerstenau, D.W. Trans. AIME 254, 123 (1973).

145. Rendall, M.M. and Smith, A.L. Surface Active Agents p37 (Soc.Chem.Ind., London, 1979).

146. Shinoda, K., Tamamushi, B., Nakagawa, T. and Isemura, T. Colloidal Surfactants. (Academic Press, 1963).

147. Flengas, S.N., Rideal,E. Trans.Far.Soc. 55, 339 (1959).

148. Blair, C.M. J.Chem.Phys. 16, 113 (1948).

149. Lavionov, C. Zh. Fiz. Khim. 52 (1973) 2118.

150. Nunn,C., Schechter, R.S. and Wade, W.H. J.Coll.Int.Sci 80, 598 (1981).

151. Nunn, C. and Everett, D.H. J.Chem.Soc. Far.Trans. I 79, 2953 (1983).

152. Wang, H.L., Duda, J.L. and Radke, C.J. J.Coll.Int.Sci. 66, 153 (1978).

153. Muramatsu, M. Surface and Colloid Science. Vol 6 p101 (ed. Matijevic, Wiley, 1973).

154. Trojus, F.J., Sophany, T., Schechter R.S. and Wade, W.H. Soc.Pet.Eng.J. Oct. p339 (1977).

155. Lawrence, S.A., Pilc, J.A., Readman, J.R. and Sermon, P.A. Chem.Comms. 13, 1035 (1987).